Biotransformation of Thiomersal by Naturally Mercury Resistant Isolates and Genetically Engineered Microorganisms

Von der Fakultät für Lebenswissenschaften
der Technischen Universität Carolo-Wilhelmina
zu Braunschweig
zur Erlangung des Grades einer
Doktorin der Naturwissenschaften
(Dr.rer.nat.)
genehmigte
D i s s e r t a t i o n

von Wanda Fehr
geboren Teheran/ Iran

1. Referent: PD Dr. Irene Wagner-Döbler

2. Referentin oder Referent: Prof. Dr. Dieter Jahn

eingereicht am: 17.03.2006

mündliche Prüfung (Disputation) am: 24.04.2006

Vorveröffentlichungen der Dissertation

Teilergebnisse aus dieser Arbeit wurden mit Genehmigung der Fachbereich für Biowissenschaften und Psychologie, vertreten durch Mentorin Dr. habil. I. Wagner-Döbler, in folgenden Beiträgen vorab veröffentlicht:

Publikation:

Felske AD, Fehr W, Pauling BV, von Canstein H, Wagner-Dobler I. Functional profiling of mercuric reductase (*mer*A) genes in biofilm communities of a technical scale biocatalyzer. *BMC Microbiol*. 2003 Oct 27; 3(1):22.

Tagungsbeiträge:

Wanda Fehr and Irene Wagner-Döbler. Microbial degradation of an organic mercury compound (Thiomersal). Roskilde, Sectoral meeting, June 14-16, 2000, Roskilde, Denmark.

Weitere Veröffentlichungen:

Brummer IH, Fehr W, Wagner-Dobler I. Biofilm community structure in polluted rivers: abundance of dominant phylogenetic groups over a complete annual cycle. *Appl Environ Microbiol.* 2000 Jul; 66(7):3078-82.

Uphoff HU, Felske A, Fehr W, Wagner-Dobler I.The microbial diversity in picoplankton enrichment cultures: a molecular screening of marine isolates. FEMS Microbiol Ecol. 2001 May; 35(3):249-258.

Vorträge:

Irene Wagner-Döbler1, Harald von Canstein1, Andreas D.M. Felske1, Johannes Leonhäuser, Björg V. Pauling, Wanda Fehr, Wolf-Dieter Deckwer. New tricks of old bugs. VAAM Frühjahrstagung, March 28-31, 2001, Braunschweig, Germany.

CONTENTS

1 Introduction

1.1 Mercury in the Environment

Mercury is an element occurring naturally in the earth's crust with an average concentration of 0.08 ppm. Since ancient geologic times mercury has been buried as a component of highly insoluble mercury ore (mercuric sulfide) along with other minerals and has only been released into the atmosphere during earth movements such as volcanic outbreaks and similar thermal situations. The amount of mercury today is identical to that present at the time when the earth was formed, but the global distribution has been drastically changed as a result of continuing offgassing from the earth, increasingly wide industrial use and subsequent release of fumes from burning coal and oil and the disposal of mercury containing products. Although the precise amount of mercury released to the environment is unknown, the annual natural emission is estimated to be between 2700 and 6000 tons, of which some can be attributed to previous anthropogenic activity (Lindberg *et al.*1987; WHO 1991). In total, human activities have been estimated to constitute 2000–3000 tons of the total annual release of mercury to the global environment (WHO 1991). For example, the Almaden mercury mine in Spain, just one of over 3000 natural mercury reservoirs in the world (others are e.g. in former Yugoslavia, Russia, and North America), has produced in the past more than 1000 tons of mercury per year (U.S. Geological Survey 1998) and represents more than 30% of the total known mercury produced throughout the world (mining activity at the Almade´n mine ceased in May 2002).

Environmental transport and the distribution of mercury can be described in terms of a global cycle that involves two scopes: elemental mercury evaporates from land and water surface to the atmosphere and is globally transported. Locally, mercury can be converted to different soluble compounds, and it returns to land and water by various depositional processes.

Mercury is easily transformed into several forms. It occurs naturally in three oxidation states: metallic mercury (Hg0), monovalent (HgI) and divalent ions (HgII). The distribution of mercury between these three oxidation states is determined by the redox potential, pH, and the anions present. Mercury (I) always exists in the dimeric form (Hg_2^{2+}) and all of its derivates are ionized in solution. Mercury (II; Hg^{2+}) forms both covalent and ionic bonds. By accepting pairs of electrons from ligands, it can also generate complexes. The covalent property of mercury (II) allows a stable mercury–carbon bond and the formation of organometallic compounds, especially those containing sulphur (amino acids, oxycarbonic acids etc.) and

natural compounds of higher molecular weight like fulvic and humic acids (from degraded plant material etc.). In natural waters, mercury compounds are strongly bound to particulate matter and are readily transported in aquatic systems such as rivers. In addition to hydrophobic organic complexes, Hg (II) can form, microbiologically and chemically, water and lipid-soluble organomercurial compounds consisting of linear hydrocarbons (alkyl derivates, e.g., methylmercury and dimethylmercury).

The transformation of mercury in aquatic systems (Figure 1-1) is believed to be mediated by biological processes, although scientists attribute the process to abiotic conversion (Roger 1976; Wood *et al.* 1983). Usually, mercury accumulates in the aquatic food chain, primarily in the form of methylmercury, a well-studied organomercurial. Methylmercury (MHg) occurs in the water column of an aquatic system contaminated with inorganic mercury as a consequence of biogeochemical transformation in the sediment resulting in a rapid flux of methylmercury to the water column (Ikingura *et al.* 1999). Organic forms of mercury are more easily absorbed by biological membranes when ingested. They are less readily eliminated from the body than inorganic forms of mercury. Therefore, mercury attains its highest concentrations in large predatory species at the top of the aquatic food chain.

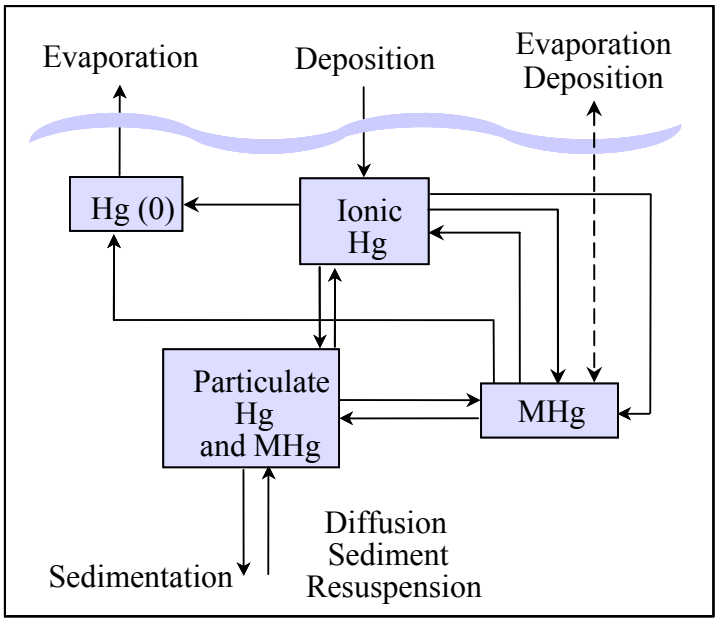

Figure 1-1. Dynamic interaction of different mercury species in aquatic systems (based on Mason and Fitzgerald 1996). Hg(0) = elemental mercury, MHg = methyl-mercury.

The degree to which mercury will become a hazard to the environment and human health depends on parameters such as alkalinity, pH, specific conductivity and dissolved nutrients. Swain and Helwig (1989) correlated lower pH with enhanced mercury accumulation in fish, which they attributed to an increased production of methylmercury. Also, the quality and the quantity of dissolved organic carbons (DOC) can have a strong influence on the fate and transformation of mercury in the environment (Babiarz *et al.* 2001; Cai *et al.* 1999). There are a number of studies that show increasing bioaccumulation with increasing DOC concentration. Richardson *et al.* (1995) found a positive correlation between fish tissue levels and DOC concentrations. Further evidence is provided by data collected by the Georgia Environmental Protection Division (GA EPD), which shows that the highest mercury concentrations in fish tissue occur in waters of the Coastal Plain where DOC levels are highest. This may be because abiotic mercury methylation is enhanced by humic substances (Weber 1993). DOC also helps to retain mercury in the water column where methylation may occur.

1.2 Toxicity of Mercurial Compounds

Mercury strongly bioconcentrates and has only harmful effects with no useful physiological functions (Hill *et al.* 1996; Trakhtenberg 1974). The toxicity and mode of action of mercury depends on its chemical and physical forms, which exceedingly differ in their toxicokinetics. Following general toxicological considerations, the way of assimilation in the organism is the major determinant for its bioavailability and toxicity. Mercury can be absorbed through the skin, respiratory, or gastrointestinal tract or can be injected (e.g., vaccination). While elemental mercury is poorly absorbed in the gastrointestinal tract (< 0.001% in rats), 10–15 % of ionic mercury and almost 100% of organomercurials are absorbed in the gastrointestinal tract and retained in body tissues. In contrast, vaporized Hg^0 is more toxic to animals than is Hg^{2+} because it penetrates the blood–brain barrier more readily and severely damages the brain (WHO 1976).

Owing to three large epidemics (Minamata and Niigata, Japan, and several provinces in Iraq) much more is known of the clinical toxicology of organomercurials, primarily of methylmercury, than of the effects of ionic mercury in human beings. The toxicity was first recognized during the late 1950s and early 1960s when industrial discharge of mercury in Minamata Bay, Japan, led to widespread consumption of mercury-contaminated fish (Harada 1995). Epidemics of methylmercury poisoning also occurred in Iraq during the 1970s when

seed grain treated with a methylmercury fungicide was accidentally used to make bread (Bakir *et al.* 1973). During these epidemics, fetuses and children were found to be more sensitive to the effects of mercury than adults. But even adults showed sensory and motor neurologic dysfunction, such as paresthesia[1], visual changes, dysarthria[2], and hearing defects; ataxia[3] and paraplegia[4] were observed among adults several weeks after the acute intoxication.

Based on the events in Japan, Iraq and in the experimental data, various agencies have developed guidelines for safe exposure to mercury, including the U.S. Environmental Protection Agency (EPA; Mahaffey *et al.* 1997), the Food and Drug Administration (FDA; Federal Register 1979), the World Health Organization (WHO 1996), and the Agency for Toxic Substances and Disease Registry (ATSDR). The guidelines include an estimate of the daily human exposure to methylmercury that is likely to be without appreciable risk of adverse toxic health effects over the specified exposure duration (Table 1-1).

Table 1-1. Safety exposure guidelines.

Agency	Exposure guideline	Terminology
EPA	0.1µg / kg bodyweight/ day	RfD
ATSDR	0.3µg / kg bodyweight/ day	MRL
FDA	0.4µg / kg bodyweight/ day	ADI
WHO	3.3µg / kg bodyweight/ week	PTWI

RfD: Oral reference dose
MRL: Minimal risk levels
ADI: Acceptable daily intakes
PTWI: Provisional tolerable weekly intake. Expressed on weekly basis to emphasize that long-term exposure is important (for contaminants that accumulate in body)

It must be pointed out that the values of exposure are based mainly on methylmercury. These guidelines may be used as indicators in risk assessments. Nevertheless they do not completely rule out the possibility of intoxication. And since they are based mainly on methylmercury,

[1] abnormal sensations associated with peripheral nerve damage.
[2] impaired articulatory ability.
[3] unsteady and clumsy motion of the limbs or trunk due to a failure of the fine coordination of muscle movements.
[4] loss of movement in the lower half of the body.

they may not comply, for example, with ethylmercury because mercurial compounds differ greatly in their toxicokinetics. Comparisons between methyl- and ethylmercury poisoning showed more or less common symptoms (Bakir *et al.* 1973), although kinetic studies demonstrated severe differences: at equimolar doses given to rats differences of accumulation in body tissues were observed. Methylmercury caused widespread and ethylmercury only patchy damage in the cerebellum (Magos *et al.* 1985). In regard to renal accumulation, however, more mercury from ethylmercury was distributed and the damage was more widespread than from methylmercury treatment. The reason for this may be the faster renal accumulation and decomposition of ethylmercury (Suzuki *et al.* 1963).

A further aspect of mercury poisoning is the decomposition of mercurial compounds in the respective tissue. The clearance of mercury from body tissues follows a complicated pattern and the biological half-times differ according to the tissue and the time after exposure. Experiments with human volunteers demonstrated different average half-time for mercury clearance after inhalation of mercury vapor, e.g., lung 1.7 days, brain 21 days, kidney 64 days. It is quite evident, however, that minor portions of mercury remain in the central nervous system (WHO 1991).

In addition to the above-mentioned catastrophes, there are also several cases reported of acute mercury poisoning in humans from products containing thiomersal (organomercurial). Symptoms reported by these studies were local necrosis, acute hemolysis, disseminated intravascular coagulation, acute renal tubular necrosis, and central nervous system injury including obtundation (cognitive impairment), coma, and death (Powell 1931; Kinsella 1941; Axton 1972; Fagan 1977; Matheson 1980; Rohyans 1984; Lowell 1996; Pfab 1996).

1.3 Thiomersal

Thiomersal is also known as thimerosal, mercuriothiolate, sodium o-mercaptobenzoate or ethylmercurithiosalicylate sodium. It is chemically synthesized from ethylmercuric chloride and thiosalicylic acid (Figure 1-2) and contains 49.6% mercury by weight. The carboxylic group of thiosalicylic acid makes thiomersal water soluble and at physiological pH the compound is present as a sodium salt. The known properties of thiomersal are listed in Table 1-2.

Table 1-2. Selective properties of thiomersal (The Merck chemical databases: www.chemdat.merck.de).

Molecular formula	$C_9H_9HgNaO_2S$
Molecular weight	404.8
Appearance	White powder with faint yellow cast
Density	0.93 g·cm^3
Molar volume	435 cm^3·gmol^{-1}
Melting point	232–233°C
Water solubility	100 mg·ml^{-1} at 19°C
Free mercury ions	< 0.7%
LD 50 oral Rat	75 mg·kg^{-1}

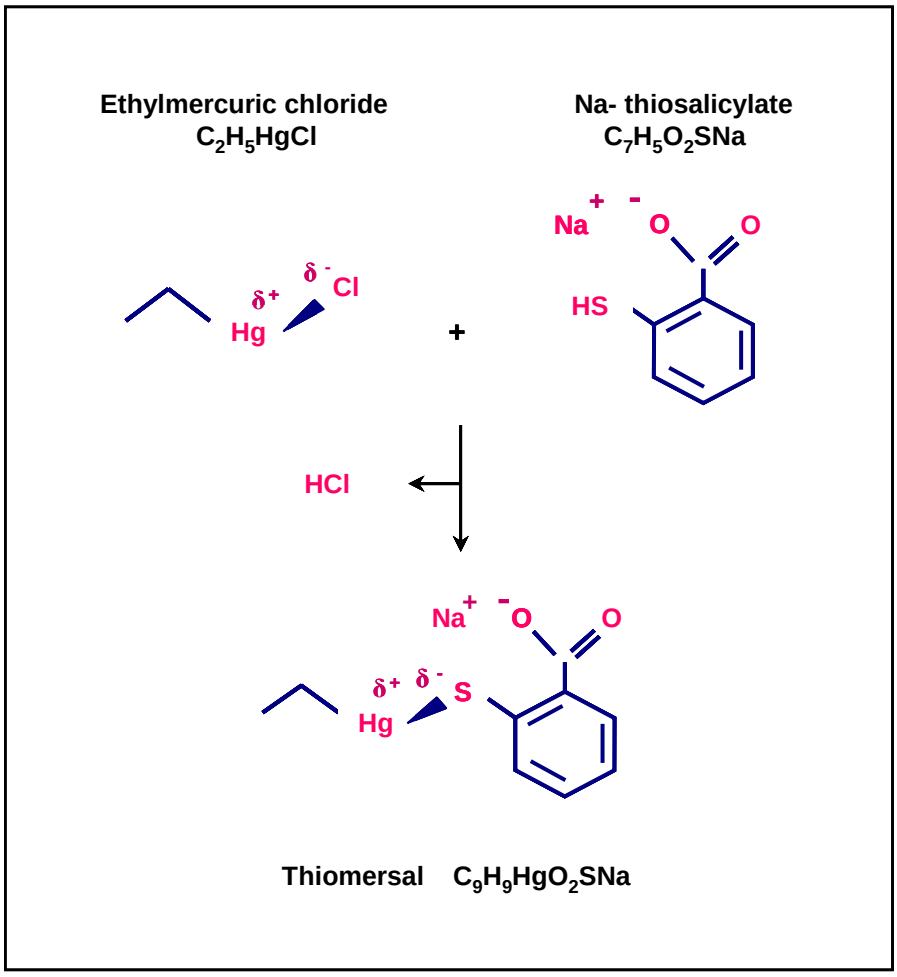

Figure 1-2. The schematic formation of thiomersal (Pirker 1993).

Thiomersal is able to penetrate cell membranes like lipid-soluble mercurial compounds; it enters the cell as a free acid, which is formed in equilibrium with the charged carboxylate form (Evans *et al.* 2000). It has been observed by many investigators that the compound responsible for the toxicity of thiomersal is ethylmercuric chloride (Pirker 1993; Wantke 1994). Just like other heavy metals, thiomersal has a high affinity to thiol groups (–SH) due to the presence of charged mercury. Mercury (II) is known to react rapidly and selectively with sulfhydryl groups, bridging vicinal pairs of cysteines and forming an intermolecular mercury-linked dimer (Arnon *et al.* 1969). Therefore, thiomersal has the ability to act as sulfhydryl reagent (Pintado *et al.* 1995; Evans *et al.* 2000). Sulfhydryl reagents, which reduce intracellular –SH levels, induce a variety of diverse physiological and pathological processes (Hecker *et al.* 1989; Song *et al.* 2000). For example, protein cysteine residues are known to be sensitive towards the cellular redox state and participate in the regulation of cellular functions. It has been shown that the redox modification of cysteine SH groups alters the function of various ion channels. Thiomersal interferes with this activation process of the channels. The harmful effect of thiomersal on cell function is mostly the inhibition of calcium-mobilization within the cells (Hatzelmann 1990; Martin 1991; Van Gorp 1997). If thiol groups are part of an enzyme's active site, the reaction between thiomersal and the sulfhydryl compound will result in inactivation of that enzyme and can cause devastating effects (Stüning *et al.* 1988). These chemical properties make thiomersal an effective antibacterial and antifungal agent.
It should be noted that a large number of studies on thiomersal toxicity were carried out on eukaryotic cells and are not conclusive for bacteria.

1.4 Thiomersal Utilization

Thiomersal is widely used as a preservative in pharmaceutical products such as ointments, contact lens cleaners, nasal sprays, but also in cosmetics (Decicco *et al.* 1982; Tosi *et al.* 1989; Wekkeli *et al.* 1990). Thiomersal (TH) was developed by Eli Lilly & Company in the 1920s, and it has been used since the 1930s for vaccine production and for preventing potentially life-threatening contamination with harmful bacteria, particularly in opened multidose vials (American Academy of Pediatrics 1999). Prior to its introduction in the 1930s, data from several animal species and humans were available providing evidence for its safety and effectiveness as a preservative (Powell and Jamieson 1931). It has been shown that thiomersal in concentrations of only 0.001% to 0.01% is effective in clearing a broad spectrum of pathogens. Worldwide, preservatives are routinely utilized in vaccines, to prevent

microbial growth in the event that the vaccine is accidentally contaminated, as might occur with repeated puncture of multi-dose vials. Incidences with tragic consequences in the use of multi-dose vials that did not contain a preservative served initially as the proof of this necessity (Wilson 1967). Since its introduction, thiomersal has been the subject of several studies and has a long record of safe and effective use in preventing bacterial and fungal contamination of vaccines (U.S. Pharmacopeia 2001).

Today, there is an increasing awareness of neurotoxicity, and even low levels of organomercurials are enquestioned. A vaccine containing 0.01% thiomersal as a preservative contains 50 μg of thiomersal per 0.5 ml dose or approximately 25 μg of mercury per 0.5 ml dose (American Academy of Pediatrics 1999). Because of the increased number of thiomersal containing vaccines that have been added to the infant immunization schedule, concerns about the use of thiomersal in vaccines have been raised over the past several years. According to the Center of Biologic Evaluation and Research (CBER) calculation, a 6-month old baby receiving all the vaccines on schedule (immunizations at 2, 4 and 6 months) would receive a total amount of 185.5 μg of mercury (Center of Disease Control 1999, see Table 1-3), that means, the average child would receive about 62.5 μg of mercury in one doctor's visit. This already exceeds the safety exposure level of about 0.1 to 0.4 $\mu g \cdot kg^{-1}$ body weight per day for the protection of human health (see guideline of methylmercury in Table 1-1).

Table 1-3. Thiomersal concentration in US-licensed vaccines and number of recommended immunizations.

Vaccine	% Thiomersal concentration	Mercury $\mu g \cdot 0.5\ ml^{-1}$	Immunization
DTaP	0.1	25	3x
Hib	0.1	25	3x
Hepatitis B	0.05	12.5	3x
Influenza*	0.05	12.5	1x

*Selective population receives one Influenza immunization.
DTaP: Diphtheria, tetanus, and pertussis vaccine
Hib: *Haemophilus influenzae* type b vaccine

By now, identified risks of thiomersal on adults at low doses are limited to hypersensitivity reactions (Cox *et al.* 1988; Grabenstein 1996; Kondler-Budde 1999; Magos 2001; Pirker *et al.*

1993). A commonly drawn parallel to the toxicity of methylmercury (WHO 2000) contains severe shortcomings, as thiomersal is a derivative of ethylmercury. Methyl- and ethylmercury are different chemical entities with different toxicity (see section 1.2). Even different toxicological effects are to be expected for thiomersal (Magos *et al.* 1985). Several gaps in the knowledge of the toxicity of thiomersal result in difficulties to evaluate the risk to cost ratio in vaccines. In fact, aforesaid studies refer solely to adults. However, with regard to children, the toxicokinetics look very different.

Consequently, the American Academy of Pediatrics demands thiomersal-free vaccines (AAP 1999). Therefore, a change in preservation practice seems to be inevitable and vaccine manufacturers are coerced into reducing and eliminating thiomersal from vaccines.

1.5 Treatment of Mercury Contaminated Wastewater

In the history of vaccine production, large quantities of wastewater containing thiomersal resulting from these processes accumulated. Up to the present, no remediation technology is available. The wastewater is delivered to municipal wastewater treatment plants and sludge containing the mercury is deposited or applied to agri- and silvicultural land.

Incineration of mercury and its compounds is not recommended as a disposal method, as it generates an increase of elementary mercury in the atmosphere. The only environmentally compatible approach implies the recycling of mercury-containing compounds. There are several methods for the treatment of mercury contaminated wastewater based on chemical, physical or biological processes. Chemical treatment, such as adsorption, chemical coagulation or precipitation is employed at many municipal treatment plants. These methods require costly downstream processes and generate hazardous by-products and residual sludge, thus creating secondary pollution (HCET Final Report 2000). An alternative, efficient and cost-effective remediation process for mercury contaminated wastewater is the application of specific bacteria. Recent studies have demonstrated an effective microbiological cleanup technology for the remediation of ionic mercury in wastewater from chloralkali industries (Wagner-Döbler *et al*. 2000; von Canstein *et al.* 1999; von Canstein *et al*. 2001).

Similar remediation of thiomersal containing pharmaceutical wastewater is hindered by the presence of a large number of complex chemical compounds. These compounds are usually present in high concentrations and because of their toxicity and complex structure, are hard to biodegrade. Often these compounds act as inhibitors of biological processes. For the degradation of complex organic compounds by bacteria in a bioreactor long-term adaptation

of microorganisms would seem to be necessary. However, adaptation would demand long retention times in the reactor (or treatment plant), which would require greater reactor volumes as well as initial investment. In spite of the long retention time in the reactors, wash out of microorganisms could still occur and reduce transformation activity.

Moreover, thiomersal is broken down to metallic mercury which is biologically methylated in the sludge. Methylated mercury and further transformation products are similarly toxic as thiomersal, which calls for new remediation strategies to be developed.

An innovative and promising system for the treatment of wastewater including toxic substances is the ion exchange membrane bioreactor (Fonseca *et al*. 2000; Velizarov *et al*. 2001). This type of bioreactor excludes direct contact of the microbial culture with the toxic wastewater. An ion exchange membrane is used as a selective barrier between the water stream and the biological compartment (Figure 1-3).

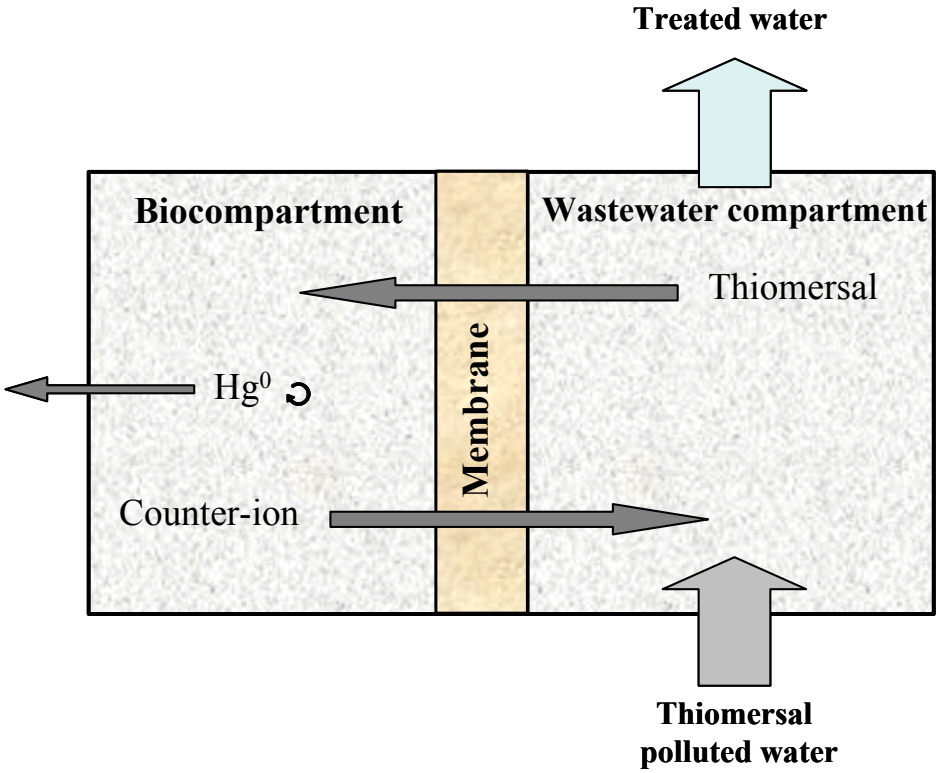

Figure 1-3. Schematic diagram of the ion-exchange membrane bioreactor.

In the presence of a suitable counter ion added to the biological compartment, the membrane should facilitate selectively the flux of thiomersal to the biocompartment, where it undergoes bioreduction. In this system, the microbial culture is completely isolated from the pollutant stream and can be optimized for the desired reaction. Even slow growing microorganisms can be efficiently enriched. Especially, the biological breakdown of organic compounds is often

carried out by bacteria having long generation times. Moreover, contamination of the treated effluent by bacteria can be avoided by this structural separation which would also allow the safe use of genetically engineered microorganisms (GEMs). The ion exchange membrane reactor would permit not only a continuous flow of thiomersal into the biological compartment but also the rate of the thiomersal transfer is adjustable and can be specifically regulated by the concentration of the counter ion. It should be emphasized that this system could be used for the treatment of wastewater containing very high concentrations of thiomersal.

1.6 Basic Principles of Biological Mercury Decontamination

Biological decontamination is defined as the process of removing or neutralizing a surface hazard through organisms such as bacteria, fungi and plants. As a response to toxic mercurial compounds that are globally distributed by geological and anthropogenic activities, microorganisms have developed a resistance mechanism to overcome the toxic environment. As aforementioned, bacteria play a major role in the natural global environmental cycle of mercury. The mercury resistant bacteria and their role in mercury detoxification have been extensively studied.

1.6.1 Mechanism of Microbial Resistance to Mercury

Microbial resistance towards mercury is based on the reduction of mercurial compounds to metallic mercury (Hg^0). Due to its properties (hydrophobic and volatile), Hg^0 can escape from the bacterial cell and leave it unharmed. This capability to detoxify mercury is an ancient and widely spread mechanism (Osborn *et al.* 1997). Two main types of mercury resistance have been described. The narrow spectrum type confers resistance to inorganic mercurial compounds only, with a minimum set of genes. More interesting for this study, however, is the broad spectrum resistance type. It confers resistance to both, inorganic and organic mercurial compounds. The genes encoding the detoxification pathway are frequently organized in regulated *mer* operons with some variations in structure (Misra 1992; Silver & Phung 1996). Several studies have shown that bacterial *mer* operons are often located on plasmids, but some have also been found on chromosomes, often as components of transposons (Wang *et al.* 1989; Rasmussen *et al*. 1998, Smit *et al.* 1998; Liebert *et al.* 1999;

Kholodii *et al.* 2000; Iohara *et al.* 2001). The bacterial resistance consists of at least three major components, with the essential genes[5] being arranged (Figure 1-4):

1. **The mercury ion (Hg^{2+}) uptake system** encoded by the transport protein genes *mer*P and *mer*T. The mechanism involves the binding of Hg^{2+} by a pair of cysteine residues on the merP protein, a periplasmatic protein, which delivers Hg^{2+} to the *mer*T transport system (integral membrane protein) and finally transfers the mercury ion into the cell cytoplasm.

2. **Enzymatic reduction** of mercury ion encoded by the mercury reductase gene, *mer*A. This reductase is a flavoprotein, which catalyzes the NADPH-dependent reduction of Hg^{2+} to Hg^{0}. The metallic mercury is then released into the cytoplasm and volatilizes passively out of cell due to its high vapor pressure.

3. **The regulatory functions** consist of regulatory genes encoded by *mer*R and *mer*D. The MerR protein promotes expression of the *mer* genes in the presence of mercury and auto regulates its own synthesis (O'Halloran *et al.* 1987; Ralston *et al.* 1990; Silver *et al.* 1989). It is transcribed separately and divergently from the structural *mer* genes. The most distal promoter gene, *mer*D, which is co-transcribed with the structural genes, down-regulates the *mer* operon. As a secondary regulator protein, the *mer*D product also binds the same operator-promoter region as the *mer*R product, although very weakly (Nucifora *et al.* 1990; Mukhopadhyay *et al.* 1992).

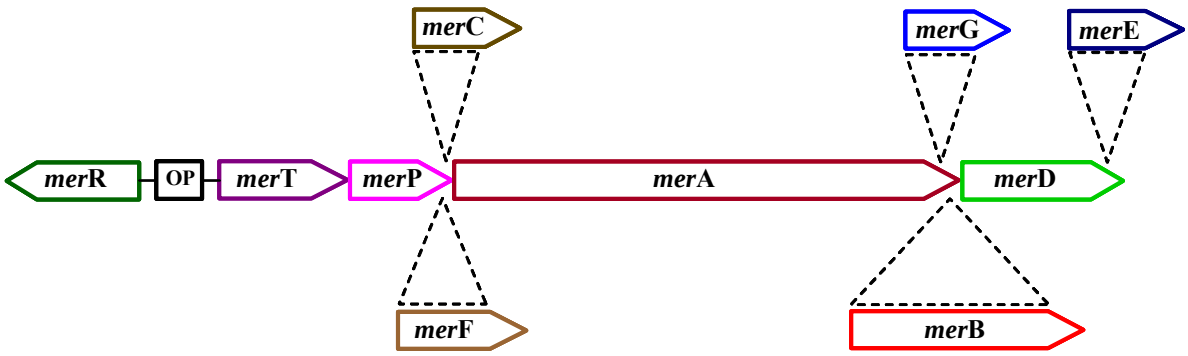

Figure 1-4. Schematic structure of mercury resistance in gram-negative bacteria. The orientation of the genes indicates the direction of transcription. OP: operator/ promoter region. *mer*: mercury resistance gene.

[5] Essential genes are defined as those genes which are found in all gram-negative mercury resistance bacteria. In contrast, accessory genes (*mer*B, *mer*C, *mer*F, *mer*G and *mer*E) are found in some but not in all examples of the *mer* operon.

The organomercurial resistance results from the presence of the *mer*B gene, which is coding for the organomercurial lyase. This accessory protein catalyses the cleavage of covalent carbon-mercury bonds (C-Hg) resulting in Hg^{2+} production (Begley 1986; Kiyono 1995).
The structure of the *mer* operons found in many gram-negative bacteria (Figure 1-4) is rather different from those of gram-positive bacteria (Huang 1999; Bogdanova *et al.* 2001;Mindlin *et al.* 2001; Narita *et al.* 2002). Nevertheless, the overall resistance mechanism remains the same both in gram-positive and gram-negative bacteria. In addition to essential genes (*mer*RTPAD) some operons encompass the inner membrane protein *mer*C or *mer*F, which have been suggested to encode mercury transport proteins (Hamlett *et al.* 1992; Wilson *et al.* 2000). However, these genes are not essential for Hg^{2+} resistance and mutating *mer*C had no effect on resistance, although it decreases the level of expression (Sahlman *et al.* 1997; Wilson *et al.* 2000). Further *mer* genes, such as *mer*G and *mer*E have recently been described (Kiyono 1999; Liebert 1999), however, their functions have not been thoroughly studied. Kiyono (1999) suggested that the *mer*G protein is located in the periplasm, where it is involved in phenylmercury resistance.

1.6.2 The Role of the *mer*B Gene

For the detoxification of organomercurial compounds, and therefore for the survival of bacteria in an environment contaminated with organic mercury, the *mer*B product (organomercurial lyase) is absolutely essential.
In gram-negative bacteria *mer*B occurs in a variety position within the operon. But in general, the additional *mer*B gene is often found immediately downstream of the *mer*A gene and without regulation of its own (see Figure 1-4).
Exceptionally, in the case of the *Pseudomona stutzeri* plasmid pPB, two functional *mer* operons were detected, one conferring narrow-spectrum and the other broad-spectrum resistance. In the broad-spectrum resistance operon of plasmid pPB, *mer*B was mapped downstream of *mer*R, together with an extra operator-promoter region. This gene structure has been unreported for any other *mer* operon (Reniero *et al.* 1998). Also, the predicted primary structure of the *mer*B protein of plasmid pPB has no similarity to that of other gram-negative *mer*B protein structures (Figure 1-5).
In general, the amino acid sequences of known *mer*B genes isolated from different microorganisms are rather dissimilar. Similarities are barely between 5-73%. The only exception is found to be in the central part of the protein (Figure 1-6). There are three

conserved cysteines (C96, C117 and C159) that play an active role in the cleavage of the C-Hg bond (pDU1358 MerB numbering). Furthermore, all organomercurial lyases have one or more additional cysteines (Misra 1992), the functions of which have not been elucidated so far.

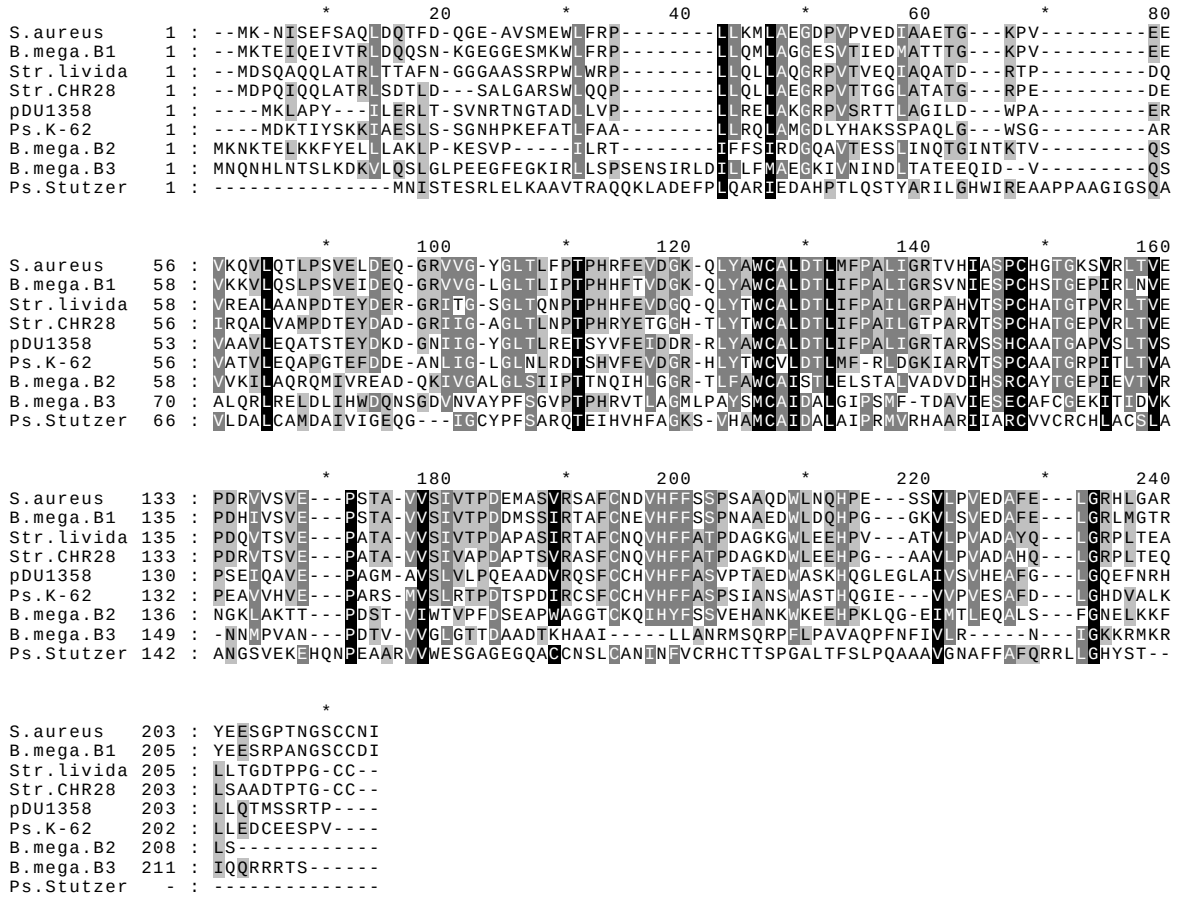

Figure 1-5. Amino acid sequences of the *mer*B proteins. Sequences from selected gram negative and gram positive microorganisms are shown. Black shade: 100%; Grey: 80%; Light gray 60%. B. mega = *Bacillus megaterium*; B1, B2 and B3 are different organomercurial lyase regions (merB1-3). Str. CHR28 = *Streptomyces sp.* CHR28; Str. livida = *Streptomyces lividans*; Str. aureus = *Staphylococcus aureus* ; Ps.K-62 = *Pseudomonas sp.* K-62 pMR26; Ps. stutzeri = *Ps. stutzeri* plasmid pPB; pDU1358 = *Serratia marcescens* plasmid pDU1358.

The function of the organomercurial lyase has been identified and thoroughly studied by Begley *et al*. 1986. A simple model of the organomercurial lyase reaction is shown in Figure 1-6. The cleavage reaction was found to work by an S_E2 reaction mechanism (bimolecular electrophilic substitution). Generally, electrophilic substitution occurs in two stages, namely the generation of an electrophile and the substitution. In an S_E2 reaction, the concentrations of two molecules determine the rate of the reaction.

The lyase catalyzes the protonolysis of the carbon-mercury bond in which the mercurated carbon has a partial negative character and mercury gains a partial positive disposition. The protein attacks the carbon with a proton while mercury attaches to an available negatively charged ligand such as protein thiolate. Hydrocarbon is released. Finally, the exchange of Hg^{2+} with thiols in the solvent leads to free organomercurial lyase. Exogenous thiols (R-SH), usually cysteine in vitro or glutathione, are essential to exempt the enzyme from mercury ions. The authors postulated that "without these excess thiols in the buffer, the enzyme will accumulate as an inhibited enzyme-Hg^{2+}-complex"(Begley et al. 1986; Silver 1991).

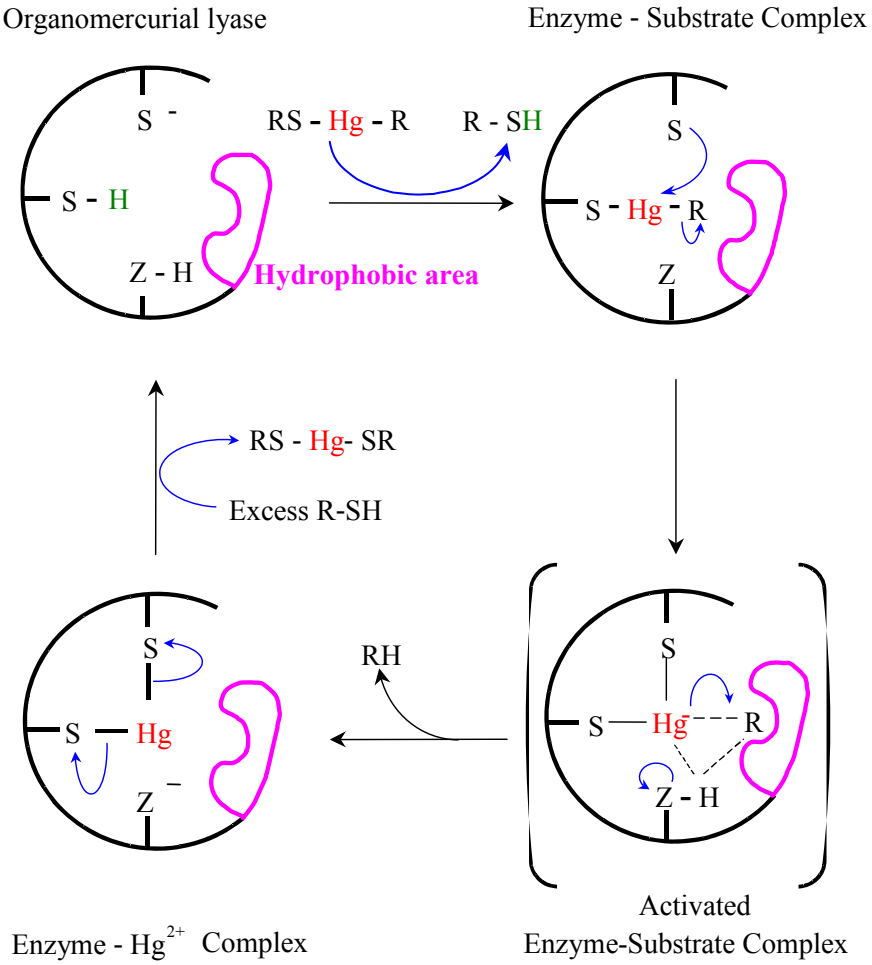

Figure 1-6. The S_E2 reaction mechanism of organomercurial lyase. The active site consists of two thiol groups (-SH), a nucleophilic group (Z), and a hydrophobic area (Begley *et al.* 1986; Silver 1991).

1.6.3 Utilization of Genetically Engineered Microorganisms

The gained knowledge about the mercurial resistance in bacteria induced research on how to utilize it to bioremediate mercury contaminated wastewater. For planned commercial products, there is often a desire to improve bacterial strains by genetic engineering techniques. Genetic engineering allows the artificial exchange of genes between genomes of very different organisms, enabling construction of gene combinations that would not be possible or take to much time to develop by traditional culturing techniques. Microorganisms created by recombinant DNA techniques are called genetically engineered microbes (GEMs). Genetic engineering techniques have been employed successfully in the chemical and pharmaceutical industry, where recombinant enzymes or drugs are produced by contained use of GEMs (e.g. tissue plasminogen activator (TPA), human insulin, human growth hormone, human serum albumin (HSA), proteins for hemophilia therapy, etc.). *Pseudomonas* strains seem to be ideal candidates for genetic engineering and applications in biotechnology, bioremediation and agriculture due to their metabolic versatility and degradative potential. Modification of *Pseudomonas* strains, including the addition of genes for enhanced and controlled bioremediation, has already been described (Ford *et al.* 1999; Ministry of Environment and Energy Denmark 2000). Especially strains of *Ps. putida*, a fluorescent, non-pathogenic bacterium, are known for their ability to degrade various toxic organic compounds and xenobiotic hydrocarbons (Vokunova *et al.* 1992; Weber *et al.* 1994; Ramos *et al.* 1995 and van Beilen *et al.* 2001). Strains of *Ps. putida* were modified by Horn *et al.* (1994) for high and constitutive expression of the mercury resistance. The aim was to construct a constitutively mercury resistant strain that would be better adapted to cope with fluctuating mercury concentrations, and especially to survive in extremely contaminated habitats owing to overexpression of the mercury resistance. For the construction of the mercury reducing GEMs, a natural plasmid (pDU1358) of *Serratia marcescens* containing only the necessary genes (*mer*TPAB) was integrated into the *Ps. putida* KT2442 and *Ps. Putida* F1 genomes. An overexpression of the mercury detoxification was attained by random mutagenesis using a mini-Tn5 transposon vector encoding only *mer*TPAB but no regulatory genes so that the expression depended on a strong host promoter. Modification of *Ps. putida* F1, a naturally occurring soil isolate harboring a chromosomally encoded pathway for the catabolism of benzene, provided the opportunity to detoxify also aromatic organomercurials (e.g. phenylmercury acetate).

In previous studies, it has been demonstrated that the constructed microorganisms have a very high and stable activity of detoxifying enzymes and were able to degrade phenylmercury

acetate (PMA) as well as ionic mercury (Brunke *et al.* 1993). Due to these biological properties the GEMs are ideal candidates for thiomersal detoxification and bioremediation.

1.7 Aim of the Work

The investigations on thiomersal as mentioned above have been mainly focused on medical effects and applications of thiomersal. Since the 1930s the pharmaceutical industry has used thiomersal to prevent bacteria and other organisms from contaminating vaccines. Thus, the wastewater resulting from vaccine production processes have been highly polluted with thiomersal. Surprisingly, demands for technological innovations for removing and treating thiomersal contamination have never been strongly expressed. The wastewater is simply disposed of at waste disposal sites. The aim of this work is to investigate the potential of treatment of wastewater contaminated with thiomersal in a biological way.

Engineered and environmental isolates have already been successfully applied to remove (ionic) mercury from Chloralkali wastewaters (von Canstein *et al.* 1999; Wagner-Döbler *et al*. 2000; von Canstein *et al*. 2001), a relatively simple and cost effective technology. Up to the present, there is no description of successful treatment of thiomersal containing pharmaceutical wastewaters by biological means due to the toxic and persistent byproducts and additives in the solution.

Selective extraction of thiomersal from wastewater by an ion exchange membrane and its subsequent degradation by microorganisms could present an effective solution. This technology would provide a complete partition of microbial compartment and wastewater. Consequently, the use of GEMs would in principle be possible without the risk of unintentional release. Bacterial culture conditions (pH, salinity, temperature, nutrition etc.) can be optimized. The transfer rate of thiomersal to the microbial compartment can be adjusted for optimal microbial transformation rates. These outstanding perspectives formed the basis for the investigation of this treatment technology for thiomersal containing pharmaceutical wastewater. The overall objective of this work is divided into four stages:

1st Stage: Microorganisms

- Selection of thiomersal degrading bacteria, such as environmental isolates and GEMs.
- Study the kinetics of thiomersal biodegradation and decomposition products using wild-type bacteria and GEMs.

- Determination of the efficacy of genetically engineered microorganisms for thiomersal degradation and comparison to wild-type bacteria.
- Determination of the thiomersal resistance level and bacterial growth inhibition, defined as the ratio of growth rates of thiomersal treated cultures versus untreated controls.
- Optimization of growth and transformation conditions by varying pH, temperature and density.

2nd Stage: Selection of counter ion for ion exchange membrane reactor

- Search for a suitable counter ion, which is added to the biological compartment to facilitate the flux of thiomersal. The elected counter ion has to be biologically inert - the applied microorganisms should not metabolize the ion.

3rd Stage: Optimization of the detoxification processes

- Application of the microorganisms (environmental isolates and GEMs) in a bioreactor for degradation of thiomersal.
- Optimization of the conditions in the bioreactor with respect to nutrient and thiomersal flow rate, as well as determination of the stability and robustness of the process.

4th Stage: Genetic analysis

- Elucidation of the genetic structure of the mercury resistance operon of the thiomersal detoxifying isolates with special attention to the *mer*B gene and comparison between the *mer* operon of the different microorganisms with regard to their thiomersal degradation capability.

Due to the legitimate complaint about thiomersal toxicity, changes in thiomersal utilization seem to be inevitable. However, the elimination of thiomersal creates several problems. The main problem is to find an alternative preservative but also new vaccine-production technology. Several local producers (e.g. 60% of DTaP[6] manufacturers), especially in some developing countries, would not have the potential to change processes to thiomersal free preservatives (WHO 2000). Thus, thiomersal contaminated wastewater will remain to be a result of vaccine production; and technological studies have to be conducted to assess the feasibility of the treatment of pharmaceutical wastewater containing thiomersal.

[6]Diphtheria, tetanus, and pertussis vaccine

2 Materials and Methods

2.1 Chemicals and Reagents

Chemicals used in this study were obtained from Merck (Darmstadt, Germany), Sigma-Aldrich (Munich, Germany), Amersham Pharmacia Biotech AB (Uppsala, Sweden), BIO-RAD GmbH, (Munich, Germany), Difco Laboratories (Detroit, USA) and Fluka Chemie AG (Neu-Ulm, Germany). For chemical and biochemical analysis the reagents were of highest grade. Acetone and methanol were of the pure grade "for residue analyses" and purchased from J. T. Baker (Deventer, Holland). Oligonucleotide primers were obtained desalted from Invitrogen - life Technologies (Karlsruhe, Germany), and used without further purification. Reagents for genetic procedures were purchased from Qiagen (Hilden, Germany), New England Biolabs (Frankfurt-Höchst, Germany), Boehringer Mannheim (now Roche-Germany), Promega (Mannheim, Germany) and Sigma (Munich, Germany).

2.1.1 Preparation of Standard Solution

Stock standard solutions were prepared by solving each analytical reference chemical with an appropriate solvent (e.g. ultrapure water, distilled water, buffer or organic solvent) in glass flasks to get a concentration of 1 $g \cdot l^{-1}$. To avoid chemical changes these stock standard solutions were stored for a maximum of 7 days in the refrigerator at 6°C.

Thiomersal stock solution with concentration of 1 $g \cdot l^{-1}$ was prepared by solving 1g ± 0.10 mg reference chemical in deionized water. These stock standard solutions were stored at - 6 °C for 7 days. Working standard solutions were freshly prepared by diluting the stock standard solutions and were used for calibrations and experiments.

All experiments with mercurial compounds were carried out in glass ware to decrease the interaction of the solvents with container material. To prevent a concentration loss of mercury by surface adsorption, glass ware was thoroughly washed, soaked for at least 72 h in 3% HCl and rinsed with distilled deionized water before use. To counteract light-accelerated degradation of thiomersal, the glass ware was coated with aluminum foil or amber glass was used. Working standard solutions were freshly prepared by diluting the stock standard solutions.

2.2 Analytical Methods for Mercury Detection

The analysis of metals in biological and environmental samples is complicated due to different organic and inorganic forms of the metal that may be present. For mercury, this complication is usually overcome by reducing all the mercury in the sample to its elemental state prior to analysis. Furthermore, mercury is relatively volatile and, therefore, easily lost during sample preparation and analysis. In spite of these complications, several methods have been developed for determining trace amounts of mercury in biological and environmental samples, even in complex media. These include atomic absorption spectrometry (AAS), atomic fluorescence spectrometry (AFS), neutron activation analysis (NAA), inductively coupled plasma-mass spectrometry (ICP), gas chromatography (GC), GC/microwave-induced plasma atomic emission detection (MPD), high performance liquid chromatography (HPLC)/UV, HPLC/ECD, and spectrophotometry. In most methods, mercury in the sample is reduced to the elemental state. Some determinations require predigestion of the sample prior to reduction. The application of each detection method depends on the nature of the sample. Cold-vapor atomic absorption spectrometry (CVAAS) is the primary method that is used to determine mercury in biological materials and environmental samples (Friese *et al.* 1990, Vesterberg 1991). Total mercury is typically determined using CVAAS after complete conversion of all mercury to the volatile elemental form using harsh (nitric acid / perchloric acid, bromate / bromide) digestions followed by reduction of ionic mercury to the elemental form. Inorganic mercury can be determined after milder digestions (HCl, sulfuric acid) and reduction.

2.2.1 Cold-Vapor Atomic Absorption Spectrometry

Cold-vapor atomic absorption spectrometry (CVAAS) is one of the best methods available for analysis of total mercury in any matrix and can be used for a great variety of conditions (Ngim *et al.* 1988, Baxter and Frech 1990, Friese *et al.*1990, Vesterberg 1991, Akagi *et al.* 1995). The flow injection CVAAS methods are characterized by high efficiency, low sample volume and reagent consumption. Moreover, using CVAAS, concentrations in the Sub-ng$\cdot g^{-1}$ (ppb) to pg$\cdot g^{-1}$ (ppt) range can be reliably measured and both direct reduction of sample (Ngim *et al.* 1988, Friese *et al.* 1990) and predigestion followed by reduction (Vermeir *et al.* 1988, 1989, Oskarsson *et al.* 1996) produce good accuracy and precision.

A 2100 Perkin-Elmer flameless cold-vapor absorption spectrometer with flow injection system (model FIAS 200, Perkin-Elmer, Überlingen, Germany), mercury hollow-cathode

lamp as radiation source and a quartz cell (160 mm length, 7 mm i.d. with quartz window) was used. The mercury resonance line was set at 253.7 nm and a slit width of 0.7 for mercury measurements, the mercury hollow-cathode lamp operated at 6 mA intensity.

The use of flow injection system (FIAS) coupled to CVAAS allows easy detection of all mercurial compounds. This system allows automation of oxidation of organomercurial prior to total mercury determination. It is necessary to use an oxidation step to convert all organomercurials into inorganic mercurial compounds prior to reduction to elemental mercury (Hanna *et al.* 1993). Sample preparation for total mercury analysis usually begins with an acid digestion (Baxter *et al*. 1990).

For total mercury measurement all chemicals used were of analytical-reagent grade. Ultrapure water from the Milli-Q system was used throughout. Potassium peroxodisulphate ($K_2S_2O_8$, 4%) as oxidizing agent was stirred and heated gently in water until dissolved completely. Potassium permanganate ($KMNO_4$, 5%), sulphuric acid (H_2SO_4, 96%), nitric acid (HNO_3, 65%) and hydroxylammoniumchloride ($K_2S_2O_8$, 10%) were used for the digestion of samples. For calibration, mercury standard solutions were prepared from a mercury nitrate stock standard solution (1000 $mg \cdot l^{-1}$, Merck) just before use by appropriately diluting the stock standard solution with hydrochloric acid (3%).

For determination of total mercury, samples of 1 ml were oxidized with 150 µl of $KMNO_4$, 10 µl H_2SO_4 and 10 µl of HNO_3. After 2 min, 100 µl $K_2S_2O_8$ was added and mixed. Then, samples were incubated by room temperature for at least 10 min and supplemented with 230 µl H_3NOHCL (hydroxylammoniumchloride). The samples were shaken until the purple color disappeared, indicating complete oxidation of sample carbon. Subsequently, the samples were injected and ionic mercury was reduced with NaBH4 (4 $g \cdot l^{-1}$) to metallic mercury, which was volatilized by the carrier gas argon into a quartz cell and detected at 253.7 nm by the CVAAS.

To analyze the standards by CVAAS for instrument calibration the guidelines specified by the instrument manufacturer was followed. For construction of a calibration curve the peak area of the standards was plotted versus mercury concentrations. The R^2 for the calibration curve was at least 0.995 or better. If the curve did not had an R^2 value equal to or better than 0.995 then the curve was rerun. If the curve still did not meet this criterion then new standards were prepared and the instrument recalibrated. All calibration points contained in the curve were within 10% of the calibration value when the calibration curve was applied to the calibration standards (see Figure D-32 in Appendix).

For the measurement accuracy, an independently prepared standard (concentrations between 0.1-100 $mg \cdot l^{-1}$) was analyzed after 20 samples. In addition, after every ten samples, a known

spike sample (standard addition) was analyzed. The measured mercury content of the spiked samples had to be within 10 % of the expected value.

2.2.2 High Performance Liquid Chromatography (HPLC)

High performance liquid chromatography (HPLC) was used for the identification and quantification of thiomersal and its decomposition products, thiosalicylic and 2,2'-dithiosalicylic acid.

A HPLC device consists of four main components: pump, injection system, separation column and detector with a processing system. The HPLC system (2690 Waters, Milford, USA) used in this work consisted of a constant flow pump. The used column (RP-18, 250 x 4.6 mm i.d.) was packed with silica particle bound to octadecylsilane. Octadecylsilane, a common stationary phase, is non-polar and it is used in combination with a relatively polar mobile phase. For each analyte injected into the column there will be equilibrium between the stationary phase and the mobile phase. A flow rate of 0.5 $ml \cdot min^{-1}$ for the mobile phase (methanol: water; 65:35:0.9 v/v) was employed and the variable wavelength detector was set at 222 nm.

In the present investigation, the stability of thiomersal in water and phosphate buffer was examined as the distribution of the thiomersal might easily be altered. Stock solution of thiomersal (1 $g \cdot l^{-1}$) was prepared freshly with Milli-Q water and was accurately diluted with volumetric flasks to end concentrations of 1, 2.5, 5, 7 and 10 ppm thiomersal. Thiomersal solution was prepared freshly in phosphate buffer (see section 2.3.2.4) by diluting 1 $g \cdot l^{-1}$ thiomersal stock solution in phosphate buffer in concentrations of 1, 2.5, 5, 7 and 10 ppm. Thiosalicylic (Aldrich-Chemie, Steinheim, Germany) and 2.2' dithio-salicylic acid (Fulka, Buchs, Switzerland) were prepared freshly in methanol (J. T. Baker) with concentrations of 0.5, 1, 2.5, 5, 7 and 10 ppm, respectively. For deterioration experiments, the samples were sealed and stored in the dark at 4°C for 1, 3 and 7 days.

Sample volumes of 1 ml were supplemented in HPLC special glass vessels and three replicate samples were prepared for each concentration. The conversion of the peak areas to concentrations was calculated using “Millenium“-Sofware (Waters, Milford, USA). The compounds were identified over the characteristic retention time (absorption interval of 0-30 min.). The quantity of the samples was calculated and plotted on the calibration graph and consequently the degree of the decomposition could be determined.

2.3 Microbiological Methods

2.3.1 Microorganisms

Microbial strains used in this study are summarized in Table 2.1. They were maintained in standard LB growth medium supplemented with glycerol at 15% (v/v) and stored at -70ºC.
The strains has been identified by the German Culture Collection of Microorganisms and Cell Cultures (DSMZ) using partial 16S rDNA sequence analysis, physiological tests, ribotyping, and fatty acid methylester (FAME) analysis.

Table 2-1. **Bacterial strains used in this work**

Strain	Abbreviation	References
Pseudomonas putida Spi3	Spi3	von Canstein *et al.*(1999)
Pseudomonas putida Spi4	Spi4	von Canstein *et al.*(2001)
Sphingomonas sp. Spi7	Spi7	von Canstein *et al.*(2001)
Pseudomonas fulva Spi11	Spi11	von Canstein *et al.*(2002)
Pseudomonas putida Elb2	Elb2	von Canstein *et al.*(2002)
Pseudomonas stutzeri Ibu8	Ibu8	von Canstein *et al.*(2001)
Pseudomonas putida Kon12	Kon12	von Canstein *et al.*(2002
Citrobacter freundii Tin2	Tin2	von Canstein *et al.*(2001)
Citrobacter freundii Bro62	Bro62	von Canstein *et al.*(2001)
Pseudomonas aeruginosa Bro12	Bro12	von Canstein *et al.*(2002)
Pseudomonas putida KT2442::*mer*-73	KT2442	Horn *et al.* (1994)
Pseudomonas putida F1:: *mer*	F1	Horn *et al.* (1994)

2.3.2 Culture Media and Buffer Solutions

The following media were used solid or in liquid form to cultivate bacteria. All media were either autoclaved for 20 min at 121°C, 1 bar vapour pressure or sterilized through a 0.22 µm membrane filter. Carbon sources, mercury, and trace elements that could not be autoclaved were filter sterilized separately by filtration (Satorius membrane filter, 0.2 µm) and aseptically added to the medium. For solid media 1.5% (w/v) agar was added to the liquid media before autoclaving.
All media were supplemented with antibiotics or heavy metals, mainly with thiomersal to create a selective pressure and prevent contamination during cultivation.
For different purposes, different concentrations of mercury in the medium were appropriate. Luria Bertani (LB) medium binds substantial amounts of mercury (see below, Chang *et al.*

1993, Farrell *et al.* 1993), owing to SH-groups present in tryptone and yeast extract (Misra 1992). Therefore, for the same bioavailable Hg-concentration more mercury needed to be added to LB medium than to a minimal medium. Moreover, *Ps. putida* tolerates many toxic (organic) compounds to a certain extent without expressing the actual resistance enzyme. This may partially be due to alterations of the outer cell membrane, e.g. mechanisms such as *cis-trans* isomerization (Heipieper, 1996). Hence, higher thiomersal concentrations were appropriate for *Ps. putida* than e.g. for *Citrobacter freundii*.

2.3.2.1 *Luria Bertani Medium (Sambrook et al. 1989)*

Luria Bertani medium (LB) was used for breeding cells from the freezer stock to prepare them for further experiments.

Bacto-Trypton	10 g
Yeast extract	5 g
NaCl	10 g
dH_2O	1000 ml

2.3.2.2 *Inoculation Medium (von Canstein et al. 2001)*

Inoculation medium (NMS medium) was utilized in experiments for the determination of the thiomersal resistance level and bacterial growth inhibition, defined as the ratio of growth rates of thiomersal treated cultures versus untreated controls.

Yeast extract	2 g
Sucrose	4 g
NaCl	10 g
dH_2O	ad 1000 ml

2.3.2.3 *M9- Pseudomonas Minimal Medium*

In all experiments in which a well-defined medium was required, e.g. effects of thiomersal decomposition products on bacterial growth, counter-ion selection and kinetic measurements, M9 was the medium of choice.

For 1 liter minimal medium:

M9-salt Solution (10x)	100 ml
Trace Element Solution (400x)	2.5 ml
dH_2O	ad 1000 ml
adjust to pH 7.0-7.2	

M9- minimal medium is composed of three parts:

1.

M9 Salt solution (x 10)	
Na_2HPO_4	70 g
KH_2PO_4	30 g
NaCl	5 g
NH_4Cl	10 g
dH_2O	ad 1000 ml

2.

Salt Solution (x 2)	
MgO	10.75 g
$ZnSO_4$ x 7 H_2O	1.44 g
$MnSO_4$ x 4 H_2O	1.12 g
$CuSO_4$ x 5 H_2O	0.25 g
$CoSO_4$ x 7 H_2O	0.28 g
H_3BO_3 x 7 H_2O	0.06 g
37% HCl	51.3 ml
$CaCO_3$	2 g
dH_2O	ad 1000 ml

$MgSO_4$: 1 M

$FeSO_4$ x $7H_2O$: 10g/ 100ml

3.

Trace Element Solution (x 400)	
2x Salt Solution	50 ml
$MgSO_4$	25 ml
$FeSO_4$ x 7 H_2O	2.5 ml
dH_2O	ad 22.5 ml

M9 minimal medium was supplemented with 20 mM sodium acetate (Fluka Chemie, Buchs, Switzerland) as carbon sources. In order to select mercury resistant cells, thiomersal was added to media in a concentration of 1 ppm for liquid cultures and for agar plates.

2.3.2.4 *Phosphate Buffer*

Thiomersal is known to be unstable in aqueous solution, predominantly in the presence of halides (Reader *et al.* 1982, Caraballo *et al.* 1993). The decomposition products have been determined as thiosalicylic and 2,2'-dithiosalicylic acid. On this account thiomersal was dissolved in a stabilized phosphate buffer (personal recommendation by Raquel Fortunato, IBET, Portugal) at pH 7. This stock solution was stored at 6°C for 7 days in the dark. The decomposition rate of thiomersal in phosphate buffer was compared with different solutions (dH_2O and M9-medium).

Phosphate Buffer		
$K_2HPO_4*7H_2O$	0.2 mM	0.5304 g
KH_2PO_4	0.2 mM	1.0614 g
dH_2O	ad 100 ml	

2.3.3 Substrate Utilization Profiles (BIOLOG)

The Biolog GN MicroPlates™ system (Biolog Inc., Hayward, CA) is primarily designed to identify bacterial isolates, but is widely used to characterize bacterial communities from various environments (Smalla *et al.* 1998; Kent *et al.* 2002). The Biolog™ bacterial identification system has also been adapted to compare sole carbon substrate utilization profiles (SCSUP) of microorganisms. The system was used here to characterize Gram-negative strains with the Biolog GN microplates with regard to their utilization of different carbon sources and to implement the most utilized substrate in minimal medium as sole carbon source, but also for a pre-selection of counter-ion.

Biolog GN microPlates are 96 well microtitre plates that contain 95 different carbon substrates and one control well containing no carbon substrate (water). The used GN

MicroPlates, specific for Gram-negative bacteria, are dominated by amino acids (*n*=20), carbohydrates (*n*=28), and carboxylic acids (*n*=24) (Table 2-2). Utilization of a carbon source is indicated by a colorless tetrazolium redox dye being reduced to a colored formazan product. Absorbance values of the color response in each microplate well are recorded with an automated Emax Precision microplate reader (Molecular Devices, Munich, Germany) at 590 nm.

Table 2-2. Carbon Sources in BIOLOG GN MicroPlates™.

Phosphorylated chemicals	Amides	Amines	Alcohols
Glucose-1-Phosphate	Succinamic acid	Phenyl ethylamine	2,3-Butanediol
Glucose-6-Phosphate	Glucuronamide	2-Aminoethanol	Glycerol
D,L- α - Glycerol phosphate	L-Alaninamide	Putrescine	

Polymers	Brominated chemicals	Aromatic chemicals	Ester
α -Cyclodextrin	Bromosuccinic acid	Urocanic acid	Methyl Pyruvate
Dextrin		Inosine	Mono-Methyl-Succinate
Glycogen		Uridine	
Tween 40		Thymidine	
Tween 80			

Table 2-2. Carbon Sources in BIOLOG GN MicroPlates (continued).

C-sources		
Carbohydrates	**Carboxylic acids**	**Amino acids**
L-Arabinose	Acetic Acid	D-Alanine
D-Arabitol	Cis-Aconitic Acid	L-Alanine
D-Cellobiose	Citric Acid	L-Alanylglycine
i-Erythritol	Formic Acid	L-Asparagine
D-Fructose	D-Galactonic	L-Aspartic acid
L-Fucose	Acid Lactone	L-Glutamic acid
D-Galactose	D-Galacturonic Acid	Glycyl-L-aspartic acid
Gentiobiose	D-Gluconic Acid	Glycyl-L-glutamic acid
α-D-Glucose	D-Glucosaminic Acid	L-Leucine
m-Inositol	D-Glucuronic Acid	L-Ornithine
α-D-Lactose	α-Hydroxy Butyric Acid	L-Phenylalanine
Lactulose	β-Hydroxy Butyric Acid	L-Proline
Maltose	γ-Hydroxy Butyric Acid	L-Pyroglutamic acid
D-Mannitol	p-Hydroxy Phenylacetic acid	D-Serine
D-Mannose	Itaconic acid	L-Serine
D-Melibiose	α-Keto Butyric acid	L-Threonine
β -Methyl-D-glucoside	α-Keto Glutaric acid	D,L-Carnitine
D-Psicose	α–Keto Valeric acid	γ-Amino Butyric acid
D-Raffinose	D,L-Lactic acid	Hydroxy-L-Proline
L-Rhamnose	Malonic acid	L-Histidine
D-Sorbitol	Propionic acid	
Sucrose	Quinic acid	
D-Trehalose	D-Saccharic acid	
Turanose	Sebacic acid	
Xylitol		
Adonitol		
N-Acetyl-D-galactosamine		
N-Acetyl-D-glucosamine		

Stock cultures were subcultured on NMS agar (see section 2.3.2) for 48 hours at 30°C temperature. To prepare the inoculum, colonies were transferred with sterile cotton swabs and suspended in sterile normal saline (0.9 % NaCl). The optical density was adjusted to 0.2 (590 nm). Biolog GN microplates were inoculated with 150 µl of this suspension per reaction well with an 8-channel repeating pipettor and incubated at 30°C in the dark. The optical density (590 nm) of each well was determined immediately, after 24 h and up to 48h with Emax Precision microplate reader. The absorbance was calculated with the Microlog software. For data evaluation, set points were used, where the average well color development reached values between 0.6 and 0.7 absorption units. This was usually the case after 45 to 48 hours of incubation at 30 °C. Data were evaluated in the following ways:

Raw difference $(RD) = X - X_0$

where X is the raw value of each well and X_0 the OD_{595} of the water blank.

Average well color development (AWCD) was calculated according to Garland and Mills (1991):

$$AWCD = \sum RD / n$$

where n is the number of substrates (GN plates, n=95). Number of substrates with RD > AWCD.

2.3.4 Counter-Ion Selection

Thiomersal removal from wastewater stream via ion exchange membrane assumes the presence of a suitable counter ion in the biological compartment. The counter ion of interest must be biologically inert and microorganisms must not metabolize the ion. It should also enhance the transport of thiomersal through the membrane. Several compounds such as carboxylic acids were considered as suitable counter-ion for selection (Table 2.3).

Table 2-3. List of possible Counter-ions.

Chemicals	Formula	Molecular weight
pivalic acid (PA)	$(CH_3)_3CCOOH$	102.13
tert-butylacetate (TBA)	$(CH_3)_3COC(=O)CH_3$	116.2
2,2 dimethylbutyric acetate (DMBA)	$(CH_3)_3CH_2CCOOH$	116.16
propylphosphonic acid (PPA)	$CH_3(CH_2)_2P(=O)(OH)_2$	124.08
tert-butylphosphonic acid (TBPA)	$(CH_3)_3CP(=O)(OH)_2$	138.10
iso valeric acid (iVA)	$(CH_3)_2C_2H_3COOH$	102.13
iso buturic acid (iBA)	$(CH_3)_2CHCOOH$	88.106

The pre-selection was based on microbial growth, both on solid and liquid medium, in the presence of the above mentioned compounds at a concentration of 20 mM. Two test series were carried out. The respective compounds were offered as sole carbon sources or they were supplemented to the growth medium with an already existing carbon source (sucrose). The batch cultivation was carried out in M9-medium and the optical density was measured after 24 h and cfu was assessed after 48h.

For the final experiments, measurements of thiomersal transformation rate (see section 2.6.3) were carried out as well as growth experiments in the presence of thiomersal.

2.3.5 Biofilm Formation Assay

Biofilms are structured communities of bacterial cells enclosed in a self-produced polymeric matrix and adherent to an inert or living surface. Microorganisms undergo profound changes during their transition from free-swimming (planktonic) organisms to cells that are part of a complex (surface-attached community). These changes are reflected in the new phenotypic characteristics developed by biofilm bacteria and occur in response to a variety of environmental signals. Recent approaches to study bacterial biofilms have identified genes and regulatory circuits important for initial cell-surface interactions, biofilm formation, and the return of biofilm microorganisms to a planktonic mode of growth.

Determining the ability of biofilm formation by investigated isolates is important in evaluating control procedures within a bioreactor. With the regard to the insertion of bioreactor for thiomersal degradation, the capability of biofilm formation of 11 bacterial

strains (see Table 2-3) was determined. The experiment was carried out according to the method of O'Toole *et al.* (1999).

The experiment was carried out in glass test tubes (internal diameter 15 mm; length 18 cm; Schott Glaswerke, Mainz, Germany). Growth was started by mixing 0.5 ml of an overnight culture with 4.5 ml of fresh M9 medium with 20 M sodium acetate. After 24 h of incubation at room temperature without agitation, 250 µl of 0.1% (wt/vol) safranin O (Sigma, Munich, Germany) was added. Tubes were incubated for 10 min at room temperature and then rinsed thoroughly with water to remove unattached cells and residual dye. The dye was solubilized in 5 ml of ethanol (absolute) for 10 min, and 200 µl was transferred into 96-well polystyrene tissue culture test plates (Techno Plastic Products, Trasadingen, Switzerland). The absorbance of safranin O was measured at 490 nm in an Emax Precision microplate reader (Molecular Devices, Munich, Germany). Uninoculated medium was used to determine the background. Biofilm formation assays were done in triplicate.

2.3.6 Carbon Source Utilization

The measurement of carbon utilization of the isolates in the bioreactors was determined by the analysis of sodium acetate (CH_3COOH) using a UV-test obtained by R-Biopharm, Germany (Cat.No.: E0148261). Determination of acetic acid concentration is based on the degree of NADH formation which is measured through an increase in light absorbance at 340 nm. The conversion results from the presence of three enzymes, acetyl-CoA synthetase (ACS), citrate synthase (CS) and L-malate dehydrogenase (L-MDH).

(1) Acetate + ATP + CoA $\xrightarrow{\text{ACS}}$ acetyl-CoA + AMP + pyrophosphate

(2) Acetyl-CoA + oxaloacetate + H_2O $\xrightarrow{\text{CS}}$ citrate + CoA

(3) L-Malate + NAD^+ $\xrightarrow{\text{L-MDH}}$ oxaloacetate + NADH + H^+

To achieve sufficiently precise results, the amount of acetic acid present in the assay had to be between 0.3 µg and 15 µg, and the measured absorbance differences (ΔA) between test samples (A1 and A2) and blank (A0) had to be at least 0.100 absorbance units. The amount of formed NADH is not direct proportional to acetic acid concentration.

Therefore, it can be calculated using the following equation:

$$\Delta A_{\text{acetic acid}} = [\,(A_2\text{-}A_0)_{\text{sample}} - \frac{(A1\text{-}A0)^2_{\text{sample}}}{(A2\text{-}A0)_{\text{sample}}}\,] - [(A_2\text{-}A_0)\,\text{blank} - \frac{(A1\text{-}A0)^2_{\text{blank}}}{(A2\text{-}A0)_{\text{blank}}}\,]$$

A0 = Blank

A1= absorbance of the test sample after 3 min start

A2 = absorbance of the test sample after approximately 10 – 15 min start

The concentration of acetic acid follows from the above:

$$C = \frac{V \times M}{\varepsilon \times d \times v \times 1000} \times \Delta A\ [g \cdot ml^{-1}]$$

with

V = final volume [ml], 3.230 ml

v = sample volume [ml], 1ml

MW = molecular weight of substance to be assayed [$g \cdot mol^{-1}$], 60.05 $g \cdot mol^{-1}$

d = light path [cm], 1 cm

ε = extinction coefficient of NADH at 340 nm = 6.3 [$L * mmol^{-1} * cm^{-1}$]

The detection limits were determined based on a sample volume of 2 ml and measurement at 340 nm of an acetic acid concentration of approximate 0.1 $mg \cdot L^{-1}$ sample solution with an Ultrospec100–Photometer (Amersham Biosciences, Freiburg, Germany). For further information see instruction leaflet by R-Biopharm (www.r-biopharm.com).

2.3.7 Determination of Protein Content

Protein concentrations of bioreactor experiments were determined by the method of Bradford (Brandford, 1976), using bovine serum albumin (BSA) as a standard. The samples were diluted with H_2O to a final volume of 800 µl and mixed with 200 µl Bradford reagent (BioRad, Richmond, USA). After 8 minutes incubation at room temperature the absorbance at λ = 595 nm was measured with a spectrophotometer (Pharmacia Biotech, now Amersham Biosciences, Freiburg, Germany) and using zeroing against 800 µl H_2O plus 200 µl Bradford reagent. The determined absorbance was compared with the absorbance of a series of standard BSA dilution solutions of known concentration and the protein content deduced.

2.4 Cultivation of Microorganisms

Cultivation of bacteria can be achieved by various methods, and the choice is dependent on the type of experiment. Of the systems available there are batch, fed-batch and continuous which are the most common modes. In this study batch and continuous cultivation methods were used.

All culture flasks, in which thiomersal was supplemented, were completely wrapped with aluminium foil to prevent photochemical degradation and photochemical induction of degradation.

2.4.1 Culture Conditions

Strains from the freezer stock were firstly inoculated on LB agar plates (Difco) and incubated for 24 h at 30°C. The fresh cells were then cultivated in a suitable medium (see above) and shaken on a rotary shaker overnight for 14–18 h at 180–220 rpm and 30°C. Generally, M9 medium was supplemented with 20 mM sodium acetate as carbon source. The cultures were subcultured in Erlenmeyer flasks in the same medium and the culture volume never exceeded 20% of the total flask volume.

The batch cultivation was oriented at optimizing parameters relevant to achieve high thiomersal transformation rates. The experiments were carried out in 250 ml Erlenmeyer flasks with 50 ml liquid culture and were incubated at 30 °C with rotary shaking at 180 rpm.

To maintain the conditions at an optimal level to extend the length of maximum growth and achieve high thiomersal transformation rates, isolates were cultivated continuously (see also

2.6.6). This is possible by feeding the bacteria continuously in a fermentor. For medium withdrawn at the same flow rate fresh medium is added and the consequence is the continuous production of cells. Using such a system offers several advantages (control of pH, redox, nutrient, etc.) over batch cultivation for interpretation of the results because of the prevailing steady state. However, disadvantages occur, such as time delay due to a contamination of the fermentor or genetic instability of microorganisms.

2.4.2 Growth Measurements

2.4.2.1 *Determination of Cell Number in Liquid Medium*

For the determination of cell number the liquid culture was diluted with 0.9 % NaCl so that colony numbers on solid medium (petri dish, ∅ 16 cm) could suitably be counted (between 30 and 300 colonies per plate). Serial dilutions (10^3, 10^4 and 10^5) of the liquid culture were prepared, of which three successive dilutions were plated in triplicates to validate the results. The results represented the average from triplicate plating.

For the adjustment of the cell number, a correlation curve was constructed by recording the optical density at 600 nm versus cell number by counting cfu on NMS medium plates. Before each experiment, the cell density of the bacteria was determined by optical density. The samples were diluted with isotonic saline solution (0.9%) in such a manner that the absorbance met the desired extension (considering the correlation curve). To control the diluted sample, aliquots were plated on NMS mediums and were counted after 48h of incubation.

2.4.2.2 *Optical Density*

The optical density of bacterial growth was measured at λ= 600 nm against the respective medium with Shimadzu Spectrophotometer (Shimadzu Deutschland GmbH, Duisburg, Germany) or Ultrospec100 (Amersham Biosciences, Freiburg, Germany). The samples were diluted in such a manner that the absorbance values were in the range of 0.1 to 0.6. Parallel measurements of cfu's (colony forming units) and the corresponding optical density allowed a correlation.

2.4.2.3 *Determination of Growth Phase*

To determine the growth phase of the isolates, each strain was grown in the respective medium and the optical density was measured hourly (see section above). As shown in Figure 2-1, the growth curve is divided in several phases, since the rate of growth is not constant over time, because conditions change in the batch culture mode. When the culture grows it depletes the nutrients in the flask and increases its use of oxygen begins to exceed the rate at which oxygen can be dissolved into the medium. In these cases, the growth rate slows because the culture has become nutrient-limited. To prevent oxygen limitation, batch cultures have to be shaken during the experiments.

All of this microbial activity causes a characteristic growth pattern that can be broken down into four phases: lag phase, exponential phase, stationary phase and death phase. The growth phases that were applied in the experiments are represented in diagram. Therefore, growth curves were initially determined for each isolate before main experiments were started.

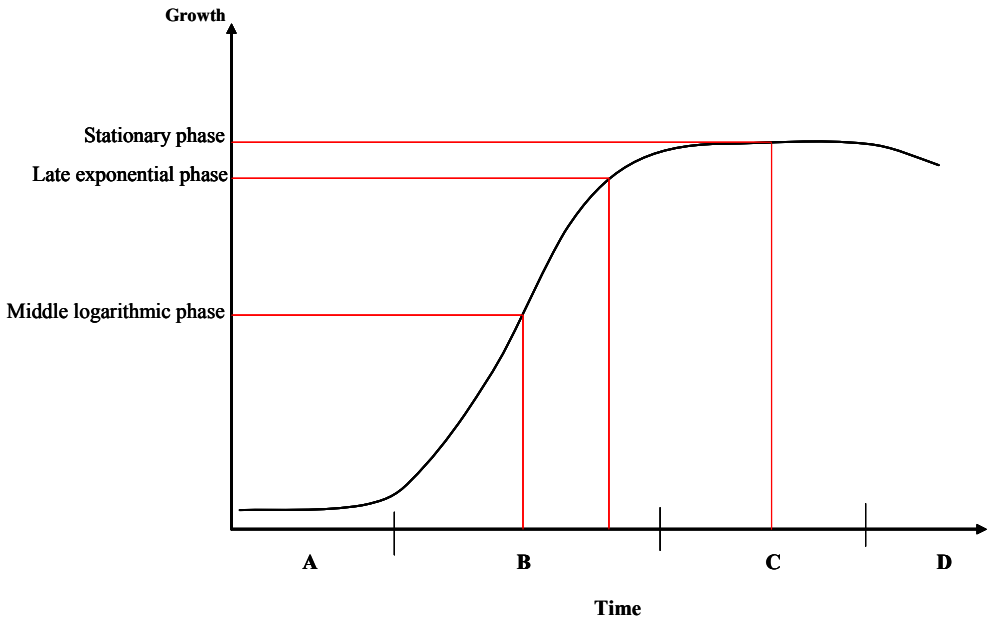

Figure 2-1. The four phases of growth. In batch culture, bacteria will proceed through four growth phases, A: lag phase, B: exponential growth phase, C: stationary phase and D: death phase. The length of time spent in each phase and the rate of growth of the isolate during exponential phase is dependent upon the species and medium conditions. Growth phases in which experiments were carried out is shown in diagram.

The lag growth phase is a stage in which bacteria often might have to adapt to the fresh medium because is different from that in which it had been growing. Enzymes may need to be synthesized to take advantage of nutrients or to better utilize the oxygen tension of the culture. The concentration of solutes may be different requiring adaptation. Adjusting to new conditions might take time and during this period of gene expression and enzyme synthesis, no or little increase in cell number is observed causing a lag in the growth of the isolate. The length of the lag phase depends upon the difference between the environment the bacterial strain found itself in before inoculation and after. If an exponentially growing culture is inoculated into an identical medium, kept at the same temperature, little or no lag will be observed. In contrast, a culture that has been growing in a rich medium and is inoculated into a minimal medium even with toxic chemicals will typically have a long lag phase while the enzymes necessary for growth and detoxification in the new environment are synthesized. Eventually all the required components for growth will be present and the cells will start to divide. Lag phase is followed by exponential growth phase which is a pattern of balanced growth wherein all the cells are dividing regularly by binary fission (see below equation 1), and are growing by geometric progression. The cells divide at a constant rate depending upon the composition of the growth medium and the conditions of incubation. The rate of exponential growth of a bacterial culture is expressed as generation time, also the doubling time of the bacterial population. Generation time is defined as the time per generation (equation 2).

Equation 1: This equation is an expression of growth by binary fission.

$$b = B \times 2^{n}$$

b = number of bacteria at the end of the time interval

B = number of bacteria at the beginning of a time interval

n = number of generations (number of times the cell population doubles during the time interval)

Equation 2: calculations of generation time

$$G = \frac{T}{n}$$

$$n = \frac{\log b - \log B}{\log 2} = \frac{\log b - \log B}{0.301}$$

$$G = \frac{T}{3.3 \log b / B}$$

When growing exponentially by binary fission, the increase in a bacterial population is by geometric progression. The generation time is the time interval required for the cells (or population) to divide. The highest rate of division is termed the maximal growth rate of the species. If conditions are not optimal, the microbe will grow more slowly, however division still occurs at an exponential rate, just not as rapidly as in the maximal growth rate. The effect of the environment on growth rate is difficult to generalize about, because each microbial species has a unique set of optimal conditions, but there are a number of factors that can affect growth. These variables include temperature, pH, solute concentration, dissolved gases, nutrients and the presence of waste products. Deviation from the ideal for a microbial strain will decrease its rate of growth.

2.5 Deoxyribonucleic Acid (DNA) Analysis

2.5.1 DNA Extraction

Total cellular genomic DNA was isolated from 1 ml of overnight cultures grown in Luria-Bertani (LB) broth at 30°C using the Nucleospin C+T Extraction Kit (Macherey-Nagel, Düren, Germany) according to manufacturer instruction. The samples were first centrifuged for 10 min at 6000 x g in an Eppendorf micro centrifuge 5415C (Eppendorf AG, Hamburg, Germany). The pellet was resuspended in the buffer T1 and supplemented with 25 µl of proteinase K stock solution, mixed by vortexing, and incubated at 56°C in a water bath. After complete lysis of the suspension (ca. 20-30 min) 200 µl of buffer 3 was added and incubated for 10 min at 70°C. Before loading in Nucleo Spin column and centrifuging, 210 µl of 98% (v/v) ethanol was added to the sample and mixed briefly. The centrifugation steps at 9000 x g and the following washing step with buffer B5 (including 96% (v/v) ethanol) were repeated twice. The flow-through was discarded every time. In the last step the column was transferred into a fresh 1.5 ml reaction tube and was supplemented with pre-heated (70°C) elution buffer BE. Finally the samples were centrifuged at 9000 x g.

2.5.2 DNA Gel Electrophoresis

The size of DNA fragments was determined by analysis on 0.8-1.5% agarose gels. The fragments moved faster if the agarose concentration was low (e.g. 0.8%) which favored the visualization of larger fragments and slower if the concentration was great (e.g. 1.5%) which favored the visualization of smaller fragments. The agarose was dissolved in 1x Tris-Acetate-EDTA (TAE)-buffer (Sambrook *et al.*, 1989) by microwave and cooled to ca. 55°C, at which it was still viscous and could be easily poured into an electrophoresis chamber (Horizontal Gel Electrophoresis Apparatus, GIBCO BRL Life Technologies, Eggenstein, Germany). After the gel had set, it was covered with 1×TAE buffer and loading dye was added to the DNA samples. DNA Ladder was loaded onto the gel. The electrophoresis was performed at 70-100 Volt/cm (BioRad, Model 200/2.0 Power Supply). The loading dye was necessary for the DNA sample to settle in the pocket, it also indicated how far the DNA fragments have been transported inside the gel by showing colored bands. After electrophoresis, the agarose gel was stained in an ethidium bromide solution (1 $\mu g \cdot ml^{-1}$ in water) for 10-15 minutes and was washed in dH_2O. DNA could be stained with ethidium bromide which intercalated with the DNA double helix and made visible with UV light (wavelength 245 nm). Gels were

illuminated with a UV Transilluminator (San Gabriel, USA, Model M-26-E) and photographed with a CCD-camera (Herolab Model 429K). Processing of the photographs was accomplished with a video printer (Mitsubishi Video Copy Processor).

TAE-Buffer (1x)	
Tris-Acetate (pH 7.5)	40 mM
EDTA (pH 8.0)	1 mM

Loading Dye	
Sucrose	40% (w/v)
Bromophenol blue	0.25% (w/v)
Xylenecyanol FF	0.25% (w/v)
EDTA (pH8.0)	0.1 M

For determination of DNA fragment length 1 kb and 2 Log DNA Ladder (New England Biolabs, Frankfurt-Höchst, Germany) were used. DNA ladders allow to estimate the mass of DNA in comparably intense samples of similar size. The approximate mass of DNA in each of the bands in the 1 kb DNA Ladder (assuming a 0.5 µg loading) and 2-Log DNA Ladder (assuming a 1 µg loading) are as follows:

2-Log DNA Ladder		1kb DNA Ladder	
Base Pairs	**DNA Mass**	**Base Pairs**	**DNA Mass**
10,002	40 ng	10,002	42 ng
8,001	40 ng	8,001	42 ng
6,001	48 ng	6,001	50 ng
5,001	40 ng	5,001	42 ng
4,001	32 ng	4,001	33 ng
3,001	**120 ng**	**3,001**	**125 ng**
2,017	40 ng	2,000	48 ng
1,517	57 ng	1,500	36 ng
1,200	45 ng	1,000	42 ng
1,000	**122 ng**	517	42 ng
900	34 ng	500	42 ng
800	31 ng		
700	27 ng		
600	23 ng		
517	**> 124 ng**		
500			
400	49 ng		
300	37 ng		
200	32 ng		
100	61 ng		

2.5.3 DNA Purification Techniques

For most molecular applications pure DNA is required as contamination may have inhibitory effects on enzymatic reactions. Hence, the removal of RNA, proteins or salts is mandatory.

2.5.3.1 *Phenol / Chloroform Extraction*

For purification of DNA from aqueous solutions phenol/chloroform extraction followed by ethanol precipitation, is commonly used. During organic extraction, protein contaminants are dissolved either in the organic phase or at the interface between organic and aqueous phase, while the nucleic acids remained in the aqueous phase. In the method presented here, phenol/chloroform/isoamyl alcohol (25:24:1) was recommended for extraction. In most cases, this mixture provides good protein denaturation and a tighter interphase between the aqueous and organic phases. Phenol used in this protocol was buffered to prevent oxidized products in the phenol from damaging the nucleic acids. Traces of the volatile chloroform disappeared if the DNA was vacuum dried (DNA Speed Vac-DNA120 SAVANT SS1, Savant Instruments, Farmingdale NY, USA).

2.5.3.2 *DNA Precipitation*

Ethanol precipitation is a convenient and rapid DNA-collecting method. The DNA sample was supplemented with 0.1 volume of 3M Sodium Acetate (pH 4.8) and 2 to 2.5 volumes of absolute ethanol. DNA was precipitated by centrifugation for 30 min at 10000 x g (Eppendorf micro centrifuge 5415C, Hamburg, Germany) and the supernatant was discarded carefully. The remaining pellet was washed with 300 µl of 70% ethanol to remove residual salt and centrifuged again for 30 min at 10000 x g. The supernatant was discarded again and the pellet dried in a vacuum evaporator (Savant DNA Speed Vac DNA A110). The pellet was resuspended appropriately in sterile dH_2O or Tris-HCl buffer. The pellet can be stored at - 20°C (Davis *et al.* 1986).

2.5.3.3 *Extraction of DNA from Agarose Gel*

Qiagen provides systems for quick and easy DNA purification for DNA between approximately 70 bp and 10 kb in size. A maximum of 10 µg can be recovered with that method. The extraction of DNA from agarose gels was also done with the help of the commercial QIAquick Gel Extraction Kit (Qiagen, Hilden, Germany). Pieces of agarose that contained the fragment of interest were excised with a lancet and incubated for 10 min at 50°C in buffer QG (3:1 of buffer to gel; v/v) to melt the agarose. The solution was transferred onto a QIAquick column and centrifuged. The column was washed with 1 gel volume of iso-propanol to increase the yield of DNA fragments <500 bp and > 4 kb. After centrifuging for 1 min at 10000 x g, the sample was supplemented with 0.5 ml buffer QG to remove all traces of agarose. The flow-through was discarded and the column was supplemented with 0.75 ml buffer PE. The sample was centrifuged twice (1 min. at 10000 x g) and the QIAquick column was placed into a clean 1.5 ml reaction tube. The DNA was eluted from the column with 15 – 30 µl 10 mM Tris-buffer (pH 8.5) or sterile H_2O by centrifugation for 1 min at 10000 x g.

2.5.3.4 *DNA Purification in Solution*

The extraction of DNA-solution (e.g. of PCR products) was done with QIAquick PCR Purification Kit (Qiagen, Hilden, Germany). The PCR sample was supplemented with buffer PB (1:5 v/v). The mixed solution was transferred to a QIAquick column, centrifuged for 30 - 60 sec and the flow-through was discarded. The column was washed with 750 µl of PE buffer and centrifuged for 1 min at 10000 x g. After removal of the flow-through and an additional

centrifugation step to remove residual traces, the QIAquick column was placed into a 1.5 ml micro centrifuge tube. The DNA was eluted from the column with 15 – 30 µl 10 mM Tris-buffer (pH 8.5) or sterile H_2O by centrifugation for 1 min at 10000 x g.

2.5.4 Polymerase Chain Reaction (PCR)

PCR is an automated in vitro method that allows rapid amplification of a DNA sequence lying between two regions of known DNA. PCR requires a thermostable polymerase (in this work Taq DNA Polymerase from Qiagen, Hilden, Germany), short DNA starting molecules (oligonucleotide primers, usually synthesized by Gibco BRL, now Invitrogen, Karlsruhe, Germany), 2.5 mM of each deoxynucleotide triphosphate (dNTP; MBI Fermentas, St. Leon-Rot, Germany), and suitable reaction conditions (e.g. the 1× Qiagen PCR Buffer contains 1.5 mM MgCl. Mg^{2+} cations are required by the polymerase). DMSO stabilizes single stranded DNA and was added up to 5% if the PCR did not yield any product. Qiagen offers a PCR enhancer (Q-solution) which increases the product yield and was sometimes added in the place of DMSO. PCR was performed in an Eppendorf Mastercycler®Personal (Hamburg, Germany). In the first PCR step the double stranded DNA is melted at 94°C (heat denaturation for 1 min). In the second step (annealing), the primers are given an opportunity to anneal with the template DNA. The optimal temperature for this step depends on the length and base composition of the specific primers. Strand synthesis occurs during the last step (extension) and is carried out at a temperature optimal for the enzyme (68°C for 4.5 min). This cycle was repeated 24-29 times, which was sufficient to produce ample DNA of at least 5 ng μl^{-1}. A final extension step of 68°C three times as long as the normal extension was appended to ensure that strand synthesis be completed for all products. The success of the PCR was verified on 0.8% agarose gel and the DNA was purified as described in section 2.5.3. The oligonucleotide primers used in this work and their annealing temperatures can be found in Table 2-5.

2.5.4.1 *Oligonucleotide Primer*

The *mer* operon region was amplified using primer pairs synthesized by Invitrogen – Life Technologies GmbH (Karlsruhe, Germany) that were designed after alignment of all available Gram negative *mer* operon sequences from the EMBL database with ClustalW (Table 2-5). Primers for the *mer*B gene were developed based on a sequence alignment of 10 *mer*B sequences from gram-negative and gram-positive bacteria.

Table 2-4. Sources of DNA sequence data for primer design and for alignments. Host strains carrying reference *mer* operon used as controls for PCR were pDU1358 and Tn501.

Designate *mer* operon type	Source of DNA sequence data	Accession no.	Plasmid	References
pDU1358	Plasmid pDU1358 from *Serratia marcescens*; *mer*RTPA	M24940[a]	pDU1358	H. Griffin (1987)
	*mer*A	Z49200[b]		H. Griffin (1987)
	*mer*ABD	M15049[c]	pHG103[d]	H. Griffin (1987)
Tn501	Plasmid pVS1 from *Pseudomonas aeruginosa*; *mer*RTPAD	Z00027	pVS1	N.L. Brown (1986)
Tn5041	*Pseudomonas sp.*; *mer*RTPCD	X98999		G.Y. Kholodii (1997)
Tn5053	*Xanthomonas sp.* W17; transposon Tn5053 DNA; *mer*RTPFADE	L40585	pMER419	G.Y. Kholodii (1993)
Plasmid pKLH2[e]	Plasmid pKLH2 from *A.calcoaceticus*; *mer*RTPCAD	AF213017	pKLH2	G.Y. Kholodii (1993)
Plasmid pKLH202	Plasmid pKLH202 from *Acinetobacter lwoffi*: *mer*RTPCAD	AJ486857	pKLH202	G.Y. Kholodii (2004)
Plasmid pMER327/419	Plasmid pMER327/419 from *Ps. fluorescens*; *mer*RTPFA	X73112	pMER327	J. Hobman (1994)
Plasmid R100[f]	pR100 from *Shigella flexneri* 222; *mer*RTPCAD	AP000342	pR100	G. Sampei (unpublished)
plasmid pPB	Plasmid pPB from *Pseudomonas stutzeri*; *mer* RTPAD	U80214	pPB	D. Reniero (1995)
	*mer*RBTPCA	U90263	pPB	D. Reniero (1998)
Plasmid pSB102	Plasmid pSB102 from *Sinorhizobium meliloti* FP2: *mer*RTPABD	NC003122	pSB102	S. Schneiker (2001)
Plasmid pMR26	Plasmid pMR26 from *Pseudomonas sp.* K-62: *mer*RTPAGB	D83080	pMR26	M. Kiyono (1997)
plasmid pRJ28	Plasmid pRJ28 from *Streptomyces sp.* CHR28: *mer*B	AF222792	pRJ28	Ravel J. (2000)
Genomic DNA	*Bacillus megaterium*: *mer*R_2B_2	AB027307	Genomic DNA	C. Huang (1999)
	merB_3	AB027306		C. Huang (1999)
Tn5084	Tn5084 from *Bacillus cereus:* *mer*B_3R_1ETPA$R_2B_2B_1$	AB066362	Genomic DNA	A. Gupta (1999)
Plasmid pI258	Plasmid pI258 from *St. aureus* merR, ORF_{234}TAB	L29436	pI258	R.A. Laddaga (1987)
Genomic DNA	*Streptomyces lividans*: *mer*B	X65467	Genomic DNA	R. Sedlmeier (1992)

[a] The end of this sequence overlaps the beginning of sequence Z49200.
[b] This sequence completes the gap in the previously incomplete *mer*A sequence of pDU1358.
[c] The beginning of this sequence overlaps the end of sequence Z49200.
[d] This subclone carries only the broad-spectrum mer locus of pDU1358.
[e] pKLH2 plasmid including aberrant mercury resistance transposon TnPKLH2
[f] Plasmid R100 is also referred to as NR1

To compensate for a possible failure of the primers to anneal to unknown *mer* genes sequences, several specific primers were used with the genomic DNA of mercury reducing strain. The following parameters were considered for primer design:
Length between 19-22 nucleotides, at least two guanine and / or cytosine molecules at the 3'end, similar melting temperatures for both primers, avoid once of palindromic and self complementary sequences. The melting points were estimated by the following equation (Rychlik *et al.*1990)

$$Tm = 4°C\ (n_G+n_C) + 2°C\ (n_A+n_T)$$

To obtain complete sequences of the respective *mer* genes, a large number of primers were used to create enough overlapping PCR products to cover the entire operon by sequence. The corresponding locations of the priming sites in the *mer* operon are depicted in Figure 2-2 and primer sequences are listed in Table 2-5.

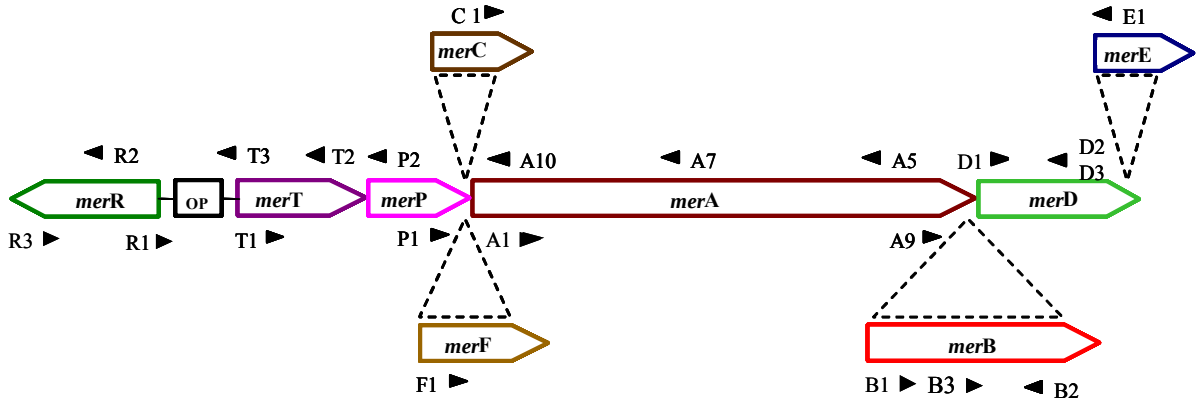

Figure 2-2. Schematic representation of the *mer* operon of gram-negative bacteria. The locations of the *mer* PCR primers and the direction of the primers are indicated by arrowheads.

Table 2-5. Primer sequences and annealing temperatures for PCR analysis of all *mer* genes. F = Forward and R = Reverse

mer primer	Direction	Nucleotide sequence [5‘ to 3‘]	Annealing Temp. [°C]	Reference
R1	R	GCC GAT TTC ACG AAT CGC A	58	Pauling (unpublished)
R2	F	ACG GAT GGT CTC CAC ATT G	58	Liebert *et al.* 1997
R3	R	ATC AGC GGG CAG GAA ACG TT	62	This study
T1	F	GCT TGG ATC GGC AAC TTG A	58	Pauling (unpublished)
T2	R	AAT CGC GCA GAC CTC ACC	58	Pauling (unpublished)
T3	R	AGC GYA TGT CTG AAC CWC AA	60	This study
P1	F	GGC TAT CCG TCC AGC GTC AA	64	Liebert *et al.* 1997
P2	R	TCT TCG GTG GCC TTG GTC A	60	Pauling (unpublished)
C1	F	TTT CYG CGA TGG GCT GCG	58	This study
A1	F	ACC ATC GGC GGC ACC TGC GT	68	Liebert *et al.* 1997
A5	R	ATC GTC AGG TAG GGG AAC AA	60	Liebert *et al.* 1997
A7	R	TTG CGC ATT GAC AGT GAC CC	62	This study
A9	F	GAA YTG ATC CAG ACG GCK G	60	This study
A10	R	TGT GTG CCG TCC AAG ATC A	58	This study
B1	F	TCG CCC CAT ATA TTT TAG AAC	58	Liebert *et al.* 1997
B2	R	CAT GTN CAY TTC TTY GCN TCTC	64	This Study
B3	F	TAY NCC TGG TGY GCN CTG GA	64	This Study
B4	R	TCS CCY TGY GMC GCM ACC GG	64	This Study
D1	F	ATG AAC GCC TAC ACS GTG TC	62	This Study
D2	R	CTG GAA GTG CAG TTG GCC	58	This Study
D3	R	GCG GAG AGT YTG CCA TGA	56	This Study
E1	R	ATC GGT TTG TGC GTC TCG GA	62	This study

2.5.5 Sequencing and Sequence Analysis

DNA sequencing was carried out by the Gatc Biotec AG (Konstanz, Germany) using ABI 3700 sequencing instruments, or PCR products were sequenced using ABI PRISM™ 377 and ABI PRISM™ 3100 Genetic Analyser (at GBF Braunschweig, Germany), as described in the protocols recommended by the manufacturer (Perkin Elmer Biosystems) for the Taq Dye Deoxy Terminator Cycle Sequencing kit. This sequencing method is based upon the dideoxy mediated chain termination method devised by Sanger *et al.* (1977). The labeling of the DNA fragments is accomplished through the incorporation of fluorescence-dye-labeled didesoxy-nucleotides, causing a termination of the DNA chain synthesis. Subsequently, the labeled DNA fragments are separated by denaturing polyacrylamide gel electrophoresis and the detection system consists of an argon laser.

The sequencing reaction was carried out in a total volume of 20 µl with approximately 75-100 ng of the purified (QiaEx or PCR purification kit, Qiagen, Hilden Germany) DNA template, 10 pmol of the sequencing primer, 6 µl of “Big Dye TerminatorTM v. 2.0 Ready

Reaction Mix" (containing the terminators, dideoxynucleotide triphosphates, $MgCl_2$, and AmpliTaq® DNA Polymerase FS). Termination fragments were produced in 30 cycles of PCR in an Eppendorf Mastercycler®Personal (Hamburg, Germany) with a pre-denaturation step at 94 °C for 1 min; 30 cycles of 94 °C for 15 sec, 56 °C for 30 s, and a final extension step at 68 °C for 4.5 min. The termination products were precipitated by addition of 10 µL 3M Na-Acetate (pH 4.8), 80 µl dH_2O and 250 µl absolute Ethanol (98 % v/v) and mixing and centrifugation for 20 - 30 min at 15000 x g. The supernatant was removed and pellets were washed by adding 300 µL 70 % (v/v) ethanol and centrifuging for 20 min at 15000 x g. After removing the supernatant, pellets were dried in a vacuum centrifuge (DNA Speed VAC-DNA 120 SAVANT SSI, Savant Instruments, Farmingdale NY, USA). Sequence evaluation and first corrections were done with Chromas Version 1.41 (Brisbane, Australia) by comparing the automatically extracted sequence and chromatograph signals. Further analysis of sequence and gene context was done case-by-case, including Blast searches (Altschul *et al.* 1997) for homologs in several sequence databases. Variants in *mer* operons were characterized by the length of the *mer*R-T, *mer*P-A, and *mer*A-D PCR amplicons. DNA samples from reference *mer* operons (Tn501, plasmid pDU1358 and plasmid pHG106 respectively) were used as positive controls in PCR to confirm that observed PCR products from natural isolates did contain *mer* genes.

DNA sequences were either aligned "directly" with ClustalX or were aligned with multiple alignment tool ClustalW at EBI (ClustalW: http://www.ebi.ac.uk/clustalw). For protein analysis nucleotide sequences were translated to amino acid sequences by using translation tool of ExPASy (ExPASy Molecular Biology Server: http://www.expasy.org) and the secondary structure elements reported were analyzed by Predict Protein at EMBL-EBI: PredictProtein (http://cubic.bioc.columbia.edu/predictprotein).

The protein sequence clustering tool ClustalX (Thompson *et al.* 1997) was used for more detailed phylogenetic analysis of protein family relationships. The phylogenetic unrooted tree shown in this study was drawn by using TreeView belonging to the Phylip package program.

2.5.6 Phylogenetic analysis

Protein sequences were aligned using ClustalX 1.83 (Thompson et al. 1997) with pairwise gap penalties of 35 for gap opening and 0.75 for gap extension, and multiple alignment penalties of 15 for gap opening and 0.3 for gap extension. Changing gap penalties will have a bearing on mismatches. Decreasing gap penalty will allow the introduction of more gaps and will thus produce fewer mismatches in the alignment, but may also result in spurious matches that do

not really reflect homology (identity by descent). Increasing gap penalties (from 10 to 35 and 0.10 to 0.75) will have the opposite effect: increasing rigor of the alignment may result in missing matches that actually do not reflect homology (Hall 2004).

DNA sequences were either aligned "directly" with ClustalX using the default gap opening penalties of 15 and gap extension penalties of 6.66 for both the pairwise and multiple alignment stages, or they were aligned, as indicated, according to the corresponding protein sequence alignment using CodonAlign 2.0 (Hall 2004).

In neither case were alignments optimized either by modifying global gap penalties or by modifying local gap penalties for selected ranges of residues. ClustalX calculates a Quality Score (Q-score) for each site in the alignment and displays those scores as a histogram below the alignment pane. The Q-scores for alignments were saved to text files and the program TuneClustalX 1.01 (Hall 2004c) was used to calculate the average Q-score as a measure of the overall quality of the alignments.

Neighbor Joining, Parsimony and Maximum Likelihood trees were estimated using PAUP*4.0b10 (SWOFFORD 2000) Bayesian trees were estimated using MrBayes 3.0b4 (Huelsenbeck and Ronquist 2001).

2.6 Determination of Hg-Effect on Microorganisms

2.6.1 Growth Inhibition by Thiomersal

Growth inhibition caused by thiomersal (TH) was measured by comparing the differences in growth between a thiomersal containing culture and a control without TH. In the first experiment thiomersal (2, 5, 10, 15, 20 ppm) was added from the beginning of the experiment when inoculums of overnight culture were inoculated into fresh NMS medium. In the second experiment cultures were grown under the same conditions but with TH added at mid-log phase (OD_{600}=0.5 - 0.8). Cell growth was monitored by measuring the turbidity (OD_{600}) of the cell suspension. The growth inhibition by thiomersal was defined as the ratio of the mercury-treated growth to growth of untreated isolates (control). To determine the degradation of thiomersal by the microorganisms the total mercury content was measured during the experiments (see section 2.2.1). Physico-chemical changes of thiomersal in NMS medium were also determined in bacteria free samples (TH control sample).

2.6.2 Mercury Resistance Level

The resistance level was determined by growth of isolates on M9 minimal medium plates with various concentrations of thiomersal (1, 2, 5, 10 ppm). Aliquots of overnight liquid cultures were serially diluted in isotonic sterile saline (0.9 % NaCl) for the determination of colony forming unit (cfu) and three dilutions were plated out on M9 minimal medium in triplicate with sodium acetate (Fluka Chemie, Buchs, Switzerland) as sole carbon source. The agar plates were incubated at 30°C for 48h. For the determination of mercury-resistant bacterial numbers, samples were spread as described above on agar plates containing 5 ppm thiomersal. The detection limit was determined at 10 cfu ml^{-1}.

2.6.3 Measurement of Thiomersal transformation rate

Kinetics of thiomersal reduction by bacteria were determined based on volatized metallic mercury (Hg^0) using CVAAS (see section 2.2.1). For measurement of Hg^0 by CVAAS, scintillation vial reaction vessels were employed with 5 ml M9 medium and various concentrations of TH (Figure 2-3). The reaction vessels were closed precisely to avoid loss of transformed Hg^0. The closed reaction vessels were incubated at 30 °C in a water bath and periodically aerated with compressed air to blow the produced Hg^0 into the CVAAS. The measurements were started with aeration of the vessels for several times (approximately 5 times) to blow out all Hg^0 abound in the medium. Subsequently, the transformation was started by injection of each culture (1 ml) into the reaction vessel and was stopped after 16 min (5 blowouts). The amount of produced metallic mercury was calculated through a calibration curve obtained by the chemical reduction of a standard mercury chloride solution (1 $g \cdot L^{-1}$ $HgNO_3$) by $SnCl_2$.

The bacterial cultures were first grown overnight at 30°C on a rotary shaker at 180 rpm. 10% of an aliquot of bacterial strain was transferred into fresh M9 medium with acetate (20 mM) as carbon source. To induce the expression of the *mer* genes, 1 ppm thiomersal was supplemented. Cell cultures were used at late exponential to early stationary phase.

It is important to distinguish if the transformation has been based on living bacteria or on the enzymes of destroyed cells. Therefore the number of living cells was determined before and after each experiment by counting the colony forming units (cfu) on NMS medium (see section 2.3.2.2). On the basis of cfu, it was possible to calculate the thiomersal transformation rate per cell.

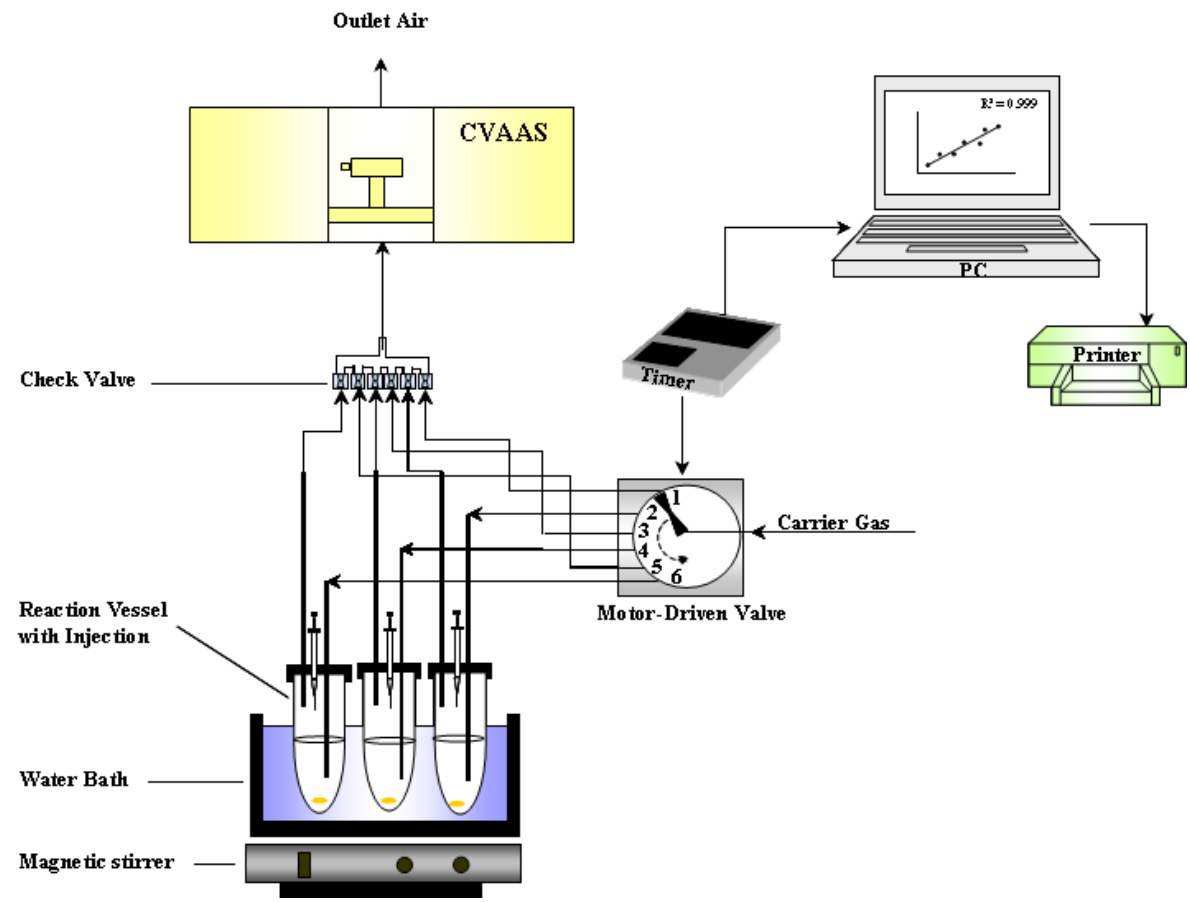

Figure 2-3. Device used for measurement of Hg(0) volatized by bacterial strain. For description see text.

For the adjustment of the cell number, a correlation curve was constructed by recording the optical density at 600 nm versus cell number by counting cfu on NMS medium plates. Before each experiment, the cell density of the bacteria was determined by optical density. The samples were diluted with isotonic saline solution (0.9%) in such a manner that the absorbance met the desired extension (considering the correlation curve). To control the diluted sample, aliquots were plated on NMS mediums and were counted after 48h of incubation.

2.6.4 Calibration of Thiomersal Transformation Measurements

Precision and accuracy of mercury determinations was assured by a calibration curve with analyzing aqueous mercury standards (Figure D-33 and D-34 in appendix). The calibration was constructed by recording the instrument response (peak area) versus the mercury standard

concentration. The calibration solution was prepared at different mercury concentrations (range of 0 to 200 ppm) by gradually dilution (in 250 ppt steps) of the mercury standard solution (c = 1,000 g·l-1 ± 0,002 g·l-1 Hg2+ Hg $(NO_3)_2$ from Merck, Darmstadt, Germany). The mercury in solution is reduced by Sn^{2+} (10% $SnCl_2$ in 1 mol-1 HCl) to form Hg^0. Before the measurements were started the closed reaction vessels were supplemented with 5 ppm distal water and 0.5 ppm $SnCl_2$ solution and were aerated with compressed air for several times (approximately 5 times) until a stable base line was reached. Subsequently, the chemical transformation was started by injection of mercury standard solution (0.5 ppm) into the reaction vessel and was stopped after 16 min (5 blowouts). The evolving elemental mercury is then aerated from the solution and the resulting vapor swept into an atomic absorption spectrophotometer. The absorption at 253.7 nm is measured and the concentration calculated from a calibration curve. The absorbency is proportional to the concentration of mercury present in a sample. The R^2 for the calibration curve should be 0.995 or better. If the curve did not had an R^2 value equal to or better than 0.995 then the curve was rerun and if the curve still did not meet this criterion then new standards were prepared and the instrument recalibrated. All calibration points contained in the curve were within 10% of the calibration value when the calibration curve was applied to the calibration standards (see Figure D-33and D-34 in Appendix).

2.6.5 Consideration of Error Propagation

Error propagation is a way of combining two or more random errors together to get a third. It can be used to combine several independent sources of random error on the same experiment or question. The error propagation is used in the measurement in question of thiomersal transformation rate per cell (see section 2.6.3), which has different random errors. The formal propagation of error approach is to compute

1. Standard deviation from the transformation measurements
2. Standard deviation from the CFU measurements

and to combine the two into a standard deviation for transformation per cell using the following approximation for products of two variables:

$$\sum sTC = 1/C \sqrt{sT^2 + T^2 / C^2 * sC^2}$$

with

sTC = estimated standard deviation of transformation rate per cell

T = transformation rate

C = cell density

sT = standard deviation of transformation measurement

sC = standard deviation of cfu determination

2.6.6 Lab-Scale Bioreactor

The degradation of thiomersal from contaminated wastewater by microorganisms could present a novel solution in bioremediation technology. Therefore, it was of interest to optimize the condition in the bioreactor with respect to nutrient and thiomersal flow, as well as to determine the stability and robustness of the process.

The Biostat MD bioreactor system (B. Braun Biotech International, Germany) shown in Figure 2-3 was furnished with an M2 culture vessel (working volume 2.0 liter). The system was equipped with automatic probes for the measurement and control of temperature, pH, foaming, and dissolved oxygen tension (DOT). Two 6-blade Rushton turbines were used for mixing. Air was added below the medium surface through a ring sparger. The culture vessel was placed on a balance (Sartorius AG, Göttingen, Germany). Feed and harvest pumps used were of type 101U/R and 505 U/RL from Watson Marlow, UK. DOT probes were calibrated with air and nitrogen gas (purity 99.5%).

Gas flows out of the Biostat MD bioreactor were channeled through a glass flask containing Potassium permanganate (5%), sulphuric acid (96%) and nitric acid (65%) to determine the amount of volatized mercury. The mercury concentration was controlled and measured with CVAAS (2100 Perkin-Elmer, Überlingen, Germany). The pH of the medium was controlled with 3 M NaOH and 3 M HCl.

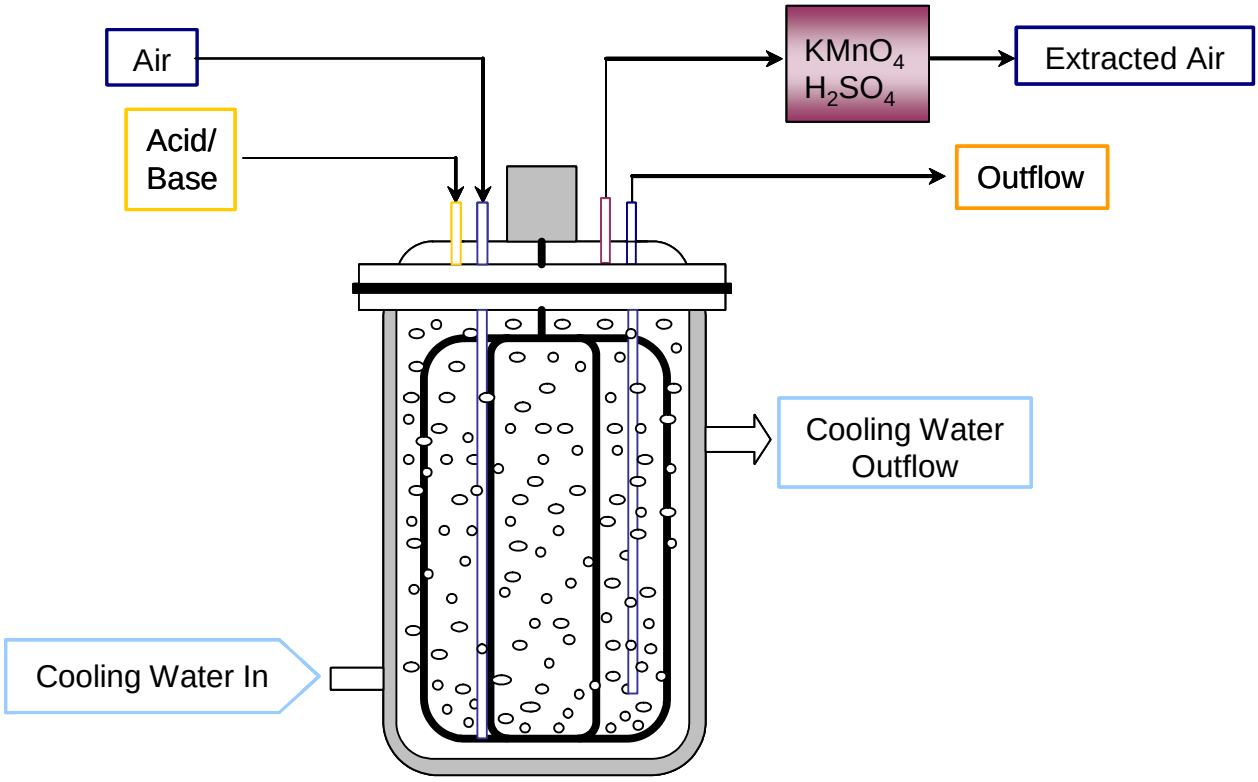

Figure 2-4. Schematic diagram of the experimental stirred bioreactor (B. Braun Biotech International, Germany).

Figure 2-4 demonstrates the inoculation protocol used in this experiment. For the first pre-culture, cells were incubated from a frozen glycerol stock on agar plates of LB growth medium in petri-dishes (9 cm in diameter) and grown for 48 h at 30°C. As a general rule, a colony was picked from these plates and inoculated into 10 ml LB growth medium for 8 h at 30 °C on rotary shaker (180 rpm). M9 medium with sodium acetate (20 mM) was then inoculated with 1 % (v/v). Thiomersal (2 ppm) was always added to the medium to prevent contamination. For the experiments in Biostat MD bioreactors, the cell biomass was produced in a 2-phase (batch + continuous culture) and the cultivation was done in M9-minimal medium with 20 mM sodium acetate and 10 ppm thiomersal. Feeding of fresh growth medium combined with 10 ppm thiomersal to the MD bioreactor was started when the cells reached late exponential growth phase.

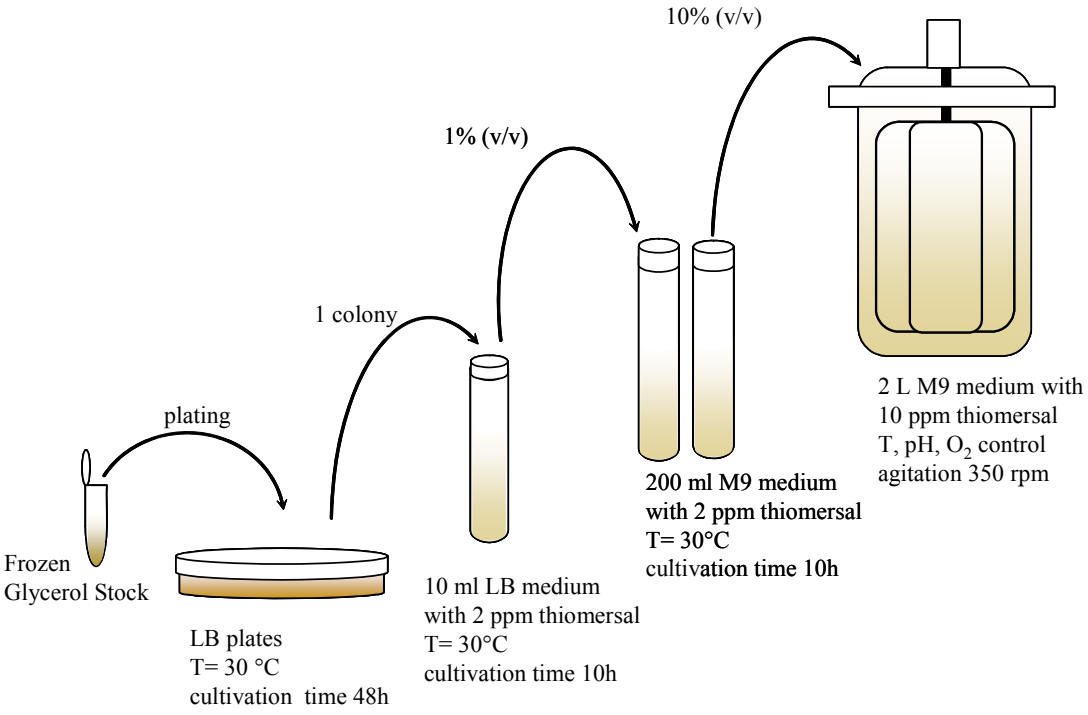

Figure 2-5. Inoculation of Biostat MD bioreactors. For description see text.

2.6.6.1 *Kinetic Model of Enzymatic Reaction*

Michaelis-Menten kinetics is a basic enzyme kinetics scheme, used for the study of enzymatic catalysis of non-inhibitory compounds. By toxic substrates it comes frequently to deviation from the hyperbolic function of Michaelis-Menten kinetics. Therefore, under conditions prevailing at the reactor operation the measured data are best described by an extended Haldane expression

$$V = V_{max} \frac{S}{S + K_s + (S^2 / K_i)}$$

with

V = specific reaction rate of Hg^{2+} to Hg^0

S = Substrate concentration

K_s = half-saturation constant or substrate concentration when $V = V_{max} / 2$

K_i = inhibition constant, which considers decreased transformation rate with increasing substrate concentration.

The transformation rate was calculated by the amount of mercury concentration in the inflow and subsracted from the amount of mercury in the outflow. Due to a high conversion the volumetric transformation rate follows the offered Hg^{2+} loading, given by

$$R_{HgV} = D\,(c_{Hg\ inflow} - c_{Hg\ outflow}) \approx Dc_{Hg\ inflow}$$

3 Results

3.1 Transformation of Thiomersal by Microorganisms

Thiomersal transformation by environmental isolates and GEMs, resistance level and growth inhibition by thiomersal (TH) were determined by two methods: measurement of transformed mercury as volatized metallic mercury (Hg^0) using cold vapor atomic absorption spectroscopy (CVAAS) and bacterial growth in liquid and solid media in the presence of various TH concentrations (for details see section 2.6.3).

To ensure accurate and reproducible results in the metallic mercury measurements, the comparability of the samples was shown in preliminary experiments. To determine if results from different thiomersal measurements are comparable between cultures and within the same culture at different stages of growth, TH transformation at various growth phases was investigated for two different strains: a naturally mercury resistant strain *Pseudomonas putida* Spi3 (Spi3) and *Pseudomonas putida* KT2442::*mer*-73 (KT2442), a genetically engineered strain which harbors mercury resistance. Furthermore, technical handling required maintaining cultures on ice before CVAAS reading for a short period of time. Therefore, it was examined for both isolates how culture storage on ice influenced TH transformation rates. *Ps. putida* KT2442::*mer*-73, is a GEM which carries a truncated *mer* operon (*mer*TPAB) randomly integrated into the chromosome by transposon mutagenesis. It was constructed by Horn *et al.* (1994) and selected for its high and constitutive mercury resistance. The rationale was that the constructed strain would be better adapted to cope with fluctuating mercury concentrations than natural bacteria with an inducible mercury resistance. On the other hand, a naturally mercury resistant strain *Ps. putida* Spi3 isolated from contaminated river sediments (von Canstein *et al.* 2001) was also shown to be resistant to mercury (von Canstein *et al.* 2002). It grew on a solid medium containing 5 ppm Hg^{2+} and was tested in the laboratory scale bioreactors in a consortium of mercury transforming bacteria.

Generally, the medium used in all transformation studies on CVAAS was *Pseudomonas* minimal medium (M9) because this medium does not form non-reducible complexes with mercury compounds. Chang *et al.* (1993) showed that the components of a complex medium such as yeast interact with mercury ions to form complexes that could not be reduced by bacteria. However, no influence on Hg^{2+} reduction could be observed using mercury containing *Pseudomonas* minimal medium.

The detection of transformed Hg^0 by microorganisms was determined by periodical aeration of closed vessels containing M9 medium and TH. Thus the TH transformation rate was determined by the volatized mercury minus the amount of formed Hg^0 measured in the control assays (chemically originated Hg^0). All experiments were performed in triplicate and carried out with a TH concentration of 2 ppm in M9 medium. The number of living cells was determined before and after each experiment by counting the colony forming units (cfu) on solid iniculum medium (NMS). This detection of living cells was essential to determine the survival of each strain during the transformation measurement and to be able to determine the mercury transformation rate per cell.

3.1.1 Influence of Growth Phase on TH Transformation Rate

The strains *Pseudomonas putida* Spi3 (Spi3) and *Pseudomonas putida* KT2442::*mer*-73 (KT2442) were examined for their capacity to detoxify thiomersal at different growth phases. The bacterial stock cultures were prepared in 100 ml NMS medium containing 1 ppm TH to ensure permanent induction of the *mer* operon. This was primarily important for the natural isolates, most of which carry resistance operons that are under the control of inducible promoters (O'Halloran *et al.* 1987; Parkhill *et al.* 1990; Ralston *et al.* 1990).

Each thiomersal reduction assay was performed in triplicate and each set of experimental conditions was also repeated three times. The initial TH concentration was 2 ppm and the initial cell density in the experiments was adjusted to 3.8–4.5 × 10^7CFU ml^{-1} for KT2442 and 1.1–1.8 × 10^7 CFU ml^{-1} for Spi3. A correlation between cell number and optical density as well as the definition of growth phases is described in Material and Methods (see section 2.4.2 and Figure 2-1).

Figure 3-1 shows TH transformation rates which are presented for 1.0 × 10^7 cells · ml^{-1} in order to represent a common denominator. The cells of both Spi3 and KT2442 exhibited the highest TH transformation rates at the mid log phase followed by late exponential phase. At the stationary phase the cells had the lowest transformation rate.

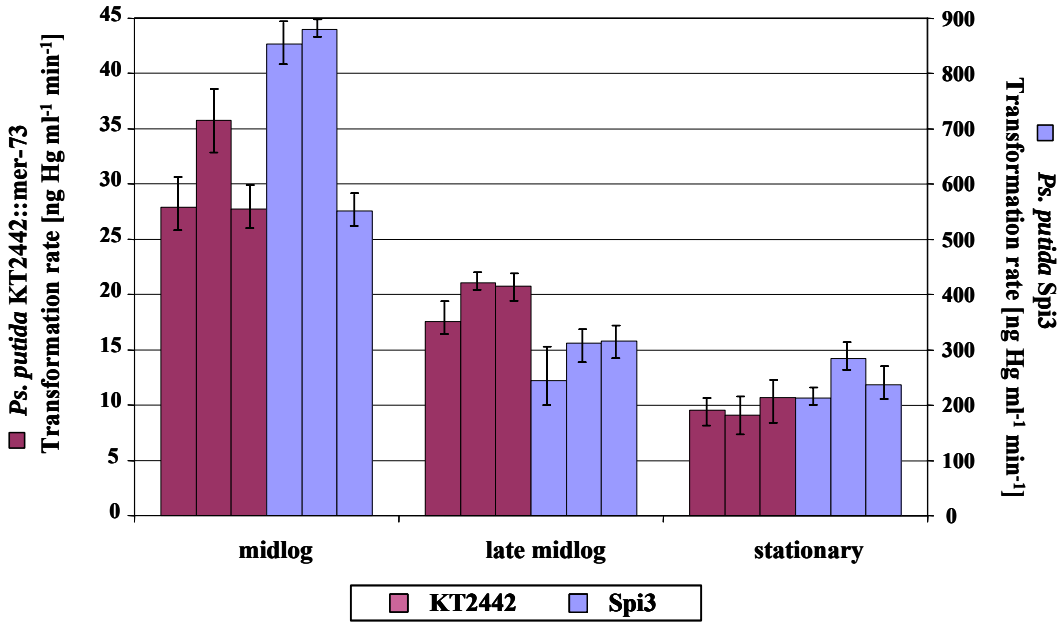

Figure 3-1. **Dependence of thiomersal transformation rates on growth phase of *Ps. putida* KT2442::*mer*-73 (KT2442) and of *Ps. putida* Spi3 (Spi3) in the presence of 2 ppm thiomersal.** The cell density was adjusted to 3.8–4.5 × 10^7CFU ml^{-1} for KT2442 and 1.1–1.8 × 10^7CFU ml^{-1} for Spi3. The reported TH transformation rates are presented for 1.0 × 10^7 cell ml^{-1}. Thus transformation rates of KT2442 and Spi3 differed by an order of a magnitude. They are shown on the primary and secondary axis, respectively.

By transforming thiomersal with unexpected high rates (14–32 fold higher than KT2442), Spi3 possessed excellent TH detoxification activity. Mercury detoxification of Spi3 during growth showed a similar trend as KT2442: TH transformation decreased with progressive cell growth. The highest detoxification rate was measured at the mid log phase with an average rate of 879 ng Hg· ml^{-1} · min^{-1} (up to 36 ng Hg · ml^{-1} · min^{-1} for KT2442) and decreased until it leveled off at approximately 250 ng Hg· ml^{-1} · min^{-1} at the stationary phase (10 ng Hg· ml^{-1} · $min^{-1}$for KT2442). The mid log phase TH transformation differed from the stationary phase by about 60% when the TH transformation rate at the middle logarithmic phase was set as 100%. Decline in the transformation rate between late exponential and stationary phases turned out smaller (19%). In conclusion, the exponential phase cells achieved transformation rates up to two times higher than the cells at all following phases.

Detecting the lowest detoxification rate during the stationary phase is reasonable because a lack of cellular metabolic energy and NADPH production limits the process of mercury transformation: the energy-driven cellular mercury transport process slows down. The supply of the cofactor for the enzymatic reduction of mercury ions ceases, resulting in an attenuation of mercury transformation (Miller *et al.* 1990; Miller *et al.* 1991; Silver and Phung 1996).

The aforementioned experiments suggest that the mercury transformation rate of growing cells is significantly higher than in resting cells, although the results showed some deviation between the triplicates in mid log cells (up to 36 and 182 ng Hg· $ml^{-1} \cdot min^{-1}$). Although the transformation rate of cells in late exponential phase was not as high as in exponentially growing cells the deviation between the parallels was negligible. Therefore, cells of the late exponential phase were chosen for further experiments.

3.1.2 Influence of Culture State on Thiomersal Transformation

The duration of one measurement with the CVAAS for determination of TH transformation rate was 45 min. Therefore the intention of this experiment was to investigate whether the same sample of culture (batch) could be utilized for several kinetic measurements. The alternatives were 1) harvest the cells from one sample by centrifugation and store of the pellets on ice resuspending each aliquot for one measurement, or 2) store the liquid culture sample on ice and take an aliquot only prior to the measurements. The third option that was tested was 3) prepare several parallel batch cultures with a temporal succession of 45 min. The samples were consequently inoculated and incubated every 45 min.

To test alternative 1 the bacterial cells of *Ps. p.* KT2442::*mer*-73 (KT2442) were cultured and harvested at the late exponential phase. To remove remaining nutrients and cell debris the cell pellets were washed and stored on ice for 0 min (1^{st} culture = control), 45 min (2^{nd} culture), 90 min (3^{rd} culture) and finally 135 min (4^{th} culture). For the measurements the aliquots were resuspended in M9 medium and incubated at 30°C for 10 min. The final cell concentration was adjusted to 3.6–4.2 × 10^7 CFU·ml^{-1}, whereby in Figure 3-2 TH transformation rates are presented for 1.0 × 10^7 cells · ml^{-1}. In the experiment, the initial TH concentration in the assays was 2 ppm. The measurements of the samples were carried out at intervals of 45 min.

The results (Figure 3-2) show a clear reduction of TH transformation between the samples over the course of time. The TH transformation rate decreased from 18.9 to 6.7 ng Hg · $ml^{-1} \cdot min^{-1}$ (64%) during 135 min of storage on ice.

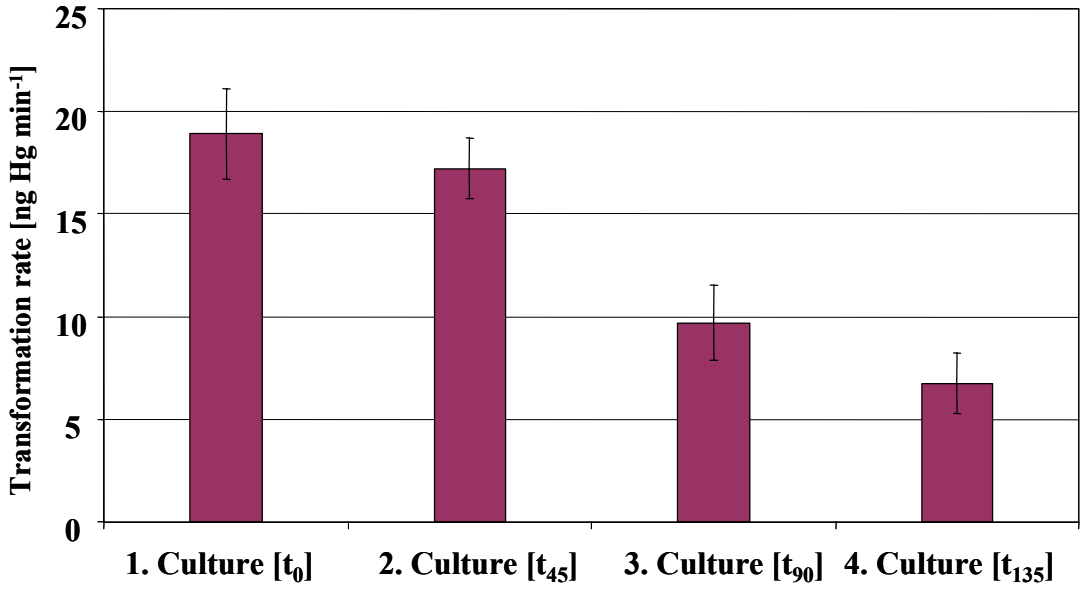

Figure 3-2. Alternative 1: "Harvesting and resuspending of Cells". Thiomersal transformation rate [ng Hg· ml^{-1} · min^{-1}] of KT2442. Rates were determined in triplicate and are presented for 1.0×10^7 cell·ml^{-1}. The first cultures from the respective series set [t = 0 min] were measured immediately. Harvested and resuspended aliquots of the second, third and fourth culture were stored on ice for 45, 90 and 135 min., respectively and resuspended in M9 medium. The initial thiomersal concentration was 2 ppm.

The TH transformation rate was slowed by 65% if the culture was stored for 135 min (4^{th} culture) in comparison to the controls. The results indicate that the preparation procedures do have a negative impact on the activity of the cells causing a substantial loss of TH transformation. Storage of aliquots on ice was therefore not an option to obtain reliable results.

Another approach to obtain comparability was to store the liquid sample on ice without harvesting the cells (alternative 2). A batch culture of *Ps. p.* KT2442::*mer*73 was grown in 50 ml NMS medium until the late exponential phase. The first sample of each batch used in measurements served as control. For further measurements the batch culture was stored on ice for the duration of the experiment (45 min). Thus, the sample was stored up to 135 min prior to CVAAS measuring. The cell density of each culture was determined by cfu after incubation of 3 ml samples for 10 min at 30°C.

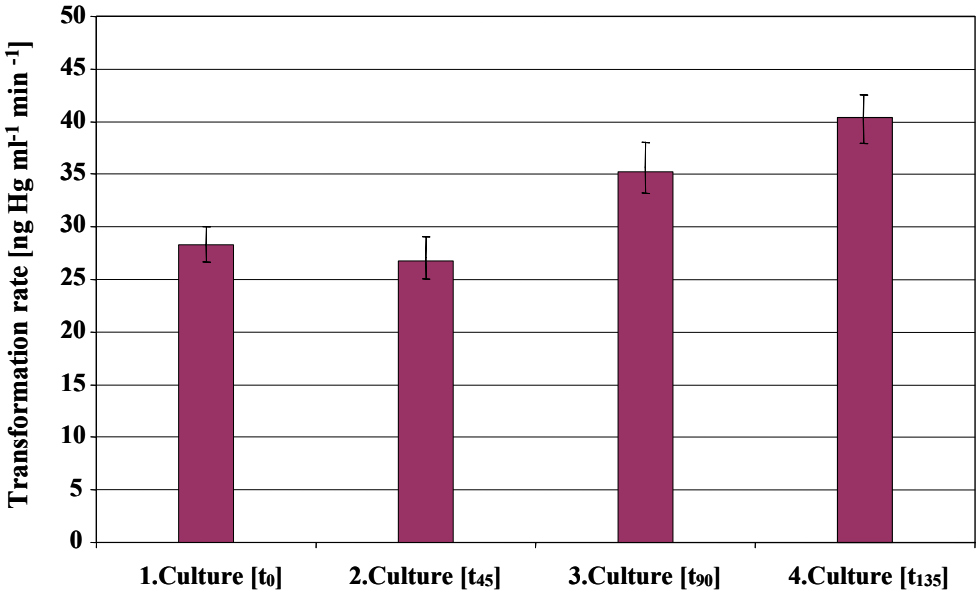

Figure 3-3. Alternative 2: "Storage of Batch Culture on Ice". Thiomersal transformation rate [ng Hg · ml^{-1}· min^{-1}] of *Ps. putida* KT2442::*mer*73 (KT2442). The TH transformation rate is presented for a cell density of 1.0×10^7 CFU ml^{-1}. Rates were determined in triplicate. The first cultures from the respective series [t = 0 min] were immediately used in the kinetic measurements. Liquid batch cultures were stored on ice for the duration of the prior measurements. The initial thiomersal concentration was 2 ppm.

As shown in Figure 3-3 the transformation rate of 2 ppm thiomersal by KT2442 varied between 26 and 41 ng Hg· ml^{-1} · min^{-1} (25–34% difference) for all four cultures. But the cell density dropped from 3.2 to 2.1×10^7 CFU·ml^{-1}, a variation between the cultures of around 35–40% (decline with aging of the cultures on ice). In terms of transformation, the measurement with the lowest cell density showed the highest transformation rate. This can be explained by fact that the cells were destroyed by the storage on ice and thus the mercury transformation enzymes were presented freely in the solution. Consequently, the enzymes transform mercury unhindered which explains the increased transformation rate with low cell number.

With respect to such a discrepancy of cell number and TH transformation rate a further experiment was carried out (alternative 3) to decide on the optimal feasibility for comparable results.

For alternative 3 batches were inoculated with a temporal succession of 45 min (2^{nd} batch was prepared 45 min after the 1^{st} sample, 3^{rd} batch was inoculated after 90 min and 4^{th} culture was inoculated with a temporal interval of 135 min). Thus the samples did not have to be set on

ice. The sample preparation was carried out as described above. In this third test series both KT2442 and Spi3 were used.

The experimental data show both isolates with an approximately constant TH transformation rate for all four cultures (Figure 3-4). Spi3 with an average TH transformation rate of 179 ng Hg · ml^{-1} · min^{-1} for 1.0 ×10^7 cell ml^{-1} surpasses KT2442 (23 ng Hg· ml^{-1} · min^{-1}) about eight-fold. The variation in the TH transformation rate of the Spi3 samples was about 8–17% and the cell density of the four batches was comparable. Similar results were determined for KT2442. Transformation rates between the four samples varied around 4–12% with almost constant cell density.

The comparability of the four samples of each isolate could be shown in this experiment. Consequently, further kinetic measurements were carried out according to this third experimental design with the cells of the late logarithmic growth phase.

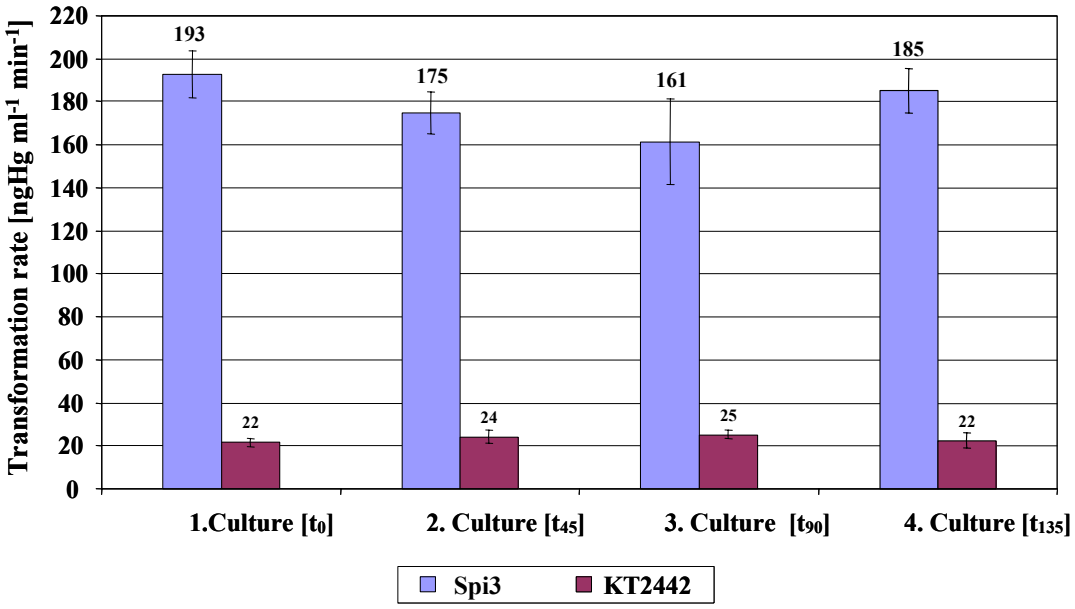

Figure 3-4. Alternative 3: "Inoculation with temporal succession". Thiomersal transformation rate [ng Hg · ml^{-1} min^{-1}] of Spi3 and KT2442 presented for 1.0 × 10^7 cell ml^{-1}. The experiments were carried out with four parallel batches of each isolate that were grown with a temporal succession of 45 min. The first cultures from the respective series were used directly in the measurements [t = 0 min]. The 2nd, 3rd and 4th culture were inoculated with a temporal interval of 45, 90 and 135 min. The initial TH concentration was 2 ppm.

3.1.3 Selection of Thiomersal Degrading Bacteria

Based on previous work (von Canstein *et al.* 2001, 2002) the seven promising naturally mercury resistant isolates of *Pseudomonas* and two *Citrobacter* strains, as well as two genetically engineered microorganisms (GEMs) were selected to determine their resistance to the organomercurial thiomersal and their capability to transform thiomersal.

The experiment was carried out with a TH concentration of 2 ppm in M9 medium and the number of living cells was determined before and after each experiment. On the basis of the previous experiments (see section 3.1.1) the late logarithmic growth phase was chosen for TH transformation measurements.

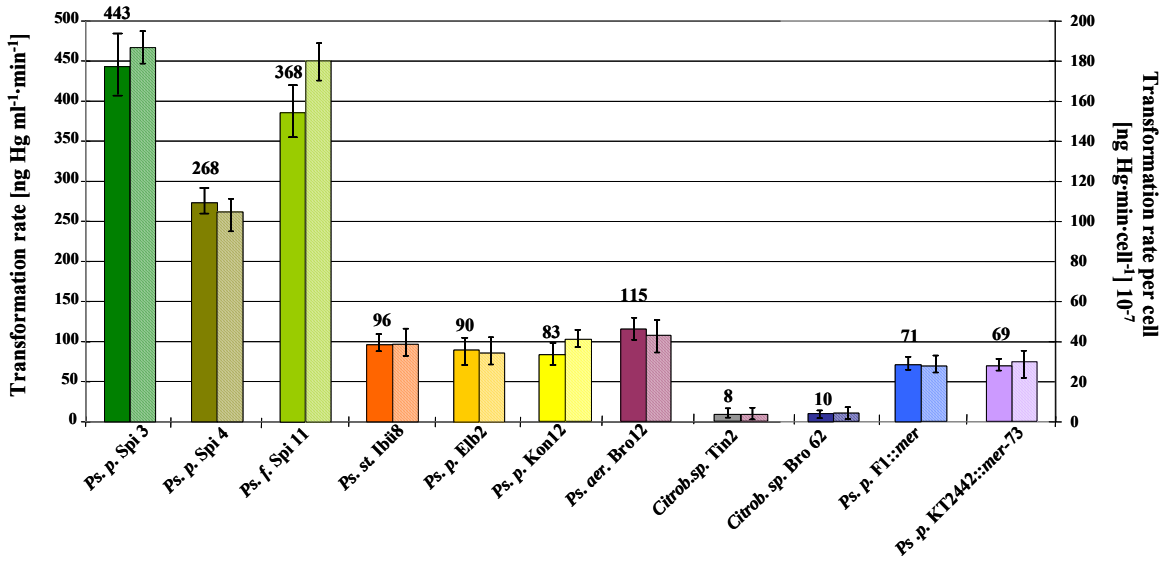

Figure 3-5. The biotransformation rate for thiomersal (2 ppm) for nine naturally mercury resistant isolates and two GEMs (*Ps. putida* F1::*mer* and *Ps. putida* KT2442::*mer*73) and TH transformation rate per cell is shown on secondary axis. Transformation was determined by measuring the amount of volatized Hg^0 by a given cell number ($1.7–2.6 \times 10^7$ cfu·ml^{-1}) upon injection into a thiomersal solution. For the transformation rate per cell, the highest cell number of the respective isolate was used (see Table 3-1).

The results showed large differences in thiomersal transformation rates (8–443 ng Hg· ml^{-1} · min^{-1}) between the investigated isolates (Figure 3-5) while all cultures were assayed at a similar cell density (Table 3-1).

Citrobacter freundii Tin2 and 62, which are highly resistant to mercury chloride in comparison with the other strains (von Canstein *et al.*, 1999, von Canstein *et al.*, 2001), could cope with thiomersal concentrations up to 2 ppm, however, with a very low transformation rate (8 and 10 ng Hg· ml^{-1} · min^{-1}). From these results, the question arises whether they are resistant to organomercurials and consequently possess the organomercurial lyase gene,

*mer*B. However, the cell number of the Tin2 did not decrease clearly after the experiment. As shown in Table 3-1 only the cell number of Bro62 decreases about 47%. Therefore, surviving in TH solution suggests that Tin2 is probably an organomercurial resistant strain but is not able to transform it well and fast. To confirm this statement, experiments have to be done with other organomercurials or the *mer* operon of Tin2 has to be sequenced to prove the presence of organomercurial lyase.

Pre-eminent among the isolates were *Ps. putida* Spi3, Spi4 and *Ps. fulva* Spi11, which showed transformation rates between 286 and 443 ng Hg· ml^{-1} · min^{-1} at a TH concentration of 2 ppm. This was 3- to 55-fold higher than the transformation rate of other strains. When the cell density of each strain was taken into consideration and TH transformation rate was computed per cell the same trend as above was observed. Again the three strains, Spi3, Spi4 and Spi11, transformed TH to metallic mercury outstandingly (Table 3-1). As shown in Table 3-1 the cell densities of all strains did not change substantially, during the measurement indicating resistance to TH. In comparison to the wild-type isolates both GEMs showed low TH transformation rates. *Ps. p.* KT2442::*mer*-73 transformed TH with a rate per cell of 29 and *Ps. p.* F1::*mer* had a transformation rate per cell of 27 [ng Hg· ml^{-1} · min^{-1} · $cell^{-1}$] × 10^{-7}, though the cell density was comparable to the other isolates and the cell densities hardly differ before and after measurements (Table 3-1). Thus the results showed a 3.8- to 6.8-fold lower rate than the three Spi-strains.

For further investigations *Ps. putida* Spi3, *Ps. putida* Spi4 and *Ps. fulva* Spi11 and also the two GEMs were selected and tested extensively.

Table 3-1. Cultivatable cell number of isolates before and after the TH transformation measurements.

Isolate	before [Cell · ml^{-1}]	after [Cell · ml^{-1}]	Transformation rate per cell [ngHg · ml^{-1} · min^{-1} · $cell^{-1}$] x 10^{-7}
Ps. putida Spi3	1.76 × 10^7	2.38 × 10^7	186
Ps. putida Spi4	2.36 × 10^7	2.61 × 10^7	105
Ps. fulva Spi11	1.91 × 10^7	2.14 × 10^7	181
Ps. putida Elb2	2.25 × 10^7	2.44 × 10^7	35
Ps. stutzeri Ibü8	2.61 × 10^7	1.95 × 10^7	39
Ps. putida Kon12	1.99 × 10^7	2.05 × 10^7	41
Ps. aeruginosa Bro12	2.68 × 10^7	1.61 × 10^7	43
Citrobacter freundii Tin2	2.69 × 10^7	2.16 × 10^7	3
Citrobacter freundii Bro62	2.32 × 10^7	1.24 × 10^7	4
Ps. putida F1::*mer*	2.40 × 10^7	1.97 × 10^7	27
Ps. putida KT2442::*mer*73	2.40 × 10^7	2.00 × 10^7	29

3.1.4 Thiomersal as a Carbon Source

Many substances considered as pollutants in the environment may serve as carbon or energy sources for microorganisms that are not negatively affected by the substance. Hence it was of interest to investigate the relevance of thiomersal as a carbon source for the mercury resistant isolates and the two GEMs.

The three natural isolates with the highest resistance towards TH, *Ps. putida* Spi3, Spi4, and *Ps. fulva* Spi11, as well as both GEMs, *Ps. putida* F1::*mer* and *Ps. putida* KT2442::*mer*73 were incubated with TH for 12h and growth was measured by turbidity (OD_{600}) and cell number. All experiments were carried out in batch cultivation. Prior, the cells were adapted to 1 ppm TH. All five isolates were incubated in M9 medium using TH as the sole carbon source in different concentrations (2, 5, 10, 15, and 20 ppm).

None of the five isolates was able to grow with TH as a carbon source and no changes in TH concentration were observed.

3.1.5 Effect of Dithiosalicylic Acid on Bacteria

The major products of thiomersal decomposition in aqueous solution have been shown to be thiosalicylic acid (THSA) and ethylmercuric hydroxide (Reader *et al.* 1982). In the presence of sodium chloride THSA undergoes irreversible oxidation to 2,2'dithiosalicylic acid (dTHSA) which might serve as energy or carbon source. In addition, it could change the reaction equilibrium and thereby have a negative influence on the wastewater treatment processes. Therefore, the effect of different dTHSA concentrations on cell densities of a the natural isolate *Ps. putida* Spi3 and the GEM *Ps. putida* KT2442::*mer*-73 was investigated (Table 3-2).

The CFU of both isolates were determined after 48h incubation on M9 medium plates with different dTHSA concentrations. Each assay was supplemented with 0, 0.25, 1.25, 2.5, 5 and 10 mg dTHSA per liter which was corresponds to 1, 5, 10, 20 and 40 ppm thiomersal. As dTHSA is almost insoluble in water, a stock solution had to be prepared by solving 100mg of dTHSA in 10 ml dimethylformamid (DMF) before addition to the M9 medium. Therefore, it was also necessary to examine the effect of DMF on bacteria. For this experiment a concentration of 1 ml DMF was chosen which was equivalent to the highest dissolved dTHSA concentration (10 ppm). Sodium acetate was used in all samples as carbon source.

Table 3-2. The effect of 2,2' dithiosalicylic acid (dTHSA) and dimethylformamid (DMF) on a natural isolate (*Ps. putida* Spi3) and a GEM (*Ps. putida* KT2442::*mer*-73). Colony forming units after growth with different concentrations of dTHSA (plus DMF) and with 1ml DMF.

dTHSA [ppm]	*Ps. p.* Spi3	*Ps. p.* KT2442::*mer*-73
0	2.4×10^7	3.6×10^7
0.25	2.5×10^7	3.5×10^7
1.25	2.7×10^7	3.6×10^7
2.5	2.6×10^7	3.3×10^7
5.0	2.6×10^7	3.7×10^7
10	2.4×10^7	3.2×10^7

DMF [ml]	*Ps. p.* Spi3	*Ps. p.* KT2442::*mer*-73
1	2.6×10^7	3.3×10^7

The cell density of both the isolate and the GEM was found to be approximately the same in all samples after 48 h compared to a control that was only supplemented with 20 mM sodium acetate, as carbon source. The results in Table 3-2 showed clearly no changes of cell numbers depending to dTHSA or DMF. These results showed that dTHSA was not utilized as energy source and on this account; the effect of dTHSA during all experiments with thiomersal can be neglected.

3.1.6 Thiomersal Resistance of the Environmental Isolates and GEMs

3.1.6.1 *Effect of Thiomersal on Bacterial Growth*

These experiments were performed to determine if the chosen isolates were able to cope with thiomersal up front if they had previously been adapted to a mercury-free medium. As mentioned above strains Spi3, Spi4, Spi11 and the two GEMs, KT2442 and F1 were capable of detoxifing up to 2 ppm TH. Therefore, growth experiments were carried out with these strains for 10 h to 12 h in batch mode, using inoculum medium (NMS medium) with different initial thiomersal concentrations (0, 2, 5, 15, 20 ppm). Pre-cultures for inoculation were grown in a mercury-free medium. A control culture was grown under the same conditions but in the absence of TH. A second control batch was prepared only with TH in the medium but without microorganisms to determine chemical changes of TH during the experimental period. The growth yield of the isolates was determined in the form of total viable-cell counts and turbidimetrically at 600 nm. Thiomersal contents were measured via mercury

concentration in the solution using a CVAAS. The mercury transformation rate was calculated by the residual mercury concentration in the samples as a function of time.

Figure 3-6 (A) and 3-7 show clearly that only *Ps. putida* Spi3 was able to grow with TH up to 20 ppm. No growth was observed for the other four isolates (3-7 A–D) in a TH environment and a complete inhibition of growth was still observed up to 2 days. The number of CFU remained below detection due to TH toxicity (Table 3-3).

No growth was also observed with both KT2442 and F1 (Figure 3-7 C and D): The effect of TH on growing cells was devastating: no cell growth could be detected (Table 3-3). This finding was remarkable because both GEMs have been constructed and selected for their high and constitutive mercury resistance (Horn *et al.* 1994). Moreover, they have been especially provided with the resistance against organic mercury. The *Ps. putida::mer* isolates described by J. Horn have the potential to cope with mercury chloride ($HgCl_2$) and phenylmercuric acetate (PMA) in concentrations up to 60-80 ppm. However, thiomersal could not be transformed by the strains under the conditions used in this experiment and entirely repressed their growth.

Table 3-3. Cell number [cfu ml^{-1}] of the isolates after 10h of incubation in M9 medium containing different thiomersal concentrations (5, 10, 15, 20 ppm). The density of all isolates was 1.3×10^8 cfu·ml^{-1} initially. Only Spi4 had an initial cell density of 6.1×10^7 cfu per ml. The cell number of Spi4, Spi11, F1 and KT2442 were below detection up to 2 days. * bd =below detection

	Thiomersal concentration [ppm] Cell density after 10 h incubation [cfu·ml^{-1}]					
	0	2	5	10	15	20
Spi3	1.3×10^8	1.6×10^8	1.0×10^8	9.7×10^7	1.1×10^8	8.9×10^7
Spi4	6.7×10^7	bd	bd	bd	bd	bd
Spi11	1.1×10^8	bd	bd	bd	bd	bd
KT2442	4.7×10^8	bd	bd	bd	bd	bd
F1	1.0×10^8	bd	bd	bd	bd	bd

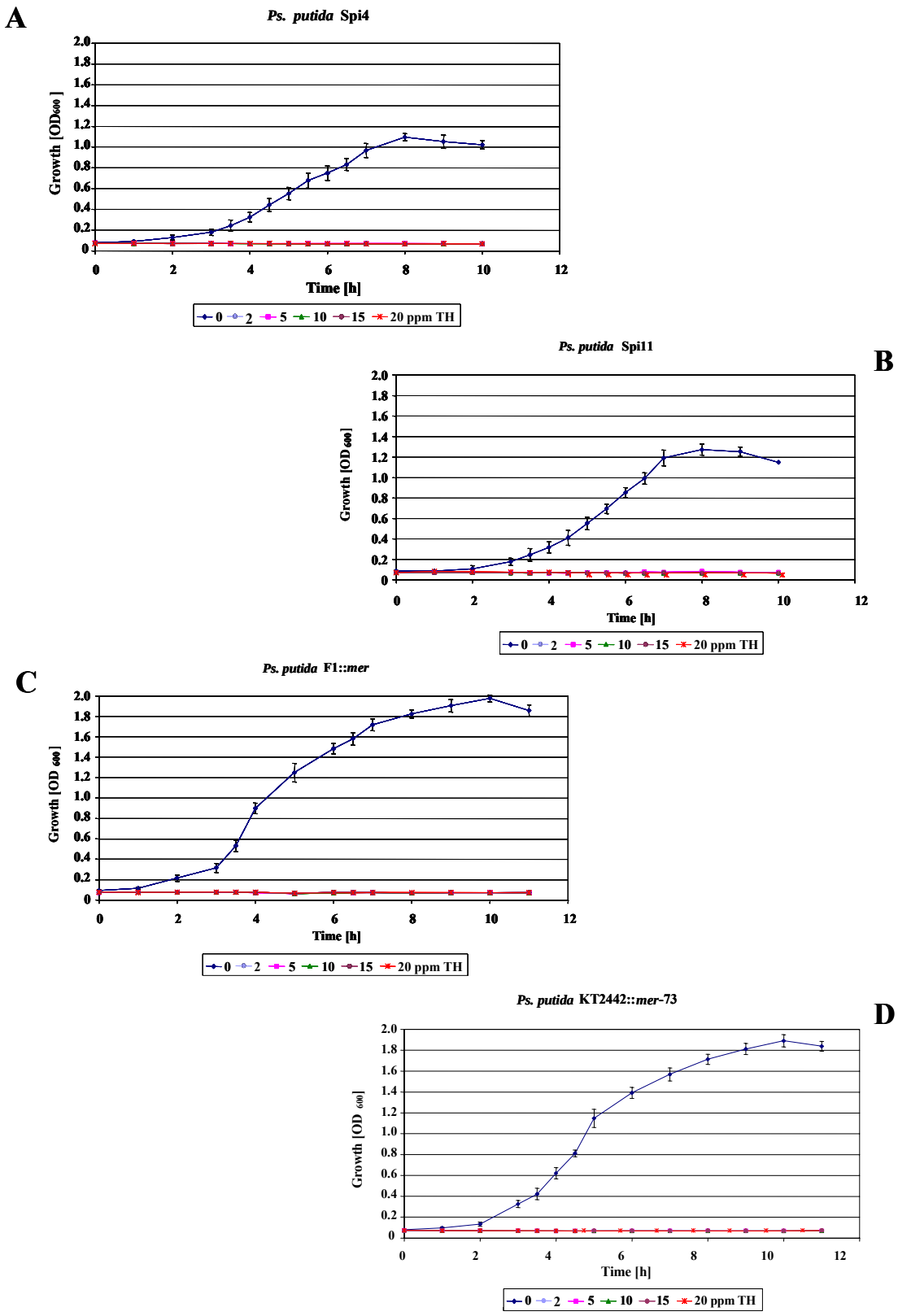

Figure 3-6. Effect of different thiomersal (TH) concentrations (0, 5, 10, 15, 20 ppm) on growth of *Ps. p.* Spi4, *Ps. fulva* Spi11, *Ps. p.* F1::*mer* and *Ps. p.* KT2442::*mer*-73. TH was added to the samples from the beginning of the experiment. The results are mean values of triplicates.

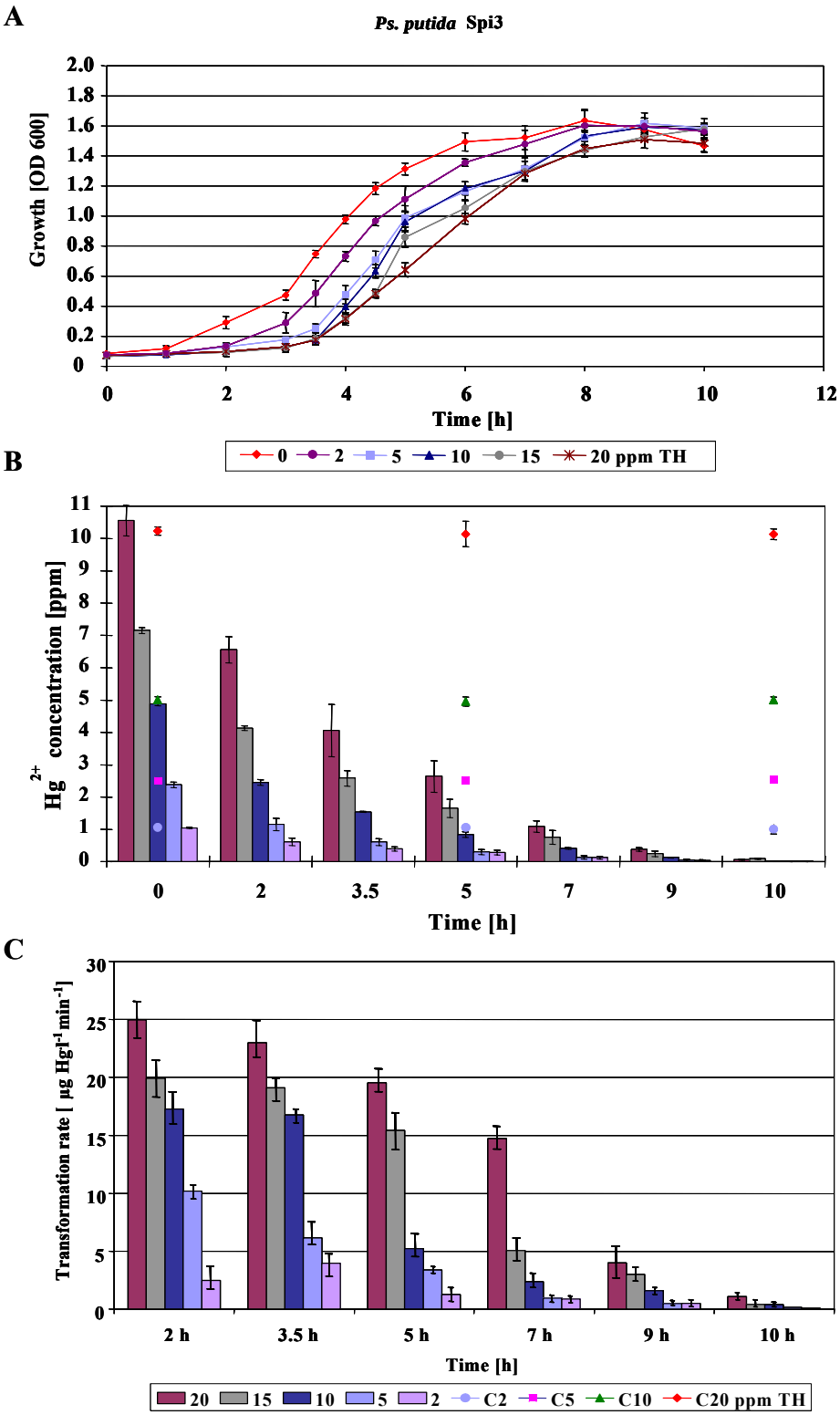

Figure 3-7. Effect of different thiomersal (TH) concentrations (0, 2, 5, 10, 15, 20 ppm) on bacterial growth of *Ps. putida* Spi3 (A). Thiomersal was added to the samples from the beginning of the experiment. The preculture used for inoculation did not contain mercury. **B:** Mercury (Hg^{2+}) concentration in different batch cultures during the growth of Spi3. Note TH contains 49.6% mercury by weight thus Hg^{2+} concentration is about half of TH. Control samples without cells but with different TH concentrations (C2, C5, C10, and C20 ppm) are represented as dots. The results are mean values of triplicate measurements. **C:** Thiomersal transformation rates [µgHg l^{-1} min^{-1}] during the growth. Transformation rates per minute were calculated from total mercury concentration using the interval 0–2, 2–3.5, 5–7, and 9–10 h.

The data showed that Spi3 coped particularly well with TH. The strain showed a delayed lag phase compared to the control in the presence of TH but attained approximately the same maximum optical density. The results of the growth curves were also reflected in the cell density after 10 h incubation in different TH concentrations. No significant differences could be detected in the maximum cell number between the Spi3 samples. Only the growth of Spi3 in 20 ppm TH was slightly decelerated and the maximum density reached 93% (8.9×10^7 cfu per ml) as compared with the control culture.

Figure 3-7 B shows the concentration of Hg^{2+} during the growth of Spi3. Note that thiomersal contains 49.6% mercury by weight and thus Hg^{2+} concentration is about half of the given TH concentration. The results show clearly the constant decrease of mercury in all samples, until it leveled off between 0.002 (for 2 ppm TH) and 0.06 ppm (20 ppm TH). On the other hand, there was no mercury removal in the control sample without cells. The transformation of TH was only based on microbial activity.

With the total mercury measurements during the growth of Spi3 (as shown in Figure 3-7B), it was therefore possible to calculate the thiomersal transformation rate during the growth (Figure 3-7 C). In spite of probable cell death during the lag phase, the total mercury concentration decreased from the onset of the cultivation. High transformation activity occurred mainly during the first 5 hours of growth at concentrations of 5, 10, 15, 20 ppm TH and sequentially decreased. But the highest transformation rates were calculated in the first 3.5 h. This observation could be explained by the fact that lag phase cells may spend most of their resources to reduce mercury to survive the toxic environment and thereafter start to grow. Nevertheless, with increasing thiomersal concentrations (15 and 20 ppm TH) the exponential phase cells of Spi3 (3.5 to 5 hours) achieved better transformation rates so that the rate between 2 and 5 h of incubation became considerably smaller. In contrast to the other TH samples the bacterial transformation activity at 20 ppm TH was very high in the first 7 h and dropped drastically. A remarkable finding was also the dependence of the mercury transformation rate on initial thiomersal concentrations, namely higher transformation rates with higher initial thiomersal concentrations. At 20 ppm TH, the transformation rate was highest. Future experiments will have to show the optimal thiomersal concentration for the highest possible mercury transformation rate.

3.1.6.2 *Biotransformation of Thiomersal at Mid Exponential Phase*

As mentioned above, the four isolates Spi4, Spi11, and the GEMs KT2442 and F1, were unable to grow in the presence of thiomersal, if it were added to the medium from the beginning. Since all of these strains had been shown to be able to transform TH before (Figure 3-5), it was of interest to see whether they could withstand and transform thiomersal if it was supplemented to mid-log phase (OD_{600} = 0.5–0.8). Concurrently, the biotransformation of TH was determined as described in 2.2.1. In addition to the control culture without TH, a second control sample containing TH but no bacteria was examined to detect any chemical changes of thiomersal in solution. All tests were prepared in triplicate.

Figure 3-8 – 12 show the growth of the five strains in liquid inoculum medium (NMS) containing different TH concentrations, from 2 to 20 ppm.

Figure 3-8 illustrates that a TH concentration up to 10 ppm had hardly any effect on the growth of Spi3. Bacterial growth was slightly decelerated at the beginning but attained approximately the same maximum optical density. Growth inhibition was only detected at 15 and 20 ppm with a slight reduction of the maximum optical density (OD) of 3% and 9% at 20 ppm TH. Mercury was reduced extensively during the exponential growth phase and the concentration of mercury was volatized up to 60% after 1.5 h of incubation in TH medium. Almost 99.7 % of the total mercury was reduced up to stationary phase. Interestingly, the cells at exponential phase in this experiment exhibited a very high transformation rate due to higher cell density compared to the previous experiment (Figure 3-7C and Figure 3-8C).

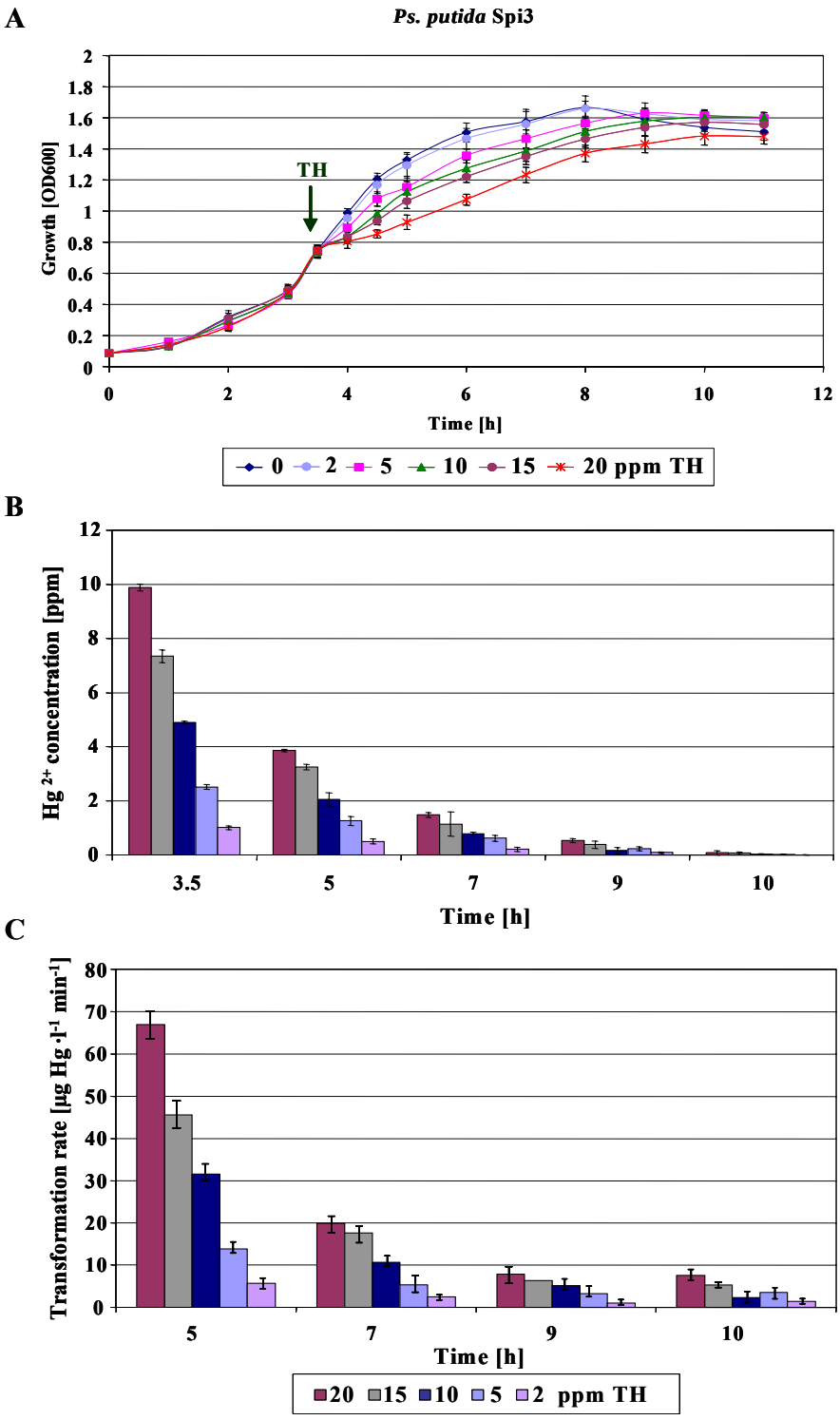

Figure 3-8. Addition of different thiomersal concentrations (2, 5, 10, 15, 20 ppm) to cells of middle logarithmic phase from *Ps. p.* Spi3. A: The cell growth was measured at 600 nm. **B:** TH was added to the samples after 3.5 h of growth. The Hg^{2+} concentration [ppm] during the experiment was measured with CVAAS. **C:** TH transformation rate [µg Hg·min^{-1}] during the growth. The rates were calculated from Hg^{2+} concentration in the respective sample using the intervals 3.5-5 h, 5-7 h, 7-9 h and 9-10 h. The results are mean values of triplicates.

No bacterial growth was observed when TH was added from the beginning of the experiment (see Figure 3-6). By supplementing TH to middle logarithmic phase almost all isolates grew in the presence of TH (3-9, 3-10, 3-11 and 3-12). Even, two strains were able to cope with TH up to 20 ppm. However, all four isolates showed growth inhibition already at concentrations of 2 ppm, i.e. cell death occurred at the beginning of each TH addition. The extent of cell death becomes even more significant at increasing TH concentrations. For Spi4 a considerable decrease in growth by up to 30% was observed at a TH concentration of 10 ppm and nearly no growth was observed after addition of 20 ppm TH (Figure 3-9 A). However, the total mercury amount was reduced between 40 % at 20 ppm and 74 % at 2 ppm TH (Figure 3-9 B). In the first 1.5 h after TH addition the amount of Hg^{2+} decreased extensively (up to 50 %) but slowed down in the following hours (Figure 3-9 C), so that between 8 and 10 h of growth, no significant changes was measured for TH transformation rate.

Ps. putida KT2442::*mer*-73 was able to grow well in TH environment up to 10 ppm but a considerable decrease in growth was observed at a TH concentration of 15 ppm (Figure 3-10 A). At 20 ppm TH the cell number decreased about 20 % below the cell number before TH addition. However, approximately 40–92 % (20–2 ppm) of total mercury was reduced after 11 h of growth. Also in this batch experiment the TH concentration decreased drastically in the first 1.5 h. Moreover, the transformation rates of KT2442 was increased with higher TH concentrations between 2 and 15 ppm and showed a maximum at 15 ppm TH.

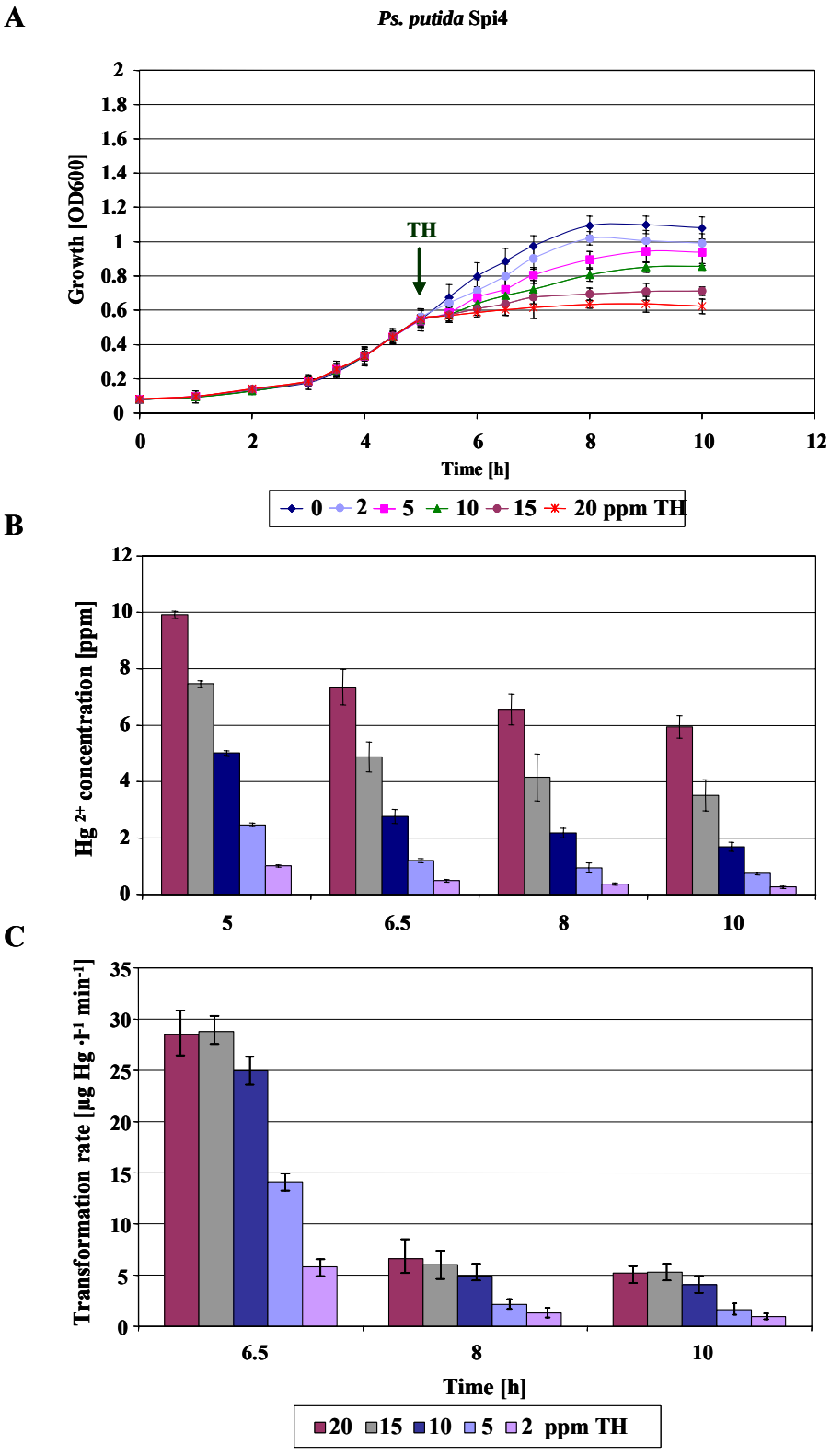

Figure 3-9. Addition of different thiomersal concentrations (2, 5, 10, 15, 20 ppm) to cells of middle logarithmic phase from *Ps. p.* Spi4. A: The cell growth was measured at 600 nm. **B:** TH was added to the samples after 5 h of growth. The Hg^{2+} concentration [ppm] during the experiment was measured with CVAAS . **C:** TH transformation rate [µg Hg·min^{-1}] during the growth. The rates were calculated from Hg^{2+} concentration in the respective sample using the intervals 5–6.5 h, 6.5–8 h and 8–10 h. The results are mean values of triplicates.

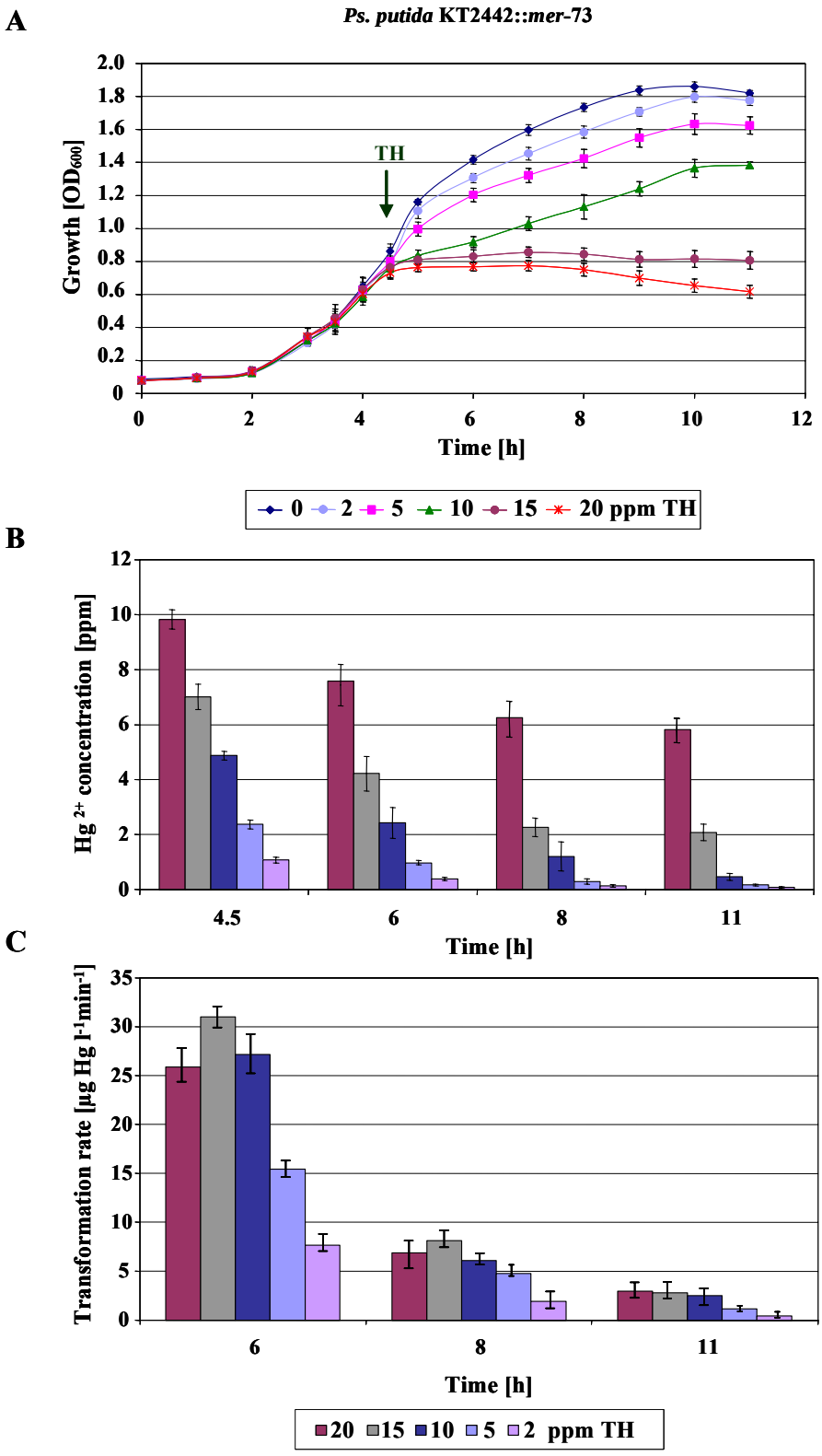

Figure 3-10. Addition of different thiomersal concentrations (2, 5, 10, 15, 20 ppm) to cells of middle logarithmic phase from *Ps. putida* KT2442::*mer*-73. A: The cell growth was measured at 600 nm. **B:** TH was added to the samples after 4.5 h of growth. The Hg^{2+} concentration during the experiment was measured with CVAAS. **C:** TH transformation rate [µg $Hg \cdot min^{-1}$] during the growth. The rates were calculated from Hg^{2+} concentration in the respective sample using the intervals 4.5–6 h, 6–8 h and 8–11 h. The results are mean values of triplicates.

In contrast, cell growth was observed in all TH concentrations for Spi11 and F1 (Figure3-11 and 3-12), similar in both samples. Only the optical density of F1 was much higher. Nevertheless, the reduction of the growth was nearly proportional to TH concentration. The growth of the two strains decreases up to 10% at 5 ppm while it reduces to 16% at 10 ppm and 22% at 15 ppm thiomersal concentration. At 20 ppm TH, a nearly 35% reduction in optical density was observed. In medium containing 2 - 10 ppm TH 98-93 % of mercury was volatized by F1 strain while 56% of Hg^{2+} remained in the solution as the cells reached the stationary period. Same results were observed by Spi11 but at 20 ppm TH only 66% of thiomersal was reduced up to the stationary phase.
A high TH transformation rate was also seen in the first 1.5 h after TH supplementation but it depended on thiomersal concentration. Increase in thiomersal concentration caused augmentation in TH transformation rate. At 20 ppm TH, the transformation rate was highest.

This capability of *Ps. putida* Spi3 to cope with high TH concentrations initiated further experiments on its resistance against thiomersal (minimum inhibitory concentration [MIC]) and on the kinetics of TH transformation to research if parameters such as density, temperature and pH have an influence on the transformation rate of thiomersal.

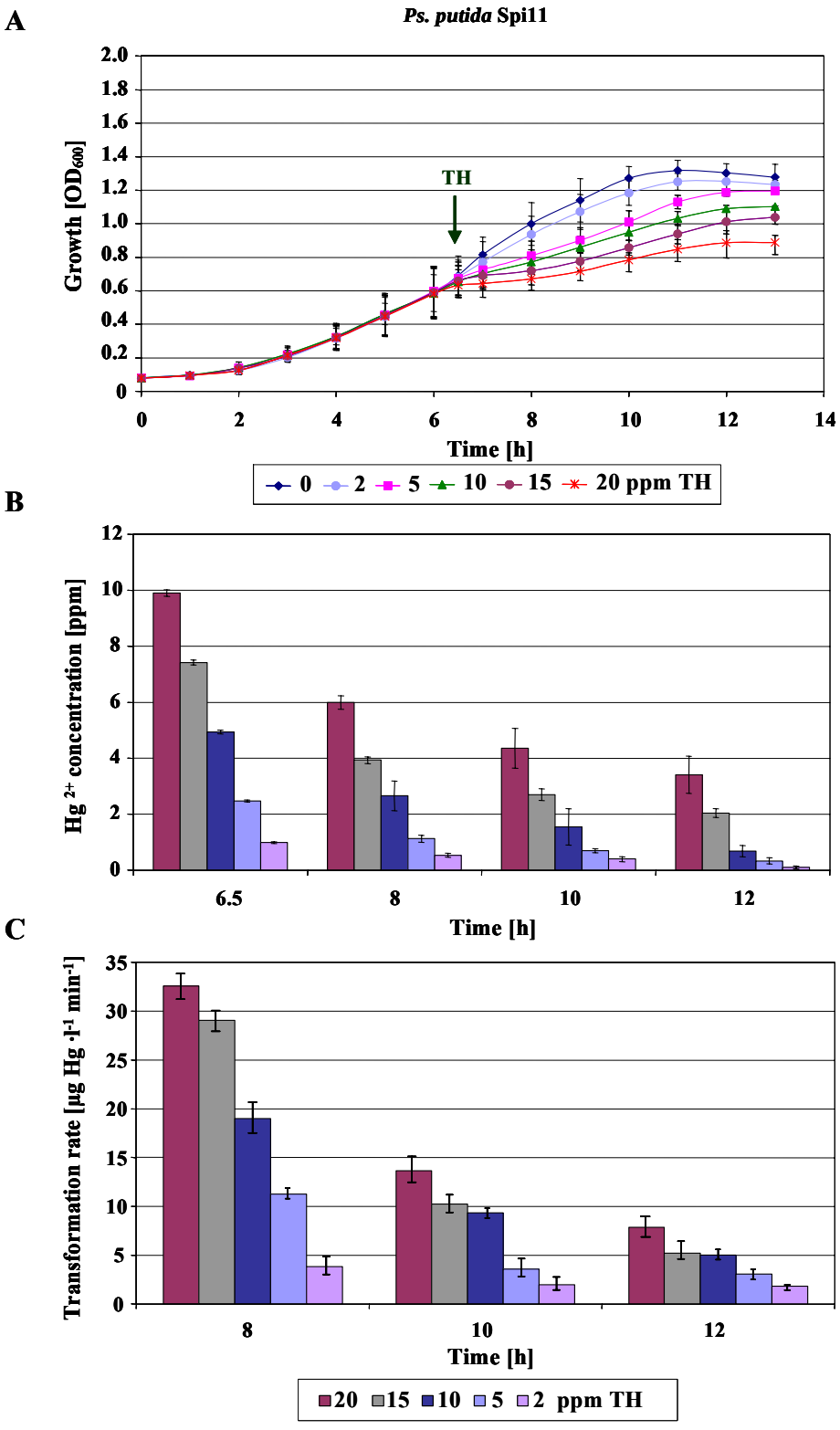

Figure 3-11. Addition of different thiomersal concentrations (2, 5, 10, 15, 20 ppm) to cells of late logarithmic phase from *Ps. fulva* Spi11. A: The cell growth was measured at 600 nm. **B:** TH was added to the samples after 6.5 h of growth. The mercury ion concentration during the experiment was measured with CVAAS. **C:** TH transformation rate [µgHg l^{-1} min^{-1}] during the growth. The transformation rates were calculated from Hg^{2+} concentration in the respective sample using the intervals 6.5–8 h, 8–10 h and 8–12 h. The results are mean values of triplicates.

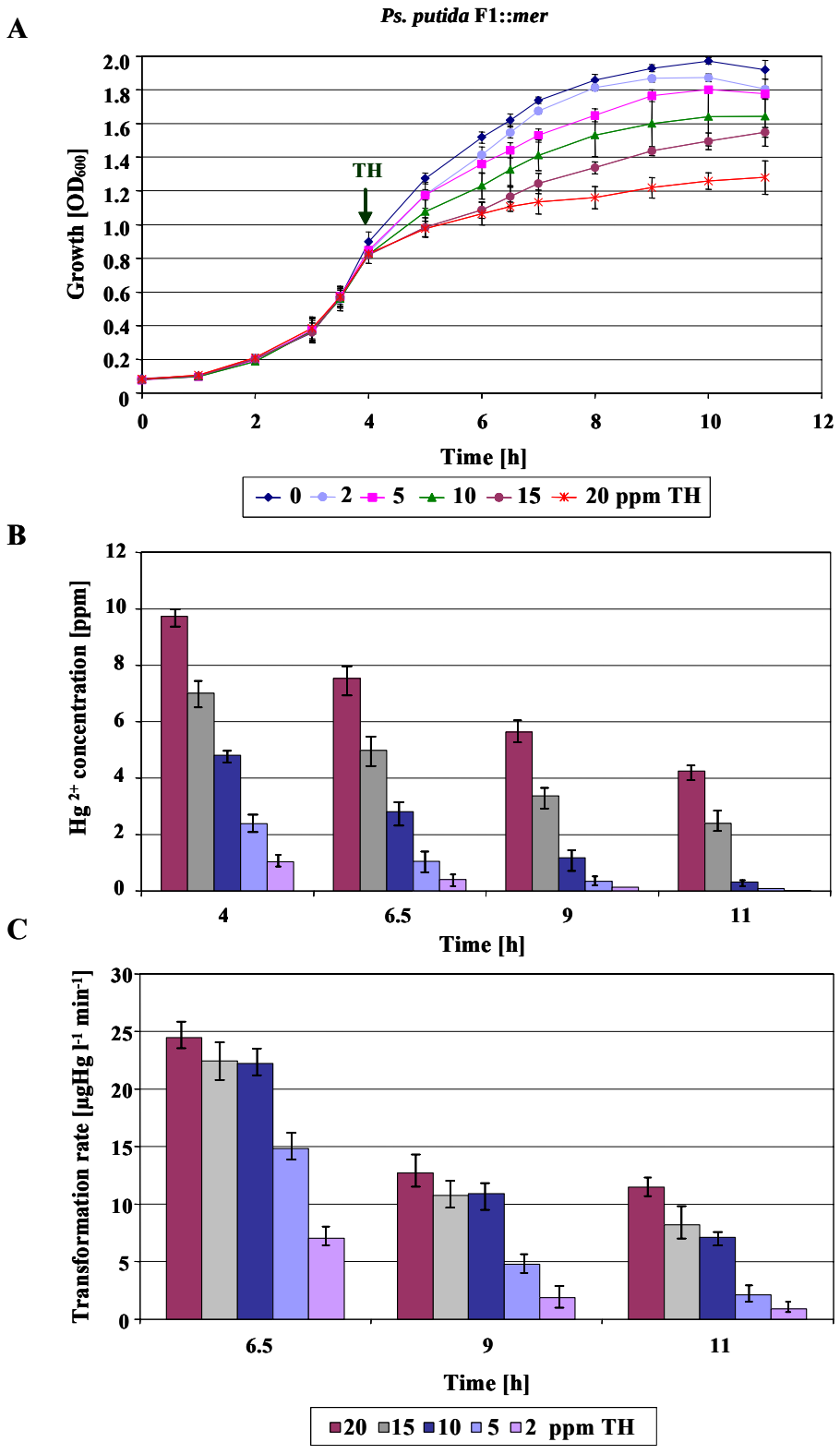

Figure 3-12. Addition of different thiomersal concentrations (2, 5, 10, 15, 20 ppm) to cells of late logarithmic phase from *Ps. putida* F1::*mer*. A: The cell growth was measured at 600 nm **B:** TH was added to the samples after 4 h of growth. The mercury ion concentration during the experiment was measured with CVAAS. **C:** TH transformation rate [µgHg l^{-1} min^{-1}] during the growth. The transformation rates were calculated from Hg^{2+} concentration in the respective sample using the intervals 4–6.5 h, 6.5–9 h and 9–11 h. The results are mean values of triplicates.

3.1.7 Thiomersal Transformation by *Ps. putida* Spi3:

Effect of TH concentration, Temperature, pH and Cell Density

3.1.7.1 *Determination of Upper Resistance Level towards Thiomersal*

The high thiomersal transformation rate of *Ps. p.* Spi3 caused to investigate further experiments to evaluate the highest TH concentration which still allowed transformation in liquid M9 minimal medium. The transformation of TH was determined using CVAAS by measuring volatized metallic mercury (for detail see section 2.6.3). The concentrations up to 120 ppm TH were done in triplicate whereas the concentrations of 140 to 160 ppm TH were carried out in sextuple.

Figures 3-13 A and B and Figure 3-14 show the transformation rates of *Ps. p*. Spi3 cells at different initial TH concentrations (5–160 ppm). The results show that the transformation rate increased with higher initial TH concentration. Spi3 was preeminent in its capability to cope with TH concentrations up to 140 ppm at which the strain achieved a transformation rate of 1488 ng Hg· ml^{-1} · min^{-1}. The different TH transformation rates between the first (Figure 3-13 A), second (Figure 3-13 B) and third experimental series (Figure 3-14) are based on the fact that the cells of different growth phases were used. The cells of the first experimental series (5-80 ppm TH) were taken at late logarithmic phase. When the dependence of the transformation rate on the TH concentrations was examined, Michaelis-Menten kinetic was observed (a nearly hyperbolic curve). With increasing TH concentration from 5 to 80 ppm the transformation rate increased to approximately 2013 ng Hg· ml^{-1} · min^{-1}, which is 3fold faster compared to the transformation rate at 5 ppm.

The TH transformation rate was determined in the second experimental series (Figure 3-13 B) with cells in the early stationary phase (1 h later than the previous measurement, due to technical problems). As a consequence the TH transformation rate was lower than in late exponential phase. Compared to prior experiments the ability to transform TH at 80 ppm (transformation rate of 823 ng Hg· ml^{-1} · min^{-1}) decreased by up to 60% due to the physiological state of the cells ("decreased activity in stationary phase cells," see also section 3.1.1). Nevertheless the TH transformation rate slightly increased about 1.8fold from 80 to 140 ppm but drastically dropped at TH concentrations of 150 and 160 ppm to approximately 350 and 155 ng Hg· ml^{-1} · min^{-1} respectively. Also, the cell number decreased drastically about 74–78 %.

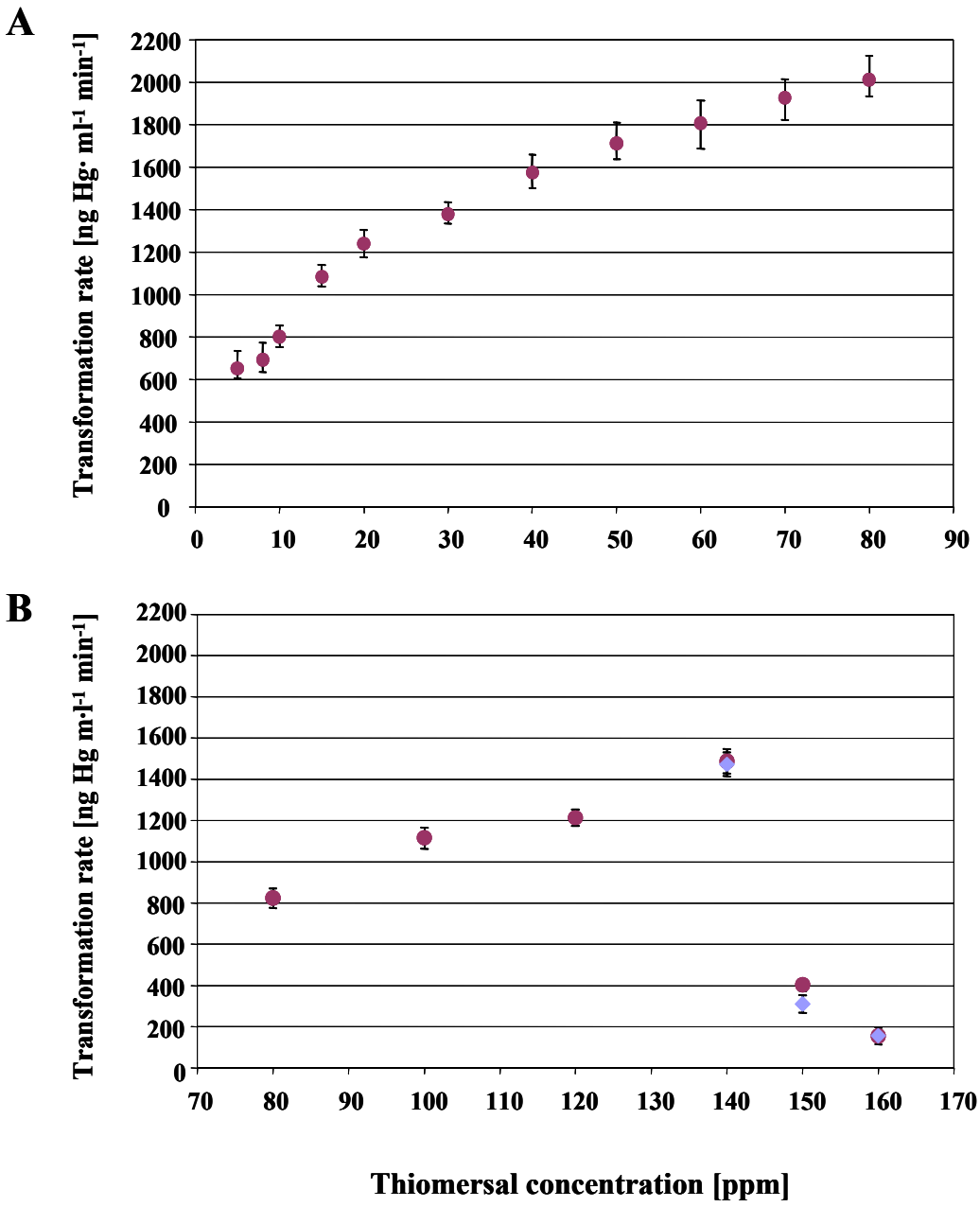

Figure 3-13 A-B. **Thiomersal transformation rate of *Ps. p.* Spi3 in M9 medium with different TH concentrations by measuring volatized Hg^0.** TH concentrations were 5, 8, 10, 15, 20, 40, 60 and 80 ppm. The cells of late exponential phase were used in the experiment and the cell density was approximately 1.9×10^7 cells ml^{-1}. **B:** TH concentrations were 80, 100, 120, 140, 150, 160 ppm. The cells of early stationary phase were injected into the M9 medium with a cell density of approximately 1.8×10^7 cells ml^{-1}. The measurements were carried out in triplicate up to 120 ppm TH in triplicate (red dots ●) and thiomersal concentrations of 140 and 160 ppm were carried out in two series and also in triplicate (● red and ◆ blue dots).

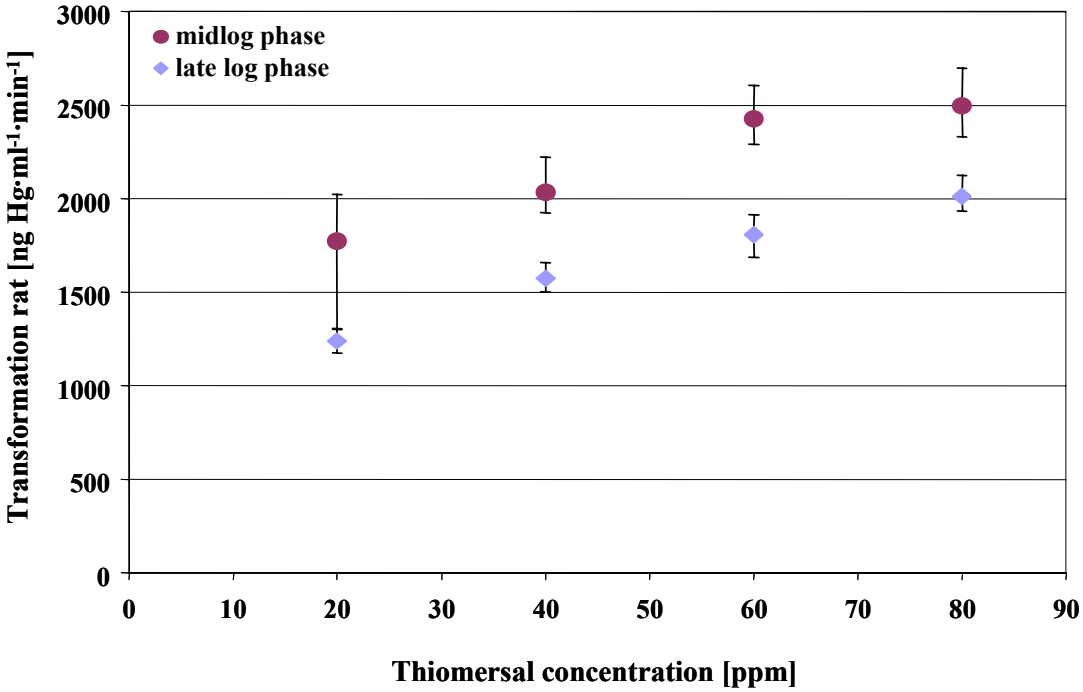

Figure 3-14: Thiomersal transformation rate of *Ps. p.* Spi3 at different TH concentrations (20, 40, 60 and 80 ppm). The cells of the 3rd Experiment were harvested at midlog phase with a cell density of approximately 1.6×10^7 cells ml^{-1} (● red dots) and cells of the 1st Experiment were harvested by late logarithmic phase (◆ blue dots). The cell density was approximately 1.9×10^7 cells ml^{-1}. Only the transformation rates of 20, 40, 60, 80 ppm TH from the 1st Experiment are represented in this figure (see also Figure 3-13).

Because it had been observed that aged cells loose their ability to transform TH efficiently, a third series of experiments was conducted to determine the impact of cell aging on thiomersal degradation. Figure 3-14 shows the thiomersal transformation activity of *P. putida* Spi3 cells at late logarithmic phase (1st experiment) and middle logarithmic phase (3rd Experiment). The detoxification rate of aged cells was clearly decreased by up to 30 %. Whereas the reduction of TH in both experiments was increased approximately to the same degree (1.5fold) as the TH concentration was increased from 20 to 80 ppm.

3.1.7.2 *Effect of pH on Thiomersal Transformation*

To determine the effects of pH on thiomersal transformation, the pH of the M9- medium was adjusted after autoclaving to 5.0 and up to 8.0 by adding concentrated HCl or NaOH to the tubes. The experiment was carried out with 5 ppm thiomersal and the final cell concentration was adjusted to 2.6×10^7cells ml^{-1}.

Figure 3-15 shows the pH dependence of the TH biotransformation rate, which is dependent on the enzyme activity of the thiomersal transforming enzymes mercuric reductase and organomercurial lyase. An optimal thiomersal biotransformation was reached at pH values of 7.0 with a maximum transformation rate of 814 ng Hg· ml^{-1}· min^{-1}. However, pH values higher and lower than 7.0 rapidly caused reduction in the TH transformation rates to 176 ng Hg· ml^{-1} · min^{-1} at pH 6 and 462 ng Hg· ml^{-1} · min^{-1} at pH 8, respectively. The transformation rate was reduced even up to 50% if pH was reduced from 7.0 to 6.5. This result clearly indicates that TH transformation of the strain Spi3 was preferentially maintained at a neutral pH, a pH optimum which is equal to the cytoplasmatic pH of *Pseudomonas*. Moreover, the data demonstrated that TH transformation is extremely sensitive to external pH values below 7.

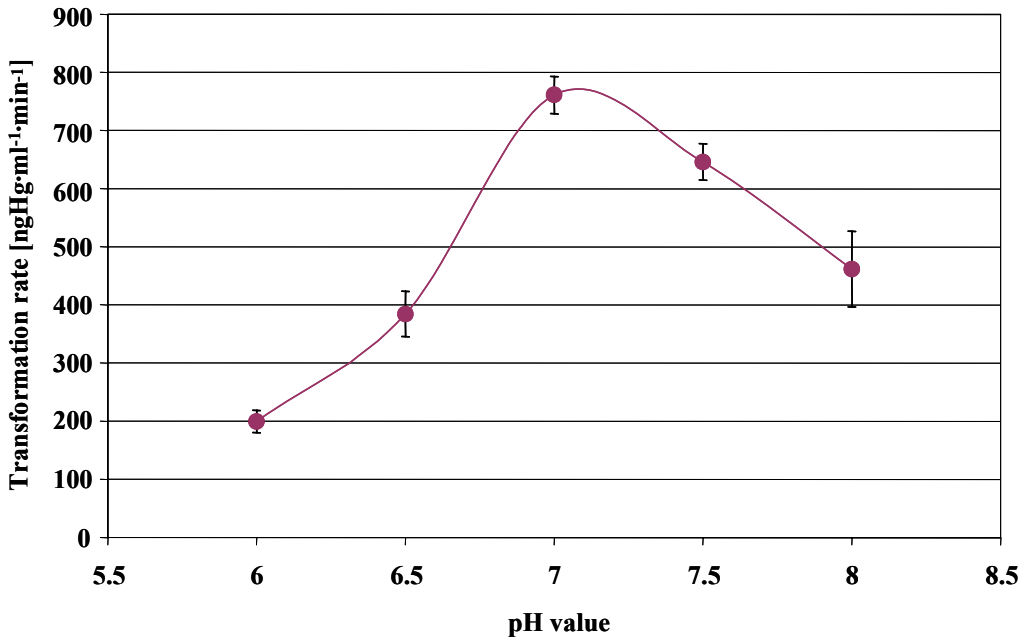

Figure 3-15. **The effect of pH on thiomersal detoxification of *Ps. putida* Spi3.** The cell density was adjusted to 2.6×10^7 cells ml^{-1}. The operation temperature was 30°C and the initial thiomersal concentration 5 ppm. The results shown are mean values of triplicates.

Due to the pH sensitivity of Spi3 for TH degradation and the pH value of 6 to 6.6 of industrial wastewater (dependent on vaccine type of GlaxoSmithKline), it is essential to pre-treat the polluted water and adjust it to a neutral pH.

3.1.7.3 *Effect of Temperature on Thiomersal Transformation*

Temperature is an important parameter affecting enzyme reaction rates. Therefore the effect of temperature on thiomersal transformation by Spi3 was investigated at 15, 20, 25, 30 and 40°C and the results are shown in Figure 3-16.

Thiomersal biodegradation was observed under a wide range of temperatures. As shown in Figure 3-16 the maximum transformation rate of approximately 700 ng Hg· ml^{-1} · min^{-1} occurred at 30 °C, a temperature that is most favorable for growth of Pseudomonads. The degradation efficiency of TH at 15°C was approximately 170 ng Hg· ml^{-1} · min^{-1} which is 4fold less than maximal transformation rate. Increasing the temperature from 15 to 20 °C led to an increase of the thiomersal transformation rate from 172 to 450 ng Hg· ml^{-1} · min^{-1} (about 60-63%). However, the transformation rates decreased by 15-32% as temperature increased from 30 to 40 °C. Therefore the results from this experimental series clearly indicate the significant influence of temperature on the TH transformation rate.

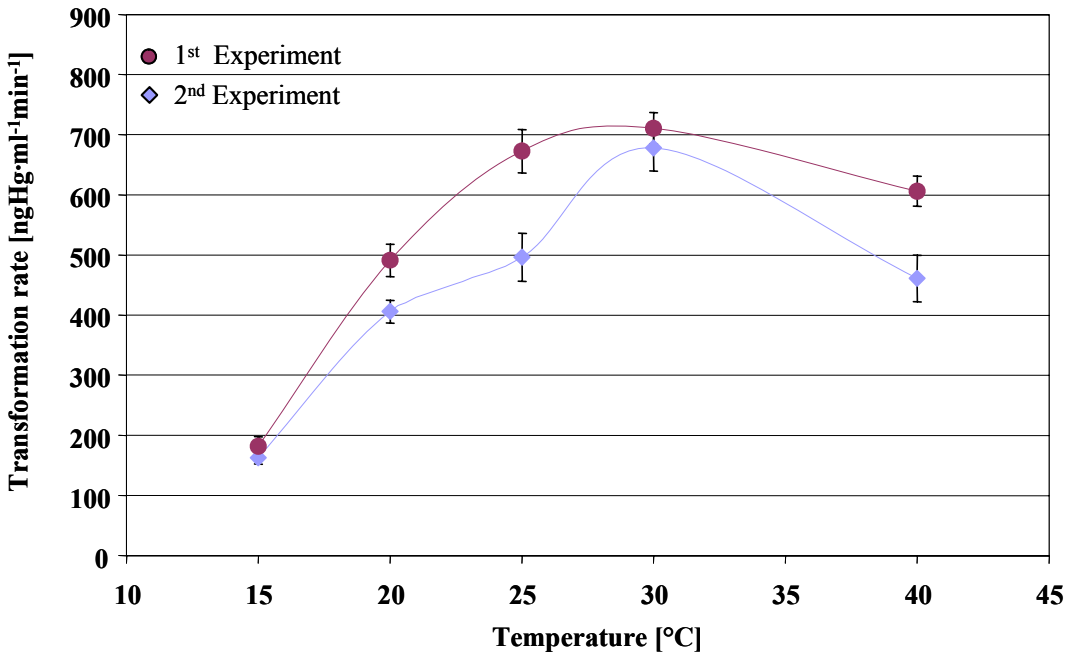

Figure 3-16. **Dependence of *Ps.p.*Spi3 thiomersal transformation on temperature with a thiomersal concentration of 5 ppm.** The cell density was adjusted to 2.7 × 10^7 cells ml^{-1}. The results are mean values of triplicate.

3.1.7.4 *Effects of Cell Density on Thiomersal Transformation*

Neither biotransformation nor growth could be observed if thiomersal was present at the beginning of the lag phase, nevertheless high biotransformation rates were measured if TH was added at midlog phase. These findings led to study the kinetics of the bacterial TH degradation process depending on cell number. The effect of cell density on TH transformation rate is shown in Figure 3-17.

When the cell number of the inoculum was below 10^5 in liquid medium containing 5 ppm thiomersal, no sign of transformation could be observed. Assays with cell density of 2×10^5 cells ml^{-1} showed a weak transformation rate of only 5-8 ng Hg per minute. However, if the initial cell number was increased to 2×10^6 (3×10^6 cells ml^{-1} respectively) the transformation rate rose to 86 ng Hg· ml^{-1} · min^{-1} (46 ng Hg· ml^{-1} · min^{-1}). A rise in the initial cell number from 10^6 to 10^7 cells ml^{-1} resulted in an additional increase of transformation rate up to 412 ng Hg· ml^{-1} · min^{-1}.

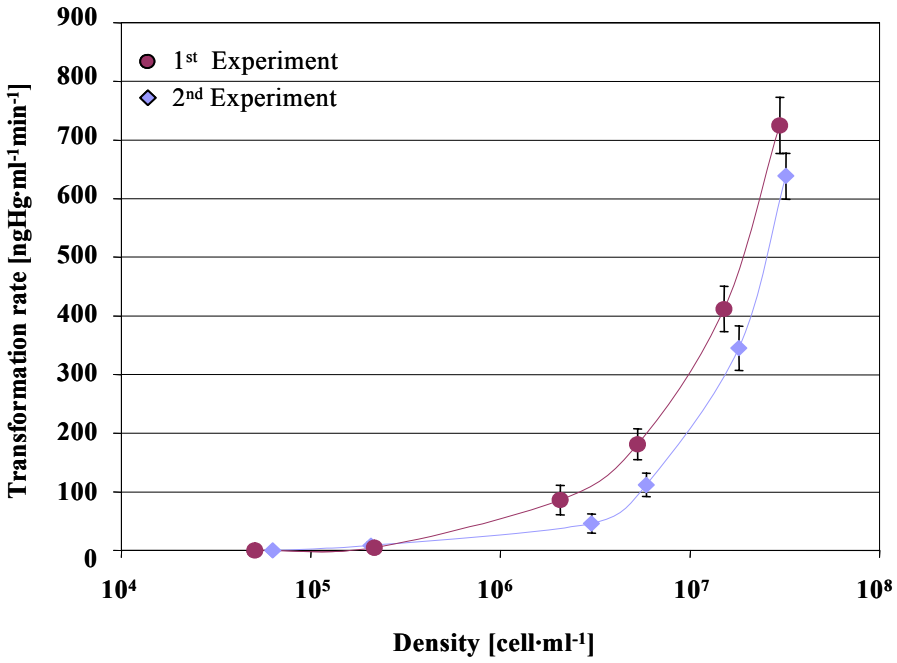

Figure 3-17. Dependence of thiomersal transformation by *Ps. p.* Spi3 on cell density at a thiomersal concentration of 5ppm. The experiments were carried out at 30 °C and a pH of 7. Two experimental series were carried out in triplicate. The results are displayed as the mean values of each experimental series.

Due to the toxicity of thiomersal, a variation in the initial cell concentration resulted in exponential differences in TH transformation rate, indicating that cell survival in the presence

of TH is very sensitive to the inoculums size. If the initial cell concentration is high enough to reduce mercury to sub-toxic levels before all the cells are killed, surviving cells would grow.

3.1.7.5 *Analysis of the Stability of Mercury Resistance in Ps. putida Spi3*

This experiment was designed to study the stability of the mercury resistance in the strain *Ps. p.* Spi3. Mercury resistance genes are often located on plasmids or transposable elements and may be lost in a mercury-free environment. If mercury resistance is located on the chromosome, it is considered to be stable. For Spi3 the location of the *mer* operon is not known. If Spi3 was used in a bioreactor that is exposed to fluctuating mercury concentrations, resistance could be lost during times when no mercury is present.

Plasmids are defined as extrachromosomal circular or linear genetic elements. Many of them are capable of self-replication and of transferring genes horizontally from one bacterium to another by which dissemination of *mer* genes occurs. R-plasmids (R = resistance) commonly carry a variety of antibiotic and heavy metal resistance genes. Plasmid loss is described as an event where plasmids are "lost" from dividing cells during replication. Bacteria lose their plasmids because of different reasons.

Firstly, maintenance of large plasmids causes a fitness reduction in the bacterial host in nutrient-limiting culture conditions (Caldwell *et al*. 1989; Modi and Adams 1991; Rhee *et al.* 1994). Studies indicate that when strains are starved, the plasmid is lost unless carrying essential genes for nutrient uptake and the rate of loss is positively correlated with the size of the plasmid (Griffiths *et al.* 1990).

Secondly, plasmids can be spontaneously lost by bacteria in an environment without selective pressure (Firshein *et al.* 1997; Gil-Turnes *et al.* 2001; Paulsson 2002). This raises the question if mercury resistant bacteria would lose their mercury resistance in a mercury-free environment.

The strain Spi3 was grown at 30°C for 10 days in mercury-free M9 minimal medium (M). The control cultures were grown under the same conditions but in the presence of 2 ppm thiomersal (MTH). Every 24 hours culture samples were inoculated into a fresh batch of the respective medium (M or MTH) and plated onto M9 agar plates with 0 or 2 ppm TH. After 10 days of incubation in medium M or MTH cells of Spi3 were inoculated in M9 medium with 0, 5 and 10 ppm thiomersal.

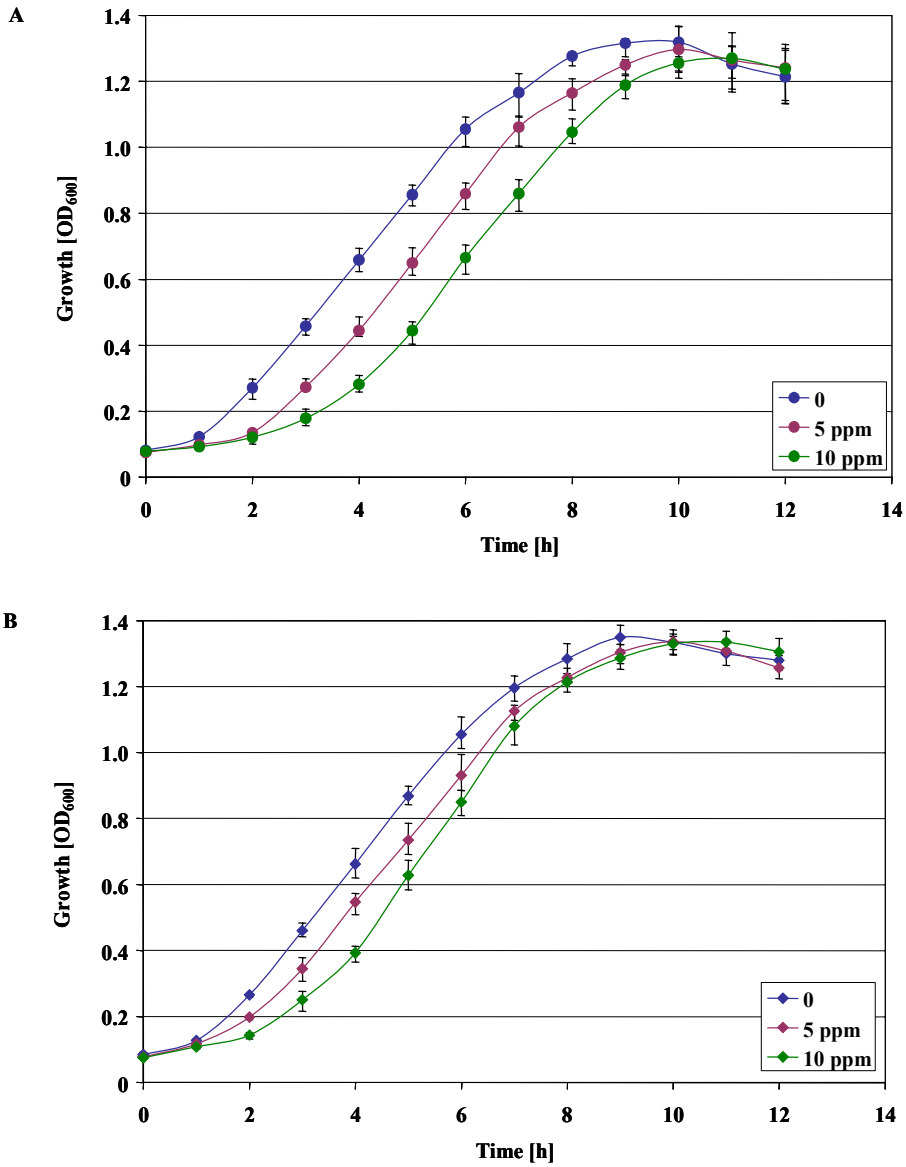

Figure 3-18. **Growth of *Ps. putida* Spi3 in M9 minimal medium containing 0, 5, and 10 ppm thiomersal (TH). A:** growth curve of cells after 10 days incubation in mercury-free minimal medium. **B:** Growth curve of Spi3 after 10 days of incubation with 2 ppm TH.

Spi3 that was initially grown in medium M was able to grow in all cultures containing TH (Figure 3-18 A). However, the strain showed a slightly delayed lag phase compared to the control (0 ppm TH) but attained approximately the same maximum optical density. Furthermore, after 10 days of incubation in M and MTH, no differences between the growth curves could be documented (Figure 3-18 A and B). However, the samples grown in medium M showed a slightly delayed lag phase in the presence of 5 and 10 ppm TH compared to the samples grown in MTH medium. Nevertheless, they attained approximately the same maximum optical density. From these results, it can be concluded that Spi3 did not loose its resistance to mercury, thus these *mer* operons are probably located on the chromosome or on

a stable plasmid which was not lost during the cultivation used here. Moreover, it may be assumed that induced regulation is the cause for the delayed "switch-on" of the resistance genes.

Figure 3-19 shows the cell number of Spi3 that grew on 2 ppm TH plates when the strain was incubated in medium M or MTH medium. Approximately 3.4×10^7 cfu·ml^{-1} was plated as determined with a control plate not containing TH.

There are distinct variations evident in the cell number. Nearly 100% of the colonies grown in a MTH retained their resistance. Differences could be observed with cells grown in the non-TH environment (M). CFU from these cultures were always decreased on 2 ppm TH plates. The average growth inhibition of Spi3 cells was approximately 40% while cells treated prior with TH (MTH) did not reveal inhibition.

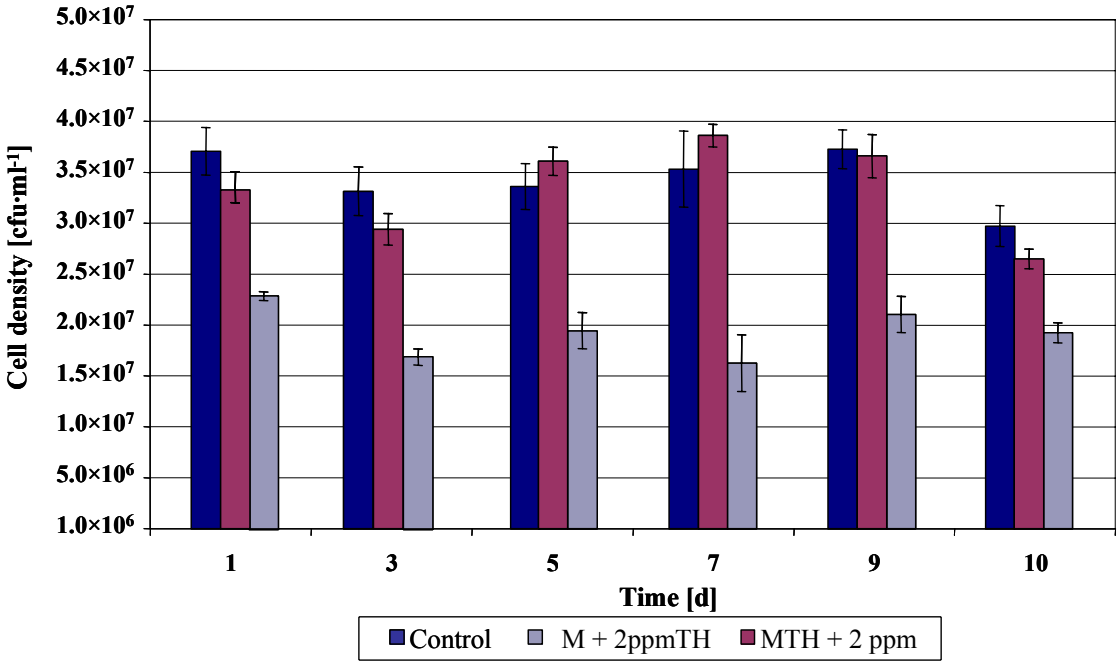

Figure 3-19. **Cell number [cfu·ml^{-1}] of *Ps. p.* Spi3 on M9 agar plates with 2 ppm thiomersal (TH) after cell growth in M9 liquid medium containing no TH (□) or 2 ppm thiomersal (■).** The control culture was grown in TH free medium and was plated on TH free plates (■). The density of Spi3 plated samples was approximately 3–3.5 × 10^7 cfu·ml^{-1} before plating.

Cell growth in liquid medium showed that resistance to mercury was not lost. However, growth was slightly delayed (see Figure 3-18), probably because induction of the *mer* operon had to occur before detoxification of mercury could take place and bacteria could begin to grow (Lund *et al* 1986; Ralston *et al.* 1990; Chang *et al.* 1998). If resistance genes were

located on a plasmid, it did not get lost. It has been shown for self-transmissible plasmids to be maintained in a culture even in the absence of a selective pressure. Nevertheless, the *mer* operon could be stably located on the chromosome. In a bioreactor, fluctuation of mercury concentration would cause no decrease in detoxification ability.

3.2 Selection of a Counter-ion for the Ion-Exchange Membrane Reactor

3.2.1 Substrate Biodegradation

The purpose of this experiment was to characterize the isolates with the Biolog GN microplate system with regard to their utilization of different carbon sources for a pre-selection of a suitable counter-ion for an ion exchange membrane bioreactor. This type of bioreactor excludes direct contact of the microbial culture with the toxic wastewater (see Figure 1-3). A suitable counter-ion, which is added to the biological compartment, enables the flux of thiomersal to the biocompartment. Therefore, the counter ion has to be biologically inert to avoid metabolization by the isolates.

The Biolog GN MicroPlates™ system (Biolog Inc., Hayward, CA) was originally designed to identify bacterial isolates on the basis of sole carbon substrate utilization profiles of microorganisms. MicroPlates are 96 well microtitre plates containing 95 different carbon substrates (see Materials and Methods, 2.3.3) and one control well containing water. Utilization of a carbon source was indicated by a colorless tetrazolium redox dye being reduced to a colored formazan product. Absorbance values of the color response in each microplate well were recorded at 590 nm.

In Figure 3-20 the variability of substrate utilization of *Ps. p.* Spi3, *Ps. f.* Spi11, *Ps. p.* F1::*mer* and *Ps. p.* KT2442::*mer*-73 is demonstrated. Substrates are grouped by their biochemical properties (carbohydrates; carboxylic acids; amines; amides; amino acids; alcohols; aromatic chemicals; polymers). The average well color development (AWCD) was calculated according to Garland and Mills (1991) as described in Materials & Methods (section 2.3.3) and the utilization is expressed as percentage of respective amounts of substrates belonging to a specific substrate group in Biolog GN microplates that could be metabolized by the isolates (see section 2.3.3).

The pattern of positive responses to the 95 substrates in Biolog GN microplates was similar for strains belonging to the same genus. For all strains, some substrates were always utilized and were scored positive in all replicates after 24 h of incubation, while other substrates were

scored as negative even after 72 h of incubation. For example, all tested strains were consistently able to utilize esters and brominated chemicals but in contrast no coloration was observed in the wells containing phosphorylated chemicals. The three *Ps. putida* strains exhibited similar profiles; each primarily metabolized amines (100% of the specific substrate group), alcohols (100%), amino acids (75-95% of the specific substrate group), carboxylic acids (63-71% of the specific substrate group) and various carbohydrates. They only showed differences with the utilization of amides and amino acids. While the strains KT2442 and Spi3 only metabolized up to 30% of the amides, *Ps. p.* F1 was able to make use of almost all amides. Slightly different results were obtained for *Ps. fulva* Spi11 which utilized the same specific groups in the Biolog GN microplates as *Ps. p.* F1, however, with different intensity. Spi11 metabolized up to 80% of the amino acids and aromatic chemicals but only 33% of the amines.

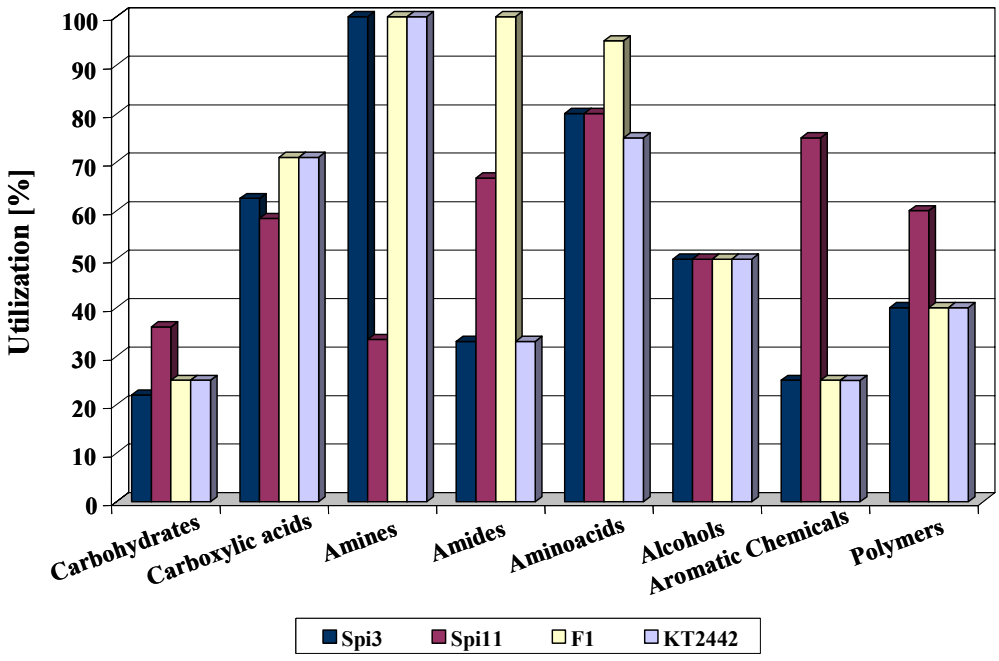

Figure 3-20. Utilized substrates in Biolog GN microplates measured as dye formation after 48h for *Ps. p.* Spi3, *Ps. f.* Spi11, *Ps. p.* F1::*mer* and *Ps. p.* KT2442::*mer*-73. Utilization is expressed as the percentage of carbon substrates in a specific group of Biolog GN microplates.

Interestingly, the utilization of carbohydrates by all strains over the experimental period was markedly narrow (22–36%). In contrast, up to 70 % of the carboxylic acids were metabolized which limits the selection of a suitable counter-ion as mainly carboxylic acids were considered as suitable counter-ion for the ion exchange membrane bioreactor to facilitates the

flux of TH to the biocompartment (Table 3-4). The non-utilized carboxylic acids (D-Galactonic acid, D-Glucosaminic acid, α-Hydroxy butyric acid, γ-Hydroxy butyric acid, p-Hydroxy phenylacetic acid, Itaconic acid, α-Keto butyric acid, Malonic acid, Sebacic acid) were not considered as suitable counter-ions due to their molecular structure as appropriate counterpart regarding to TH.

Table 3-4. Utilization of carboxylic acid by measured as dye formation after 48h for Spi3, Spi11, F1 and KT2442. Utilization of carboxylic acid is indicated as (+) and non-utilized as (–).

Carboxylic acids	Spi3	Spi11	KT2442	F1
Acetic acid	+	+	+	+
Cis-Aconitic acid	+	+	+	+
Citric acid	+	+	+	+
Formic acid	+	+	+	+
D-Galactonic	+	+	+	+
Acid Lactone	+	+	+	+
D-Galacturonic acid	–	–	–	–
D-Gluconic acid	+	+	+	+
D-Glucosaminic acid	–	+	–	–
D-Glucuronic acid	+	–	+	+
α-Hydroxy butyric acid	–	–	+	+
β-Hydroxy butyric acid	+	+	+	+
γ-Hydroxy butyric acid	–	–	+	+
p-Hydroxy phenylacetic acid	+	–	–	–
Itaconic acid	–	–	–	–
α-Keto butyric acid	–	–	–	+
α-Keto glutaric acid	+	+	+	+
α–Keto valeric acid	–	+	+	+
D,L-Lactic acid	+	+	+	+
Malonic acid	–	+	–	–
Propionic acid	+	–	+	–
Quinic acid	+	+	+	+
D-Saccharic acid	+	+	+	+
Sebacic acid	–	–	–	–

3.2.2 Selection of Possible Counter-ions

For the membrane reactor it is of particular importance to use a suitable counter-ion to facilitate the flux of thiomersal anions to the biocompartment. Selecting the appropriate counter-ion for an ion-exchange membrane depends firstly on charged substances (negatively charged) in the solution (thiomersal) and on the ion-exchange membrane. For example, it is important to use a counter-ion having no or very low affinity for the ion-exchange membrane

and to be biological inert. The following carboxylic acids were considered suitable counter-ions due to their molecular structure as appropriate counterpart regarding to TH: iso-butyric acid (iBA), iso-valeric acids (iVA), propylphosphonic acid (PPA), tert-butylphosphonic acid (TBPA), pivalic acid (PA), tertbutylacetat (TBA) and 2,2dimethylbutylacetat (DMBA). These substrates were not presented in the Biolog GN MicroPlates™ system and the degradation had to be examined additionally.

To analyze if the chosen carboxylic acids were metabolized, *Ps. p.* Spi3, *Ps. p.* Spi4, *Ps. fulva* Spi11, *Ps. p.* KT2442::*mer*-73 and *Ps .p.* F1::*mer* were incubated with 10 mM of the seven selected substrate for 24 h in M9-medium at 30 °C. Control cultures were grown under the same conditions but in the absence of carboxylic acids and with sucrose as sole carbon source. A second culture series was prepared with sucrose but also with the respective carboxylic acid to determine if there was elevated growth during the experimental period (third series in the Figure 3-21, 3-22 and 3-23). Due to the non-solubility of pivalic in medium at room temperature (melting point 36°C), batch cultures containing PA were incubated at 37 °C. The optical density was measured after 12 and 24h and the number of living cells was determined after 48 h. The results from the growth experiments with the selected carboxylic acid from growth experiment are shown in Figure 3-21, 3-22 and 3-23.

Growth was found in all cultures with iso-buturic acid (iBA), iso-valeric acids (iVA), propylphosphonic acid (PPA), tert-butylphosphonic acid (TBPA) Accordingly, elevated cell growth in the presence of these four chemicals with sucrose (Figure 3-21 and 3-22) could also be observed. iBA and iVA can be used in limited amounts for long-chain fatty acids synthesis and for amino acid synthesis through reverse reactions (Van Soest, 1989).

With iBA, iVA and PPA *Ps. p.* Spi3 could grow to the same optical density as with sucrose. In contrast Spi4 and KT2442 were not able to utilize iBA and iVA for growth.

In the presence of PA, TBA and DMBA there was no cell growth and the turbidity at 600 nm of approximately 0.07 that was detected at the end of the experiment was similar to the initial cell turbidity (Figure 3-23). Pivalic acid was excluded from further experiments due to its non-solubility at 30°C and due to the fact that maximum TH transformation rate occurred at 30 °C (see Figure 3-16). However, PA was tested as a carbon source at 37°C. Tertbutylacetat (TBA) and 2,2dimethylbutylacetat (DMBA) were therefore selected as candidates to be used as counter ion. To have more detailed results growth experiments and measurements of Hg^0 volatilization by bacteria were carried out with thiomersal in the presence of the two carboxylic acids.

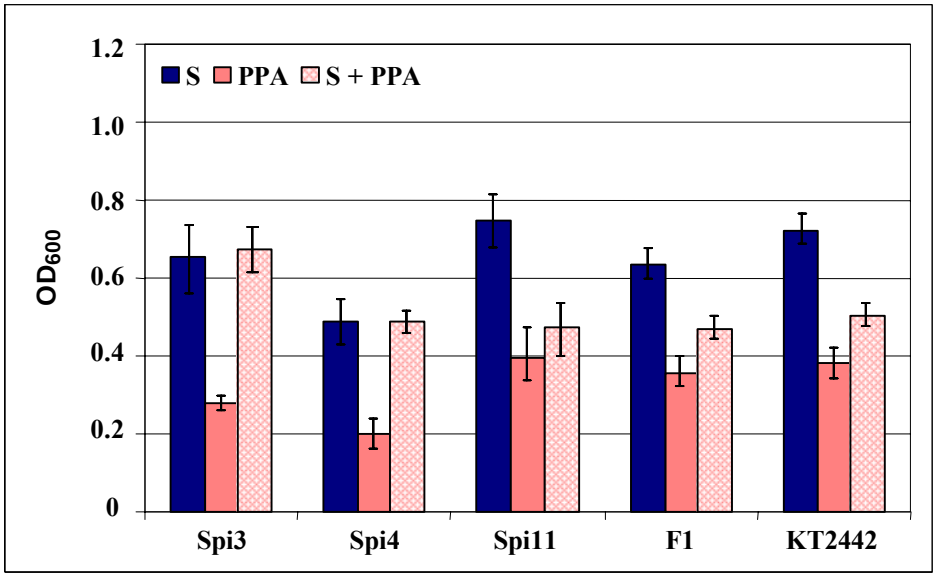

Figure 3-21. **Utilization of propyl phosphonic acid (PPA) as carbon source by different isolates.** Each culture was grown under three conditions: with sucrose as control (S = Sucrose), only with the propyl phosphonic acid (PPA) and with sucrose and PPA. The results are mean value of triplicate samples.

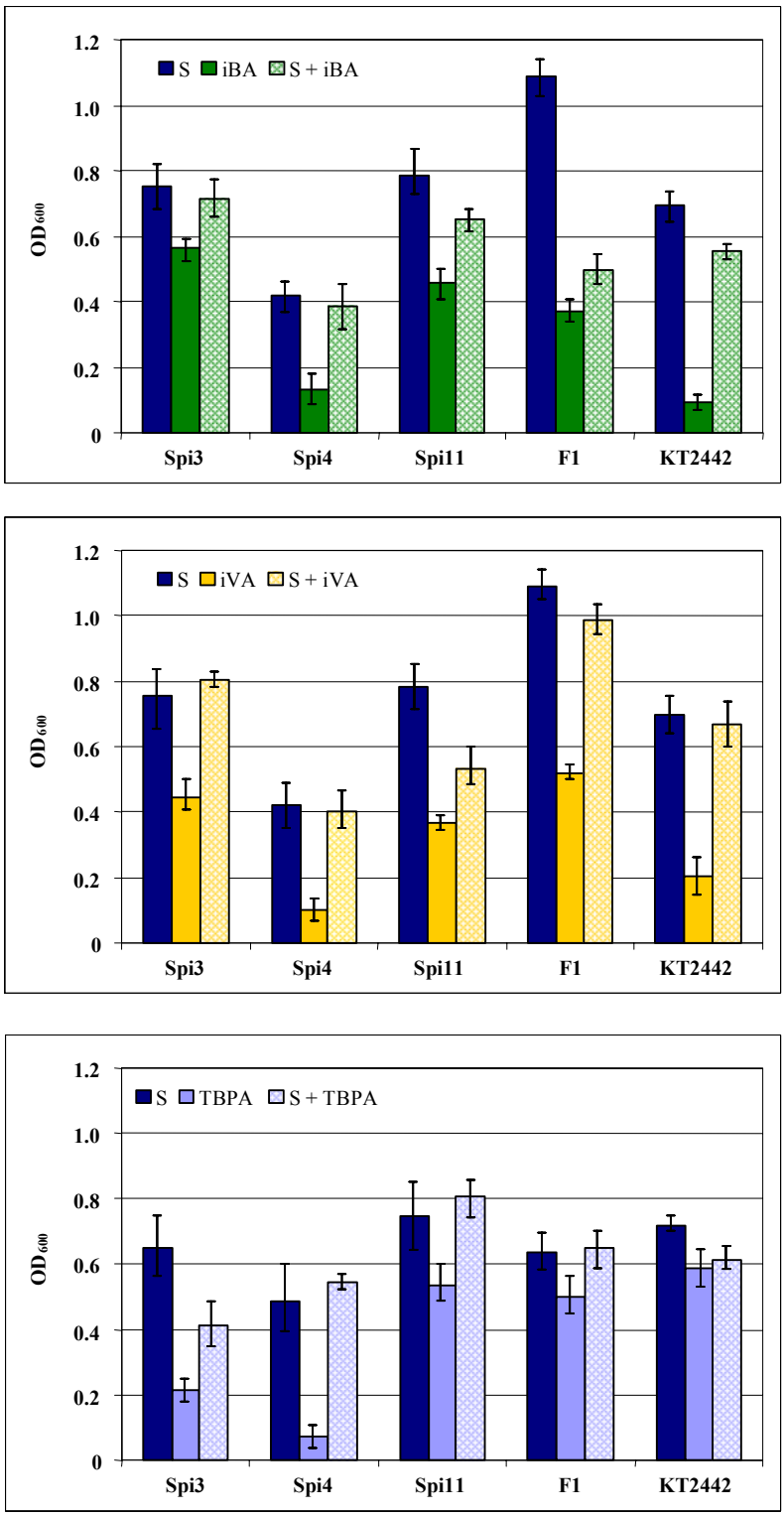

Figure 3-22. Utilization of three different carboxylic acids (iBA, iVA and TBPA) as carbon sources by different isolates. S = Sucrose; iBA = iso-buturic acid; iVA = iso-valeric acids; TBPA = tert-butylphosphonic acid. Each culture was grown under three conditions: with sucrose as control, with the respective carboxylic acid (iBA, iVA and TBPA) and in with sucrose and the respective carboxylic acid. The results are mean value of triplicate samples.

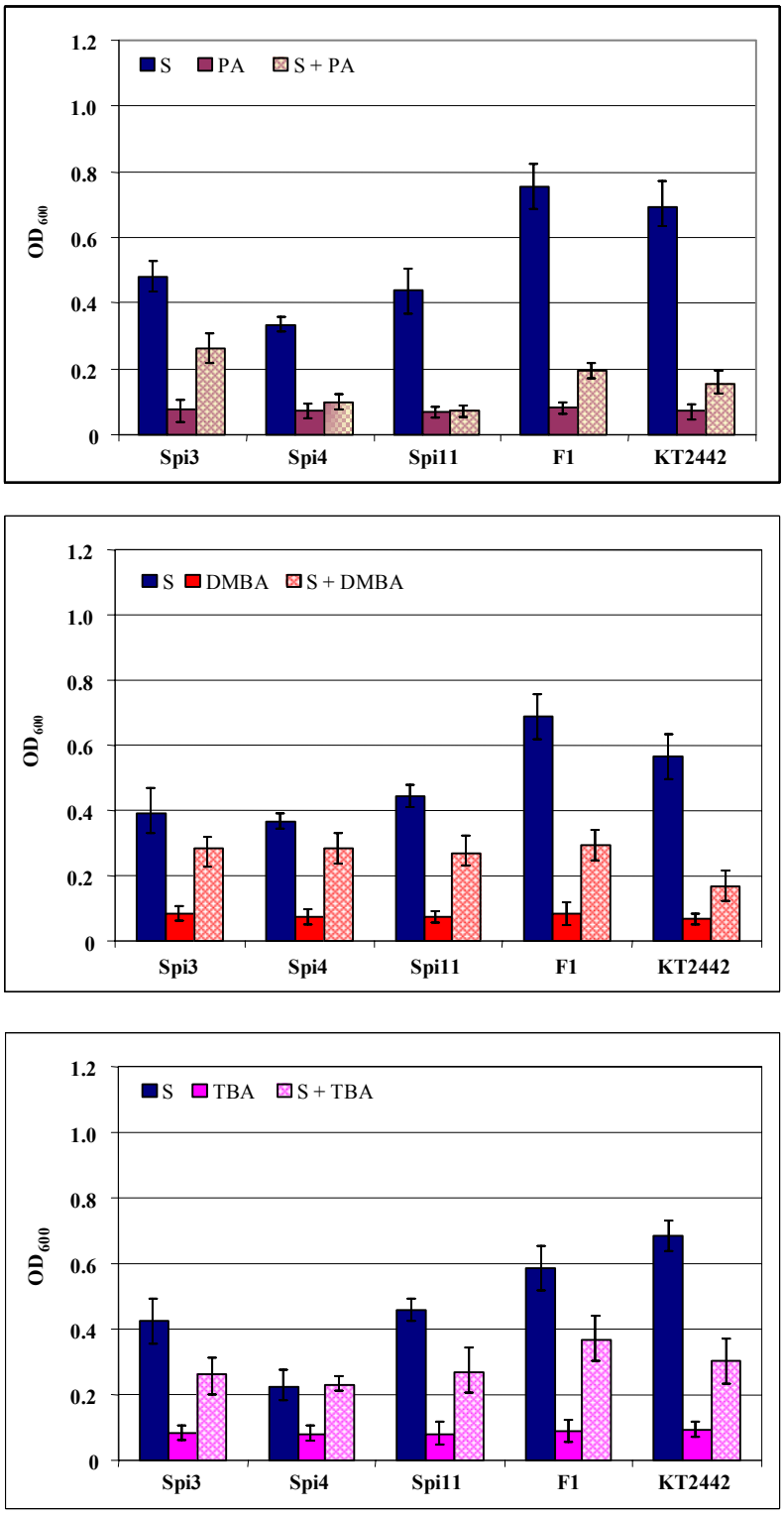

Figure 3-23. Utilization of another three carboxylic acids (PA, DMBA and TBA) as carbon sources by different isolates. S = Sucrose; PA = pivalic acid; DMBA = 2,2'dimethylbutylacetat; TBA = tert-butylacetat. Each culture was grown under three conditions: with sucrose as control, with the respective carboxylic acid (PA, DMBA, TBA) and with sucrose and the respective carboxylic acid. The results are mean value of triplicate samples.

3.2.3 Growth of *Ps. p.* Spi3 in the Presence of Counter-ions and Thiomersal

As shown above, all isolates were incapable of utilizing tertbutylacetat (TBA) and 2,2dimethylbutylacetat (DMBA) as sole carbon sources. Thus they are candidates to be used as counter-ions in the membrane reactor. Consequently, growth experiments were carried out in batch mode, using M9 medium to determine the effect of the TBA and DMBA on *Ps. p.* Spi3 growth in the presence of 5 ppm TH. In all samples 10 mM sucrose was used as carbon source. A control culture was grown under the same conditions but in the absence of carboxylic acids and TH. A second control sample contained only 5 ppm TH. Test cultures and the control cultures were prepared in triplicate. Of each carboxylic acid (TBA and DMBA) 10 mM were added to the medium from concentrated stock solutions.

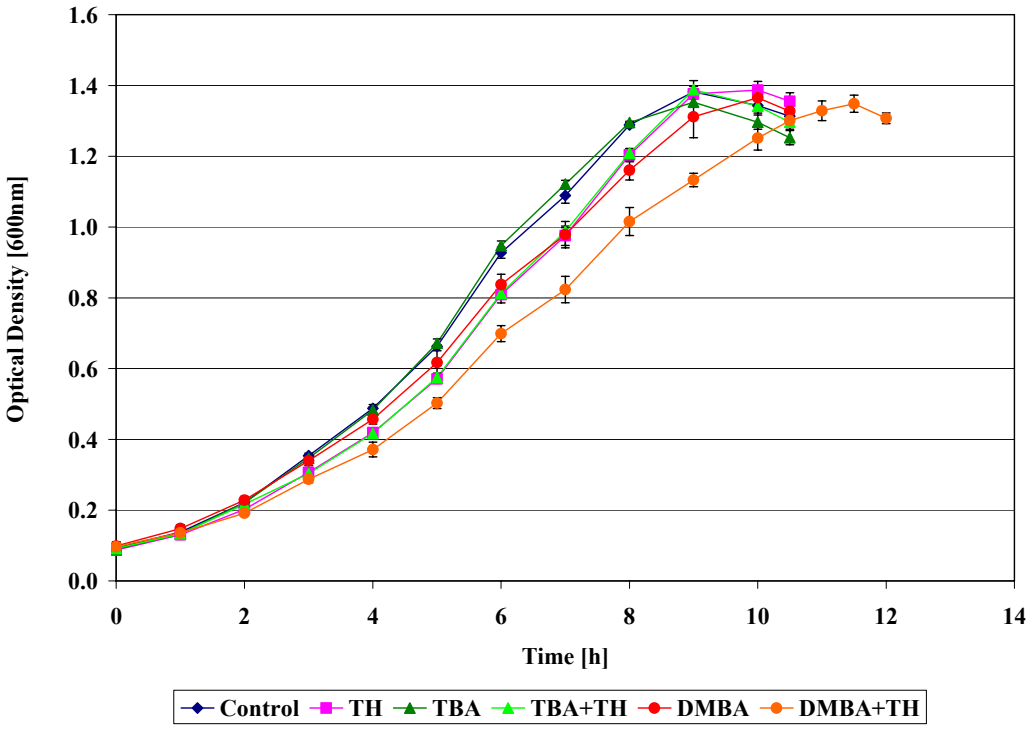

Figure 3-24. Growth of *Ps. p.* Spi3 with tertbutylacetat (TBA) or 2.2′dimethylbutylacetat (DMBA) in the presence or absence of thiomersal (TH). Sucrose was used as carbon source in all samples. The values shown represent the average of triplicate cultures.

Growth yields of Spi3 did not differ greatly among the substrates tested (Figure 3-24). In the presence of the counter-ions neither a clearly marked inhibition nor promotion of cell growth was observed. Solely, the samples containing DMBA with thiomersal had a slower rise but

grew to similar maximum optical density. A comparable growth curve was observed with the TH control samples and the cultures containing TBA + TH. However, if the cell density was observed, distinct differences between the samples could be found (Figure 3-25).

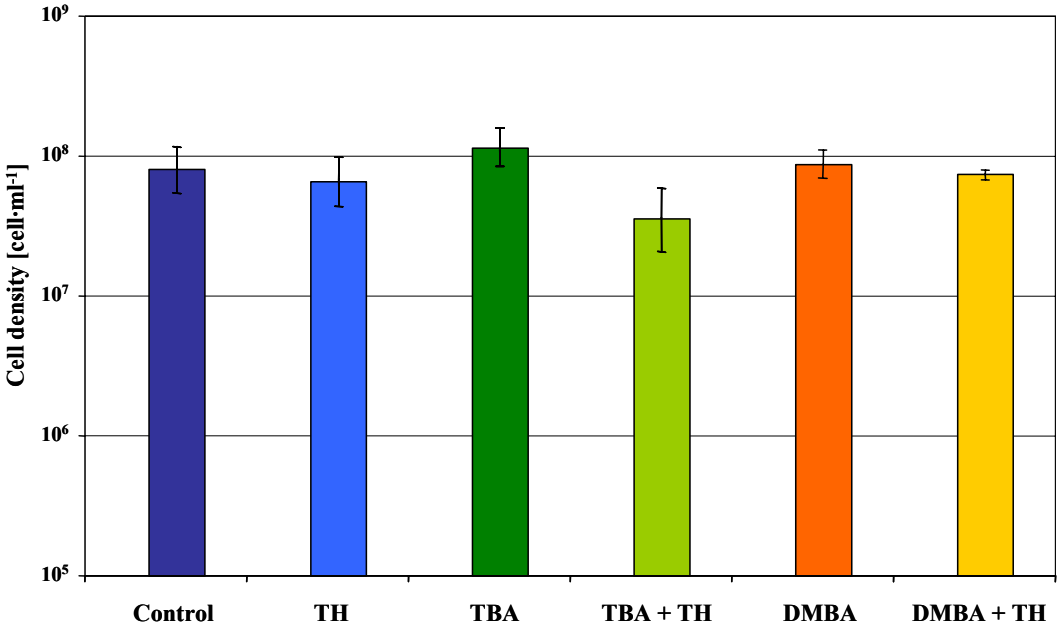

Figure 3-25. Cell number [cell·ml^{-1}] of the *Ps. p.* Spi3 after 10-11h of growth with thiomersal (TH), tert-butylacetate (TBA) and 2,2 dimethylbuturic acid (DMBA). In each case the samples were with or without thiomersal (as indicated). The initial Spi3 density in all samples was 1×10^6 cfu·ml^{-1}. The control culture was grown only with sucrose as sole carbon source.

The cell number in the samples containing TBA were up to 42 % increased (1.14 x 10^8 cell·ml^{-1}) as compared to the sucrose control culture while TBA samples with thiomersal (TBA + TH) showed an inhibition of Spi3 cells of about 56 % (3.55 x 10^7 cell·ml^{-1}). In contrast on this the cell number of the batch cultures containing sucrose and TH was only slightly inhibited (6.54×10^7 cell·ml^{-1}). *Ps. p.* Spi3 cells in DMBA + TH had a decelerated growth but grew to similar maximum optical densities (Figure 3-24). The cell density was approximately equal to the TH and control samples. Also the cell number of Spi3 in the presence of DMBA reached a similar density as the control culture. This could be an indication that DMBA was biologically inert while TBA was metabolized.

3.2.4 Effect of the Selected Counter ion on TH Transformation

Further investigations were carried out by measuring the volatized Hg^0 in the presence of DMBA and TBA with CVAAS.

The M9 minimal medium used in the assay contained 5 ppm TH with 10 mM sucrose and further assays included in addition 10 mM TBA or 10 mM DMBA. The initial cell concentration was adjusted to approximately 2×10^7 cells· ml^{-1}.

Figure 3-26 demonstrates the effect of DMBA and TBA on TH transformation by *Ps. p.* Spi3 cells. The results showed little differences among the transformation rates of all three samples. Nevertheless, TH transformation was slightly inhibited by 10 mM TBA while thiomersal transformation did not differ in the presence of 10 mM DMBA.

From these experiments DMBA and with similarly good characteristics TBA could be selected to be the counter-ion of the choice.

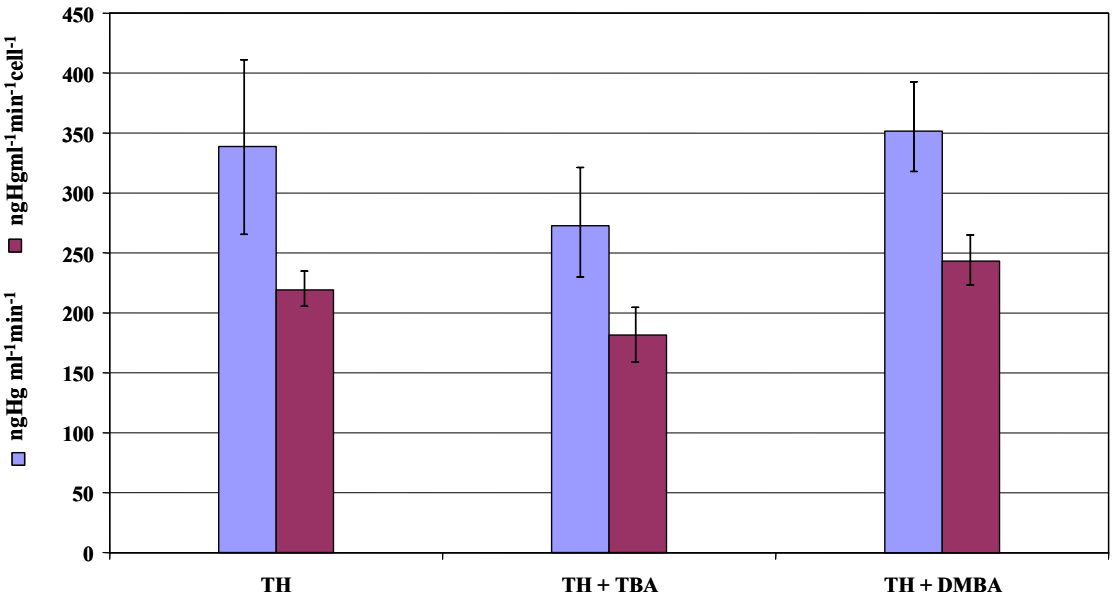

Figure 3-26. **Biotransformation of 5 ppm thiomersal (TH) in M9 minimal medium containing 10 mM of tertbutylacetat and 2,2′dimethylbutylacetat.** The initial cell density was adjusted to approximately 2×10^7 Cell·ml^{-1}. Sucrose (10mM) was added to all samples as carbon source.

3.3 Optimization of the Cultivation Condition for Thiomersal Detoxification

3.3.1 Biofilm Formation

Direct microscopically observation of a wide variety of natural habitats has shown that the majority of microbes persist attached to surfaces within a structured biofilm ecosystem and not as free floating organisms (Costerton *et al.* 1995). Bacterial communities in nature play a key role in the degradation of many environmental pollutants, such as heavy metals. Most of these natural processes require the concerted effort of bacteria with different metabolic capabilities. It is likely that bacteria residing within biofilm communities carry out many of these complex processes. With respect to an ion exchange bioreactor a biofilm can be developed on the membrane surface, where pollutants undergo a bioreduction reaction inside this biofilm. Moreover, biofilm development might be considered beneficial for mass transfer and consequently increase the degradation process. In the course of the process evolution, however, the specific detoxifying activity of the biofilm could decrease, thus leading probably to an extended reaction zone required for bioreduction, and a corresponding increase of the biofilm thickness and overall mass transfer resistance (Velizarov *et al.* 2001). Therefore, it is important to determine the ability of biofilm formation by the investigated isolates. The ability of each strain for biofilm formation was tested in M9 medium with 20 mM sodium acetate. On the basis of retained safranin O on the glass test tubes the relative amounts of produced biofilms could be derived.

The results of bacterial growth and safranin O absorption representing biofilm formation are shown in Figure 3-27.

Nine of ten isolates were able to form a biofilm within 24 h but the capacity for biofilm formation varied extensively. While Ibü8 and Kon12 clearly produced higher biofilm mass, Bro12 and Tin2 showed a minimal formation of biofilm. Biofilm did not seem to correlate with the maximum optical density at 650 nm of the growth experiments. The two GEMs differed greatly in their biofilm formation. Even though F1 reached the highest cell number of the ten tested strains, the biofilm formation was minimal (second lowest). KT2442 on the other hand formed distinctly higher biofilm mass (third highest) compared to cell growth while the cell density was only mediocre compared to the other strains. The natural isolates Spi3, Spi4 and Spi11 showed similar biofilm formation between each other.

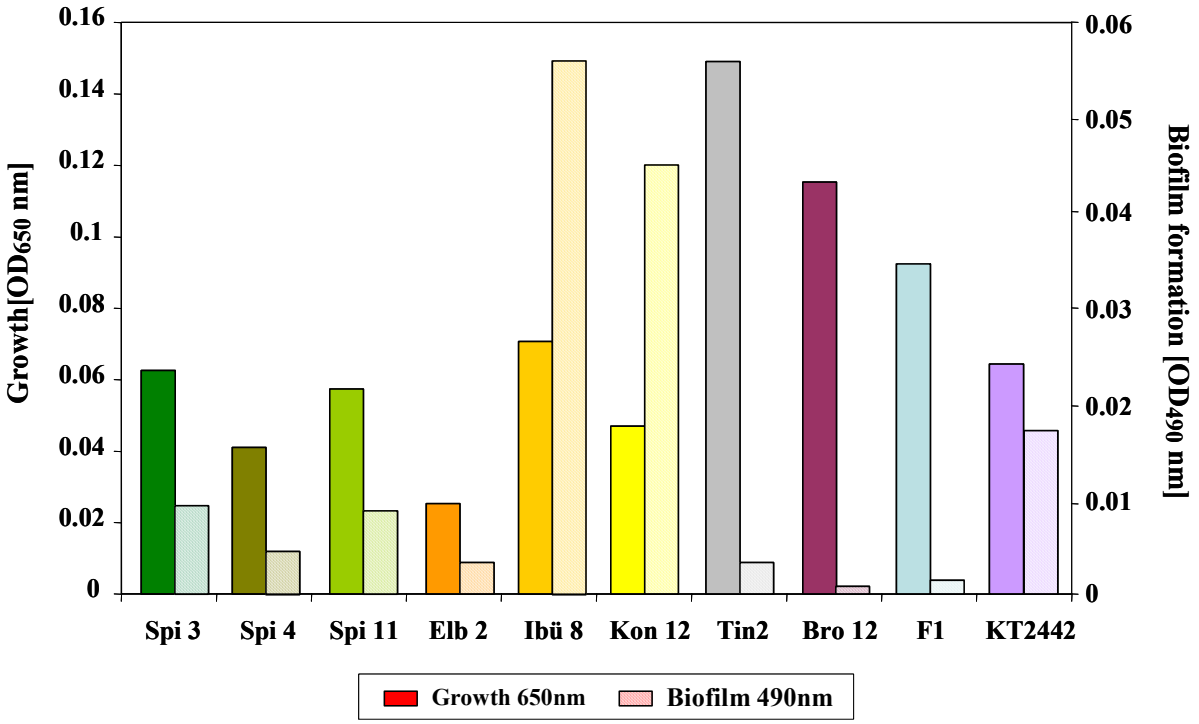

Figure 3-27. **Microbial growth and biofilm formation in M9 minimal medium after 24 h incubation.** Microbial growths of 10 isolates are measured at 600nm and are illustrated as filled columns. The biofilm formations are measured at 490 nm and are shown as dashed columns. The results of biofilm formation are presented on the secondary y-axis.

3.4 Biotransformation of Thiomersal under Steady State Conditions

The cultures so far discussed for growth of bacterial populations are called batch cultures. Since the nutrients are not renewed, exponential growth is limited to a few generations. Bacterial cultures can be maintained in a state of exponential growth over long periods of time using a system of continuous culture. The addition of fresh medium to such a batch culture during exponential growth at a suitable rate would allow growth to proceed indefinitely at a given rate. Consequentially, the culture volume and biomass would increase exponentially without the removal of culture at the rate of fresh medium input, as occurs in continuous culture. The advantage of this system is that the microbial population within the bioreactor then grows at a constant rate in a constant environment and assumes a ‘steady state’. Environmental factors such as pH, nutrient concentration (including oxygen) and metabolic products can be varied, controlled and optimized. The aim of this experiment was to determine the thiomersal transformation rate under steady state conditions. It also means that no component is truly exhausted, thus avoiding stress response transcription which could mask effects resulting specifically from nutrient limitation.

A lab-scale bioreactor using *Pseudomonas putida* strains was set up and operated continuously to investigate the applicability for treatment of TH contaminated environment. As described by Farrell (1993), the chemical composition of a medium containing yeast extract can have a significant effect on the reactivity and bioavailability of mercury. Hence, an accurately defined mineral salt medium (M9-medium) with sodium acetate was chosen as growth medium for more genuine results with regard to the bio-availability and toxicity of TH and its product, the mercury ion (Hg^{2+}). Each dilution rate was kept up at least 1.5 times longer than the corresponding cell retention time.

The steady-state data are expressed as the average of values obtained from samples at steady state (at least three times for each run). Results of experimental runs performed at different dilution rates are shown in Figures 3-28 and 3-29. At the beginning of the cultivation the bioreactors were inoculated with 10 % of the respective inoculum. The experiment started when the cultures reached stationary phase with a cell density of 7.6×10^7 cfu ml^{-1} in the bioreactor A (*Ps. putida* Spi3) and 8.5×10^8 cfu ml^{-1} in bioreactor B (*Ps. putida* KT2442::*mer*-73). Then, the M9 medium containing TH (10 ppm) was continuously fed into the bioreactor with a peristaltic pump. To prevent washout of biomass the dilution rate in a chemostat has always to be lower than the maximal growth rate ($D < \mu max$). Due to growth curve calculations both bioreactors were run with a dilution rate of 0.01 h^{-1} but the bioreactors were not stabilized after 24–48 h. Probably as a response to the stress situation, the cell density decreased by approximately three orders of magnitude to $<10^5$ cfu ml^{-1} with an increase of TH concentration in the reactor. Consequently the dilution rate was set to 0.005 h^{-1} and stepwise increased to 0.007, 0.01, 0.012, 0.014 h^{-1}. Runs in bioreactor A were increased to a dilution rate of up to 3.2 h^{-1}.

Thiomersal and its decomposition products (thiosalicylic acid and 2,2'dithiosalicylic acid) were measured with HPLC, while the mercury content in the inlet and outlet liquid flow and in the gas trap device was measured every day by using CVAAS.

With the gradual rise in dilution rates, TH concentrations in both bioreactors fell below the detection limits and only the mercury concentration of the aerated biomass suspension (Hg_{Total}) and the biomass free liquid phase (supernatant after centrifugation: Hg^{2+}) were detectable. The results are summarized in Table 3-5 for *Ps.putida* Spi3 and in Table 3-6 for *Ps. putida* KT2442::*mer*-73.

The results of the the experiments shown in Table 3-5 demonstrated that *P. putida* Spi3 was able to reduce the high TH inflow concentration to a TH outlet concentration below the detection limit and the mercury removal was through out the experiment more than 99 %. Due

to this high conversion the volumetric Hg^{2+} transformation rates (R_{HgV}) at steady state were in the range of 0.5–0.16 $mg \cdot l^{-1} \cdot h^{-1}$. The Hg^{2+} transformation rates for steady state continuous cultures of Spi3 confirm that the microorganisms applied possess a large potential for removing Hg^{2+} and are able to cope with high concentration of TH.

Table 3-5. Thiomersal removal in continuous stirred tank reactor with Spi3. Mercury ion concentration (Hg^{2+}), total mercury residual concentration (Hg_{Total}l), mercury transformation rate (R_{HgV}), and percentage of mercury removal in a bioreactor for different dilution rates. TH concentration in the bioreactor was below the detection limit (bd).

D $[h^{-1}]$	TH inflow $[mg \cdot l^{-1}]$	TH outflow $[mg \cdot l^{-1}]$	Hg^{2+} outflow $[mg \cdot l^{-1}]$	Hg_{Total} outflow $[mg \cdot l^{-1}]$	Hg^{2+} Removal [%]	R_{HgV} $[mg.l^{-1} \cdot h^{-1}]$
0.010	10	bd	0.009	0.037	99.8	0.0499
0.012	10	bd	0.005	0.062	99.9	0.0599
0.014	10	bd	0.008	0.067	99.8	0.0699
0.018	10	bd	0.040	0.210	99.2	0.1587
0.020	10	bd	0.040	0.333	99.2	0.1587
0.023	10	bd	0.030	0.286	99.4	0.1590
0.026	10	bd	0.043	0.233	99.1	0.1289
0.029	10	bd	0.030	0.146	99.4	0.1441
0.032	10	bd	0.036	0.134	99.3	0.1588

Furthermore HPLC analysis showed a total consumption of thiosalicylic acid, a degradation product of TH. Transformation of thiosalicylic acid and aromatic thiols is extensively studied (Weisinger *et al.* 1980; Drotar *et al.* 1987; Carrithers and Hoffman 1994). One way of degradation is to form their methyl derivate. Thus methylation is important for degradation of sulphur metabolites in microorganisms but also in animals.

a

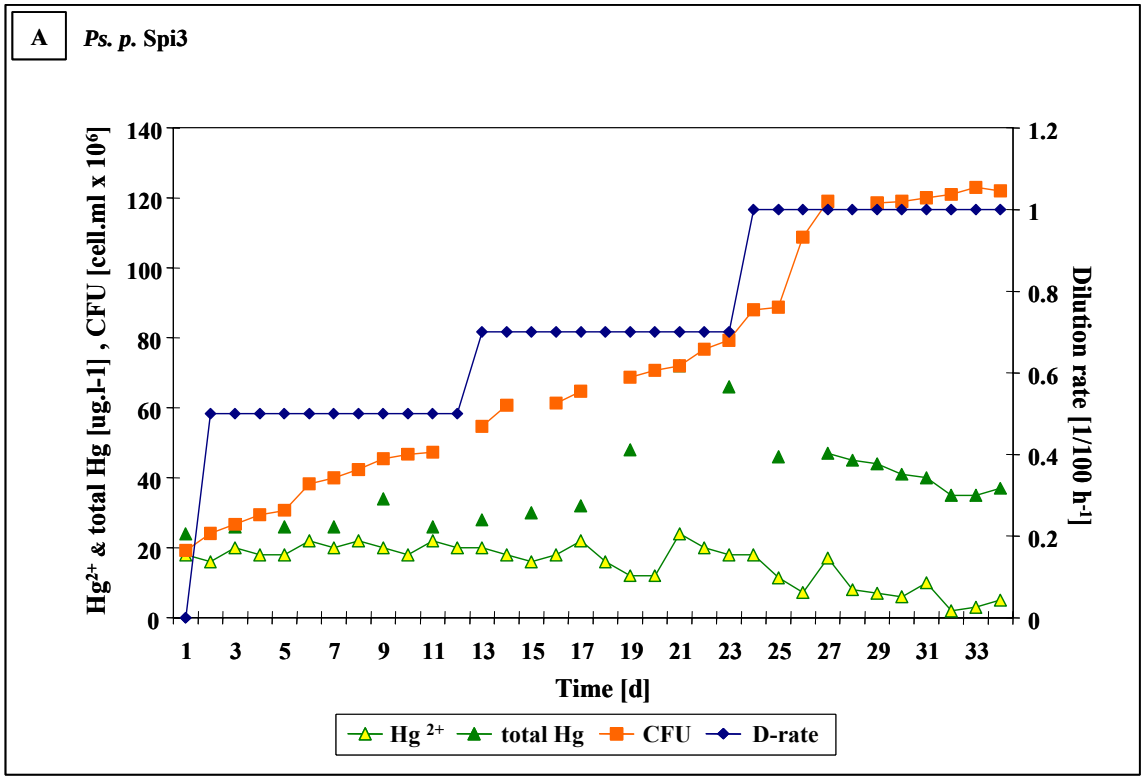

b

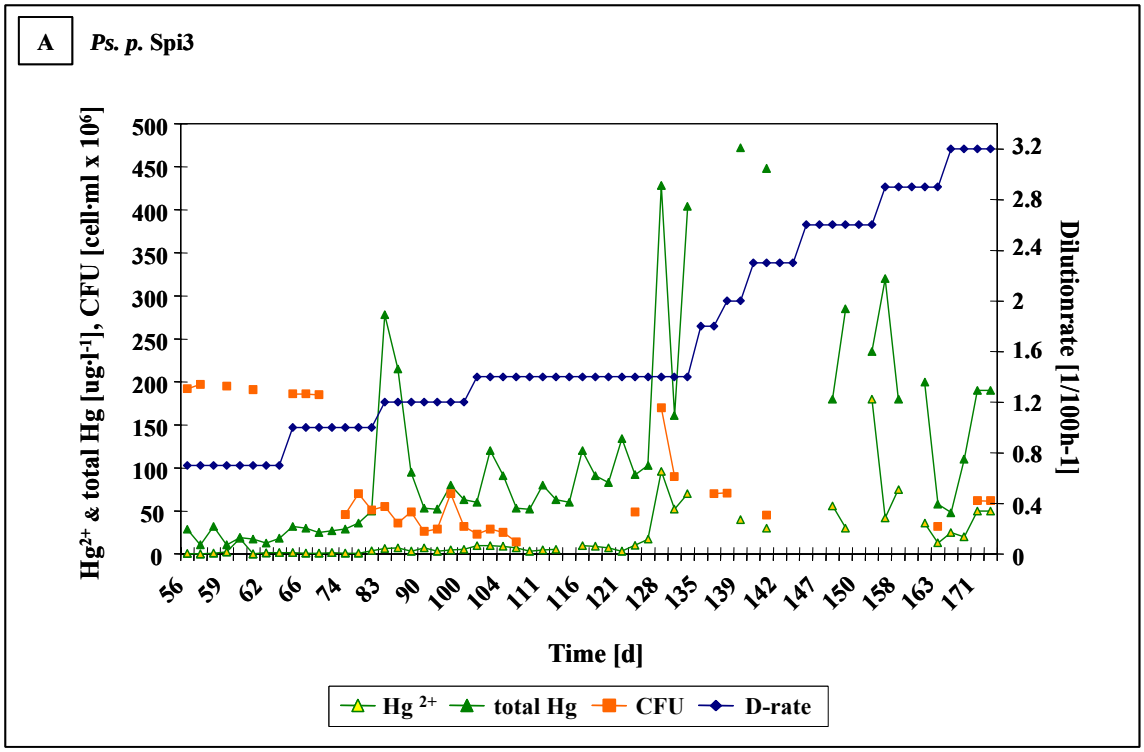

Figure 3-28. **Reactor A:** effect of dilution rate on thiomersal degradation and cell density in the bioreactor using *Ps. putida* Spi3. Experimental data of Hg^{2+} (△), mercury concentration with cell suspension (▲), colony forming units (■) and dilution rate (◆) are presented. (a) Experimental run from days 0 to 34 and (b) days 56 to 172.

Throughout the entire experiment physical and chemical stresses (unintended pH fluctuations, blocking of nutrient inflow e.g.) were exerted on the cells, however from every disturbance they recovered within a few days. As a result of the interferences high mercury peaks and dithiosalicylic acid could be measured.

Similar observations were made with *Ps. putida* KT2442::*mer*-73 in bioreactor B (Figure 3-29). The results are summarized in Table 3-6, TH was never detected at the bioreactor outlet during the experimental period. As a result, the rate of TH transformation was assumed equal to the thiomersal-feeding rate. With increasing the dilution rate and TH feeding rate respectively, the TH transformation rate increased prpotional. The Hg^{2+} and total mercury residual concentration (Hg_{Total}) in the bioreactor was also measured. The mercury removal efficiency was above 99 %. The minimum Hg^{2+} concentration in the filtered supernatant of bioreactor B was between 5–20 $\mu g \cdot l^{-1}$ at all dilution rate, whereas the total mercury concentration (samples with cell suspension) was considerably higher during the whole experiment. This finding may be due to dead mercury containing cells and not caused by the washed-out cells.

As a result, the TH transformation rate for steady state continuous cultures of KT2442 was within the range 0.1–0.14 mg l^{-1} h^{-1}. The results obtained showed that KT2442 culture is capable of degrading high concentration TH. When operated continuously, the cells were able to deal with fluctuations.

Table 3-6. Thiomersal removal in continuous stirred tank reactor with KT2442. Mercury ion concentration (Hg^{2+}), total mercury residual concentration (Hg_{Total}), mercury transformation rate (R_{HgV}), and percentage of mercury removal in a bioreactor for different dilution rates. TH concentration in the bioreactor was below the detection limit (bd).

D [h^{-1}]	TH inflow [$mg \cdot l^{-1}$]	TH outflow [$mg \cdot l^{-1}$]	Hg^{2+} outflow [$mg \cdot l^{-1}$]	Hg_{Total} outflow [$mg \cdot l^{-1}$]	Hg^{2+} Removal [%]	R_{HgV} [$mg.l^{-1} \cdot h^{-1}$]
0.010	10	bd	0.013	0.0387	99.739	0.0999
0.012	10	bd	0.017	0.0283	99.669	0.1198
0.014	10	bd	0.033	0.0647	99.344	0.1395

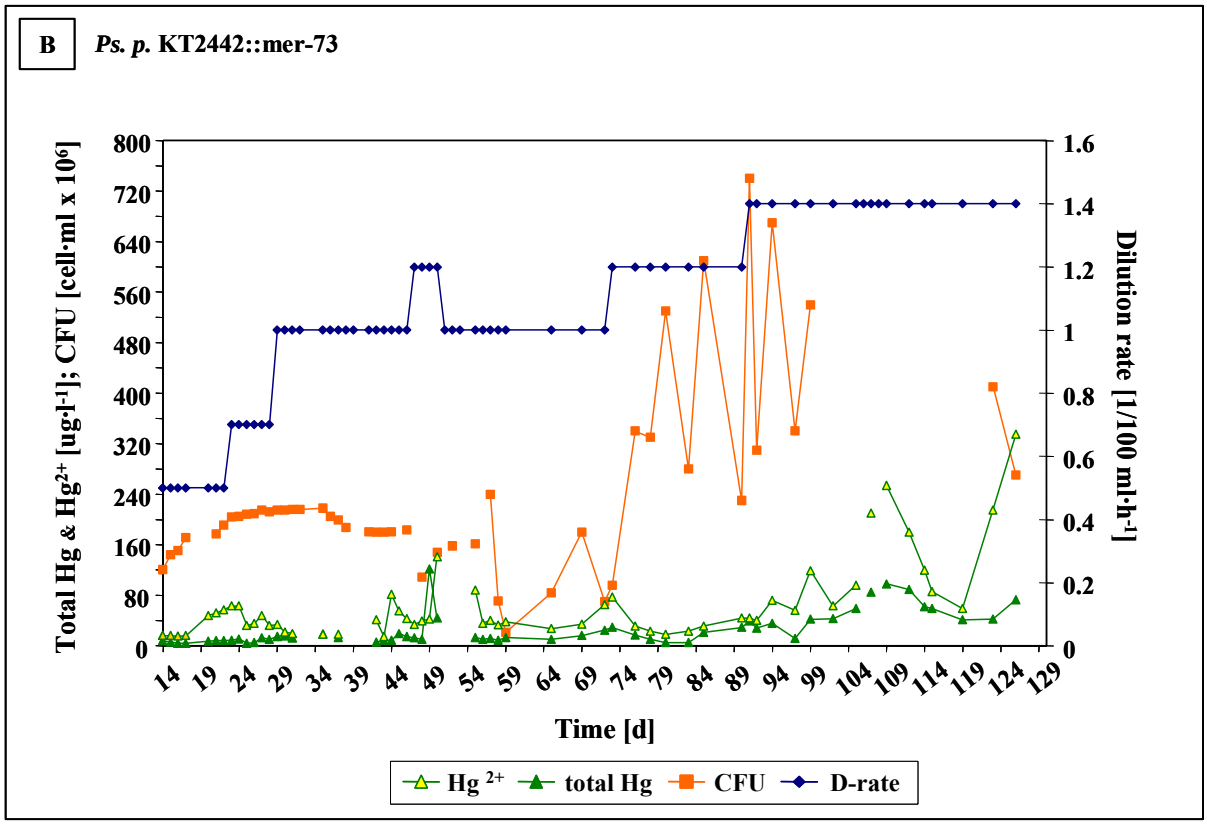

Figure 3-29. **Reactor B:** effect of dilution rate on thiomersal degradation respectively Hg^{2+} and cell density in the bioreactor using *Ps. p.* KT2442*::mer*-73. Experimental data of Hg^{2+} (△), mercury concentration with cell suspension (▲), colony forming units (■) and dilution rates (◆) are presented.

3.5 The Mercurial-Resistance Determinants of the Naturally Thiomersal Resistant Isolates

The significantly differing thiomersal transformation rates of the isolates (see Figure 3-5) and the extremely high resistance of *Ps. putida* Spi3 to thiomersal raised the questions: (1) whether the strains contained multiple operons, (2) if the genes of *mer* operon were very diverse and (3) if this diversity was reflected in the thiomersal transformation capability.
Although a recurring *mer* gene arrangement pattern can be observed in most mercury resistant microorganisms, eminent differences also exist. The characterization of the *mer* operons may thus shed light on the genetic basis for the diversity in the levels of resistance. Special attention was also given to the *mer*B gene which encodes the organomercurial lyase. This protein catalyses the cleavage of covalent carbon-mercury bonds (C–Hg) resulting in Hg^{2+} production, it is responsible for the resistance to thiomersal and other organomercurials.
Therefore, the *mer* operons were characterized with specific intragenic PCR primers to amplify and sequence distinct regions of the typical gram-negative *mer* operons. The desired region was amplified and sequenced as described in Material and Methods (see section 2.5.5). Blast searches were performed at the website of the National Center for Biotechnology Information for identification and search for sequences related to the amplified ORFs (open reading frames). Due to the overlapping regions of the sequences, the mer operon could be assembled.

3.5.1 Specificity of the Designed PCR Primers for *mer* Genes of Gram Negative Bacteria

To obtain complete sequences for the *mer* operon of the strains a large number of primers were used to create enough overlapping PCR products to cover the entire operon by sequences. These primers (R, T, P, A, C, D against the *mer*R, T, P, A, C, D genes) were designed from conserved DNA sequences of published *mer* operons of gram-negative bacteria and are listed in Table 3-7 (see also section 2.5.4.1). The priming sites and regions of the *mer* operon which are amplified by the primers are depicted in Figure 3-30 (sequences and the priming sites are also shown in Figure 11 in the Appendix).

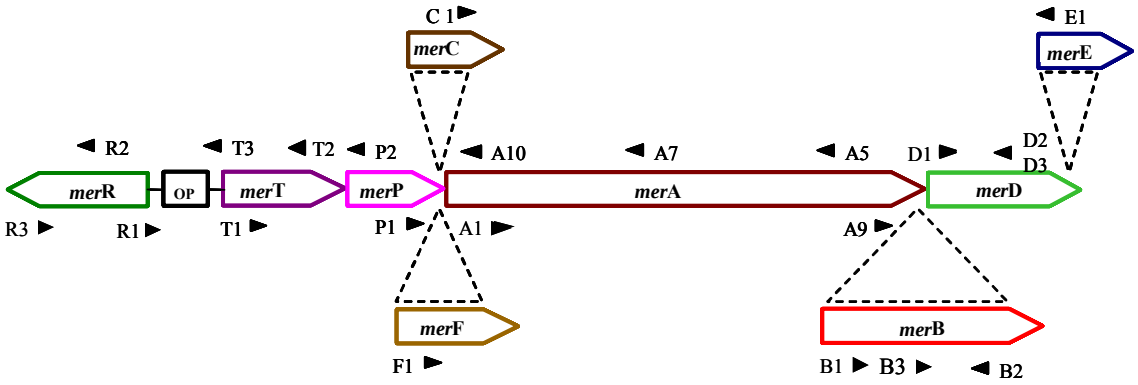

Figure 3-30. Schematic representation of the *mer* operon commonly found in gram-negative bacteria. The location of the *mer* PCR primers and the direction of the primers are indicated by arrowheads.

Table 3-7. Primer sequences and annealing temperature for PCR analysis of all *mer* genes. F = Forward and R = Reverse

mer primer	Direction	Nucleotide sequence [5‘ to 3‘]	Annealing Temp. [°C]	Reference
R1	R	GCC GAT TTC ACG AAT CGC A	58	Pauling (unpublished)
R2	F	ACG GAT GGT CTC CAC ATT G	58	Liebert *et al.* 1997
R3	R	ATC AGC GGG CAG GAA ACG TT	62	This study
T1	F	GCT TGG ATC GGC AAC TTG A	58	Pauling (unpublished)
T2	R	AAT CGC GCA GAC CTC ACC	58	Pauling (unpublished)
T3	R	AGC GYA TGT CTG AAC CWC AA	60	This study
P1	F	GGC TAT CCG TCC AGC GTC AA	64	Liebert *et al.* 1997
P2	R	TCT TCG GTG GCC TTG GTC A	60	Pauling (unpublished)
C1	F	TTT CYG CGA TGG GCT GCG	58	This study
A1	F	ACC ATC GGC GGC ACC TGC GT	68	Liebert *et al.* 1997
A5	R	ATC GTC AGG TAG GGG AAC AA	60	Liebert *et al.* 1997
A7	R	TTG CGC ATT GAC AGT GAC CC	62	This study
A9	F	GAA YTG ATC CAG ACG GCK G	60	This study
A10	R	TGT GTG CCG TCC AAG ATC A	58	This study
B1	F	TCG CCC CAT ATA TTT TAG AAC	58	Liebert *et al.* 1997
B2	R	CAT GTN CAY TTC TTY GCN TCTC	64	This Study
B3	F	TAY NCC TGG TGY GCN CTG GA	64	This Study
B4	R	TCS CCY TGY GMC GCM ACC GG	64	This Study
D1	F	ATG AAC GCC TAC ACS GTG TC	62	This Study
D2	R	CTG GAA GTG CAG TTG GCC	58	This Study
D3	R	GCG GAG AGT YTG CCA TGA	56	This Study
E1	R	ATC GGT TTG TGC GTC TCG GA	62	This study

Suitable priming regions for *mer*RTPAD were mainly identified within the part of the sequences coding for the reaction centers. However, no conserved DNA sequence regions could be identified for the *mer*B gene due to high sequence variability (Figure 3-31). Primers for the *mer*B gene were developed based on a sequence alignment of eight *mer*B sequences from gram-negative and also from published gram-positive bacteria.

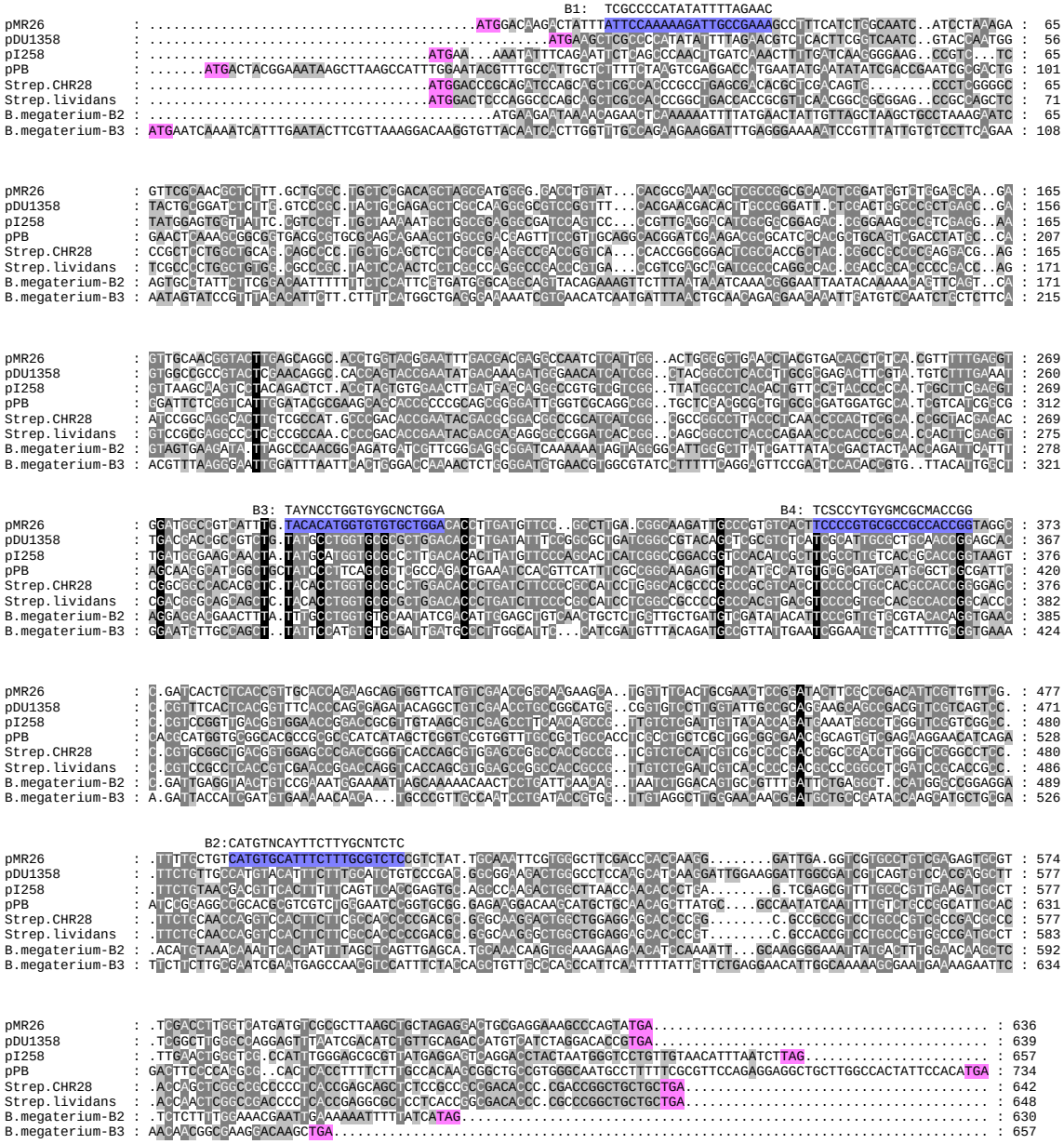

Figure 3-31. Alignment of the published *mer*B sequences with specific primers. The primers (forward primer: B1 and B3; reverse primer: B2 and B4) are colored in blue. Plasmid pDU1358: *Serratia marcescens*: M24940; Plasmid pMR26: *Pseudomonas sp.* K62: MerB$_2$: AB013925; Plasmid pPB: *Ps. stutzeri*: *mer*RBT: U90263; Plasmid pRJ28: *Streptomyces sp.* CHR28: AF222792; *Strep. lividans*: X65467; *Bacillus megaterium*: *mer*B2: AB027307; *Bacillus megaterium*: *mer*B3: AB027306. Black shade: 100% similarity; Gray: 80% similarity; Light gray 60% similarity. Start and stop codon are colored pink.

In agreement with the rules for primer sequence design (Innis and Gelfand 1990) 22 primers were chosen for the analysis, resulting in several possible combinations. However, 11 favorable combinations were chosen for the detection of the *mer* genes. In order to obtain also the accessory genes (*mer*C, *mer*F, and *mer*B) which are located between *mer*P and *mer*A, and between *mer*A and *mer*D primer combinations such as R-T, P-A and A-D were chosen.

To enhance the probability for desired matches with unknown *mer* gene sequences, an annealing temperature of about 5–8°C below the lowest temperature of the primer set was applied. Two sequenced *mer* operons (pDU1358 and Tn501) were used as positive controls in the PCR reactions. Primer pairs, PCR annealing temperatures, and product sizes are listed in Table 3-8.

Table 3-8. **PCR primer pairs used for sequencing of the *mer* genes of the eight naturally mercury resistant isolates.** The given DNA sizes represent amplicon sequence lengths calculated from the control sequences pDU1358 and Tn501.

Primer Pair	Annealing Temp. [°C]	Size of the amplicons [bp]	Amplified Gene
R3-T2	56	672 for Tn501	*mer*R, *mer*T
R3-T3	58	432 for Tn501	*mer*R
R3-P2	58	922 for Tn501	*mer*R, *mer*T, *mer*P
T1-A5	58	2211 for Tn501	*mer*T, *mer*P, *mer*C or *mer*F, *mer*A
P1-A10	60	540 for Tn501	*mer*C or *mer*F, *mer*A
A1-A5	60	1182 for Tn501	*mer*A
A1-A7	60	715 for Tn501	*mer*A
A9-D3	58	458 for pDU1358	*mer*B, *mer*D
B1-D2	55	1068 for pDU1358	*mer*B, *mer*D
B2-B3	54	235 for pDU1358	*mer*B
D1-E	58	411 for Tn501	*mer*D, *mer*E

The resulting amplicons from PCR with these primers were sequenced using ABI sequencer (for detail see section 2.5.5). The readable length of the sequenced amplicons was between 500 to 900 nt and the *mer* genes were identified by BLAST analysis (Altschul *et al.* 1997). The DNA sequences were compared using the programs ClustalW and Genedoc. Phylogenies based on sequences were derived for the amplicons rendered by the individual strains.

The primers were found to be specific for their target groups (Table 3-9). The primers based on the genes *mer*R, *mer*A, *mer*T, or *mer*P yielded a product in 94% of the performed PCR reactions and proved suitable for an analysis of the operon. However, the primers were not successful in amplifying *mer*B and *mer*E gene sequences from wild-type isolates known to contain at least one *mer*B gene because of their resistance to thiomersal.

More detailed information about the specific primers and the amplicons will be presented in the respective sections.

Table 3-9. **PCR results of the *mer* genes from the eight wild-type isolates.** Sizes of *mer* amplicons from the control sequences pDU1358 and Tn501 are given underneath the primer pairs. The given DNA lengths represent the length of amplified sequences. The letters in the designation of the primer represent the respective *mer* genes. ms = mismatch, sequence did not represent *mer* gene, (-) = no PCR product.

Strains	***mer* amplicons with primer pairs (bp)[α]**					
	R3-T2 672 bp	R3-T3 432 bp	R3-P2 922 bp	T1-A5 2211 bp		P1-A10 540 bp
				T1	A5	
Spi3	472	1554 [γ]	922	880	610	537
Spi4	473	432	927	910 [δ]	856	537
Spi11	637	432	922	820 [δ]	872	900 [δ]
Elb2	694	–	922	847 [ε]	840	534
Ibü8	445	–	924	811	744	534
Kon12	–	432	924	841	688	519
Tin2	672	432	922	859 [δ]	796	924 [δ]
Bro12	462 [β]	–	922	810	622	526 896 [δ]

Strains	***mer* amplicons with primer pairs (bp)[α]**				
	A1-A5 1182 bp	A9-D3 458 bp	B1-D2 1068 bp	B2-B3 235 bp	D-E 411
Spi3	1182	488	1093	235	–
Spi4	1179	–	–	–	–
Spi11	1182	–	–	–	–
Elb2	1179	485	–	–	–
Ibü8	1182	1197	1068	235	–
Kon12	1182	ms	1062	235	–
Tin2	1194	ms	–	–	–
Bro12	1179	–	–	–	–

[α] Nucleotide sizes are approximated by comparison to amplicons from sequenced *mer* operon of the control DNA (pDU1385 and Tn501).

[β] The amplicon of 462 bp represents only the *mer*R gene sequenced with primer R3. Primer T2 amplified a gene region of unknown function from *Pseudomonas aeruginosa* PAO1(AE004961) with 98% similarity, apparently not belonging to the *mer* operon.

[γ] The 1554 nt fragment contains the 3' end of *mer*R and the 5' end of *mer*T, but additionally a *mer*B gene could be found between *mer*R and *mer*T.

[δ] Strains with large amplicons contain the *mer*C gene between *mer*P and *mer*A.

[ε] The amplicon of T1-A5 contains the additional gene *mer*F between *mer*P and *mer*A.

3.5.2 Identification of the Regulatory Gene *mer*R

Two primer sets (R3-T2 and R3-T3) amplified the 3' end of *mer*R, *mer*O/P, and the 5´end of *mer*T in all of the eight naturally mercury resistant isolates, however, with different amplicon lengths (Table 3-8). The primers R3 and T2 amplified a region of approximately 670 bp and *mer* genes from *Ps. putida* Spi3, *Ps. putida* Spi4, *Ps. fulva* Spi11, *Ps. putida* Elb2, *Ps. putida* Ibu8 and *Citrobacter freundii* Tin2 and *Ps. aeruginosa* Bro12 could be detected. The primer pair R3-T3 yielded a product of approximately 470 bp (according to the control sequence) and amplified *mer*R, *mer*O/P, and *mer*T in Spi3, Spi4, Spi11, Tin2 and *Ps. putida* Kon12 (Figure 3-32).

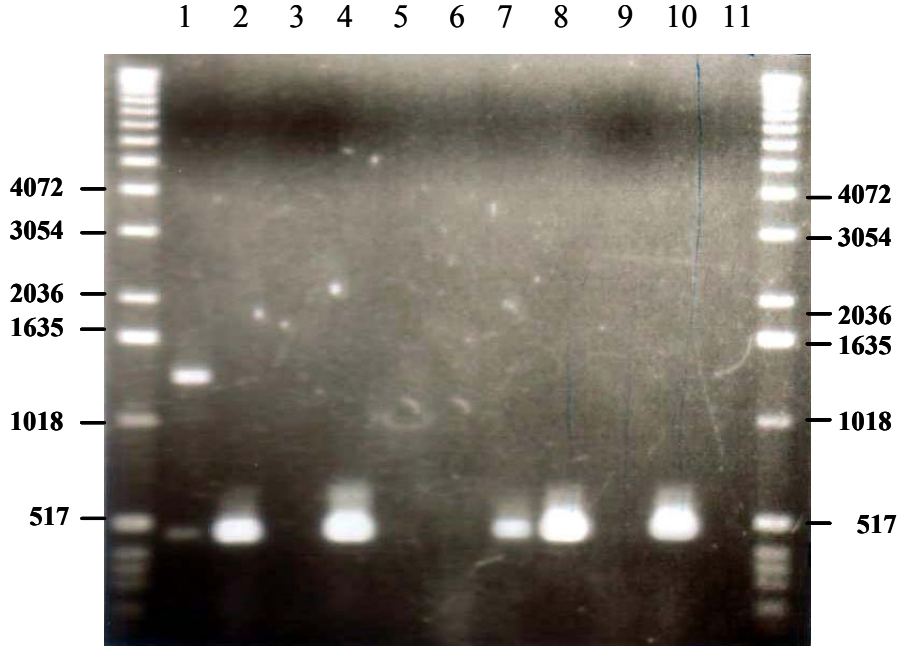

Figure 3-32. Amplification of *mer*R genes (470 bp) from mercury resistant strains using primers R3 and T3. Lane 1: Spi3; Lane 2: Spi4; Lane 3: Spi7; Lane 4: Spi11; Lane 5: Elb2; Lane 6: Ibü8; Lane 7: Kon12; Lane 8: Tin2; Lane 9: Bro12. Genomic DNA from Lane 3 (*Sphingomonas sp.* Spi7) does not yield any signal band and therefore it will not be mentioned anymore. The positive control (lane 10) contained Tn501 as template and the negative control (Lane 11) did not contain any DNA template. The marker used was a 1 kb ladder (see section 2.5.2).

The PCR products were sequenced and the *mer*R alignment of the isolates is shown in Figure 3-33. Note that by the use of primer R3 approximately 70 bp of the end of *mer*R genes could not be detected. The overall similarity between these *mer*R sequences is very high. Since the *mer* operon is often located on transposable elements or plasmids, it is not surprising to find

*mer*R genes although from phylogenetically distant organisms to be highly related, e.g. the mercuric regulatory genes from pMER327, Tn5057 and Tn5053 are identical, although originating from *P. fluorescens*, *E. coli* and *Xanthomonas sp.*, respectively.

The Spi3 amplicon placed an exception among the isolates because it gave two signals in the agarose gel (Figure 3-32). The amplicons had a nucleotide sequence length of 432 bp and 1553 bp (Table 3-8). When sequenced and blasted, it was revealed that the small fragment represented the 3' end of *mer*R (*mer*R_1) and the 5' end of *mer*T. The amplified *mer*R_1 gene in Spi3 is highly homologous to already known *mer*R genes (Figure 3-33). The predicted 119 amino acid (aa) polypeptide of Spi3 merR_1 showed 100% identity with Tn501 (accession no: AAA27432) and the mercury regulatory protein of *Wautersia eutropha* (accession no: AAR31069). The larger fragment also contained the 3' end of *mer*R (*mer*R_2) and the 5' end of merT, but additionally a *mer*B gene could be found between *mer*R and *mer*T which is corresponding to the *mer*B gene of *Ps. stutzeri* pPB. The predicted 119 aa polypeptide of merR_2 was 100% identical with both the MerR protein of *Ps. stutzeri* pPB and MerR from TOL plasmid pWW0 from *Ps. putida*. As shown in Figure 3-34 the *mer*R_2 gene is immediately followed by a sequence corresponding to a typical *mer*O/P region, where the putative promoter of the structural genes (P_{merB}) is followed by the putative promoter of the regulatory gene (P_{merR}). The analysis revealed the presence of a *mer*B gene, with a putative ribosomal binding site (RBS: GAGGAA), the gene starting at 478 nucleotide (nt) and ending at 1237 nt (full length of merB gene: 759 bp). Spi3 homology with known *mer* operons continues to the 3' end of *mer*B showing two elements also identical with pDU1358: Spi3 P_{merT} is followed by a *mer*T gene that is identical to that of plasmid pPB and highly homologous to *mer*T of both pDU1358 and Tn501 (Figure 3-34).

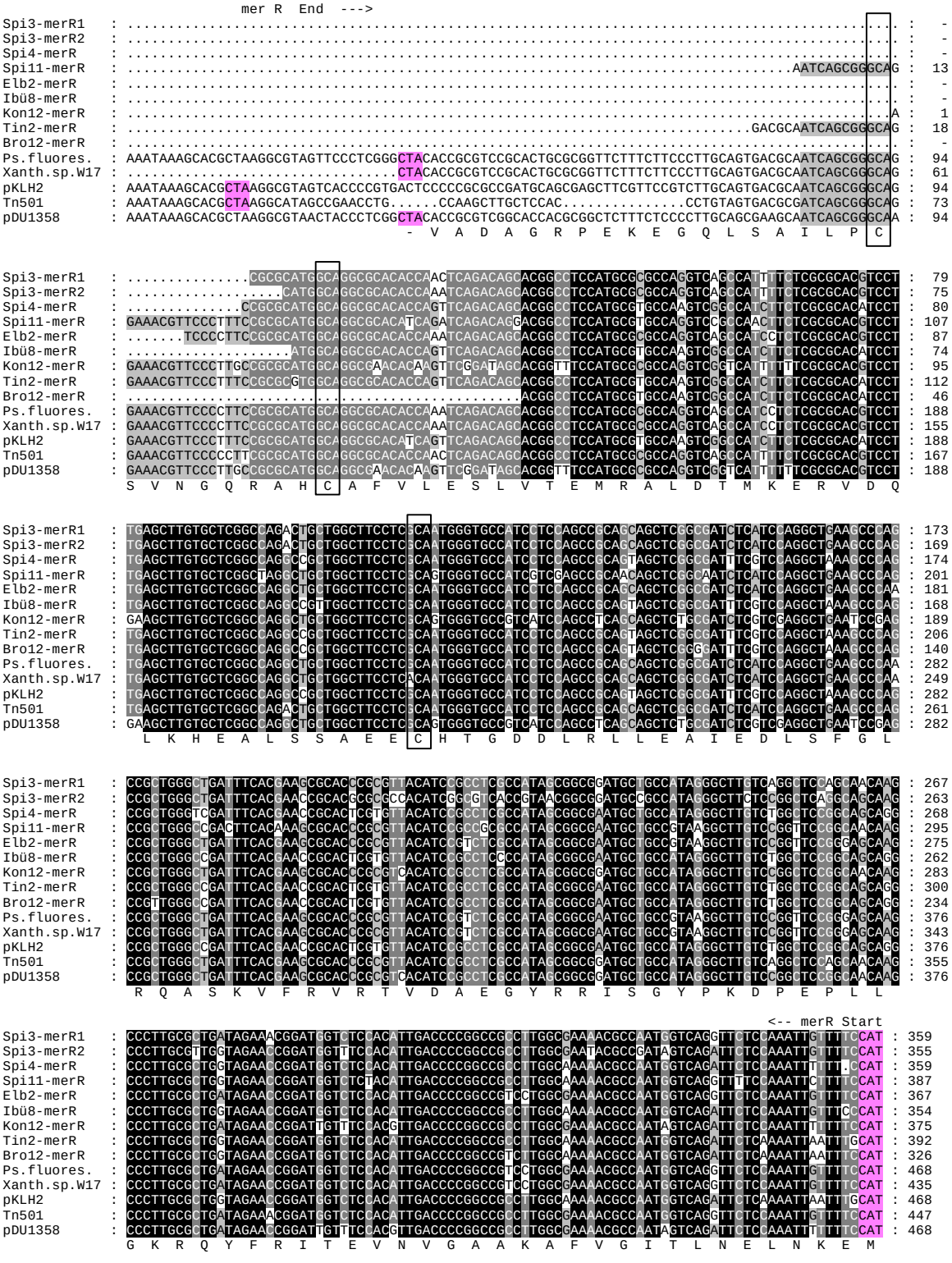

Figure 3-33. *mer*R alignment of 8 environmental isolates with published genes. The references are *Ps. flourescens*: X73112; *Xanthomonas sp. W17*: Tn5053: L40585; Tn501: *Ps. aeruginosa*: Z00027; Plasmid pKLH2: *Acinetobacter calcoaceticus*: AF213017; Plasmid pDU1358: *Serratia marcescens*: M24940. The amino acid sequence of Plasmid pDU1358 is shown as standard single letter below the DNA sequence line. The stop codon is represented as (-). The three completely invariant cysteine residues; Cys82, Cys117, and Cys126 are boxed. Black shade: 100% similarity; gray: 80% similarity; light gray 60% similarity.

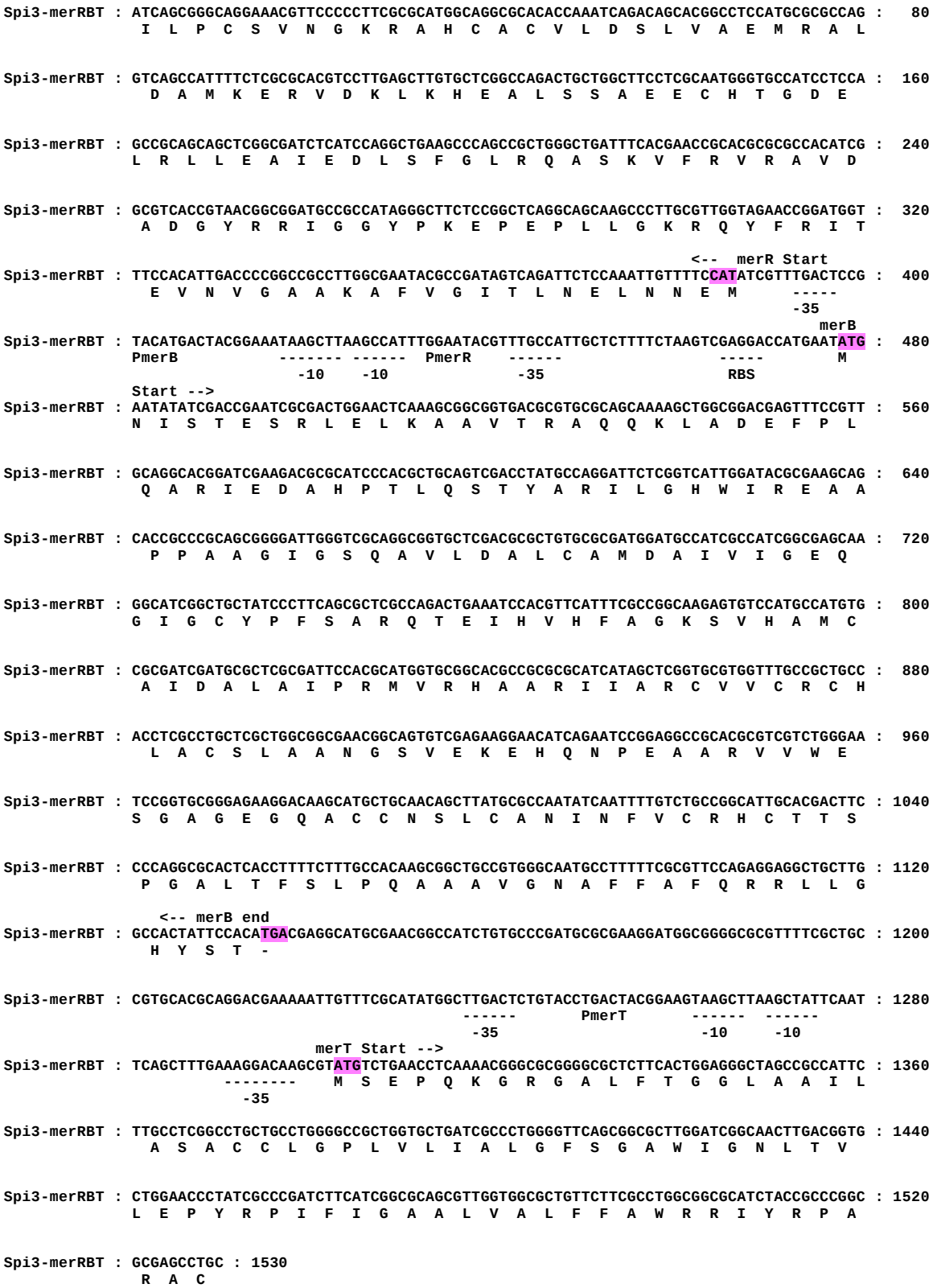

Figure 3-34. **Nucleotide sequence of 1530 bp from *Ps. putida* Spi3 broad spectrum mercury resistance gene cluster.** This region includes the genes *mer*R_2B, merO/P_2 and the 5' end of the *mer*T_2 gene. Promoters, ribosomal binding site (RBS), Startcodons (colored in pink) and the predicted polypeptide (aa) sequences are shown. The stop codon of MerB is represented as (–). Note that by the use of primer R3 approximately 70 bp of the end of *mer*R gene could not be detected.

3.5.3 Identification of Mercury Resistance *mer* Promoters

Regulation of the transcriptional initiation of the mercury resistance operon occurs from two divergent promoters. The region containing these two adjacent promoters lies between the structural genes (*mer*TPAD) and the regulatory gene *mer*R. During repression, both promoters are negatively regulated by MerR bound to a dyadic operator located between the -10 and -35 hexamers of *mer* gene promoter (P_{TPAD}). Upon Hg^{2+} induction, MerR activates transcription only from P_{TPAD} and continues to repress transcription from *mer*R promoter (P_R).

As shown in Figure 3-35 the nucleotide sequences from the *mer* promoter / operator (*mer*OP) were compared with that of published *mer*OP regions. The nucleotide sequences of all isolates showed a strong similarity to each other. The *mer*OP contained good potential -35 and -10 sequences (TTGACT and TAAG[G]T respectively), but with a spacing of 19 base pairs between them, 2 bp more than the optimal spacing for efficient transcription by the *Escherichia coli* σ70 RNA polymerase (Harley *et al.* 1987; Ansari et al. 1992). Comparative studies on *E. coli* promoters have revealed a number of conserved features, e.g. spacing of 17 bp between hexamers. Changing the spacing of the -35 and -10 sequences generally gives a down-promoter phenotype (Lund *et al.* 1989). Two 7 bp dyad sequences are located within the -35 and -10 hexamers (blue box) and are interrupted by 4 bp. The 19 bp spacing, dyad sequences, and relative position of the dyad sequence with respect to the -10 and -35 sequences are important for induction and repression of the operon. Generally, the dyad domain consists of the four highly conserved inner bases (….GTAC….GTAC….) of the seven-base interrupted dyad, alteration of which severely modifies both MerR and RNA polymerase contacts in the promoter region. Dyad sequences of 4 isolates (Spi4, Elb2, Tin2 and Bro12) in the putative operator region have one base pair mismatch at -22 (GTAC….CTAC) and the 7 dyad sequence of Spi11 and Ibu8 have even 2 bp mismatch (GTAC….CTCC). On the other hand the isolates Spi3 *mer*OP1 and Kon12 share an inverted repeat of the sequence GTAC flanked by potential transcription promoter elements. Generally, the MerR-Hg^{2+} complex binds DNA in the promoter region and underwinds the spacer region of the promoter, thus facilitating the formation of a transcriptionally active open complex by RNA polymerase. Ansari *et al.* (1992) showed that the Hg-MerR-induced DNA distortion corresponds to a local underwinding of the spacer region of the promoter by about 33 degrees relative to the MerR-operator complex. The magnitude and the direction of the Hg-MerR-induced changed in twist angle were consistent with a positive control mechanism involving reorientation of conserved promoter elements and were consistent with a role for torsional stress in formation of an open complex. Furthermore, Lee *et al.* (1993) revealed that

mutants in this dyad central region generally allow constitutive open complex formation at the *mer*R promoter. Therefore, it indicates that these positions are more significant in repression and activation. Especially, the position in the right arm of the dyad (G -22 of Spi4, Elb2, Tin2 and Bro12) is required for activation process. As shown in Figure 3-35, *mer*OP_2 from Spi3 takes an exceptional position. It has already been mentioned about the position of the *mer*B promoter downstream of *mer*R gene followed by *mer*R promoter (Figure 3-34). In addition, the *mer*OP_2 region of Spi3 has two mismatches, one in the right dyad arm at position -22 and another at position -14. Since both promoters overlap to some degree, a change in base pair (mutation) could affect both promoters. Therefore, it is of interest whether the effect of these mutations in nucleotide sequence will have consequence for the activities of *mer*OP_2.

To determine the activities of the *mer*OP region (*mer*R repression, *mer*TPAD repression, and Hg dependent *mer*TPAD activation) with respect to the ability to bind MerR protein in vitro in the presence and absence of mercury, the effect of given mutation should be investigated.

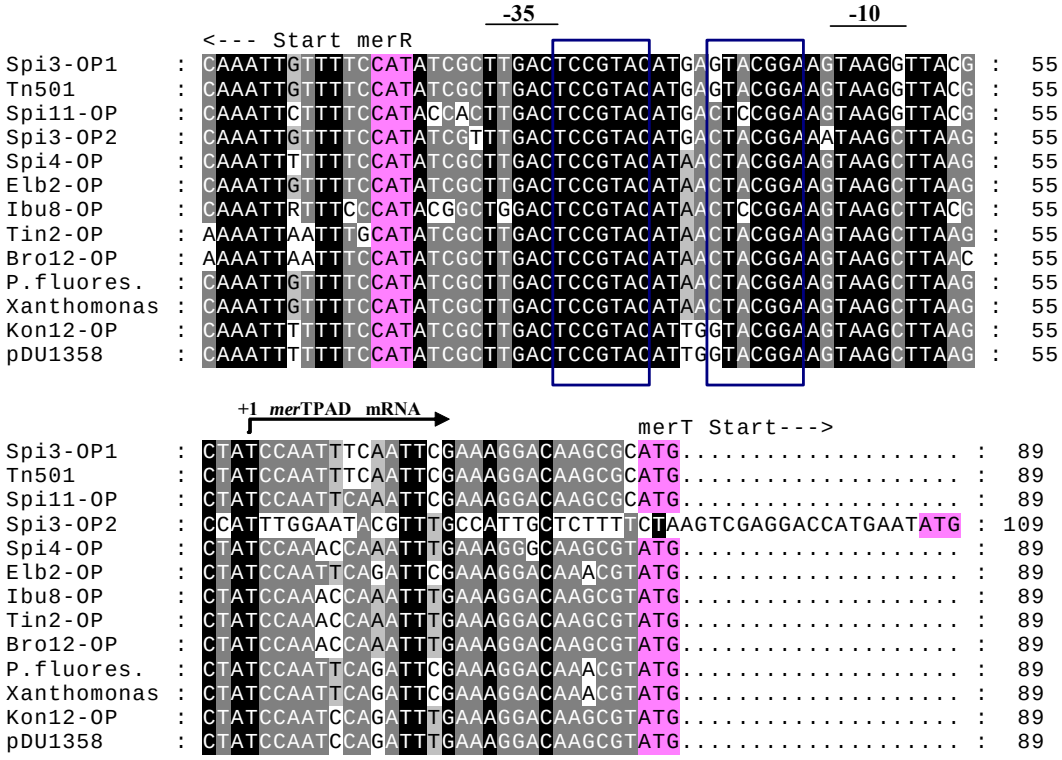

Figure 3-35. Alignment of the MerO/P nucleotide sequence of the 9 wild-type isolates with published *mer*O/P sequence. References are Plasmid *Ps. flourescens*: X73112; *Xanthomonas sp. W17*: Tn5053: L40585; Tn501: *Pseudomonas aeruginosa*: Z00027; Plasmid pDU1358: *Serratia marcescens*: M24940. Regions with similarity to the consensus -35 and -10 recognition elements for RNA polymerase are marked above the nucleotide sequences, and elements of dyad symmetry (conserved GTAC: TCC**GTAC**....**GTAC**GGA) are boxed. The start site of transcription from the wild-type *mer* promoter is indicated with arrow (+1). Black shade: 100% similarity; Gray: 80% similarity; Light gray 60% similarity.

3.5.4 Identification of the Transport Gene *mer*T

The primer pair R3-P2 which yielded a PCR product of approximately 960 bp in the control amplified the full *mer*T region, a structural gene of the *mer* operon that is involved in the uptake of Hg^{+2} into the cell. The amplicons obtained from the isolates with the primer R3-P2 are shown in Table 3-9.

The complete *mer*T sequences (348 bp encoding a 117 aa protein) could be detected in all investigated isolates. Two *mer*T genes could be detected for of *Ps. putida* Spi3 but the second *mer*T_2 ABI sequence (*mer*R_2BT_2) missed approximately 123 bp at the 3' end. Nevertheless, the eight other *mer*T genes including the Spi3 *mer*T_1 were aligned to other *mer*T sequences that have been published and were found to be highly similar (Figure 3-36). Minor dissimilarities could be observed at the nucleotide level. While Spi3 *mer*T_1 was 100% similar to *Ps. stutzeri* and Tn501, Spi4 was 99% similarity to Tn5041. The strain *Ps. fulva* Spi11, which was able to transform thiomersal with at a rate similar to Spi3 (see Figure 3-5), harboured a *mer*T gene similar to that of *Ps. stutzeri* and Tn501, however only with 91% DNA sequence identity. Two *mer*T genes were also detected for the strain Elb2 which indicated the presence of two different *mer* operons: The first *mer*T gene (merT_1) was very closely related to the one of Tn5053 of *Xanthomonas sp.* (99 % nucleotide identity) and the second *mer*T (*mer*T_2) showed 93% similarity in DNA sequence to the published sequence of transposable element Tn5041. The *mer*T of the strain *Ps. aeruginosa* Bro12 showed a very close relationship to the mercuric transport gene from plasmid pKLH201 (99% nucleotide identity). The strain *Citrobacter freundii* Tin2 which had a very low resistance to thiomersal showed 99% nucleotide identity to that of *Alcaligenes sp.* plasmid pMER610 and the *mer*T sequence of Kon12 was closely related to pDU1358 (99 % DNA similarity). The sequence analysis of the strain Ibu8 showed fainter similarity to already known mercuric transport genes (around 91 % nucleotide identity). The predicted 115 amino acids could be identified for Ibu8 with low agreement with the protein of *Pseudomonas sp.*, respectively of Tn5041. Note that the *mer*T genes of all isolates contained paired cysteine residues (Cys24, Cys25 and Cys76, Cys 82) which have been shown to be essential for mercury transport (Morby *et al.* 1995).

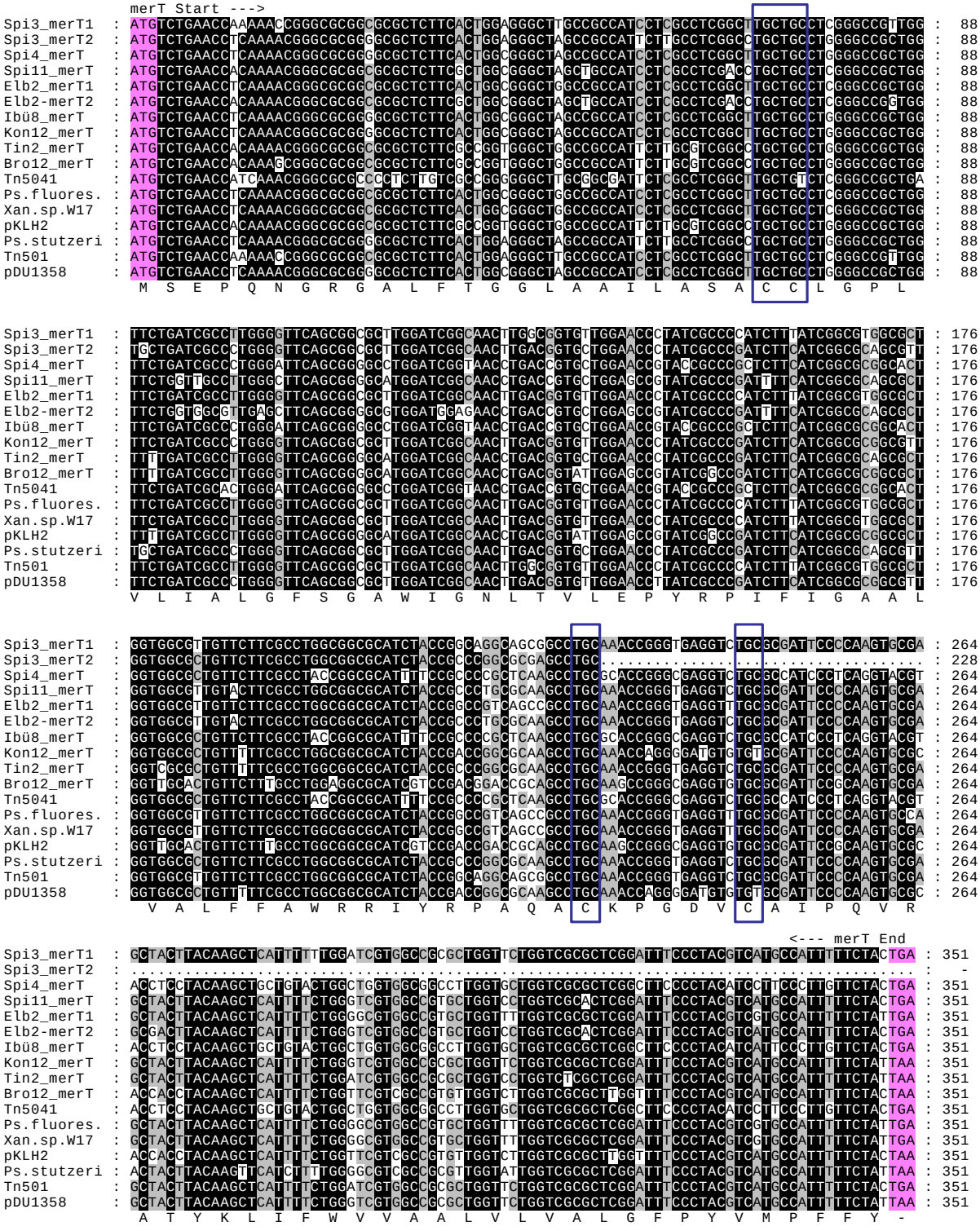

Figure 3-36. Alignment of the *mer*T genes of the 8 natural isolates and published *mer*T genes. The references are *Pseudomonas sp.*: Tn5041: X98999; *Ps. fluorescens*: X73112; *Xanthomonas sp. W17*: Tn5053: L40585; Tn501: *Pseudomonas aeruginosa*: Z00027; Plasmid pKLH2: *Acinetobacter calcoaceticus*: AF213017; Plasmid pDU1358: *Serratia marcescens*: M24940. Amino acid sequence of Plasmid pDU1358 polypeptide is shown as standard single letter below the DNA sequence line. The stop codon is represented as (-). The paired cysteine residues (Cys24, Cys25 and Cys76, Cys 82) are boxed. Black shade: 100% similarity; Gray: 80% similarity; Light gray 60% similarity. Start and stop codon are colored pink.

Interestingly, Opella and coworkers (2002) report the xxCC motif to be specific for Hg(II) transport. The xxCC motif found in the first transmembrane region of MerT could make the transport protein the central piece in selection of the metal to be incorporated by the bacteria (Figure 3-37). Another cysteine pair is located in the peptide lying in the cytoplasm and connecting the second and third transmembrane helixes (Figure 3-38). Moreover, the coordination-induced structural organization is favored by the presence of a proline-glycine motif in the CKPGEVC sequence (boxed sequence in Figure 3-37) that induces a β-turn bringing the two reactive cysteines closer and forming a cytoplasmatic loop. One can thus describe the cytoplasmic loop as a pre-organized cyclic peptide rigidified by the β-turn and the fixation to the transmembrane. Moreover, as the cytoplasm is known to provide a reductive environment, the thiol groups would be immediately ready for the coordination of the mercury atom.

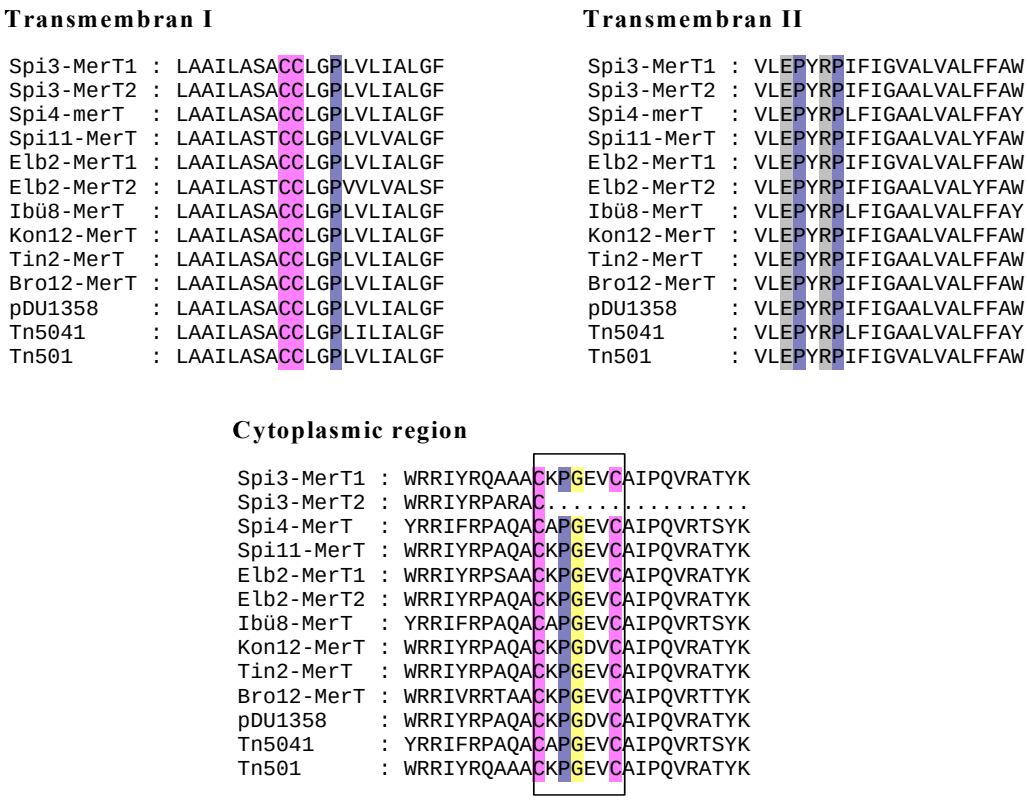

Figure 3-37. The conserved features of the MerT proteins of environmental isolates and alignment of key elements. The MerT sequences of all isolates are aligned with the publiched sequences (Tn5041: *Pseudomonas sp*: X98999; Tn501: *Pseudomonas aeruginosa*: Z00027; Plasmid pDU1358: *Serratia marcescens*: M24940). The cysteines in the first transmembrane region and in the cytoplasmic regions of MerT, are colored pink while the charged residues in the second transmembrane region are gray shaded; the proline residues are colored blue and the glycine residue is yellow shaded. The reaction center in cytoplasmic region (CxxxxxC sequence with praline-glycine motif) is boxed. Due to the gap in sequence, the alignment of the cytoplasmatic region could not be completed with the second *Mer*T2 sequence of Spi3.

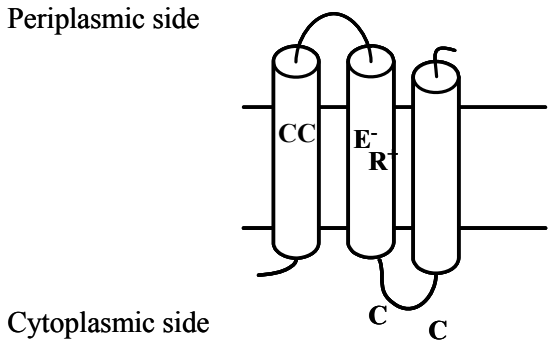

Figure 3-38. **Topological scheme of the MerT protein according to the predicted hydrophobic (membrane-spanning) elements.** MerT is predicted to contain three transmembrane helices (TM). The first TM contains two adjacent cysteine residues (Cys 24 and Cys 25) essential for the transport. Another cysteine pair (Cys 76 and Cys 82) is located in the peptide lying in the cytoplasm and connecting the second and third TM. The scheme is based on Wilson *et al.* 2000.

3.5.5 Identification of the Transport Gene *mer*P

The sequences of the mercuric transport gene *mer*P (a small periplasmic protein) were amplified by the use of primer pairs T1-A5 and P1-A10. The full length of the *mer*P gene (276 bp and 91 aa protein respectively) from all isolates could be sequenced and aligned (Figure 3-39). The similarities of the *mer*P amplicons were in accordance with the results of the *mer*T sequences. Only one *mer*P_1 gene was detected for Spi3 (downstream of the *mer*T_1 gene) and as with *mer*T this sequence showed 100% similarity both to Tn501 and plasmid pPB. In addition to *mer*P_1 of Elb2 that was 99% similar to *mer*P of Tn5053, a second *mer*P_2 was detected. This gene indicated the presence of a second *mer* operon and showed similarity to the *mer*P of the transposable element Tn5041.

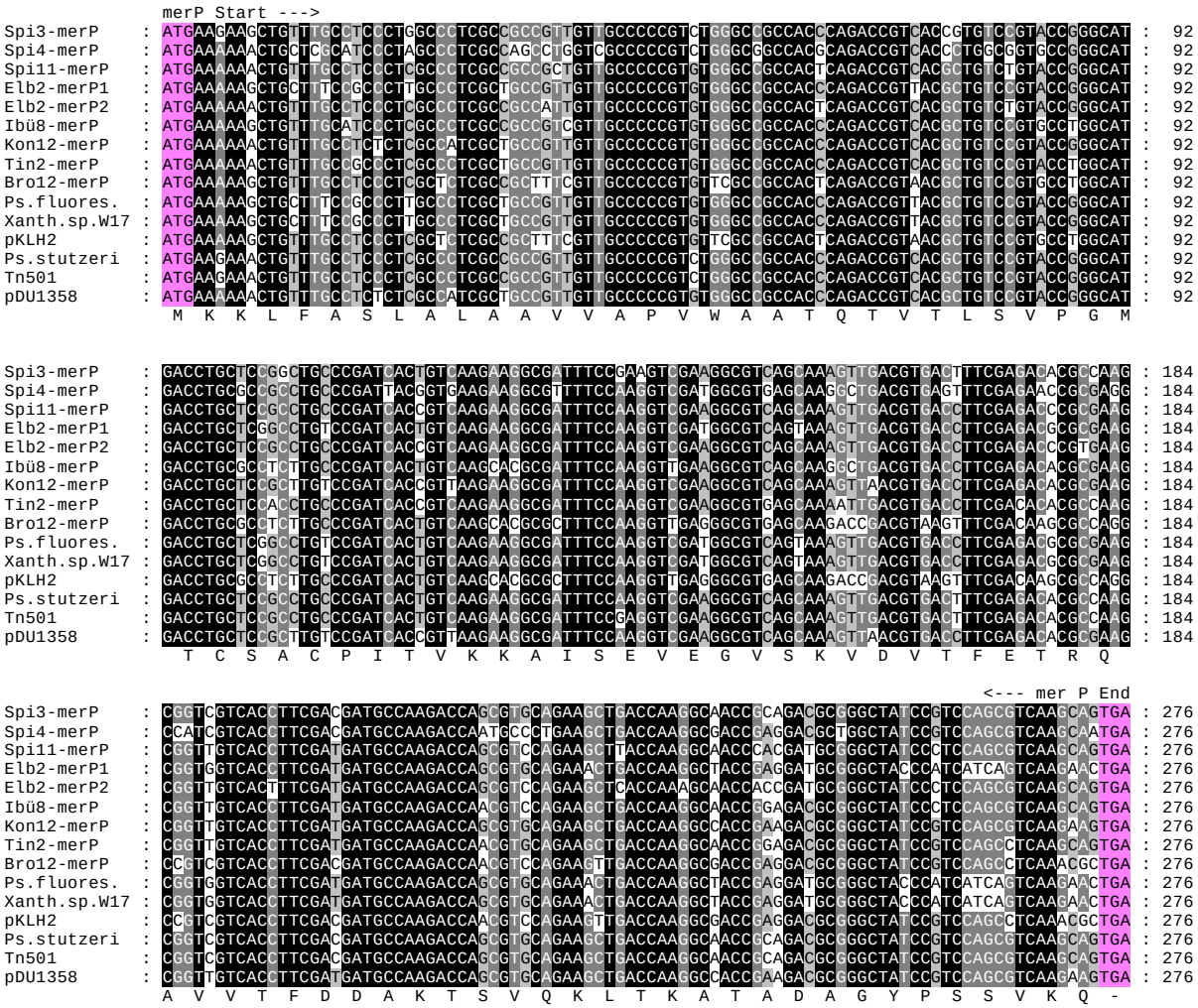

Figure 3-39. Alignment of the *mer*P genes of the 8 environmental isolates and published *mer*P genes. The references are *Ps. fluorescens*: X73112; *Xanthomonas sp. W17*: Tn5053: L40585; Tn501: *Pseudomonas aeruginosa*: Z00027; Plasmid pKLH2: *Acinetobacter calcoaceticus*: AF213017; Plasmid pDU1358: *Serratia marcescens*: M24940. Amino acid sequence of the Tn501 polypeptide is shown as standard single letter below the DNA sequence line. The stop codon is represented as (-). Black shade: 100% similarity; Gray: 80% similarity; Light gray 60% similarity. Start and stop codon are colored pink.

If one investigates the protein structure in detail, the mercury binding motif of MerP (MxCxxC) can be found in the amino acid sequence of several other proteins of prokaryotic and eukaryotic species which are proposed to bind or transport the heavy metals (Silver *et al.* 1989; Solioz and Vulpe 1996). Inspection of genomic databases reveals a significant number of homologs, which, based on sequence analysis and on the conservation of key residues, are readily segregated into a minimum of four groups: the MerP-like proteins, Atx1-like metallochaperones, CopZ-like proteins, and the domains of the P-type ATPases (Figure 3-40). The presence of metal transporters and domains of ATPases in bacteria as well as in archaea and eukaryotes, their common structure (βαββαβ fold), and the conserved MxCxxC metal

binding motif, located in the loop between strand β1 and helix α1 (Morin *et al.* 2005), indicate a common interaction mechanism.

It will be interesting to see how the functions of these small proteins and domains that emerge from this genomic survey compare with the mechanistic and functional attributes of the initially characterized members. This survey can serve as a starting point for tests of the anticipated partner proteins or of the nature of physiological metal cargo, that is, a toxic nonessential metal such as Hg(II) and Cd(II) or an essential metal such as Zn(II).

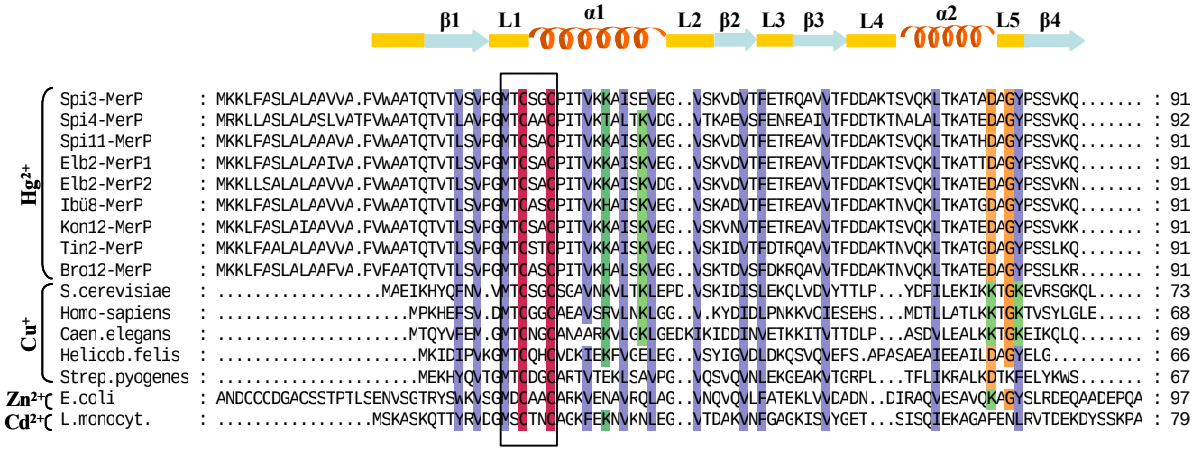

Figure 3-40. **Sequence alignment of the metal transporting proteins**: MerP, copper chaperone, zinc-transporting and cadmium-transporting ATPase. The MerP protein of the eight environmental isolates are represented and aligned with cadmium-transporting ATPase (Cadmium efflux ATPase) of *Listeria monocytogene*, zinc-transporting ATPase of *Escherichia coli* O157:H7 (BAB37741), copper chaperone of *Streptococcus pyogenes* (AAK34461), copper ion binding protein of *Helicobacter felis* (O32620), copper chaperonin of *Caenorhabditis elegans* (NP_498707), copper transport protein HAH1 from *Homo sapiens* (AAC51227) and copper transporter Atx1 from *Saccharomyces cerevisiae* (NP_014140). The metal binding motif MXCxxC is boxed. The two metal-binding cysteines are shaded in red. Positions where hydrophobic residues are conserved are shaded in blue. Key positive (Arg and Lys) and negative (Glu and Asp) residues are indicated in green and in orange, respectively. The secondary structure elements reported above the alignment were analyzed by Predict Protein at EMBL-EBI: PredictProtein. Secondary structural motifs are α-helix (α1 and α2), β-sheet (β1-β3) and protein loops (L1-L5).

3.5.6 Identification of Further Transport Genes *mer*C and *mer*F

Two primer pairs T1-A5 and P1-A10 were used to amplify the regions immediately flanking *mer*A to detect possible gene insertions and/or deletions that are responsible for the structural variations of the *mer* operons. The chosen primers generated PCR products which indicated

the presence of the *mer*C or *mer*F gene neighboring *mer*P (Figure 1-4 and 3-30). From the different isolates two types of signal length were obtained: some amplicons were approximately 2600 bp (if the primer pair T1-A5 is used) or 960 bp in lenght (P1-A10), these amplicons contained *mer*C. With a fragment length of 2460 bp (T1-A5) or 790 bp (P1-A10) the sequence contained the *mer*F gene while PCR products of approximately 2210 bp (T1-A5) or 540 bp (P1-A10) lacked both *mer*C and *mer*F (see Table 3-8).

The PCR products of the two primer pairs (T1-A5 and P1-A10) were sequenced and aligned with sequences from plasmid pR100, transposon Tn5053, plasmid pKLH2 (containing *mer*C), plasmid pMER 327/419 (containing *mer*F) and plasmid pDU1358 (possesses neither *mer*C nor *mer*F).

The primers P1 and A10 amplified a region of approximately 530 bp from *Ps. putida* Spi3, *Ps. putida* Spi4, *Ps. putida* Elb2, *Ps. stutzeri* Ibü8, *Ps. putida* Kon12 and *Ps. aeruginosa* Bro12 (Figure 3-41). The sequenced amplicons contained the 3' end of *mer*P and the 5' end of *mer*A, without further genes. The similarity of the sequence to those of Tn501 in Spi3 could be confirmed by "blasting" the *mer*PA region. Amplification of this region with this primer pair and *Ps. putida* Spi4 DNA with this primer pair revealed fragments of a *mer* operon by generating a 537 nt PCR product harboring the *mer*PA region, however lacking *mer*C and being identical to the *mer*A gene from the *Klebsiella pneumoniae* plasmid pRMH760 (100% DNA sequence identity, which is similar to the broad spectrum *mer* module in pDU1358). The strain Kon12 also showed also a very close relationship to the *mer*PA genes from plasmid pDU1358 (99.0 % nucleotide identity). Whereas the strain Ibü8 had a remote similarity to the defined region from *Acinetobacter calcoaceticus* KHW14 including Tn5047 (91 % nucleotide identity).

In contrast *Ps. fulva* Spi11, *Citrobacter freundii* Tin2 and *Pseudomonas aeruginosa* Bro12 showed a signal of approximately 900 bp. In these strains *mer*C was found between the *mer*P and the *mer*A gene (Figure 3-41). Sequencing of the defined region revealed that the entire 3' *mer*P, *mer*C and 5' *mer*A (PCA) region of Spi11 was 91% identical to its closest relative, *Pseudomonas sp.* (with regard to the *mer*PCA genes). On the other hand the *mer*C sequence of the strain Tin2 showed a very close relationship to the transmembrane protein MerC of Tn5047 from plasmid pKLH201 (97 % DNA sequence identity). The strain *Ps. aeruginosa* Bro12, which transformed thiomersal moderately (see Figure 3-5), had a 90 % similarity to the MerC protein of *Pseudomonas sp*. on transposable element Tn5041. Interestingly, Bro12 was the only strain that showed a second band in the 517 bp range besides its main signal around 1018 bp (Figure 3-41). The smaller PCR amplicon was identified with BLAST

analysis to be the 3' end of *mer*P and the 5' end of *mer*A lacking the *mer*C gene. This finding indicated the presence of a second *mer* operon in *Ps. aeruginosa* Bro12. The sequence of the second *mer*PA region was supported with the primer pair T1 and A5 (see Figure 3-42).

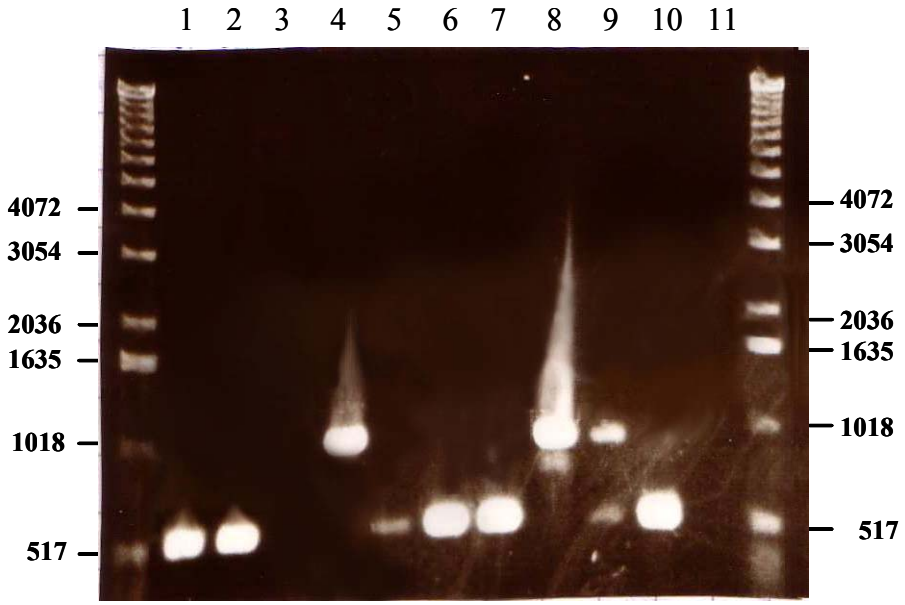

Figure 3-41. Amplification of the *mer*C (960 bp) or *mer*F gene (790 bp) from mercury resistant strains using P1 and A10 primer set. PCR products of 540 bp did not contain *mer*C or *mer*F. Lane 1: Spi3; Lane 2: Spi4; Lane 3: Spi7; Lane 4: Spi11; Lane 5: Elb2; Lane 6: Ibü8; Lane 7: Kon12; Lane 8: Tin2; Lane 9: Bro12. The positive control (lane 10) contained Tn501 as template and the negative control (Lane 11) did not contain any DNA template. The marker used was a 1 kb ladder.

The nucleotide sequence of the *mer*TPCA region amplified with the primers T1 and A5 comprised approximately 2600 bp nucleotides and the presence of the *mer*C gene in this region was confirmed for the strains Spi11 and Tin2. A further *mer*C gene was discerned in the *mer* operon of *Ps. putida* Spi4 (Figure 3-42). The presence of *mer*C in the T1-A5 amplicons of *Ps. putida* Spi4 was revealed by alignment of the approximately 2660 bp nucleotide sequence with DNA sequences specific for the *mer*C gene mentioned above. The highest similarity score for Spi4 obtained from BLAST analysis was the *mer*C gene from *Pseudomonas sp.* Tn5041 showing a 99% identity in nucleotide sequence. Alignment of all isolates possessing the *mer*C gene is depicted in Figure 3-43).

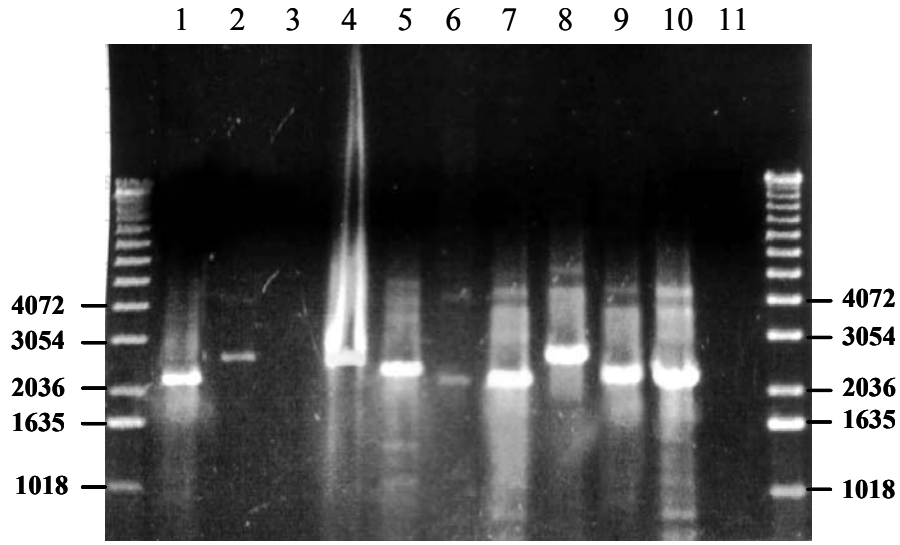

Figure 3-42. Amplification of the *mer*C (2600 bp) or *mer*F gene (2460 bp) from mercury resistant strains using T1 and A5 primer set. PCR products of 2210 bp did not contain *mer*C or *mer*F. Lane 1: Spi3; Lane 2: Spi4; Lane 3: Spi7; Lane 4: Spi11; Lane 5: Elb2; Lane 6: Ibü8; Lane 7: Kon12; Lane 8: Tin2; Lane 9: Bro12. The positive control (lane 10) contained Tn501 as template and the negative control (Lane 11) did not contain any DNA template. The marker used was a 1 kb ladder.

Unlike the four mentioned isolates (Spi4, Spi11, Tin2 and Bro12 possessing the *mer*C gene), *Ps. putida* Elb2 harbored a *mer*F gene lying between *mer*P and *mer*A instead of *mer*C (Figure A-7 in Appendix). The PCR product of Elb2 amplified with primer pair T1-A5 confirmed the presence of the *mer*F gene (Figure 3-42) which was 99% identical to the published sequence of *Xanthomonas sp.* W17 mercury resistance transposon Tn5053. Since previously a *mer* region was amplified using the primer pair P1-A10, which was too small (533 bp) to contain any additional genes (see Figure 3-41), it appears that Elb2 carries at least two *mer* operons. When sequenced this fragment lacked both *mer*C and *mer*F and was 99% identical to the *mer*PA region of plasmid pDU1358.

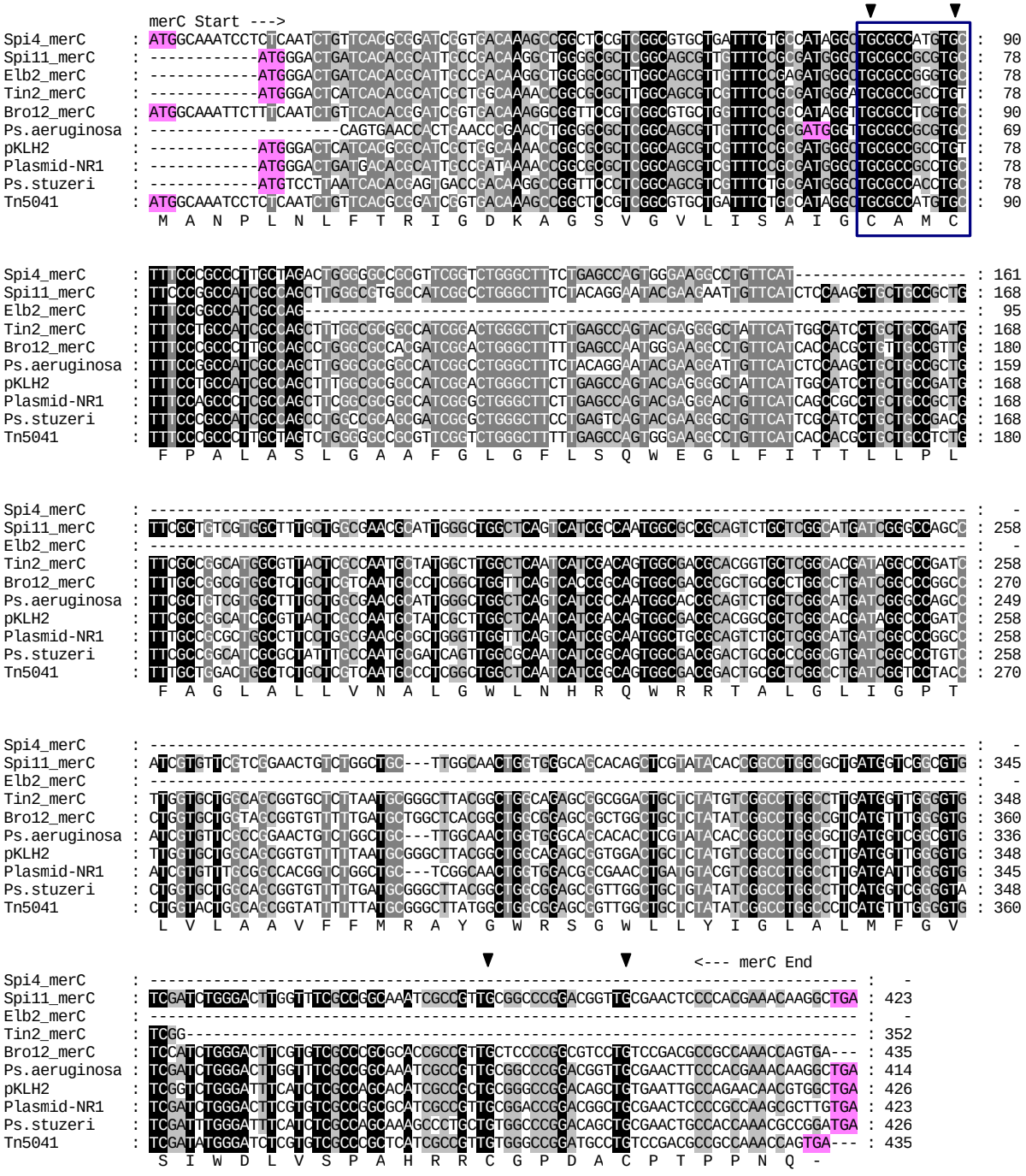

Figure 3-43. Alignment of the *mer*C genes of the 5 isolates and published *mer*C genes. The references are *Pseudomonas sp.*: Tn5041: X98999; Plasmid pKLH2: *Pseudomonas sp.*: Tn5041: X98999; *Ps. stutzeri*: plasmid pPB: U90263; Plasmid pKLH2: *Acinetobacter calcoaceticus*: AF213017; Ps. aeruginosa: AF120971. The *mer*C genes of Spi4, Elb2 and Tin2 were partly sequenced. Amino acid sequence of Tn5041 polypeptide is shown as standard single letter below the DNA sequence line. The four cysteine residues are marked with arrows above sequences and the typical metal binding motif (CxxC) on the N-termini of MerC is boxed. The stop codon is represented as (-). Black shade: 100% similarity; Gray: 80% similarity; Light gray 60% similarity. Start and stop codon are colored pink.

In the determination of *mer*C genes, a further primer pair R1 and D2 was used to amplify the DNA sequence of the strain Elb2 which according to the control sequence (pDU1358) was expected to yield a fragment length of approximately 3.5 to 4.0 kb.

The PCR gave four signals at 4 kb, 3 kb, 0.4 and 0.3 kb (Figure 3-44). The control PCR gave the expected signal at 4.0 kb and an additional signal at 0.7 kb. The latter and the 0.4 and 0.3 kb fragments of Elb2 were not further investigated. Both Elb2 signals of 4.0 kb and 3.0 kb were sequenced and contained *mer* genes. The 3.0 kb amplicon in addition contained *mer*C between *mer*P and *mer*A and this region was 92% similar in nucleotide sequence to the equivalent region of transposon Tn5041. On the other hand, the 4.0 kb fragment was 99% similar to the pDU1358 *mer* operon (without the *mer*C or *mer*F gene).

Overall, Elb2 appears to possess three *mer* operons: a *mer* operon containing the *mer*F gene between *mer*P and *mer*A (99% identical to Tn5053 of *Xanthomonas sp.* W17), the second possesses *mer*C (92% nucleotide identity to Tn5041) and the third *mer* operon lacked both *mer*C and *mer*F and was 99% identical to the *mer* operon of plasmid pDU1358.

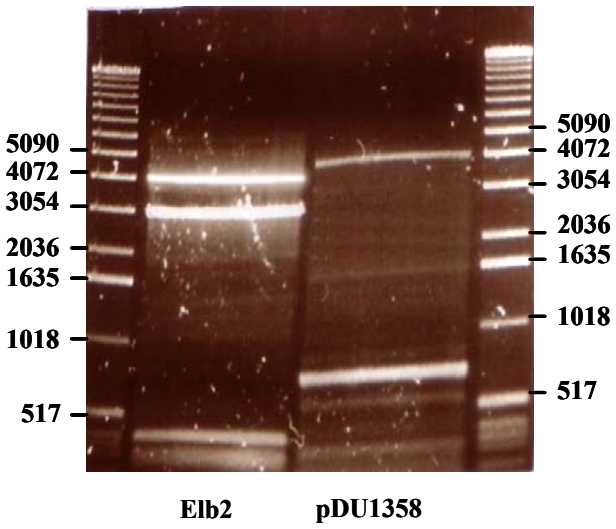

Figure 3-44. Amplification of *mer* operon from the strain *Ps. putida* Elb2 using primers R1 and D2. Two amplicons could be generated a first band in the 3054 bp range besides a second signal around 4072 bp. The signals at 0.3, 0.4 and 0.7 were shown not to be *mer* genes. The positive control contained pDU1358 as template and showed one signal at 4072 bp. The marker used was a 1 kb ladder (see section 2.5.2).

After careful analysis of the predicted MerC proteins from Spi4, Spi11, Elb2, Tin2 and Bro12 it became evident that all contained a cysteine pair located in the first transmembrane region with the motif: Cys-Ala-Ala-Cys and Cys-Ala-Met-Cys (Figure 3-45). Exchange of methonine against alanine is biochemically insignificant. From mutagenesis studies with the MerC protein there is clear evidence that these cysteine residues are required for mercuric ion transport (Sahlmann *et al.* 1999). Translation of the *mer*F nucleotide sequence sequence of Elb2 to protein sequence revealed conserved features of the MerF protein (cysteines) in the first transmembran region (Cys-Cys) and in the cytoplasmic regions of MerF (Cys-Cys). Given this homology it can be considered that MerC and MerF may function by equivalent mechanisms, with mercury-binding cysteines within a transmembrane helix.

The amino acid proline at the carboxy-terminal side of this cysteine motif, marked blue in Figure 3-45, is conserved. As already mentioned, studies have emphasized the importance of proline for the structure and function, due to its capacity to expose Cys residues to solvent as may the proline residues in the second transmembrane regions (Brown *et al.* 2002; Wilson *et al.* 2000). A statistical analysis of Brandle and Deber (1986) revealed that proline residues are frequently found in the transmembrane segments of ion channels and transporters but not in the transmembrane segments of proteins that have no transport function. Having prolines in the middle of protein could be important for the mechanism of transport since proline residues are considered to be helix-breakers because they lack amide hydrogen and because they cause a kink of about 26° in the α -helix. Proline-kinks in α-helices may pack to form either funnel- or cage-like structures, which have the potential to form either a channel vestibule or ion binding site(s) (von Heijne *et la.* 1991, Williams *et al.* 1991). Whereas the relevance of this motif to Hg(II) uptake in MerF is not known, the occurrence of the helix-breaker proline in the middle of a transmembrane α-helix is reminiscent of the P-type ATPases which often occur in metal ion transport systems (Lutsenko *et al.* 1995; Solioz *et al.* 1996). Heavy metal ATPases commonly contain the consensus motif CxxC and they feature a conserved intramembranous CPC motif (CPx motif respectively).

Transmembran I

```
Spi4-MerC   : LISAIGCAMCFPALARLGAA
Spi11-MerC  : VVSAMGCAACFPAIASLGVA
Elb2-merC   : VVSEMGCAGCFPAIASLGAA
Tin2-MerC   : VVSAMGCAACFPAIASFGAA
Bro12-MerC  : LVSAIGCASCFPALASLGAT
Tn5041-MerC : LISAIGCAMCFPALASLGAA
Elb2-MerF   : GTTLVALCCFTPVLVILLGV
Tn5053-MerF : GTTLVALCCFTPVLVILLGV
```

Transmembran II

```
Spi11-MerC : EELFISKLLPLFAVVALLANALGWL
Tin2-MerC  : EGLFIGILLPMFAGLALLANAMAWL
Bro12-MerC : EGLFITTLLPLFAGVALLVNALGWF
Tn5041-Mer : EGLFITTLLPLFAGLALLVNALGWL
Elb2-MerF  : ....YLDYVLLPALAIFIGLTIYAI
Tn5053-Mer : ....YLDYVLLPALAIFIGLTIYAI
```

Cytoplasmic region

```
Spi11-MerC  : IWDLVSPANRRCGPDGCELPTKQ
Bro12-MerC  : IWDFVSPAHRRCSPASCPTPPNQ
Tn5041-MerC : IWDLVSPAHRRCGPDACPTPPNQ
Elb2-MerF   : ..QRKRQADACCTPKFNGVKK..
Tn5053-MerF : ..QRKRQADACCTPKFNGVKK..
```

Figure 3-45. The alignment of the transmembrane regions in MerC and MerF with illustration of conserved amino acids of five isolates and published protein sequences. The polypeptide sequence of Spi4, Spi11, Elb2, Tin2 and Bro12 and *Pseudomonas sp.*: Tn5041: CAA67450; *Xanthomonas sp.* W17: Tn5053: AAA98325 are shown. Conserved cysteines are colored pink while the charged residues in the second transmembrane region are gray shaded; the proline residues in the first and second transmembrane region are colored blue. Due to the gap in sequence the alignment of the second transmembrane region and the Cytoplasmatic region could not be performed with the Spi4, Elb2 and Tin2 *mer*C sequences. The analysis of the transmembrane and cytoplasmatic region was carried out with NPS@ (Network Protein Sequence @nalysis: **http://npsa-pbil.ibcp.fr/**)

MerC and MerF proteins do not seem to affect the thiomersal resistance crucially since the isolates with these proteins transformed thiomersal at different, high and low rates: e.g. Spi4 and Spi11 both possessed MerC and showed high transformation rates (268 and 386 ng Hg· ml^{-1} · min^{-1}) while Tin2 only showed poor resistance (see Figure 3-5). Despite having MerC, it must be concluded that MerC was not responsible for differences in resistance. Consistent with the observation, the thiomersal transformation rate of Elb2 was not notably enhanced (90 ng Hg· ml^{-1} · min^{-1}) although it did contained both MerF and MerC. In contrast, the transformation rate of thiomersal was comparably high for Ibu8 or Kon12 (96 and 83

ng Hg· ml^{-1} · min^{-1} respectively) although they did not possess either MerC or MerF. This observation may be explained by the fact that organomercurials such as TH are sufficiently lipid-soluble to enter the cell efficiently without a specific uptake system.

A *mer*G gene (654 bp) could not be detected in any of the eight isolates although in some mercury resistant strains it has been found to be responsible for phenylmercury resistance (Kiyono *et al.* 1998). Recent work shows that the *mer*G gene is frequently found in broad-spectrum resistance operons borne by Tn5041 and carried by soil and water *Pseudomonads* (Kholodii *et al.* 2002). However, this finding did not apply to Spi4, Elb2 and Bro12 although their resistance operons are most similar to Tn5041.
Similarly, no *mer*E gene could be detected in the isolates. The *mer*E gene (237 bp) which overlaps with the 3' end of the *mer*D gene by 4 bp, encodes a predicted protein of 78 amino acids. It has been suggested that MerE plays a role in Hg(II) transport because of its similarities with mercury transport proteins (MerT, MerC, and MerF).

3.5.7 Identification and Analysis of the *mer*A gene

The *mer*A gene encodes a cytoplasmic dimeric enzyme (564 aa) and is the largest and most conserved gene in the *mer* operon. Therefore, it is widely used in microbial ecology to study functional community profiles and phylogenetic relationships among the mercury resistance bacteria (Felske *et al.* 2003; Liebert *et al.* 1997).
The primer pair A1 and A5 was designed to amplify the *mer*A gene with the 5' primer (A1) and the 3' primer (A5) lying in the highly conserved unique Hg (II)-binding domain. These domains are found in all MerA proteins. With those two primers, the *mer*A genes of all eight mercury resistant isolates could be amplified and examined. In order to obtain the complete *mer*A sequences a third primer A7 was used whose amplicon partly overlapped with the amplified sequence of the primers A1-A5. Further primers were also used such as P1, T1 and D1 which annealed to conserved regions outside of *mer*A.
After sequencing of the amplified fragments, the complete *mer*A genes were assembled and aligned (Figure 3-46 a-d). A high similarity between the *mer*A sequences of the isolates and published *mer*A sequences from natural transposons and plasmids could be found. A phylogenetic tree was generated by using the *mer*A sequences of the eight natural isolates and 26 published nucleic acid sequences of *mer*A genes and calculated with the maximum likelihood algorithm (Figure 3-47).

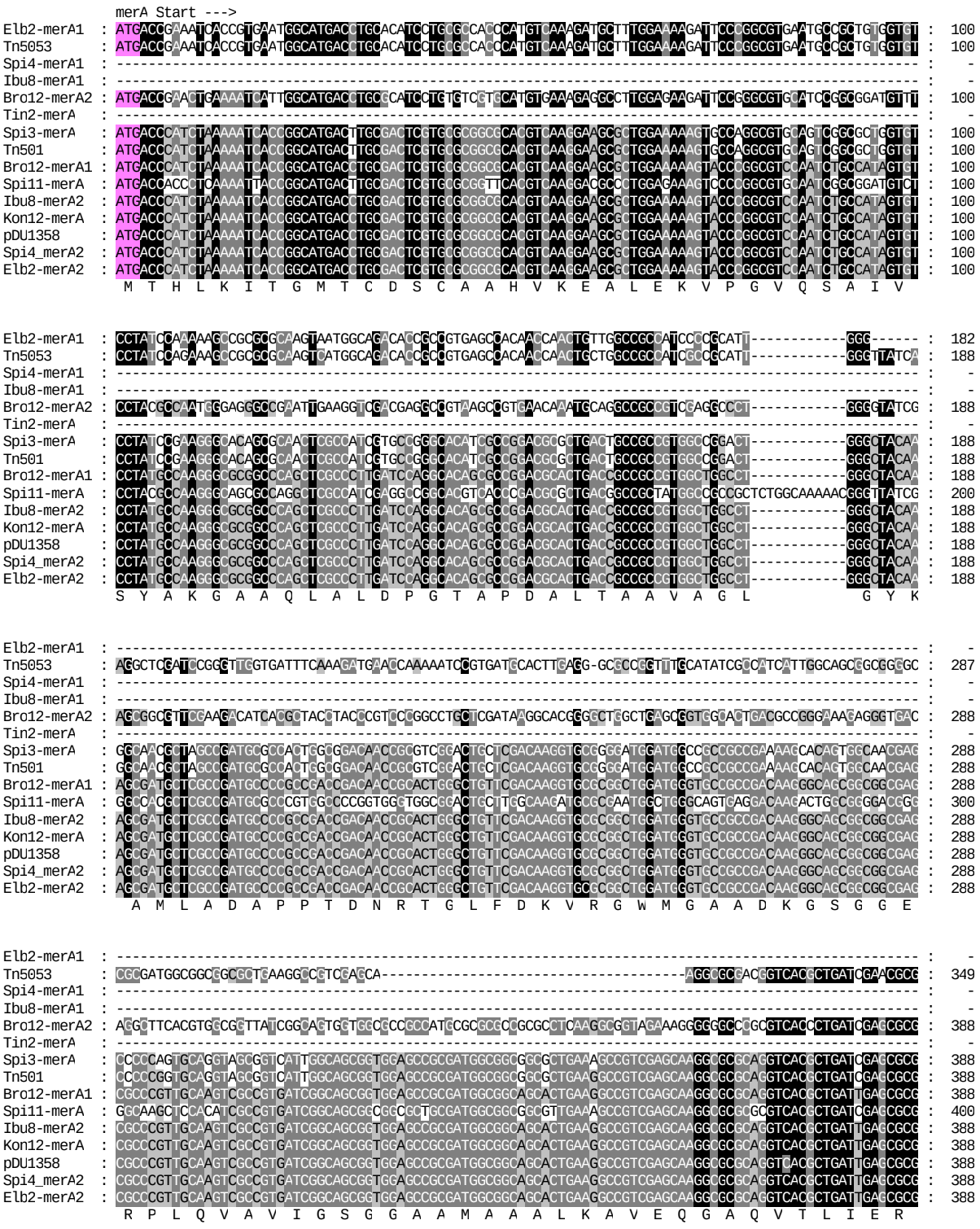

Figure 3-46a. Alignment of the *mer*A genes of the eight environmental isolates and published genes. Plasmid pDU1358: *Serratia marcescens*: M24940; *Xanthomonas sp. W17*: Tn5053: L40585; Transposon Tn501: *Pseudomonas aeruginosa* plasmid pVS1: Z00027. Gap in nucleotide sequence of Elb2-merA1 (183-389 bp numbering from pDU1358), Spi4-merA1 (up to 1126 bp from pDU1358), Ibu8-merA1 (up to 771bp from pDU1358), Tin2-merA (up to 438 bp) are not sequenced regions. Amino acid sequence of the pDU135 polypeptide (accession no. M15049, Z49200 and M24940) is shown as standard single letter below the DNA sequence line. Black shade: 100% similarity; Gray: 80% similarity; Light gray 60% similarity. Start and stop codon are colored pink.

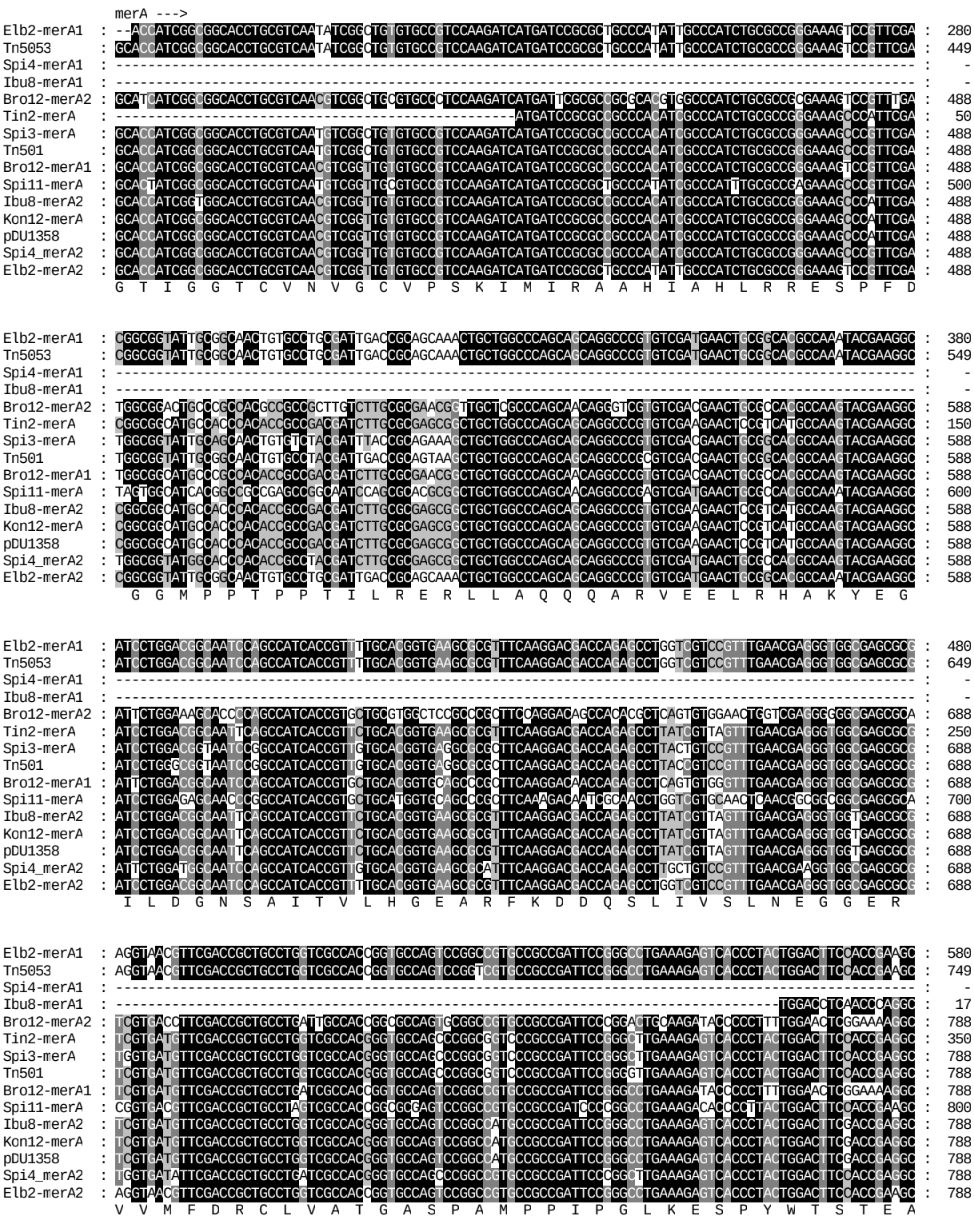

Figure 3-46b. Continuation of *mer*A sequence alignment from natural isolates and published genes (389nt-788nt).

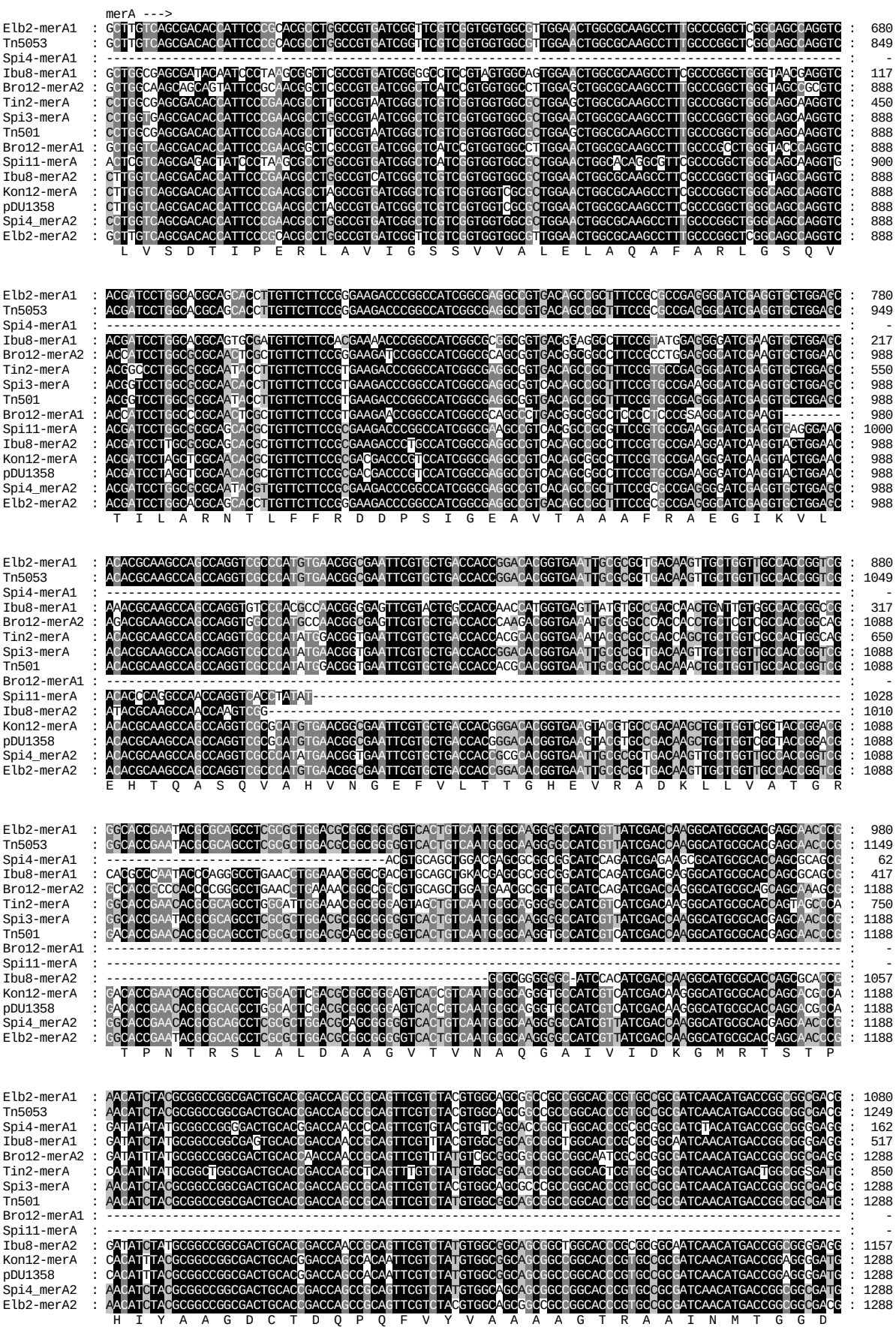

Figure 3-46c. Continuation of *mer*A sequence alignment from natural isolates and published genes (789 nt- 1288 nt).

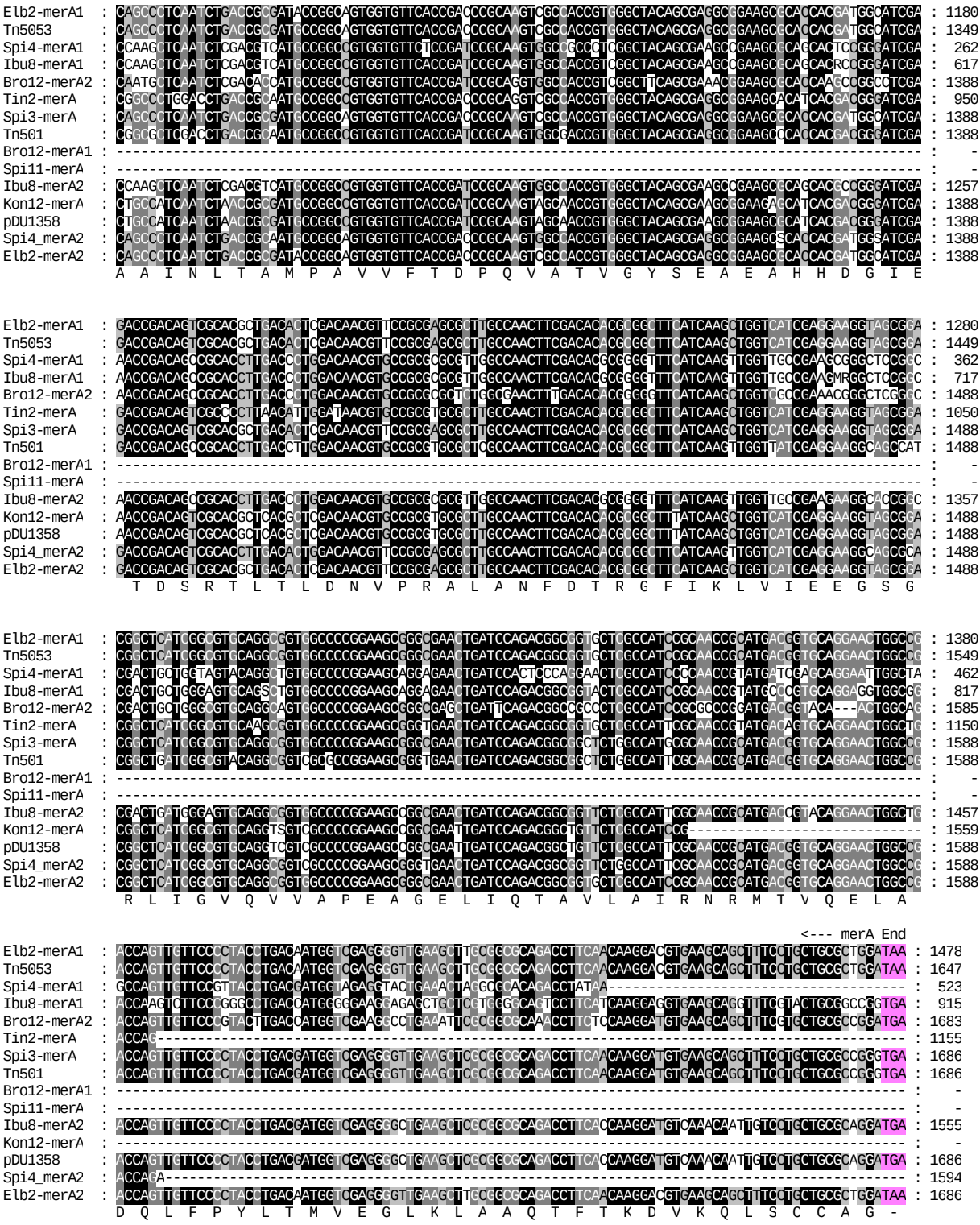

Figure 3-46d. Continuation of *mer*A sequence alignment from natural isolates and published genes (1289 nt -1686 nt). Stop codon is colored pink.

Although the *mer*A genes of the isolates were similar to already published *mer*A sequences, every strain was distinct (1-30% differing nucleotides in *mer*A). The strain Spi3 carried a mercuric reductase very closely related to the one of Tn501 (96 % DNA sequence identity, 517 of 527 amino acids identical). The strains Ibu8 and Kon12 showed a very close relationship to a mercuric reductase from plasmid pDU1358 (97.5 and 99.0 % nucleotide identity, respectively). A second 0.8 kb *mer*A fragment was sequenced from Ibu8 for which a homology search showed 96% similarity to the transposable element Tn5041. The *mer*A sequences of strains Elb2 and Spi4 were more distantly related to pDU1358 (91.1 and 93.9 % nucleotide identity) but were closely related to that of transposon Tn5041 (99% nucleotide identity). The second *mer*A gene of Elb2 showed 99% identity in nucleotide sequence to the transposable element Tn5053 of *Xanthomonas sp.* Strain Spi11 had remote similarity to a mercuric reductase from *E. coli* plasmids (<80 % nucleotide identity). The strain *Ps. aeruginosa* Bro12 possessed two *mer*A genes. While *mer*A_1 was most similar to the *mer*A gene of pDU1358 (91% identity in amino acid sequence), the second *mer*A gene (*mer*A_2) had a low similarity to already known mercuric reductases (around 80 % nucleotide identity).

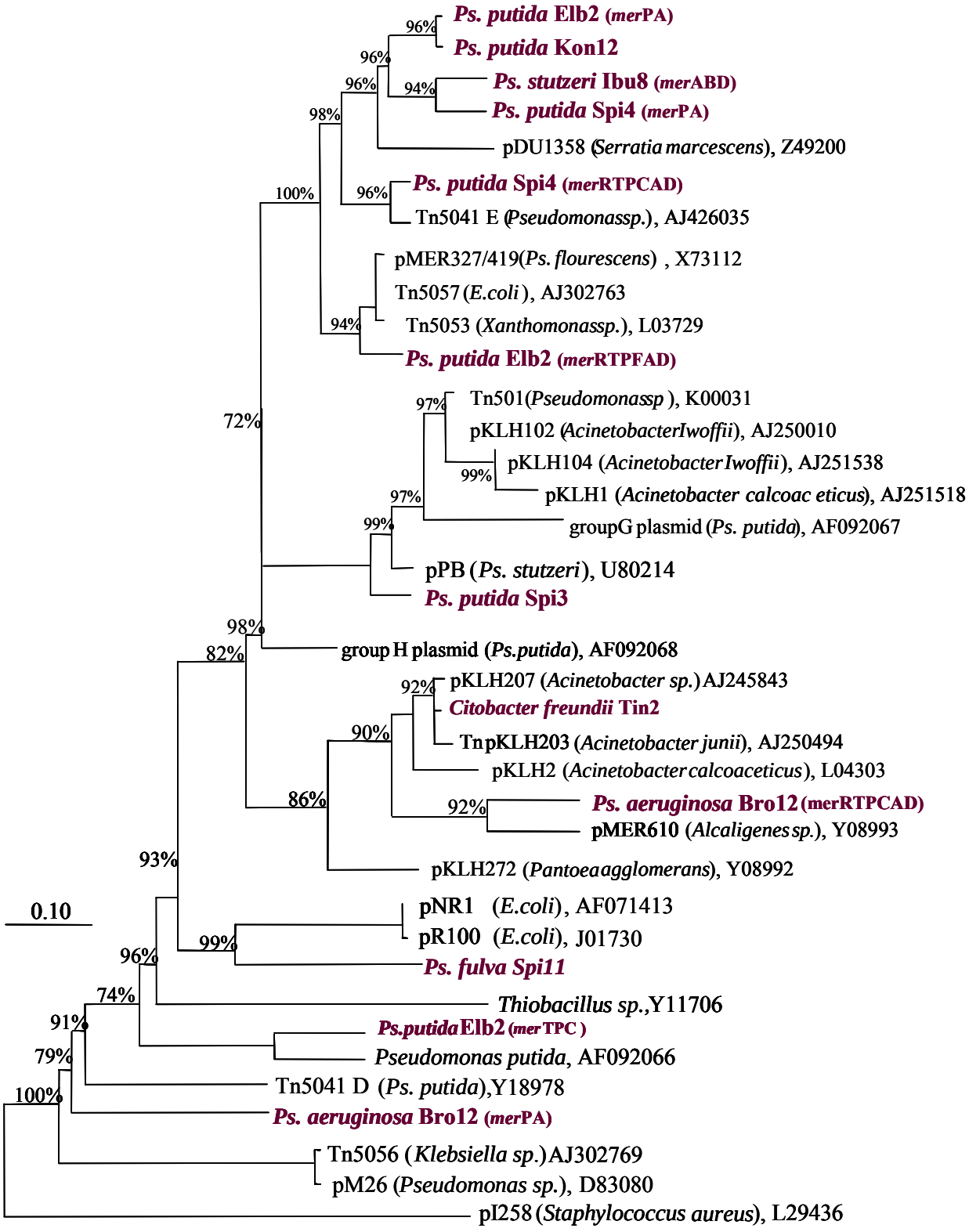

Figure 3-47. **Phylogenetic relationship between the *mer*A genes of Gram-negative bacteria.** The tree was based on an alignment of 26 published sequences and the *mer*A nucleic acid sequences of the eight investigated isolates and calculated with the maximum likelihood algorithm. Bootstrap values above 65 % are given at the branching points. The bar indicates one nucleotide exchange per ten nucleotide positions. EMBL accession numbers are given after the names. The investigated strains are shown in claret red.

3.5.8 Identification of the *mer*B Gene

Historically, the presence of the *mer*B gene was used for a classification of *mer* operons into broad range and narrow range resistance system (Laddaga *et al.* 1987, Wang *et. al* 1989). The first sequenced *mer* operon carrying *mer*B (Griffin et al. 1987) on plasmid pDU1358 had the gene organization *mer*RTPABD. A narrow spectrum operon was located nearby on the same plasmid. Restriction mapping of the *mer* operon of the *Pseudomonas stutzeri* plasmid, pPB (Reniero *et al.* 1996), revealed yet another broad spectrum operon arrangement, *mer*RBTPCAD. A narrow spectrum *mer* operon, *mer*RTPAD, was also located on plasmid pPB. Huang *et al.* (1999) revealed the occurrence of three *mer*B genes in *Bacillus megaterium* strain MB1 and suggested a functional specificity of individual organomercurial lyases for organomercurial compounds. Thus, the position of the *mer*B gene can be variable.

The different transformation rates of the isolates (see section 3.1.3) suggested that different substrate specificities of the organomercurial lyases to thiomersal might lead to differences in resistance level. As already stated in section 3.4.1, a *mer*B gene was found in Spi3 between *mer*R and *mer*T which was identical to the arrangement of *mer* genes in plasmid pPB.

With primers A9 and D3 *mer*B could be detected if positioned in a *mer* gene arrangement as in pDU1358. Two *mer*AD PCR products of different sizes were observed, a large (about 1206 bp) and a small (470 bp) product (Figure 3-48). The presence of *mer*B in the large A9-D3 amplicon was confirmed by subjecting the sequence to BLAST analysis and by alignment with DNA sequences of published *mer*B containing *mer* operons. Only *Ps. stutzeri* Ibü8 produced such a large A9-D3 amplicon and four isolates (Spi3, Elb2, Kon12 and Tin2) each produced an approximately 470 bp amplicons lacking *mer*B. However, Kon12 and Tin2 only gave faint 470 bp products which were shown not to be *mer* genes (97% identity in DNA of *Ps. putida* FruR: fructose transport system repressor region). The *mer*B gene of *Ps. stutzeri* Ibu8 was found to consist of 1196 bp nucleotides and to encode a MerB protein of 212 amino acid residues (Figure 3-49). This amplicon was significantly homologous to the *mer*ABD region of plasmid pDU1358 showing 99% identity in DNA sequence with BLAST analysis. By using PCR primers A9 and D3, it was found that Ibü8 was the only isolate that carried the *mer*B gene upstream of *mer*D within the same operon (Figure 3-49).

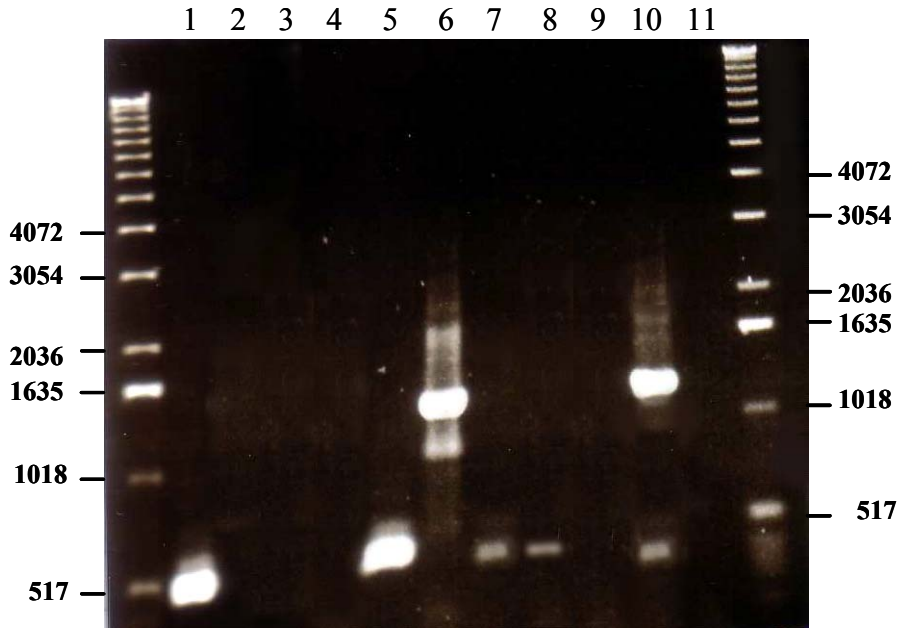

Figure 3-48. Amplification of the *mer*B gene (1200 bp) from mercury resistant strains using A9-D3 primer set. The smaller PCR products of 470 bp did not contain *mer*B. Lane 1: Spi3; Lane 2: Spi4; Lane 3: Spi7; Lane 4: Spi11; Lane 5: Elb2; Lane 6: Ibü8; Lane 7: Kon12; Lane 8: Tin2; Lane 9: Bro12. The positive control (lane 10) contained pDU1358 as template and the negative control (Lane 11) did not contain any DNA template. The marker used was the 1 kb ladder.

As shown in Figure 3-48 the two primers (A9-D3) amplified a product of approximately 470 bp with genomic DNA from *Ps. putida* Spi3 and *Ps. putida* Elb2. The analysis of these PCR products revealed the presence of the *mer*A gene followed immediately by *mer*D (but lacking *mer*B). The highest similarity score for Spi3 obtained from BLAST analysis was the *mer*A and *mer*D gene from Tn501 showing a 99% identity in nucleotide sequence (identity of 469 bp from 470 bp of the *mer*B region) and the PCR product of Elb2 showed a very close relationship to the *mer*A and *mer*D gene from *Xanthomonas sp.* W17 mercury resistance transposon Tn5053 (98 % nucleotide identity).

Since all isolates except for *Citrobacter freundii* could cope with TH concentrations up 2 ppm, it is most probable that the bacteria possessed the *mer*B gene in their *mer* operon. Nevertheless, a *mer*B gene could only be confirmed in Ibü8 and Spi3. Therefore, further PCR primers pairs (B2-B3 and B1-D2) were designed which were directed against the *mer*B gene itself.

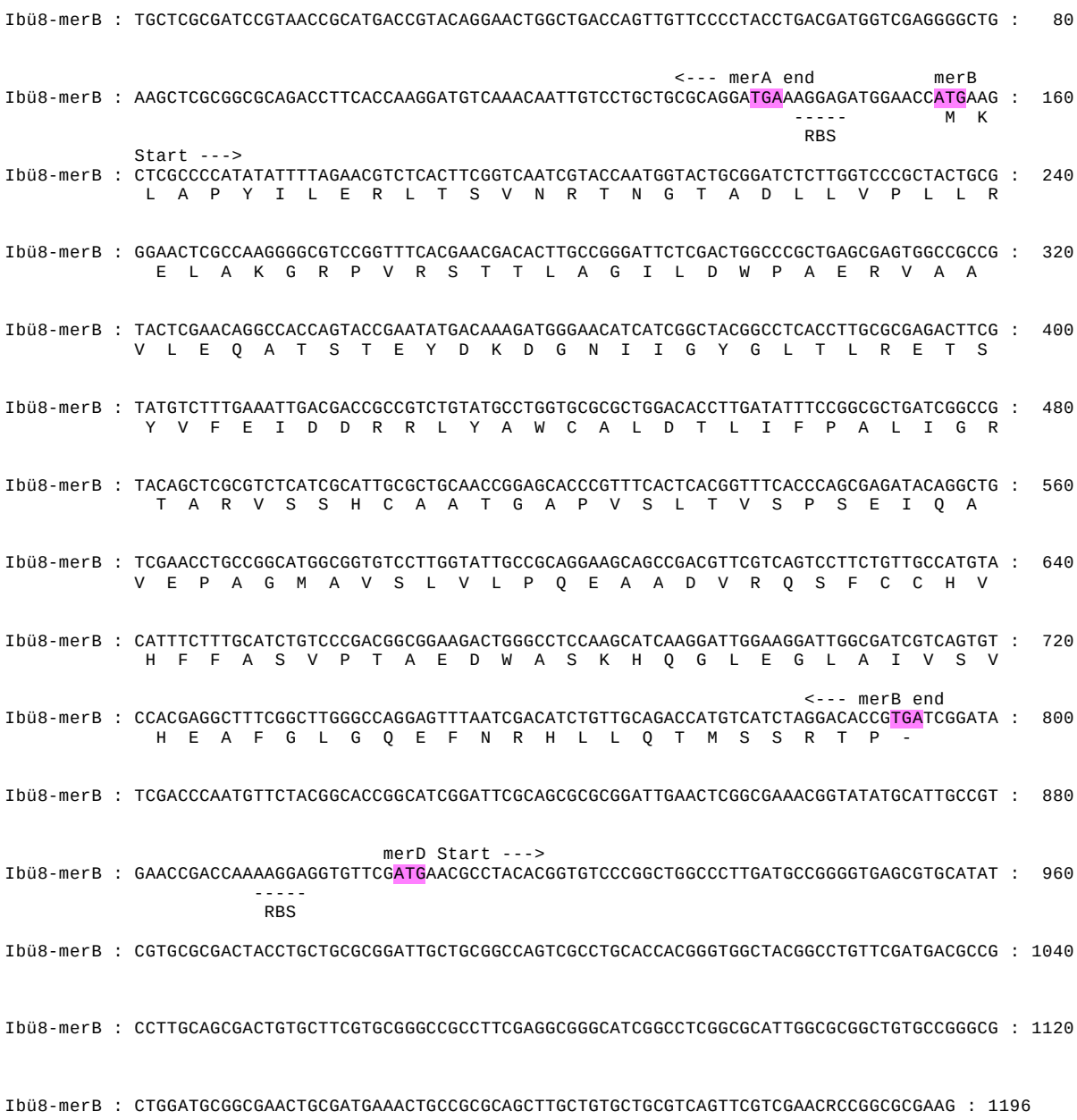

Figure 3-49. **Nucleotide sequence of 1196 bp of *Ps. stutzeri* Ibü8 broad spectrum mercury resistance, including the gene *mer*ABD.** Ribosomal binding site (RBS), Start and Stopcodons are colored in pink. The predicted polypeptide aa sequences are shown. The stop codon is represented as (-).

The PCR primers for the *mer*B gene of the isolates were developed based on a sequence alignment of published *mer*B sequences (see section 3.4.1) and conserved priming regions could not be identified due to the high *mer*B sequence variability. However, for the construction of the two PCR primers B2 and B3, two regions more than 200 bp (240 bp) distant from each other were identified (see Figure 3-31). A further primer pair was designed

which annealed to *mer*B and *mer*D (B1 and D2), generating a PCR product of approximately 1000 bp according to the control DNA of pDU1358.

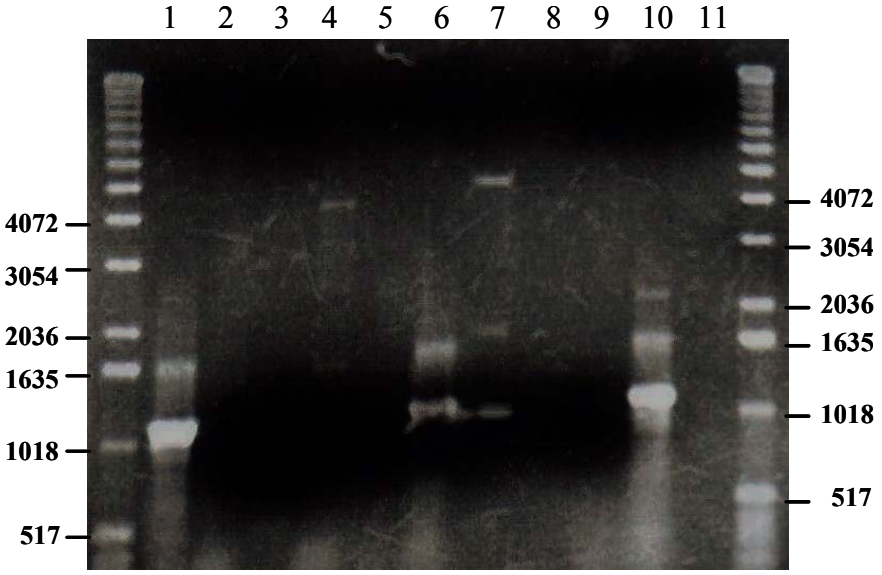

Figure 3-50. Amplification of the *mer*B gene (1000 bp) from mercury resistant strains using B1 and D2 primer set. Lane 1: Spi3; Lane 2: Spi4; Lane 3: Spi7; Lane 4: Spi11; Lane 5: Elb2; Lane 6: Ibu8; Lane 7: Kon12; Lane 8: Tin2; Lane 9: Bro12. The positive control (lane 10) contained pDU1358 as template and the negative control (Lane 11) did not contain any DNA template. The marker used was a 1 kb ladder.

These two primer sets (B2-B3 and B1-D2) amplified the desired regions of three strains: *Ps. p.* Kon12, *Ps. p.* Spi3 and *Ps. st.* Ibu8 (Figure 3-50 and Figure 3-51). Both primer pairs amplified DNA regions of Ibu8 which were identical to the previously detected *mer*B sequence (99% identity in nucleotide sequence with plasmid pDU1358). The two amplicons from Kon12 (1062 bp from primer pair B1-D2 and 235 bp from B2-B3) showed 100% identity with that of plasmid pDU1358. The *mer*B gene of Kon12 is followed by *mer*D which in sequence is also similar to the one of plasmid pDU1358.

The nucleotide sequence of Spi3 that was amplified using PCR primers B1 and D2 comprised 1093 bp and two ORFs. The first ORF which consisted of 639 bp nucleotides encoded a protein with 212 amino acid residues. It was found that it was significantly homologous to the organomercurial lyase (MerB1) from pDU1358 showing a 100% identity in amino acid sequence. The second ORF downstream of *mer*B which consisted of 366 bp and encoded a polypeptide of 122 amino acid residues was significantly homologous to the MerD protein. The BLAST analysis also showed a high similarity with the MerD protein from pDU1358.

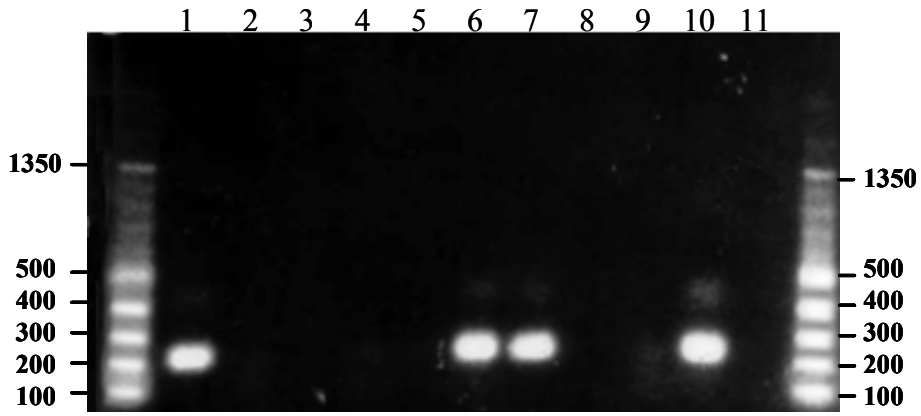

Figure 3-51. Amplification of the *mer*B gene from eight mercury resistant strains with the primer pair B2 and B3. The presence of the *mer*B gene was expected in a small amplicon of 0.2 - 0.3 kb in length. Lane 1: Spi3; Lane 2: Spi4; Lane 3: Spi7; Lane 4: Spi11; Lane 5: Elb2; Lane 6: Ibü8; Lane 7: Kon12; Lane 8: Tin2; Lane 9: Bro12. The positive control (lane 10) contained pDU1358 as template and the negative control (lane 11) did not contain any DNA template. The marker used was the 100 bp DNA ladder.

The PCR primer pair B2 and B3 revealed a second *mer*B gene in Spi3 that was more distantly related to pDU1358. Although the highest similarity score was reached with the MerB protein from pDU1358 (84%), only 183 amino acids from 209 were identical on the protein level. The central part of the deduced amino acid sequence (MerB2) had a 97 % similarity with the MerB sequences of Tn5058 from *Pseudomonas sp.* (Figure 3-52). By aligning the MerB proteins with the published proteins, a comparatively high degree of similarity can be shown in the central part of the protein (Figure 3-52). The alignment of the nucleotide sequences of the *mer*B genes are shown in Appendix (Figure A-10).

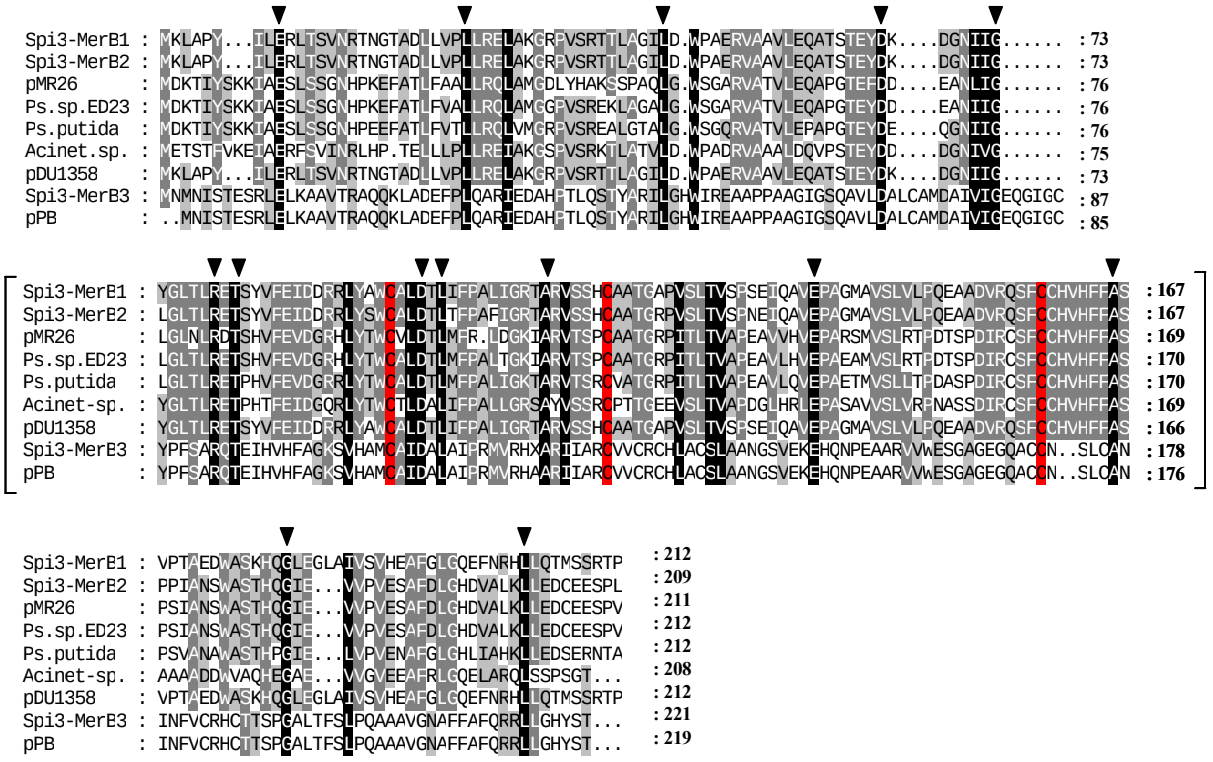

Figure 3-52. Alignment of three MerB proteins (MerB1-MerB3) from *Ps. p.* Spi3 compared with Gram-negative MerB proteins. The central region of the deduced amino acid sequences is set in the bracket. MerB1 was amplified by the primer pair B1-D2, while MerB2 and MerB3 are PCR products of the primer pair B2-B3 and R3-T2, respectively. Amino acid residues of MerB, including arginine (R-82), threonine residue (Thr-84), aspartate (D-99), three cysteine residues (Cys-96, Cys-117, Cys-159), glutamate (E-137) and one leucine residue (Leu-101), are found to be highly conserved in all MerB genes. The highly conserved amino acid residues are indicated by arrows and cysteine residues are red marked. Sequences were compared to the following *mer* operons: pDU1358 (MerB of the plasmid pDU1358, accession number P08664; Griffin *et al.* 1987), pMR26 (MerB1 of plasmid pMR26, accession nr D83080; Kiyono *et al.* 1997), *Pseudomonas sp.* ED23-33 (MerB1: accession nr. CAC14702; Mindlin *et. al* unpublisched), *Ps. putida* (accession nr. CAC86907; Kholodii *et. al* 2000), *Acinetobacter sp*. (accession nr. CAC80892; Kholodii *et. al* 2004), pPB (MerB of plasmid pPB, accession nr AAC38230; Reniero *et al.* 1998). Black shade: 100% similarity; Gray: 80% similarity; Light gray 60% similarity.

Presently there are few MerB sequences recorded in Genbank (**National Center for Biotechnology Information (NCBI)**). The MerB sequences present in the data bank show no homology with any other protein with an identified function. Therefore, it could be maintained that MerB is a unique enzyme. Moreover, the similarity between them is small. It is remarkable that with the primer pairs employed the *mer*B gene was detected only in three of the eight natural mercury resistant isolates.

Sequencing and analysis of the genomic DNA revealed three merB genes in Spi3 which are probably located in three different *mer* operons. Two of the three *mer*B genes (*mer*B_2 and

merB_3) are peculiar: While *mer*B_2 presents an unusual version of amino acid sequence except for the central part, *mer*B_3 was mapped in a peculiar position (*mer*RBT). The *mer*B genes themselves or an interaction between the three MerB proteins may be responsible for the eminently high thiomersal transformation rates of Spi3. To characterize the functional roles of each of these *mer*B genes, each *mer*B should be subcloned and characterized independently.

3.5.9 Comparison between the *mer* Operons

For a comprehensive analysis of the diversity of *mer* operons in the isolates, the overlapping individual *mer* gene sequences (see section 3.4.1) were assembled. A large number of primers were employed to create enough overlapping PCR products to cover the entire operon by sequence (see Figure 3-30). The primers based on the genes *mer*R, *mer*A, *mer*T, or *mer*D yielded a product in 90% of the performed PCR reactions and proved suitable for an analysis of the operon. The complete alignments of the *mer* operons from each strain are shown in the Appendix (Figure C-16–31).

3.5.9.1 *The mer Operons of Pseudomonas putida Spi3*

The strain *Ps. putida* Spi3 harbored a special feature, since it carried four functional *mer* operons, one conferring narrow spectrum (*mer*NS), the others broad spectrum resistance (*mer*$BS_{1/2/3}$). The completely sequenced *mer*NS operon of Spi3 had essentially the same gene organization as transposon Tn501 (97% similarity in DNA sequence). The *mer*R gene was followed by sequences corresponding to a typical *mer* O/P region and followed downstream by *mer*TPAD genes (Figure 3-53a-b). As already mentioned, the *mer* operons of bacteria are often located on plasmids and transposons. Since, mobile elements containing mercury resistant determinants were detected in 25–50% of bacteria of different species (Kelly *et al.* 1984, Dahlberg *et al.* 1995, Pearson *et al.* 1996). One of the first well-characterized mercury resistance transposon was Tn501 which was segregated from clinical isolates and define a compact group within the Tn3 family of transposons. Moore *et al.* (1989) demonstrated that resistant cells containing *mer* operon located on Tn501 were grown well at $HgCl_2$ concentrations of 25–250 µM. Owning Tn501 may confer good resistance towards mercury. Thus, Spi3 efficiently reduced $HgCl_2$ and was responsible for good performance in the bioreactors. Moreover, Spi3 was not affected by disturbances such as rapid increases of mercury or continuously high mercury concentrations (von Canstein et al. 2001).

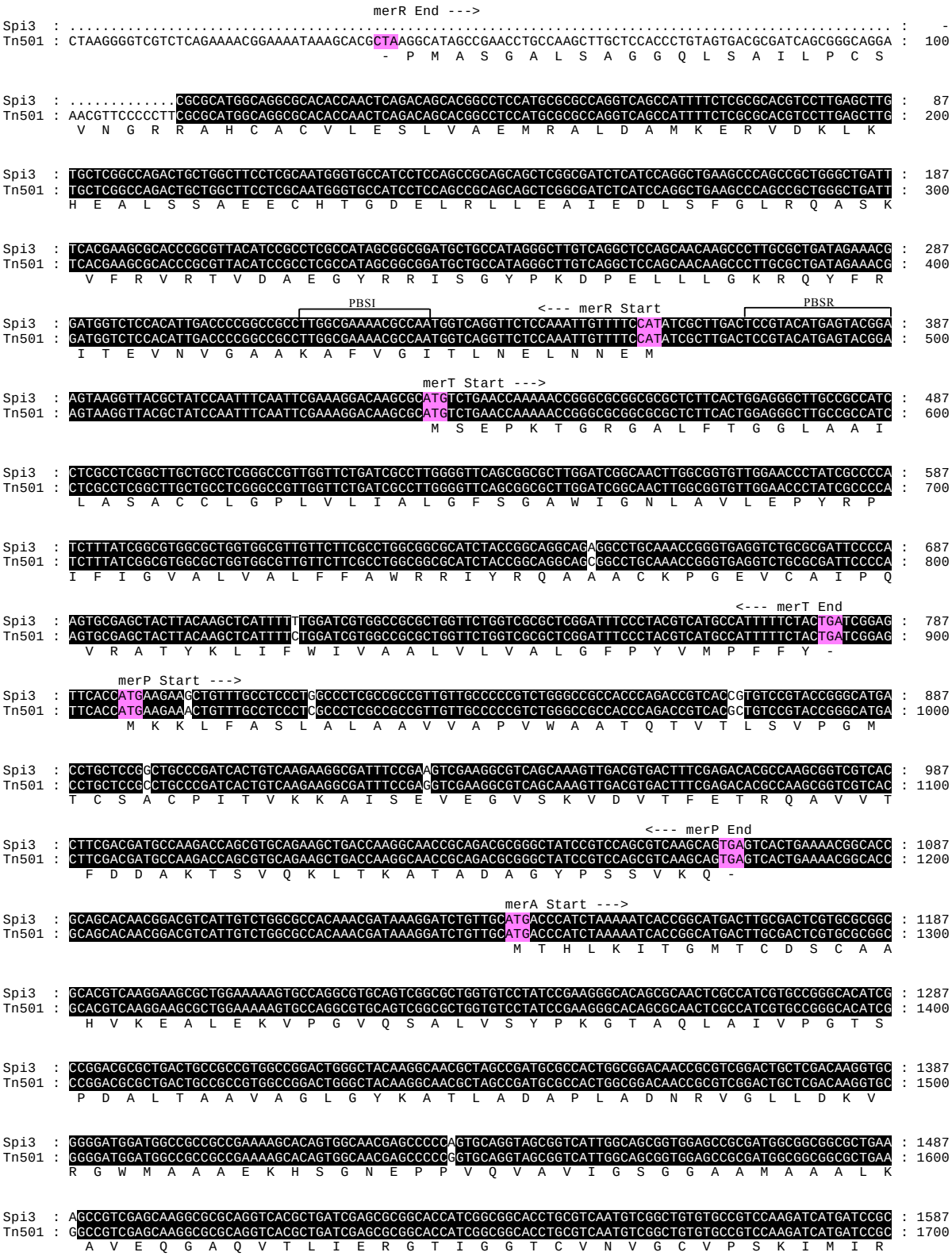

Figure 3-53a. **Nucleotide sequence of *Ps. putida* Spi3 narrow spectrum mercury resistance, including the gene *mer*RTPAD.** The *mer* operon is represented and aligned with the one of Tn501 from *Pseudomonas aeruginosa* plasmid pVS1 (Z00027). Amino acid sequence of Tn501 polypeptide is shown as standard single letter below the DNA sequence line. Black shade: 100% similarity. Start and stop codon are colored pink. The stop codon is represented as (–) and potential binding site for inducer (PBSI) and potential binding site for repressor are lined above the nucleotide sequence.

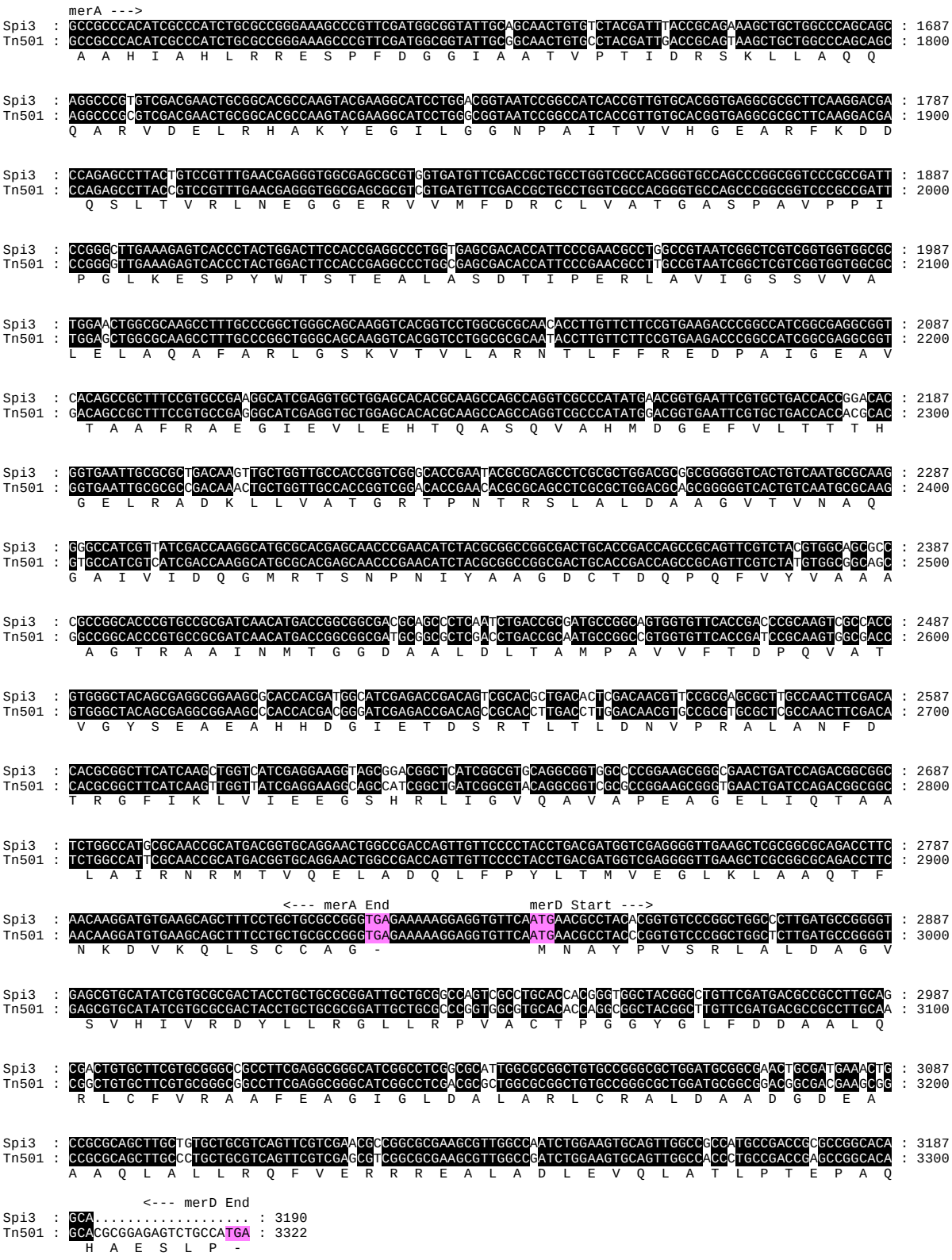

Figure 3-53b. Continuing the *mer* operon from *Ps. putida* Spi3. The nucleotide sequence is represented and aligned with Tn501 from *Pseudomonas aeruginosa* plasmid pVS1 (Z00027). Amino acid sequence of Tn501 polypeptide is shown below the DNA sequence line. Black shade: 100% similarity. Start and stop codon are colored pink. The stop codon is represented as (-).

Analysis of the broad spectrum resistance operon showed that Spi3 possesses three *mer*B genes which are probably located on three *mer* operons (Figure 3-54). The first *mer*B_1 gene which was mapped upstream of a *mer*D gene showed 100% identity to amino acid sequence of *Serratia marcescens* pDU1358. A second *mer*B_2 was also amplified upstream of a further *mer*D gene which encodes a deduced polypeptide of 209 amino acid residues that showed low similarity to MerB proteins in the databases (86% identity to *Pseudomonas sp.* K-62). In contrast to the both mentioned *mer*$B_{1/2}$, the gene arrangement of the third *mer*B_3 gene in the broad spectrum resistance operon was peculiar; the organomercurial lyase was mapped between the regulatory protein and the mercuric ion transport protein. This gene arrangement is only homologous to plasmid pPB from *Ps. stutzeri* that is described by D. Reniero *et al.* (1998). To confirm gene arrangement in Spi3 the upstream and downstream sequences of mer$B_{1/2/3}$ should be completely sequenced. Nevertheless, these four *mer* operons cause in Spi3 a high resistant to mercury chloride and organomercurials such as thiomersal. In order to obtain precise answers about the respective *mer* operons and their resistance to mercurial compounds, each cluster should be sub-cloned and characterized independently.

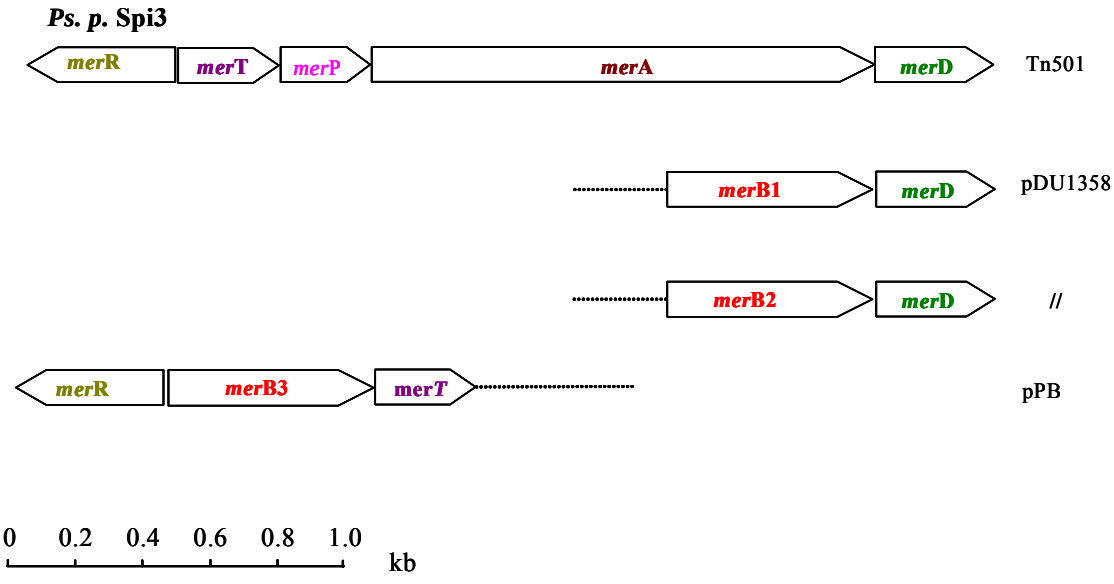

Figure 3-54. Schematic representation of the *mer* operons from *Ps. putida* Spi3. The dotted lines of *mer* operons indicate a sequence gap due to incomplete sequencing. The highest similar sequence obtained from BLAST analysis is specified at the end of the respective operon. The *mer*NS operon of Spi3 showed 97% similarity in DNA sequence to Tn501, *mer*B_1D showed 100% identity in amino acid sequence of pDU1358, *mer*B_2D had remote similarity to the amino acid sequence of Tn5058 from *Pseudomonas sp.* and the predicted polypeptide (aa) sequences of *mer*RBT was 99% similar to the one of plasmid pPB.

Like Spi3, almost all sequenced isolates carried multiple *mer* operons, as reflected by several *mer* operons that were sequenced in one isolate. The *mer* operon structure found in five isolates (*Ps. putida* Spi4, *Ps. fulva* Spi11, *Ps. putida* Elb2, *Citrobacter freundii* Tin2 and *Ps. aeruginosa* Bro12) was identical to the classical model of the narrow spectrum operon lacking *mer*B. Nevertheless, these five isolates were able to detoxify thiomersal. Therefore, one should expect MerB to be present in these strains.

3.5.9.2 *The mer Operons of Pseudomonas putida Spi4*

In Figure 3-55 a schematic *mer* gene arrangement of Spi4 is shown, a narrow spectrum resistance *mer* operon (*mer*RTPCA) and a second partly sequenced *mer* operon (*mer*PA). When the DNA sequences were analyzed, it was discovered that the narrow-spectrum resistance *mer* operon of the strain Spi4 possessed the additional gene, *mer*C, located between *mer*P and *mer*A. It should also be mentioned that no *mer*D gene could be detected. Actually, none of the published contiguous *mer* operon sequences lack *mer*D, whose translated MerD protein antagonizes the activation function of MerR (Mukhopadhyay *et al.* 1991, Champier *et al.* 2004). However, Liebert *et al.* 1997 also observed in their study contiguous *mer* operons without *mer*D. Nevertheless, the highest similarity score for Spi4 *mer*RTPCA obtained from BLAST analysis was the *mer* operon from Tn5041 showing a 97% identity in nucleotide sequence. The second partly sequenced *mer* operon, which only contained the genes *mer*P and *mer*A (900 bp), was 99% similar in DNA sequence to plasmid pDU1358. The *mer* operon of pDU1358 possesses a *mer*B gene and therefore, it is possible that this second gene arrangement is in possession of an organomercurial lyase, which causes the resistance to organomercurial compounds such as TH.

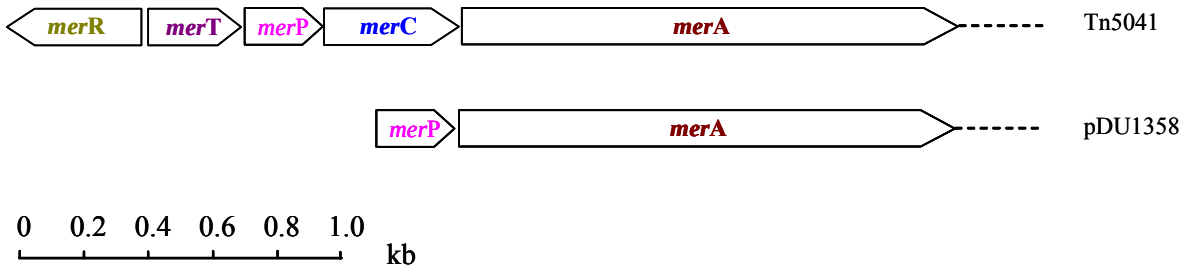

Figure 3-55. Schematic representation of the *mer* operon from *Ps. putida* Spi4. The highest similarity score obtained from BLAST analysis is specified at the end of the respective operon. The *mer*NS operon of Spi4 showed 97% similarity in DNA sequence to Tn5041, while the nucleotide sequence of *mer*PA fragment was 99% identical to plasmid pDU1358.

3.5.9.3 *The mer Operons of Pseudomonas fulva Spi11 and Citrobacter freundii Tin2*

The results of the DNA analysis from *Ps. fulva* Spi11 and *Citrobacter freundii* Tin2 showed in each case a typical and contiguous narrow spectrum resistance *mer* operon that possessed the *mer*C gene (Figure 3-56). The results of a homology search showed for Spi11 that the *mer*RTPCAD nucleotide sequence was distantly related to the mercury resistant transposon Tn21 from *Delftia acidovorans* MC1 (88 % nucleotide identity). In contrast, the sequenced *mer* operon of Tin2 with the same gene arrangement showed high similarity to the mercury resistant plasmid pMER610 from *Alcaligenes sp*. (96 % nucleotide identity).

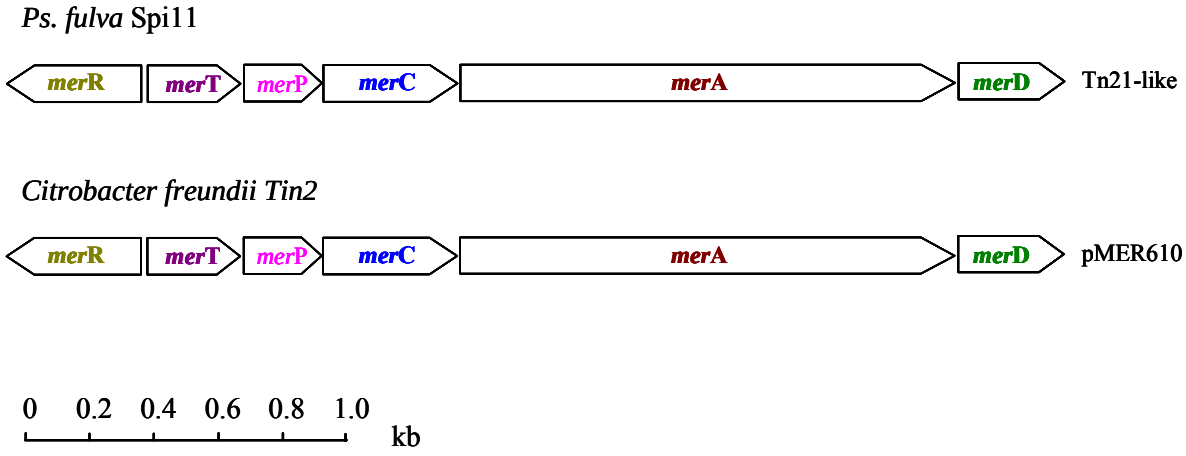

Figure 3-56. Schematic representation of the *mer* operon from *Ps. fulva* Spi11 and *Citrobacter freundii* Tin2. The highest similarity score obtained from BLAST analysis is specified at the end of the respective operon. The *mer*NS operon of Spi11 showed 88% identity Tn21-like mercury resistance transposon of *Delftia acidovorans* strain, while the nucleotide sequence of Tin2 showed 96% similarity in DNA sequence to plasmid pMER610 from *Alcaligenes sp*.

3.5.9.4 *The mer Operons of Pseudomonas aeruginosa Bro12*

A further narrow spectrum resistance operon with the same gene arrangement (*mer*RTPCAD) as mentioned above, was also identified in *Ps. aeruginosa* Bro12 (Figure 3-57). It is 3.6 kb in length and is 88% similar to its most closely related *mer* operon, Tn5047 from plasmid pKLH201 of *Acinetobacter calcoaceticus* KHW14. The second *mer* operon of Bro12, which was partly sequenced (*mer*PA with 1034 bp in length) probably, represents a broad spectrum resistance operon, in agreement with its similarity to plasmid pDU1358 (94% nucleotide identity). The broad spectrum *mer* resistance determinants from plasmid pDU1358 have been

genetically studied (Griffin *et al*. 1987, Nucifora *et al.* 1989) and the gene arrangement is in fact similar to narrow-spectrum organization, yet with an additional gene, *mer*B, specifying the organomercurial lyase enzyme, mapped immediately upstream of *mer*D. Therefore, it can be spectulated that Bro12 possesses a *mer*B gene, though none was detected here.

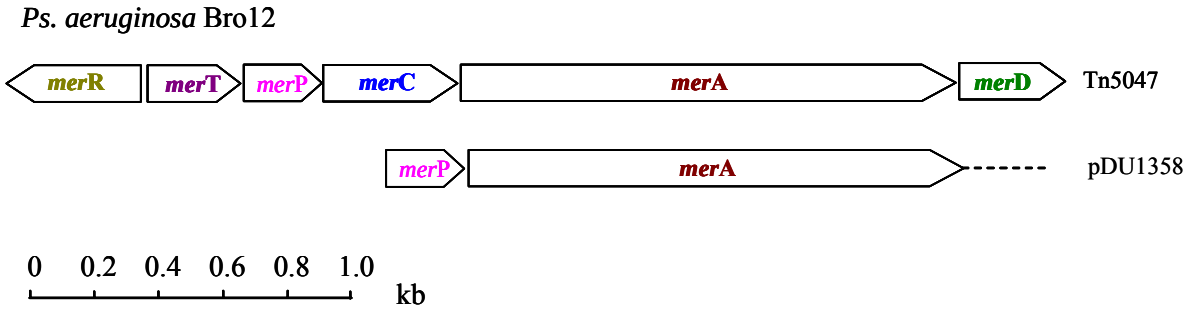

Figure 3-57. Schematic representation of the *mer* operon from *Ps. aeruginosa* Bro12. The highest similarity score obtained from BLAST analysis is specified at the end of the respective operon. The *mer*NS operon of Bro12 (*mer*RTPCAD) showed 88% similarity in DNA sequence to Tn5047 from *Acinetobacter calcoaceticus* KHW14 partial plasmid pKLH201, while the nucleotide sequence of *mer*PA fragment was 94% identical to plasmid pDU1358.

3.5.9.5 *The mer Operons of Pseudomonas stutzeri Ibu8 and Ps. putida Kon12*

It is apparent that only in the case of *Ps. stutzeri* Ibu8, *Ps. putida* Kon12 and *Ps. putida* Spi3, the *mer*B genes were mapped upstream of *mer*D (Figure 3-58), a frequently described gene order (Griffin *et al.* 1987, Sedlmeier and Altenbuchner 1992). The *mer* operon of Kon12 was furthermore highly similar (99% DNA sequence identity) to the broad spectrum *mer* operon from pDU1358 (Accession Numbers: M15049, Z49200, M24940 and AY225350).

In the case of Ibu8 only the merA, *mer*B and *mer*D region (1653 bp in length) could be sequenced, showing striking similarity to the same region of the mercury resistance operon from pDU1358 (99% identity in amino acid residue).

With the oligonucleotide primers used in this study, it was possible to amplify and sequence fragments of an additional *mer* operon from Ibu8. With the primers R-T, R-P and A-D the amplification of DNA fragments similar to those of transposable element Tn5041 (95% identity in DNA sequence) could be accomplished. The full length of the *mer*RTP region (1065 bp) and 3' end of *mer*A (900 bp) with the full length of *mer*D gene could be sequenced (1283 bp). It should be noted that the closely related operon Tn5041 encompasses the inner membrane protein *mer*C which is located between the *mer*P and the *mer*A gene

(*mer*RTPCAD) but the amplified products of Ibu8 lacked any additional *mer* genes (Figure 3-58).

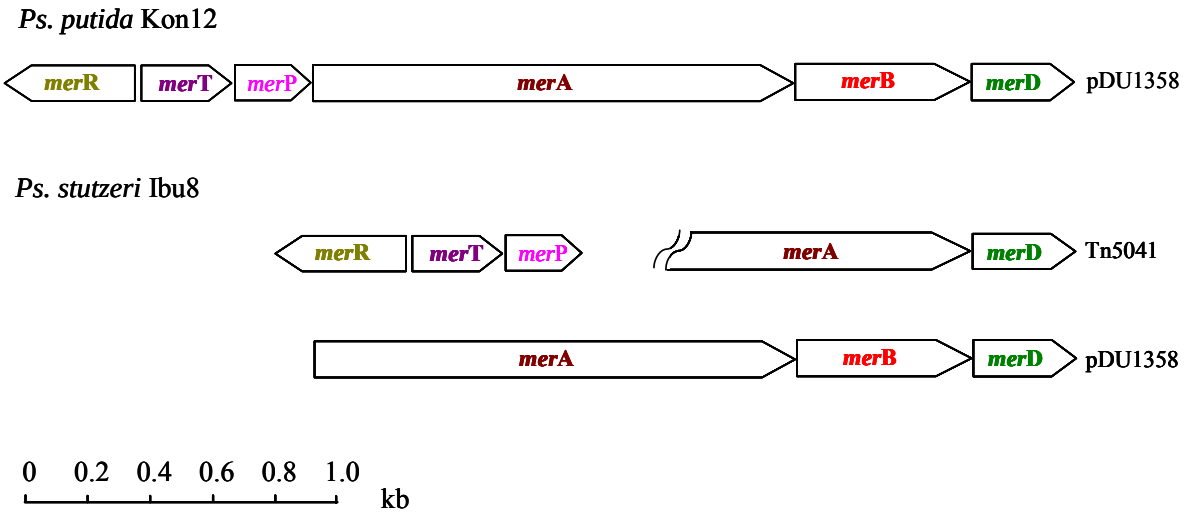

Figure 3-58. Schematic representation of the *mer* operon from *Ps. putida* Kon12 and *Ps. stutzeri* Ibu8. The highest similarity score obtained from BLAST analysis is specified at the end of the respective operon. The *mer*BS operon of Kon12 showed 95% nucleotide identity to mercury resistance operon of plasmid pDU1355. The partly sequenced *mer*NS operon from Ibu8 showed 95% identity in DNA sequence to transposable element Tn5041 from *Peudomonas* sp. (accession nr. X98999), while the nucleotide sequences of the second *mer* operon (*mer*ABD) had a 99% similarity in amino acid residue to plasmid pDU1358.

3.5.9.6 *The mer Operons of Pseudomonas putida Elb2*

Sequence analysis confirmed that *Ps. putida* Elb2 had at least three different operons that expressed resistance to mercurial compounds (Figure 3-59). A 3.4 kb region of *Ps. putida* Elb2 was mapped by sequence analysis. The *mer* operon (merRTPFAD) was expressed as a typical narrow spectrum phenotype though with the presence of a *mer*F gene, located between *mer*P and *mer*A. Blast analysis indicated for the complete *mer* genes a significant homology with Tn5053 from *Xanthomonas sp.* W17 (99% identical nucleotide sequence). The second partly sequenced *mer* operon (*mer*TPC with 833 bp in length) belongs most likely to the narrow spectrum type, in agreement with its similarity to transposable elements Tn501-Like from *Delftia acidovorans* with the gene order *mer*RTPCAD. As shown in the Figure 3-60 the nucleotide sequence from Elb2 and Tn501-like mercury resistance transposon share 92% identical positions overall (97% similarity in amino acid sequence).

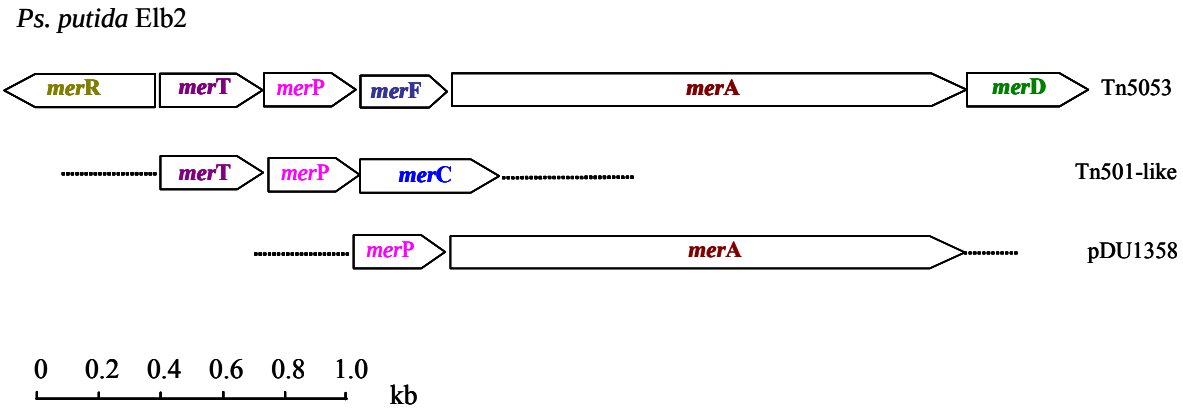

Figure 3-59. Schematic representation of the *mer* operon from *Ps. putida* Elb2. The highest similarity score obtained from BLAST analysis is specified at the end of the respective operon. The *mer*NS operon of Elb2 showed 99% nucleotide identity to mercury resistance operon of Tn5053. The partly sequenced *mer*TPC region showed 97% similarity in amino acid residue to transposable element Tn501 from *Delftia acidovorans* (accession nr. AAP88279, AAP88280 and AAP88281), while the nucleotide sequences of the third *mer* operon (*mer*PA) had a 99% identity in DNA sequence of plasmid pDU1358 (accession no. M15049, Z49200 and M24940).

To amplify the complete region of the mercury reductase of Elb2, a 574 bp DNA fragment was amplified by PCR and was subsequently mapped. The nucleotide sequence of this region comprised the 3' end of *mer*P and the 5' end of *mer*A. As shown in Figure 3-61, it is evident that this fragment ($merP_2A_2$) shows appreciable similarity in DNA sequence to mercury reductase from pDU1358 (99% identity in DNA sequence). Furthermore, *mer*A_2 differs from *mer*A_1 (operon $_{NS}$: *mer*RTPFAD) in nucleotide sequence. The homology between these two genes shows less than 83% identity. Therefore, these results indicate the presence of a further *mer* operon. Particularly, a broad spectrum resistance in agreement with its similarity to pDU1358.

In order to obtain precise results about the full length of the partly sequenced *mer* operons, each cluster should be subcloned and characterized independently.

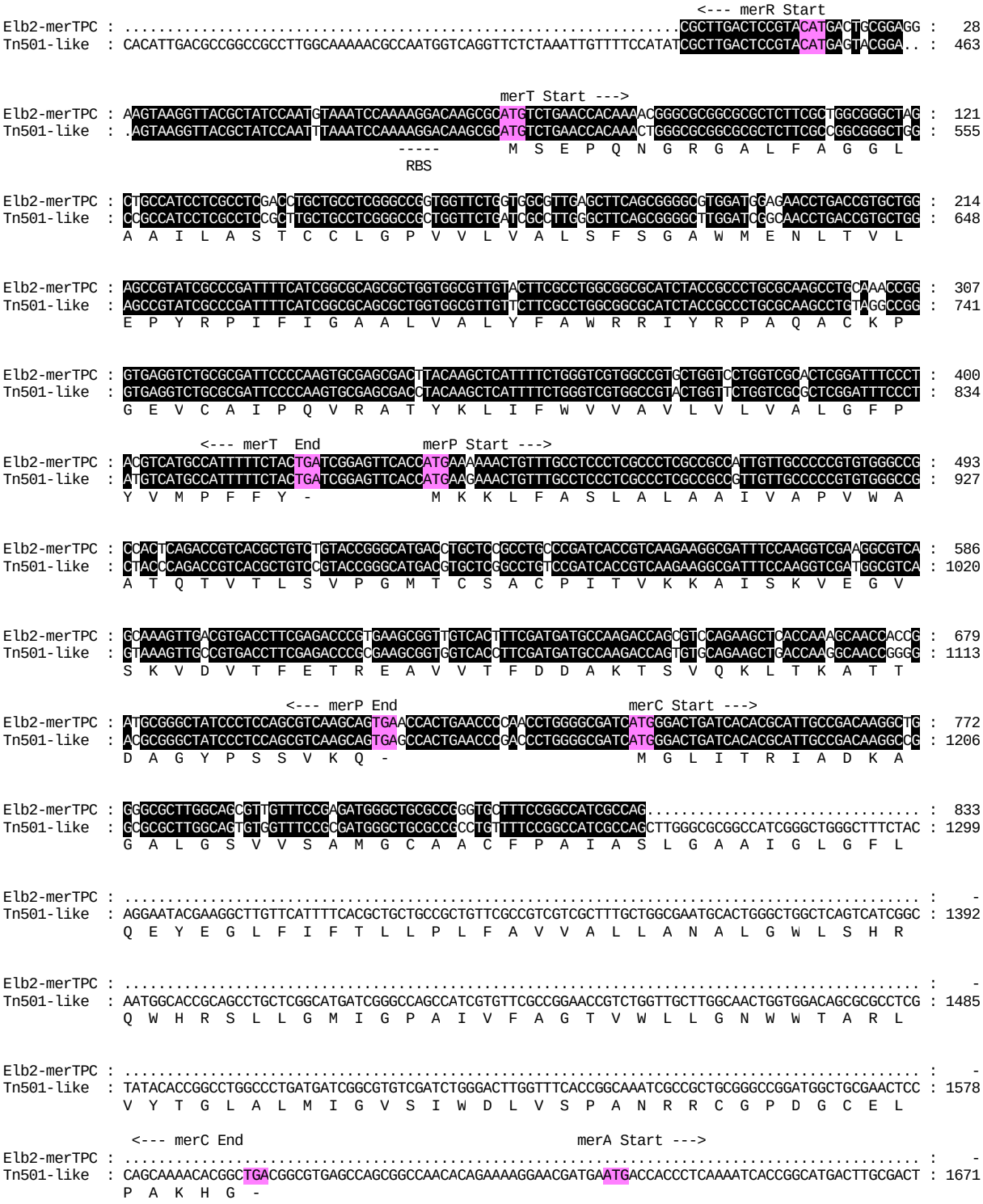

Figure 3-60. Alignment of the partly sequenced *mer* operon of *Ps. putida* Elb2, including the *mer* genes *mer*T, *mer*P and *mer*C. Amino acid sequence of Tn501-like polypeptide from *Delftia acidovorans* (accession no. AAP88279, AAP88280 and AAP88281) is shown as standard single letter below the DNA sequence line. Ribosomal binding site (RBS) is underlined. Black shade: 100% similarity. Start and stop codon are colored pink.

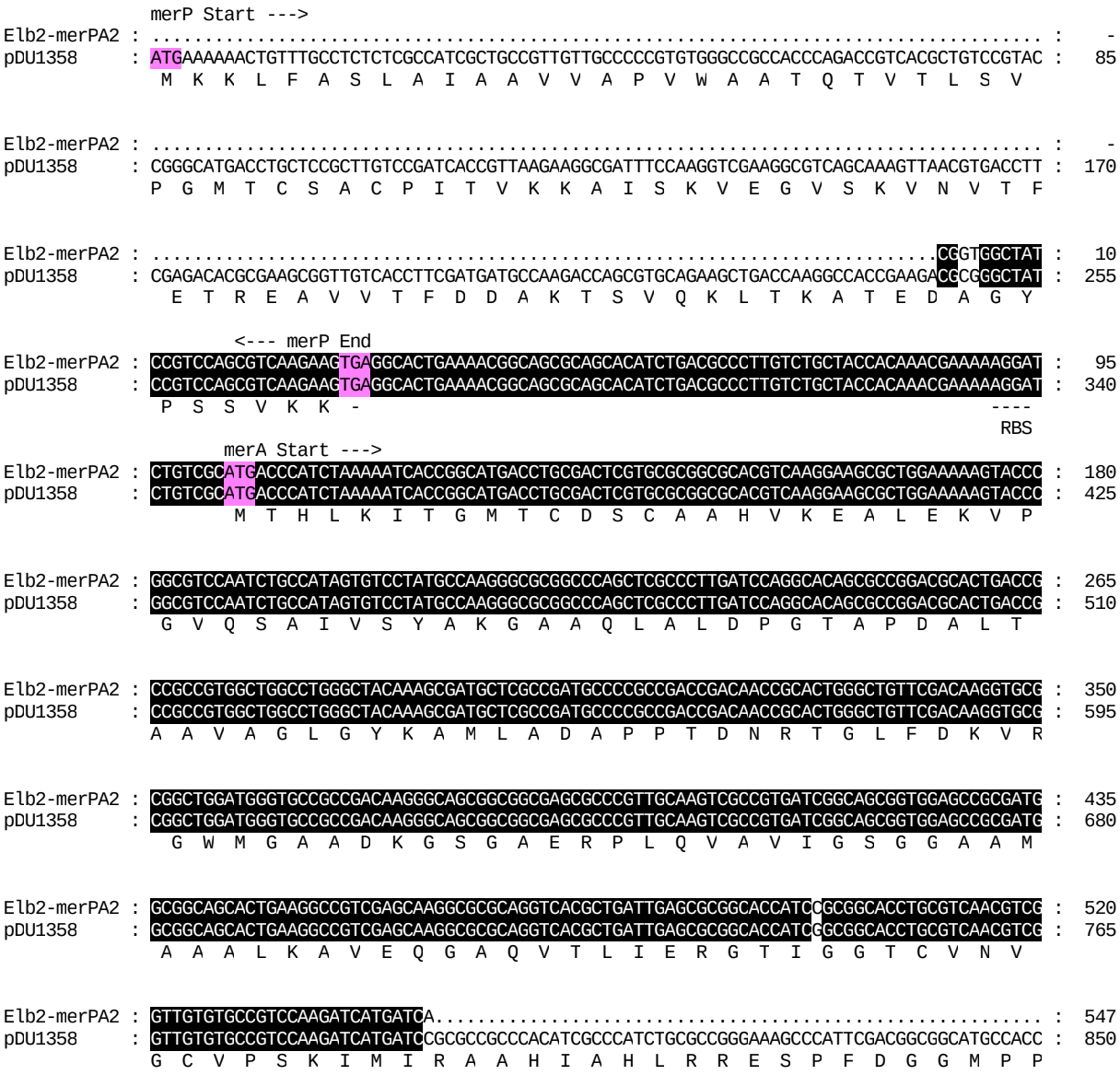

Figure 3-61. Alignment of the partly sequenced *mer* operon of *Ps. putida* Elb2 (2nd *mer* operon). This *mer* region includes the 3' end of *mer*P and 5' end of *mer*A and it is aligned with the same region of the plasmid pDU1358 (accession no. M15049, Z49200 and M24940), presumably a broad spectrum resistant operon (BS). Amino acid sequence of pDU1358 polypeptide is shown as standard single letter below the DNA sequence line. Black shade: 100% similarity. Start and stop codon are colored pink.

4 Discussion

Thiomersal ($C_9H_9HgNaO_2S$) is a water-soluble mercury containing derivative of thiosalicylic acid which is toxic for bacteria and eukaryotic cells. Thiomersal reacts with sulfhydryl groups, as a calcium mobilizer and cell-function-modulating agent (Abramson *et al.* 1995; Mezna and Michelangeli 1997; Elferink 1998). Surprisingly, little is known about its entrance into the cell and its interaction with enzymes (Stüning *et al.* 1988). The few studies on thiomersal (TH) interaction with bacteria are on the basis of resistant range assayed by minimum inhibition concentrations (Clark *et al.* 1977; Pinney 1978; Abuqaddom *et al.* 2003).
The first objective of this study was to evaluate TH degrading bacteria, such as environmental isolates and genetically engineered microorganisms (GEMs) for the remediation of vaccine production effluents of pharmaceutical industries. The wastewater resulting from vaccine production processes is highly polluted with thiomersal. Recycling of mercury containing compounds and waste water is important, since recycling will decrease the mercury load from waste sites. Natural isolates have already been successfully applied to remove mercury chloride from chloralkali wastewater (Wagner-Döbler *et al.* 2000; Canstein *et al.* 2002; Wagner-Döbler 2003), but there is no description of treatment of wastewater contaminated with thiomersal in a biological way. Therefore, the evaluation of thiomersal-resistant bacteria and the determination of optimal physiochemical parameters for transformation were of prime interest. Moreover, the question arose whether the differences in TH transformation capability of mercury resistant bacteria result of differences in genetic structure of the mercury resistance operon. Thus, an understanding of the structure of the *mer* operon could provide insights into the toxicological pathway of mercury compounds. Therefore, the gene arrangements of the isolates were identified with special attention to the gene-encoding organomercurial lyase (*mer*B).

4.1 Comparison of Thiomersal Resistant Microorganisms

The comparability of the thiomersal transformation rate of different isolates has been ensured on the basis of preliminary experiments. Therefore, TH transformation measurements on CVAAS were carried out with the cells of the late logarithmic growth phase and temporarilly shifted samples (see section 3.1.1.and 3.1.2).

Based on previous works of von Canstein *et al.* (2001 and 2002), the seven most promising naturally mercury-resistant isolates of *Pseudomonas* and two *Citrobacter* strains, as well as two GEMs, were selected to determine their resistance to the organomercurial TH and their capability to transform TH. The results show large differences in TH transformation rates (8–443 ng Hg· ml^{-1} · min^{-1}) between the investigated isolates (Figure 3-5). Frequently observed results since early studies have shown a large resistance spectrum of organomercurials, including TH among bacteria. With *S. aureus, E. coli, and Pseudomonas*, Clark *et al.* (1977) found differences in TH transformation, while strains of *Ps. aeruginosa* were able to transform TH between 0.1–0.475 nmol·$min^{-1}mg^{-1}$ of dry cells , *Ps. putida* strains were sensitive to TH (≤0.1 nmol·$min^{-1}mg^{-1}$).

The two *Citrobacter freundii* strains Tin2 and 62, proven to be highly resistant to mercury chloride (von Canstein *et al*. 1999 and 2001), could cope only with thiomersal concentrations up to 2 ppm, at very low transformation rates (8 and 10 ng Hg· ml^{-1} · min^{-1}). Interestingly, the cell number of the Tin2 did not decrease clearly after the end of the experiment. Therefore, surviving in TH solution suggests that Tin2 could probably be an organomercurial-resistant strain but is not able to transform thiomersal well. To confirm this statement, the *mer* operon of Tin2 was sequenced but the presence of organomercurial lyase was not ascertained. Furthermore, there are no published dates about Citrobacter strains and organomercurials in general. Therefore, how microorganisms survive in TH contaminated environment needs to be studied in depth.

In contrast, *Ps. putida* Spi3, *Ps. putida* Spi4 and *Ps. fulva* Spi11 were not only able to survive but were also able to transform TH rapidly. The broad resistance of *Ps. putida* to mercury compounds, heavy metals and organic solvents is often described in the literature (Williams *et al.* 1974; Higham *et al.* 1984; Diaz *et al.* 1994; Lee *et al.* 2001; Nelson *et al*. 2001; Cánovas *et al.* 2003; Pardo *et al.* 2003). These metabolically versatile microorganisms that recycle organic wastes in the environment, thus they play a key role in the maintenance of environmental quality (Short *et al.* 1992; Jenkins *et al.* 1993; Selifonova *et al.* 1996). *Ps. putida* strains are rapidly growing bacteria which have chromosomally encoded pathways for the catabolism of a variety of organic compounds. Their tendency to freely acquire plasmids

from other bacteria and their relaxed-specificity gene expression system allowing the expression of genes derived from a wide variety of different bacteria (Harayama *et al.* 1991; Ravatn *et al.* 1998; Timmis 2002; Park *et al.* 2003; Pinedo *et al.* 2005). Therefore, it is not surprising to find resistance to TH.

Moreover, growing cells of Spi3, Spi11 and Spi4 showed higher transformation rates with higher initial TH concentrations up to 20 ppm without observing a maximum of thiomersal transformation. No growth was observed for Spi11 and also for Spi4 when TH was added to the medium from the beginning. With these experiments it became evident that the extent and rate of TH transformation was strongly dependent on the cell density. With increasing cell numbers the isolates became not only better performers but were able to grow rapidly in TH environment, an observation, which is described frequently in the literature (Allard *et al.* 1985; Hendrickx *et al.* 2003; Neumann *et al*. 2004). Also the two GEMs KT2442 and F1 were not able to cope with TH from the beginning of the experiment. This finding was remarkable because the GEMs were constructed and selected for their high and constitutive mercury resistance (Horn *et al.* 1994). Moreover, they were specifically provided with the resistance to organic mercury because the *mer* TPAB genes were stably integrated by random mutagenesis into the *Ps. putida* KT2442 and *Ps. p.* F1 chromosome. A lack of the regulatory protein MerR resulted in constitutive over-expression of the transport, cleavage and reduction genes (*mer* TPAB). The aim was to construct strains to cope best with fluctuating mercury concentrations, better than natural bacteria with an inducible mercury resistance. The *Ps. putida*::mer isolates described by J. Horn have the potential to cope with mercury chloride ($HgCl_2$) and phenylmercuric acetate (PMA) in concentrations up to 60–80 ppm. However, thiomersal could not be transformed by the strains under the conditions used in this experiment and furthermore TH entirely repressed their growth. *Ps. putida* KT2442::*mer*-73 was also tested as a monospecies mercury-reducing biofilm in laboratory scale bioreactors (von Canstein *et al*. 2002a). These and previous experiments with non-sterile mercury-containing wastewater (Felske *et al.* 2001) showed the GEM to be readily lost and did not seem to establish good biofilms in the bioreactor unless feeding was increased. Insufficient growth and a prolonged lag phase were thought to be the reason for this. Experiments in this study demonstrated clearly that the TH transformation efficiency of the strains is closely related to the initial cell density. Bacterial cells at the middle logarithmic phase proved to be best suited. Under this condition wild type isolates and the two GEMs too were able to transform TH. The transformation rates of F1 and KT2442 were also increased with higher

TH concentrations between 2 and 15 ppm and showed a maximum at 15 ppm TH (12 and 10 $\mu g \cdot min^{-1}$, respectively).
The outstanding capabilities of Spi3 prompted us to perform a detailed investigations of this strain.

4.2 Selection of a Counter-Ion for the Ion-Exchange Membrane Reactor

The use of an ion-exchange membrane bioreactor can excludes direct contact of the microbial culture with the wastewater to be treated. This integrated membrane process combines continuous ion exchange transport (Donnan dialysis) of the pollutant through a non-porous membrane, selective for the transport of mono-anions, from its simultaneous bioconversion to harmless products in a biocompartment. Up to the present the ion exchange membrane bioreactor was studied and utilized for drinking water denitrification and for removal of micropollutants such as perchlorate and bromate from polluted waters streams. The counter-ion is usually chloride, and less frequently is bicarbonate. One of the technical challenges for the development of an ion-exchange membrane bioreactor system is the extension of its application, as for TH bioremediation. Therefore, it is of particular importance to use a suitable counter-ion to facilitate the flux of TH anions to the biocompartment. Furthermore, it is important to use a counter-ion having no or very low affinity for the ion-exchange membrane and one that is biological inert.
One possibility to select a suitable counter-ion is offered by the Biolog GN MicroPlates™ system. Basically, Biolog™ (carbon source utilization profile) has been introduced as a mean of classifying microbial communities on the basis of heterotrophic metabolism (Garland and Mills 1991). Such a classification system might allow microbial ecologists to compare the metabolic roles of microbial communities from different environments without involving tedious isolation and identification of community members. The simplicity of the method and the commercial availability of Biolog GN Microplates™ are particularly attractive. In this study, the use of the Biolog GN Microplates™ system containing 95 carbon substrates was needed to limit the search for suitable counter-ions. The utilization of carboxylic acids are of interest, since they were considered as suitable counter-ions for the ion exchange membrane bioreactor to facilitate the flux of thiomersal to the biocompartment. The results demonstrated that up to 70% of the carboxylic acids were metabolized, which limits considerably the selection of a suitable counter-ion. The unutilized carboxylic acid of Biolog could not be taken into account due to their molecular structure as an appropriate counterpart to TH.

Therefore, another seven counter-ions (iso-butyric acid [iBA], iso-valeric acids [iV], propylphosphonic acid [PP], tertbutylphosphonic acid [TBP]), pivalic acid [P], tertbutylacetate [TBA] and 2,2′dimethylbutyl-acetate [DMBA]) were chosen as possible candidates. As shown in the results, isolates were incapable of utilizing tertbutyl acetate (TBA) and 2,2´dimethylbutyl acetate (DMBA) as sole carbon sources. TBA ($C_6H_{12}O_2$ with a molecular weight of 116.16 g·mol^{-1}) occurs in natural and food products, but it is also produced chemically. But there are severely limited data on butyl acetate isomers (n-, iso-, sec- and tert-butyl acetate). Nevertheless, the few data available indicated that butyl acetate isomers are metabolized in the body to acetic acid and their respective butanols; TBA, however, slower than the other isomers (Girkin & Kirkpatrick, 2000). Moreover, depending on the microorganisms presented, TBA was either inherently biodegradable or readily biodegradable (Hotta *et al.* 2002; Stouten and Bogaerts 2002; WHO 2005). This observation did not correspond with the experiments carried out here. Since, TBA had been hardly utilized by the isolates. However, in-depth experiments indicated that DMBA was completely biologically inert, while in the presence of TBA the cell number slightly increased.
DMBA ($C_6H_{12}O_2$ with a molecular weight of 116.16 g·mol^{-1}), a plasma metabolites of simvastatin (a Cholesterol-lowering agent), is also a butyric acid such as TBA. But it has not been reported by EU Industry and is not listed in a priority and risk assessment information list (Council Regulation (EEC)). Moreover, there is no information available on the effect of DMBA on microorganism in the literature. Nevertheless, since DMBA but also TBA were not utilized by bacteria and no toxic effect were observed, these carboxylic acids could be selected as candidates to be used as a counter-ion in an ion-exchange membrane bioreactor.

4.3 Determination of Process Optima

One of the major constraints in implementing in situ bioremediation could be the lack of understanding of how physical, biological and chemical factors affect microbial activity particularly with respect to thiomersal degradation. In an attempt to understand how these factors impact thiomersal bioremediation, investigations were carried out to determine the optimal parameter. Two microorganisms, the naturally mercury resistant isolate *Ps. putida* Spi3 and *Ps. putida* KT2442::*mer*-73, a genetically engineered isolate, were chosen for laboratory scale continuous-culture and batch culture systems to analyze the microbial transformation of thiomersal. As already reported for Spi3 the optimal transformation rate of TH was determined at a temperature of 30°C and pH of 7.

Another important aspect that has to be taken into consideration is the effect of TH decomposition products on bacteria. As an ethylmercury derivate, it has been reported that thiomersal desintegrates, especially in liquid solutions containing sodium chloride (Reader *et al.* 1982; Fleitmann and Patridge 1991). The main decomposition products are thiosalicylic acid (THSA) and ethylmercuric hydroxide. However, in the presence of sodium chloride, THSA undergoes irreversible oxidation to 2,2′dithiosalicylic acid (dTHSA). This highly polar organic compound can serve as an energy or carbon source. Bressler and Fedorak (2001) reported that dTHSA can serve as the sole carbon and sulfur source in aerobic soil enrichment cultures. Therefore, experiments were carried out to determine the total amount of dTHSA utilization by *Ps. putida* Spi3 and *Ps. putida* KT2442::*mer*-73. The results of the investigation showed that dTHSA did not act as an anitimicrobial agent and was not utilized by Spi3 and KT2442 as an energy source (biological inert). Therefore, the effects of dTHSA in all TH experiments could be neglected.

A further aspect that had to be clarified was the ability of biofilm formation of mercury resistant isolates. Bacteria used in remediation processes need to establish good biofilms to cope well with disturbances (temporary high inflow, mercury concentrations, temperature fluctuation, oxygen and nutrient gradients). Direct observation of a wide variety of natural habitats has established that the majority of microbes persist attached to surfaces within a structured biofilm ecosystem and not as free-floating organisms (Costerton *et al.* 1995). Teitzel *et al.* (2003) compared by exposing equal numbers of *Ps. aeruginosa* cells to various heavy metal concentrations and they found that biofilms were more resistant to heavy metals than either stationary-phase or logarithmically growing planktonic cells of *Ps. aeruginosa*. There was an approximately 600-fold increase in resistance for copper-treated biofilms compared to the resistance of free-swimming cells. These data are not surprising since *Ps. aeruginosa* biofilms have been reported to be more resistant to a variety of antimicrobial stresses than free-swimming cells (Costerton, *et al.* 1999; Hentzer *et al.* 2001). Persistor cells, as described by Lewis *et al.* (2000 and 2001), were observed in biofilms in which less than 1% of the original population was extremely difficult to kill with elevated concentrations of heavy metals. Therefore, it is of vested interest to determine the biofilm formation of the investigated isolates.

On the other hand, in an ion exchange membrane bioreactor biofilms tend to develop on the membrane surface (Van der Hoek and Klapwijk, 1987; Beeton *et al.* 1991; McCleaf and Schroeder, 1995). Consequently, the biofilm would have a significant effect on the bioremediation of the wastewater, particularly in the course of the time. Studies have shown

in an ion exchange bioreactor, the membrane provided a surface for biofilm growth, facilitated the transport of pollutant, and prevented mixing of treated water and bioreactor medium (Casey 1999; Fonseca *et al.* 1999). Velizarov *et al.* (2002) determined a fast denitrifying reaction in the early stage of the process as a result of biofilm formation. In the course of the process evolution, however, the specific denitrifying activity of the biofilm decreased and a corresponding increase of the biofilm thickness was observed. Therefore, they concluded that the biofilm contribution to the improvement of the nitrate flux to the biocompartment was time-dependent, being most significant in the early stage of the process.

Results from the analysis of the biofilm development in this study indicated that nine of ten isolates were able to form a biofilm within 24 h but the capacity for biofilm formation varied extensively. Only the strain *Ps. aeruginosa* Bro12 could hardly produce biofilm at all. This result was unexpected, since Bro12 remained stable for 240 days in the community composition of a bioreactor biofilm and temporarily overgrew the other strains. But on the other hand, it is known that certain criteria and characteristics affect the biofilm development (Stoodley *et al.* 1997). For example, James *et al.* (1995) showed that biofilm thickness could be affected by the number of component organisms. Pure cultures of either *K. pneumoniae* or *P. aeruginosa* biofilms in a laboratory reactor were thinner (15 µ and 30 µ respectively), whereas a biofilm containing both species was thicker (40 µ). Jones *et al.* noted that this could be because one species enhanced the stability of the other. Studies have described good and stable performance of the multispecies biofilms in contrast to monospecies, resulting in the effective remediation of wastewater (Caldwell 1995; Costerton *et al.* 1995; Canstein *et al.* 2002).

The extent of biofilm formation of *Ps. stutzeri* Ibu8 was very high, which was equivalent to the finding in the study of Canstein *et al.* (2002). They observed that Ibu8 temporarily overgrew the other strains while most of the other inoculum strains dropped below the detection limit within the first month. The strains Spi3, Spi4 and Spi11 showed only mediocre performance like those in bioreactor investigations of von Canstein (2002). In contrast to the "Spi" isolates, KT2442 produced a high biofilm mass but it failed to establish good biofilm in laboratory-scale bioreactor (von Canstein *et al.* 2002) and has been gradually washed out. Felske *et al.* (2001) demonstrated that KT2442 even disappeared quickly in a lab-scale bioreactor with nonsterile Hg^{2+}-contaminated wastewater and was replaced by ubiquitous mercury-reducing bacteria.

What constitutes a mercury-resistant community? A performance of the multispecies bioreactors clearly showed with respect to Hg^{2+} reduction that the presence of several

community members, although with very low abundance, improved a very effective biofilm activity. Therefore, it can be declared that biofilm with different bacterial populations increases the chance that a well-adapted strain acts effectively and protects the less-adapted microorganisms. This assumption corresponds to the statement of Shapiro proposing the view of bacteria as interactive organisms capable of significant collective activity as a general bacterial trait (Shapiro 1988 and 1998). The ability to use intercellular interactions and communication to facilitate their adaptation to changing environmental parameters was stated by Kaiser *et al.* (1993). Therefore, it is not surprising that the results of the aforementioned experiments showed inconsistent outcomes, i.e. performance in biofilm formation did not prove to be a good predictor for bioreactor potential. Concerning the extraordinary robustness of the multispecies community it should be considered if a multispecies bioreactor would achieve better results in wastewater treatment than monospecies bioreaktor.

4.4 Thiomersal Detoxification Capacity of *Ps. putida* Spi3

The strain *Ps. putida* Spi3 is an example of mercury-reducing microbes that have been shown to be efficient in mercury retention in a bioreactor (von Canstein *et al.* 2002). A mixed culture of several mercury-resistant isolates, including Spi3, efficiently retained $HgCl_2$ from a laboratory-scale bioreactor and was not affected by disturbances such as rapid increases of mercury or continuously high mercury concentrations (Wagner-Döbler *et al.* 2000; von Canstein *et al.* 2001). However, von Canstein *et al.* (2002) showed by analyzing the physiological traits of adaptive relevance in packed-bed bioreactors with mercury-polluted chlor-alkali wastewater that Spi3 was a moderately mercury-reducing isolate. Moreover, it did not perform extraordinary well with other species and was temporarily present in very low abundance. An increase of inflow mercury concentration to 7 ppm resulted in a decrease of Spi3 cell number even below the detection limit. By reducing the selection pressure to 2 ppm Hg^{2+} the initial diversity was restored and Spi3 was detectable. Consequently, Spi3 cells did not die out but dropped below the limit of detection under unfavorable conditions.

By contrast, Spi3 proved in this study to be an excellent strain for thiomersal detoxification. It was able to cope with thiomersal concentrations up to 140 ppm at which Spi3 achieved the highest transformation rate of 1488 ng Hg· $ml^{-1} \cdot min^{-1}$. This exceptional capability of *Ps. putida* Spi3 to cope with high TH concentrations was also shown in growth experiments. It was the only strain that could detoxify thiomersal from the moment of inoculation, while all other strains were not detectable. Additionally, the results of the growth experiments showed

that the cells at lag phase exhibited the highest thiomersal transformation rates, followed by those at the exponential phase. At the stationary phase the cells had the lowest transformation rate. This trend is caused by the physiological state of the cells in different growth phases. In the lag phase the cell density was very low and thus the TH-to-cell ratio was higher than that of other growth phases. To survive the toxic environment, lag phase cells tend to dedicate most of their resources to reducing the thiomersal concentrations only and thereafter start growing. Therefore, lag phase cells achieved better transformation rates than cells at any other phases. As the exponential growth phase is reached, the mercury-to-cell ratio is reduced significantly due to higher cell density. Thus, according to the reaction kinetics, the transformation rate becomes lower since TH concentration dropped. It also seems reasonable to observe that the lowest transformation rate occurred at the stationary phase, because the cells in this period enjoy the lowest thiomersal-to-cell ratio. Teitzel *et al.* (2003) sought to assess the effects of heavy metals (Zn^{2+}, Pb^{2+} and Cu^{2+}) toxicity on *Ps. aeruginosa* and compared the relative susceptibilities of logarithmic- and stationary phase *Ps. aeruginosa* liquid cultures. Significantly, logarithmically growing *Ps. aeruginosa* was found to be more resistant than stationary phase cells. These results are confirmed by findings in this study. Thus, during the stationary phase the metabolic energy and NADPH production is limited, so the supply of the cofactor for the enzymatic reduction of Hg^{2+} is consequently insufficient (Misra 1992). These factors result in a decrease in thiomersal transformation rate as observed here.

One of the major aspects of implementing in bioremediation is the understanding of physical, biological and chemical factors affecting microbial activity. Therefore, further investigations were conducted to determine how TH transformation rate, is affected by temperature, pH, and initial cell number (between 10^4–10^8) in *Ps. putida* Spi3. The detected optimal physiological parameters were equal as the favorable condition for growth of Pseudomonads. The optimal temperature for the reduction activity was 30 °C. Deviation caused a rapid reduction in the TH transformation rate. The optimal pH was neutral (pH 7), above which the activity decreased. Over the ranges of temperature and pH evaluated, transformation rate varied by more than four orders of magnitude. Throughout the experiments, it turned out that the TH transformation efficiency was found to be closely related to the initial cell density. Therefore, it was of great interest to determine the influence of cell density of Spi3 on TH transformation capability. A positive correlation of cell density on TH transformation rate in medium containing 5 ppm thiomersal was observed. Increase in the cell number caused an increase in transformation rate. As the cell number went below 10^5 cells · ml^{-1}, no sign of transformation

could be observed. A rise in the initial density from 10^6 to 10^7 cells·ml^{-1} resulted in an increase in the transformation rate of up to 412 ng Hg· ml^{-1} · min^{-1}. Thus, in dynamic systems, changes in cell number will have significant effects on the magnitude and timing of the transformation rate.

Furthermore, it is important to test the stability of the mercury resistance in Spi3 as a consequence of genomic changes and loss of mercury-resistant plasmids. It has often been suggested that the rates of phenotypic and genomic changes were discordant both across replicate populations and over time within a population. Divergence from the ancestor increases over time, as does genetic diversity within each population. It can be concluded that Spi3 did not lose its resistance to thiomersal and probably did not undergo a molecular evolution, leading to extensive changes in its genome structure during 10 days of adaptation to a mercury-free environment in which it received nutrients every day.

Initially, it can be supposed that the *mer* genes are probably located on the chromosome or stable plasmid, since it has been shown that self-transmissible plasmids are maintained in a culture even in the absence of a selective pressure. Moreover, the fitness of the bacteria and the TH transformation capability lead to the assumption that there was no genomic change. On the other hand, the incubation time for Spi3 of 10 days might be too short to determine any genomic variation concerning mercury-resistance ability. The investigation of Papadopoulos *et al.* (2000) sought to examine directly the concordance between phenotypic and genomic changes. Their results demonstrated that the experimental populations of *E. coli* underwent rapid molecular evolution, leading to extensive changes in their genome structure. They serially propagated *E. coli* B for 10,000 generations (1500 days) in a glucose-limited minimal medium. They analyzed the genomes for restriction fragment length polymorphisms (RFLP) using seven insertion sequences (IS) as probes after 500, 1000, 1500, 2000, 5000, 8000 and 10,000 generations. The evolving genomes became increasingly different from their ancestor over time. Moreover, tremendous diversity accumulated within each population, such that almost every individual had a different genetic fingerprint after 10,000 generations. More generally, their data showed that the genome is highly dynamic even over a time scale that is, from an evolutionary perspective, very brief. This finding is very important for the biological treatment of contaminated wastewater, especially in respect to long-term utilization of microorganisms in bioreactors.

4.5 Biotransformation of Thiomersal under the Steady State Condition

In batch-culture experiments, either the consumption of the growth-controlling substrate or the increase in biomass concentration as a function of time is usually monitored. Inherent in this system is that the cell's environment and hence the cell's composition and physiological state changes during the experiment (this has already been recognized and discussed in the classical studies Tempest 1970, Koch 1976 and Tempest and Neijssel 1978). However, in continuous culture, an equilibrium concentration of the growth-controlling substrate is established independently of culture density and time. This allows the culture to grow at the set dilution rate by maintaining stable environmental growth conditions and hence the same physiological state. Therefore, in an ideal continuous culture, more precise, reproducible and statistically relevant data can be collected than those obtained from batch cultures (Senn *et al.* 1994; Kovárová *et al.* 1997).

To overcome the analytical difficulties of determining maximal TH inhibition concentrations, maximal transformation and kinetic experiments with set dilution rates were carried out in batch cultures. The specific growth rate was determined by measuring the cell density (by optical density). In this experiment a low initial dilution rate was set (0.01 h^{-1}), because the two bioreactors were not stabilized within 24–48 h. Probably as a response to the stress situation, the cell density decreased by approximately three orders of magnitude to $<10^5$ cfu·ml^{-1}. Another possible reason for this effect could be the choice of cultivation and feeding medium. The chemical composition of a medium containing yeast extract (such as LB and NMS medium) can have a significant effect on the bioavailability of mercury. Chang *et al.* (1993) observed a loss of free Hg^{2+} in complex media. The time course analysis for Hg^{2+} and total mercury in LB medium clearly showed an interaction between Hg^{2+} ions with tryptone and yeast extract. Furthermore, they showed that the formed mercury complexes with yeast or tryptone are not direct substrates for the mercury reductase enzyme and therefore not bioavailable. To prevent this effect, M9 minimal medium was selected for the bioreactor performance. On the other hand, Begley *et al.* (1986) postulated the necessity of thiol groups in the solution for organomercury detoxification. Without an excess of thiol in the medium there is no formation of an irreversible enzyme inhibitor complex. Exchange of Hg^{2+} with thiol in the solvent releases the active site of the enzyme, making it ready for another catalytic cycle (see Figure 1-6). Several research groups suggested that enzymatic protonolysis of organomercurial compounds by organomercurial lyase is best explained by S_E2 reaction type mechanism (Begley *et al.* 1986a and 1986b; Sandstöm and Lindskop 1988;

Silver *et al.* 1992). Therefore, a thiol-free medium (such as M9 minimal medium) would lead to unstable cell cultivation and an inefficient transformation of thiomersal as well.

Nevertheless, thiomersal concentrations in both bioreactors fell below the detection limits and only minimal Hg^{2+} concentration was detectable. In both reactors mercury removal efficiency was reached over 99 % as a result of high microbial transformation activity. No comparison could be drawn between the bioreactors due to a contamination of bioreactor A containing the strain *Ps. putida* Spi3. The results of bioreactor B suggested that *Ps. putida* KT2442::*mer*-73 was able to deal with high TH inflow concentrations.

As indicated, dilution rates of 0.01 h^{-1} (which is already a low rate) resulted in significant decreases of cell concentration during the first 3 h of continuous cultivation, indicating that for the early hours of cultivation, the rate of dilution of cell culture following the addition of medium was higher than the rate of cell growth. Apparently, feeding rates are inappropriate for the stirred bioreactor mercury detoxification process, in which the mercury solution will be fed into cell culture along with the medium, causing further decreases in cell concentration due to toxic effects of mercury. Consequently, the separation of TH from the feeding medium is necessary. Not only the availability of carbon and energy can be adjusted by the carbon feeding rate but also the TH feeding rate can be accurately adapted to the microbial population. According to the reaction kinetics, higher TH feeding rates are normally preferred to enhance mercury detoxification activity. However, the mercury feeding rate should not be so high to cause significant inhibition to cell viability.

In conclusion, the results showed that the stirred bioreactor with the recombinant mercury-resistant strain enabled detoxification of TH from environment. Additionally, it was possible to obtain a bioreactor outflow with a mercury concentration below the European limit ($50\ \mu g \cdot l^{-1}$) for mercury effluent discharges, even though the feeding strategy was not optimized. Therefore, there is still much room for improvement.

4.6 Analysis of the *mer* Operon Structure of the Thiomersal Resistant Bacteria

The *mer* operon is widely distributed among bacteria and it is required to enable resistance to mercurial compounds. Several variations on the structure and organization of *mer* operons are known, reflecting the mosaic nature of the operon (Liebert *et al.* 1997; Kholodii *et al.* 2002). There are some characteristic differences between the operons of Gram negative bacteria that are reflected in the length of *mer*RT, *mer*PA and *mer*AD amplicons. These differences lay in the presence and arrangement of essential (*mer*RTPAD) and accessory genes (Summer 1986;

Osborn *et al.* 1996). And exactly these differences were shown to cause the differences in TH transformation rate. Therefore specific primers were designed to identify the mercury resistant *mer* operon. According to the size and sequence of the PCR amplicons, the organization of *mer* operons from the natural mercury-resistant isolates could be identified (see section 3.4.1). From the sequence analysis it turned out that nearly all bacteria (except for *Ps. putida* Kon12 and *Citrobacter freundii* Tin2) have multiple *mer* operons. Seven strains (except for *Ps. putida* Kon12) have a narrow spectrum resistance *mer* operon plus their resistance to thiomersal that resulted in the presence of a broad spectrum resistant *mer* operon which includes the organomercurial lyase, MerB. The possession of several *mer* operons (at least two) in each strain presumably increased the resistance towards mercury. Philippidis *et al.* (1991) evaluated the effect of gene amplification by increasing the gene copy number on enzyme activity. They showed that the maximal mercuric ion reduction rate increased linearly with the gene copy number. Qualitatively, the same phenomenon has been observed with the resistance levels to chloramphenicol and streptomycin of intact *E. coli* cells harboring plasmid R1 and copy number derivatives of this plasmid (Uhlin and Nordstrom 1977). Multiple *mer* operons resulting in possession of the same number of regulatory genes (*mer*R_1 and *mer*R_2), each preceded by its own proposed operator/promoter (O/P) region, activate independently transcription of the respective *mer* genes. This fact leads to a better resistance toward mercury. The regulatory function of MerR, however, does not always exist, which is reported for some Gram-positive *mer* operons. The analysis of transcriptional regulators from *Bacillus cereus* RC607 and *Bacillus megaterium* strain MB1 revealed that MerR proteins in a bacterium differ from each other in a number of ways, particularly if two MerR proteins occurred (Gupta *et al.* 1999). Firstly, the location of cysteine residues can differ. While cysteine residues of the first $MerR_1$ are located at the position Cys-79, Cys-114, Cys-123, only one cysteine residue (Cys-50) appeared in the second $MerR_2$ amino acid sequence. Secondly, the homology between MerR proteins showed remote identity (less than 30% identity). Thirdly, the highly conserved inner bases (GTACnnnnGTAC) in each dyad arm of the *mer* promoter/operator (Summers 1992), which are also found in the operator regions of Gram-positive bacteria, do not appear in the second *mer*R operator (Gupta *et al.* 1999). Therefore, $MerR_2$ cannot respond to and bind Hg^{2+} in a manner similar to that of the first $MerR_1$ protein (Helmann *et al.* 1989; O'Halloran 1993).

In this study, the regulatory functions of *mer*R genes in all eight isolates are given by the fact that each of the MerR proteins contained three completely invariant cysteine residues, Cys82, Cys117 and Cys126 (see Figure 3-36), binding Hg^{2+} and provoking an allosteric change in the

protein which is propagated to the DNA of the operator region (Helmann *et al*. 1989; Shewchuk *et al.* 1989; Silver and Walderhaug 1992). Also the degree of amino acid conservation between the MerR regulator proteins is very similar (90–96% identity). The strikingly conserved region in all aligned MerR proteins (see Figure A-2 in the Appendix) is the proposed amino-terminal helix-turn-helix DNA-binding motif. This region is the likely interface between the MerR proteins and their target operator sequences. It contains all of the recognized structural features of helix-turn-helix units (Pabo *et al.* 1984; O'Halloran 1993). The observation that MerR protein bound to operators with comparable affinity strongly implicates the evolutionarily conserved GTAC residues (see Figure A-3 in the Appendix) as primary contact points for sequence-specific recognition. This *mer*O/P region (25 bp region), shown in Figure A-3, is characterized by the centrally located GTAC (7-base dyad TCCGTAC....GTACGGA) repeats and by -35 and -10 consensus elements for RNA polymerase recognition. Unlike the majority of described transcription activator proteins (Ribaud and Schwartz 1984), the MerR proteins bind between the -35 and -10 consensus elements of the target promoter DNA. These *mer* promoter elements all share the conserved -35 and -10 sequence features of promoters. The importance of spacer length to promoter activity is apparent from genetic analyses: mutation away from the optimum length of 17 bp generally decreases promoter activity both in vivo and in vitro (Mulligan *et al.* 1985; Harley and Reynolds 1987; O'Halloran *et al.* 1989; Warne and deHaseth 1993).

Interestingly, the *mer* operons of each strain that were sequenced were not closely related to each other. Taking the assumption of substrate specificity for *mer* genes (specifically *mer*B gene), it could refer to the complete *mer* operon, with closer attention to the *mer* operator/promoter region. Thus the variant in the *mer* O/P region enhanced the gene expression. This hypothesis is not yet confirmed by experiments for these mercury-resistant isolates but seems more than likely, especially in the light of mercuric ion results (von Cansteins and own previous data not shown). Nevertheless, a clear demonstration of the differences in substrate specificity and sequence variation has to be obtained by analysis of the performance of the different determinants on mercury. Especially the examination of in vivo gene transcription, specifically the kinetics of gene expression, has to be studied.

4.6.1 Transport of Mercury into the Cell

As mentioned in section 1.6.1 the *mer* operon of bacteria, which encodes the proteins responsible for the bacterial mercury detoxification system, has the ability to transport Hg^{2+}

across the cell membrane into the cytoplasm where it is reduced to Hg^0. The structures of the reduced and mercury bound forms of *mer*P, the periplasmic protein, which binds Hg^{2+} and transfers it to the membrane transport protein *mer*T, have been already studied extensively (Lund *et al.* 1987; Hamlett *et al.* 1992; Morby *et al.* 1995; Hobmann *et al.* 1996; Steele and Opella 1997; Serre *et al.* 2004). However, the mechanism of protein-mediated transport of mercuric ions across the bacterial membrane is not yet understood in great detail, especially the mercury transport mechanism of the inner membrane proteins, MerC, MerF and possibly MerE.

It is evident that Hg^{2+} can get into a cell without a dedicated transport system. Transcriptional induction of the repressed *mer* operon is detectable within 30 s after the addition of Hg^{2+} to cells carrying a *mer* operon (Gambill and Summers 1992). Condee and Summers (1992) also showed that in the complete absence of any *mer* transport proteins, transcription is observable within 2–3 min after exposure to sub-micromolar Hg^{2+}. Thus it appears that mercury reduction is substantially more efficient with than without any transport proteins and accelerated mercury reduction increased the survival.

Regarding thiomersal, the role of the transport proteins has not been not clarified. Moreover, it is not clearly understood how TH penetrates into the cell. It is clear that TH as an organomercurial compound with sulfhydryl reactive properties diffuses easily into the cell as a result of its chemical structure, due to its lipophilicity, and reacts as a thiol oxidizer. Hence, thiomersal can freely diffuse across the cell membrane, arguing against differences due to reactions with thiol residues located on the intracellular site of the channel molecule and cytosolic side of the membrane. Consequently, it inhibits a number of enzymes possibly via the sulfhydryl group (Pintado 1995). This group of TH is converted into the thiomercuryethyl derivate, which can no longer react as a sulfhydryl group. But no data suggest a requirement for the reaction between thiomersal and thiol groups.

Nevertheless, since the diffusion of TH into the cell is not well known, the transport genes (*mer*T, *mer*P, *mer*C and *mer*F) were considered more closely. All of the *mer* operons had the *mer*P and *mer*T genes and high similarities (92–99%) were among the respective proteins. Studies have shown that both *mer*T and *mer*P are required for full expression of Hg^{2+} resistance, but loss of *mer*P is less deleterious than loss of *mer*T. This fact is due to protein structure. MerT contains paired cysteine residues (Cys24, Cys25 and Cys76, Cys82) which have been shown to be involved in mercuric ion hypersensitivity (Brown *et al.* 1991; Morby *et al.* 1995). Site-directed mutagenesis of any of the four cysteine residues abolishes mercuric ion resistance in vivo (Hobmann and Nigel 1996). The MerT peptide contains vicinal

cysteines, CCxx that bind mercury exclusively. DeSilva *et al.* (2002) suggested that a large part of the specificity in the mercury detoxification system lies with the metal transport protein MerT due to the vicinal cysteines, rather than the periplasmic protein MerP, which can bind many different metals because it has the CxxC sequence in its metal-binding loop. This is in view of the fact that the CxxC motif is a typical heavy-metal binding motif. On the one hand, Cu^{+}-chaperones bearing this motif were identified for their ability to interact with their Cu^{+}-ATPase targets in prokaryotes as well as in eukaryotes and, on the other hand, the target Cu^{+}-ATPases were identified as having the same CxxC motif at their N-terminus. In addition, non-Cu^{+} heavy-metal ATPases were also found (see Figure 3-42), which bear the same CxxC motif at their N-terminus and are involved in Cd^{2+}, Zn^{2+} or Pb^{2+} resistance of prokaryotes (Nucifora *et al.* 1989; Rensing *et al.* 1997). It is tempting to examine whether MerP and MerT could fulfill the role of transport protein regarding TH and in which manner the interaction occurs.

One difference between the bacterial *mer* operons was the presence or absence of the inner membrane proteins MerC and MerF. The *mer* operons of five strains (Spi4, Spi11, Elb2, Tin2 and Bro12) could be grouped on the presence of the *mer*C gene and *Ps. putida* Elb2 was the only strain in which a *mer*F gene could be detected. A high degree of similarity was observed for each transport protein of all eight strains, especially for the crucial regions (see Figure 3-46). Though these five strains transformed thiomersal in very different rates. While Spi4, Spi11 showed high transformation rates, Bro12 showed lower rates. Although Elb2 did contain both MerC and MerF proteins the thiomersal transformation was not notably enhanced. Therefore, it can be maintained that these proteins do not play a crucial role for thiomersal transformation.

Generally, the role of *mer*C in *mer* operons remains a puzzle. The Tn501 *mer* operon, however, lacks a *mer*C gene but nonetheless has a functional Hg^{2+} binding system. Hamlett *et al.* (1992) provided evidence that *mer*C does not have a role in Hg^{2+} transport or in resistance in the Tn2l *mer* operon, respectively Tn501. Moreover, the CxxC peptide residue in MerC is also in the metal binding loop. It can bind many different metals and is possibly not highly specific for mercury ions such as the MerP protein. These conclusions raise the question of whether *mer*C has any function in mercurial resistance mechanisms. However, several studies (Gilbert and Summers 1988; Olson *et al.* 1991; Liebert *et al.* 2000) showed that the *mer*C gene is widely distributed in nature, suggesting that it may have a role yet to be determined.

The situation for the *mer*F gene is different, particularly on the protein level. Different than MerC, both of the mercury binding sites in MerF have vicinal cysteine residues, CCxx (see Figure 3-45). As reported for the MerT protein, vicinal cysteine residues binds mercury exclusively, suggesting that the specificity in the mercury detoxification system lies with the metal transport proteins, rather than the periplasmic protein MerP and MerC, which can bind many different metals because they have the CxxC sequence in their metal-binding loop. DeSilva *et al.* (2002) supposed that perhaps the close proximity of the vicinal cysteine residues requires linear bicoordinate geometry which consequently leads to a high metal-binding affinity and selectivity.

To define precisely the roles of MerT, MerP, MerC and MerF in thiomersal resistance, binding and operon induction, it is necessary to construct in vitro precise deletion and frameshift mutations that eliminate each of the *mer*T, *mer*P and *mer*C genes singly and in combination while leaving the other genes intact and expressed from the *mer* promoter. Results of these studies have to be combined with an analysis of the protein structure to develop a molecular picture suggesting alternative pathways for binding of mercury substrates (thiomersal) that lead to reduction and/or inhibition depending on the nature of the ligand (thiosalycylic acid).

4.6.2 Mercury Transformation Enzymes

The most important role in organic mercury detoxification systems is played by the organomercurial lyase, MerB, and mercuric reductase, MerA. As already mentioned, mercury-resistant bacteria eliminate organomercurials by producing organomercurial lyase (MerB) that catalyzes the protonolysis of the carbon–mercury bond (Begley *et al.* 1986). The products of this reaction are an inorganic species, Hg^{2+}, and a reduced carbon compound. On the basis of isotope effects and conservation of stereochemistry, Begley *et al.* (1986) concluded that MerB acts by electrophilic substitution (S_E2), an unusual concerted mechanism that has only been proposed for two other enzymes: tryptophan indole-lyase and orotidine 5′-monophosphate decarboxylase (Sloan and Phillips 1996; Kulikova *et al*. 2003).

In this study we detected five organomercurial lyases in three strains. *Ps. putida* Kon12 and *Ps. stutzeri* Ibu8 each possessed one MerB protein which was highly similar (98–99% amino acid identity) to the one of plasmid pDU1358 (Figure 3-53 and also A-10 in the Appendix).

Hongri Yu *et al.* (1994) demonstrated that the broad spectrum resistant operon from pDU1358 is resistant to Hg^{2+} and a number of organomercurial compounds, such as thiomersal. The *mer*

operon was inducible by six different organomercurial compounds. The minimum inhibitory concentrations of cells harboring the intact broad spectrum *mer* operon for thiomersal and phenylmercuric acetate were at the same rate (8 ppm) and were almost 50% lower than for the mercuric ion (18 ppm). The exact analyzed values cannot be compared with the ones of this study, since LB medium was used. Nevertheless, they are a good clue for the sensitivity of the plasmid pDU1358 MerB protein.

Ps. putida Spi3 also contains one *mer*B gene similar to the one of pDU1358 (100% amino acid identity) in addition to two other *mer*B genes. The three MerB proteins of Spi3 are quite dissimilar in sequence, with only 14–72% nucleotides matches upon alignment and therefore probably did not arise by gene duplication. Due to its superior position concerning transformation ability and unusual genetic structure, Spi3 will be discussed in detail in section 4.6.3.

The MerB protein is a unique enzyme and does not have homologies with any other protein of identified function. Also the similarities among the MerB proteins are very small (see Figure 1-5). Therefore, it is not uncommon that only five *mer*B genes could be detected while most of the strains (except *Citrobacter freundii* Tin2 and Bro62) were resistant to thiomersal. There is good sequence conservation in the central region of all sequenced MerB proteins, including four cysteines at positions 96, 117, 159 and 160 (pDU1358 MerB numbering, Figure A-11 in the Appendix).

In the majority of the Gram-negative examples, Cys159 is part of a cysteine pair with Cys160. As mentioned above, pairs of cysteine residues play a key role in the mercury transformation process, since they bind mercury exclusively (Morby *et al.* 1995). Site-directed mutagenesis of any of these four individual cysteines to alanine caused a loss of resistance to organomercurials, suggesting that all of the four cysteines play an important role in MerB's activity (Moore *et al.* 1990; Pitts and Summers 2002). These studies showed that the Cys96 and Cys159 mutations lead to a complete loss of enzymatic activity, whereas the Cys160 mutation results in the retention of about 37% of the wild-type activity. On the other hand, the enzymatic activity of the Cys117 mutant could not be assessed because of its tendency to form insoluble precipitates. Therefore, Pitts and Summers (2002) suggested that the highly conserved Cys117 could play a structural role.

It has been hypothesized that vicinal cysteine residues produce an even greater enzymatic activity. Therefore the organomercurial substrate could make initial contact with Cys 159 and Cys 160 of MerB, since the highly conserved carboxyl-terminal cysteine pair of MerA (Cys558 and Cys559) has been shown to be required for the removal of tightly bound thiol

ligands from mercuric ion substrates (Engst and Miller 1999). Because MerB can be thought of as a very large, tightly bound thiol ligand, it is a reasonable hypothesis that the carboxyl-terminal cysteines of MerA are involved in removing the mercuric ion directly from MerB. Such a direct transfer of mercuric ions may occur in at least two other steps of the mercury detoxification process. MerP sequesters mercuric ions, and MerT transports mercury ions across the cell membrane. There is evidence that mercury ions are transferred directly from MerP to MerT through a trigonal intermediate (Brown *et al.* 1991). It has also been proposed that the mercuric ion is transferred directly from the cytosolic side of MerT to MerA (Brown *et al.* 1991). Direct transfer of mercuric ions between MerB and MerA, and between other proteins in the mercury resistance system, would prevent the need for free release of the toxic product of MerB.

After formation of mercuric ion, MerA (flavoprotein disulfide oxidoreductase) catalyzes the two electron-reductions of Hg^{2+} to Hg^0 by NADPH. As with all the members of this class of proteins (e.g. glutathione reductase and lipoamide dehydrogenase), the enzyme is a dimer of identical subunits with two active sites per dimer, each composed of one FAD (flavin adenine dinucleotide) and catalytically essential residues from both subunits (Dym and Eisenberg 2001). These residues include at least FAD and Cys135 and Cys140 from one subunit and Cys558 and Cys559 from the other (see Figure 3-47 and A-9 in the Appendix). The carboxy-proximal thiol pair, Cys558, Cys559, clearly communicates with the active-site dithiol pair, Cys135, Cys140, and plays an essential role in binding and positioning Hg^{2+} for reduction (Miller *et al.* 1989; Moore and Walsh 1989; Barkay *et al.* 2003). This carboxy-proximal cysteine pair, which is completely conserved in all analyzed sequences in this study and which is absent from the other members of this class of flavoproteins, confers on mercuric reductase the unique ability to reduce the toxic Hg^{2+} ion rather than merely bind it (Van Driessche *et al.* 1996; Truffault *et al.* 2001). As shown in Figure A-9, the amino-proximal thiol pair (GMTCxxC: Cys10 and Cys13) is not essential for efficient reduction of Hg^{2+}. Fox and Walsh (1983) postulated that removing the first 85 amino acids of mercuric reductase from Tn501 showed no effect on catalytic activity. Therefore, they suggested that this N-terminal cysteine pair might be involved in a cytoplasmic Hg^{2+}-transport or -binding function. The high degree of conservation of the domain and its obvious homology to metallochaperones and other metal binding proteins (Arnesano *et al.* 2002; Barkay *et al.* 2003) strongly suggest an important function for the domain in metal ion binding and transfer. But the evidence for a functional role of the highly conserved metal binding N-terminal

domain of the MerA protein in the acquisition and delivery of Hg^{2+} to the catalytic core for reduction must still be proven.

MerA occurs in all sequenced isolates, even multiply (Spi4, Elb2, Ibu8, Bro12 and highly probably Spi3 and Spi11). As shown in Figure A-9 (Appendix), MerA proteins are highly conserved and since they catalyze the conversion of the thiol and Hg^{2+} to the uncharged Hg^0, they are not substrate specific. Thus the MerA structure does not play a special role regarding thiomersal transformation, but most likely its number in a strain. An increase in the *mer*A gene copies per cell increases the transcription and consequently the reduction of mercury ion. All isolates which transform TH over 90 ng Hg· ml^{-1} · min^{-1} had at least two or more MerA proteins (see Figure 3-5).

The MerA protein reduces Hg^{2+} to Hg^0 at a much faster rate (several orders of magnitude higher) than organomercurial lyase. The MerB protein reacts extremely slowly with its substrates, for example, it reacts with a turnover rate of 1 min for methylmercuric chloride and 240 min^{-1} for butenylmercuric chloride (Begley *et al.* 1986). Therefore, if the cells are exposed to an organomercurial compound such as TH, it must synthesize the maximum level of organomercurial lyase and other *mer* gene products in order to thrive in a TH-contaminated environment. Since mercuric ion reductase could reduce Hg^{2+} at a rate much faster than it is produced from the organomercurial substrates by the organomercurial lyase, it would be beneficial for the resistant cells to recognize the organomercurial substrates as direct inducers of the *mer* operon, specifically the direct expression of *mer*B by it own promoter such as plasmid pPB.

4.6.3 Genomic Analysis of Mercury Resistance of *Ps. putida* Spi3

The mercury resistance determinant of *Ps. putida* Spi3 is unusual in several aspects.

Firstly, Spi3 is able to cope with thiomersal concentrations up to 140 ppm with a transformation rate of 1488 ng Hg· ml^{-1} · min^{-1}. This extremely high resistance of Spi3 to TH has never been reported for other natural environmental bacteria and for recombinant microorganisms.

Secondly, four mercury-resistant operons, in other words, three broad spectrum resistant operons with three differently related *mer*B genes, and one narrow spectrum resistant operon, occurred in Spi3.

Generally, all known MerB organomercurial lyase sequences are homologous, although the diversity of sequences is great. For example, *Ps. p.* Spi3 MerB1 and MerB3 show only 26%

identical amino acids while $MerB_3$ is highly similar to MerB of *Ps. stutzeri* plasmid pPB and $MerB_1$ to plasmid pDU1358. A more detailed analysis is now needed to establish the substrate specificities of the three protein products, by subcloning analysis of these three *mer*B genes (*mer*B_1, *mer*B_2 and *mer*B_3) using a host strain and testing against a spectrum of organomercurial compounds. Huang *et al.* (1999) undertook a similar analysis with three MerB proteins from the Gram-positive bacterial transposon TnMERII of *Bacillus megaterium* MB1. The resistance spectrum was assayed by the MICs of several organomercurials and the *mer*B genes conferred different patterns of organomercury resistance on the host bacterial strain. Therefore, the level of understanding of the organomercurial lyase enzyme (Walts and Walsh 1988) does not allow us to draw conclusions with regard to substrate specificity from the protein sequences.

A further distinctive feature is the presence of an unusual version of *mer*B located in a peculiar position. Regularly, *mer*B genes lie at the 3′ end of *mer*A; an often described position in Gram-negative bacteria (Griffin *et al.* 1987; Silver and Walderhaug 1992). In the case of Spi3, *mer*B_3 is located between the *mer*R and *mer*T genes and the presence of two typical O/P regions, both upstream and downstream of *mer*B_3 was ascertained (see Figure 3-37). Reniero *et al*. (1995) first described a similar *mer*B gene (99% amino acid identity) in such a peculiar position. They suggested that the *mer*B gene has been secondarily acquired by an insertional event from an unknown source. This hypothesis might also explain the presence of promoters both upstream and downstream from the *mer*B gene that showed a high similarity to that of Tn5053. Thus, the promoter downstream of *mer*B may represent the remains of the original operon after the insertion of *mer*B itself. The fact that the *mer*B gene has its own promoter and ribosomal binding site may account for Spi3's extremely high resistance to thiomersal. It has been well known that a transcriptional gradient occurred over the length of a *mer* operon (Gambill and Summers 1992). Distal genes of the mercury-resistance operon encoded by Tn21 on the monocopy IncFII plasmid R100 were transcribed more slowly and at lower levels. The authors observed considerable variation in the rates of mRNA synthesis from the beginning to the end of the operon. Specifically, mRNA corresponding to the promoter-proximal genes, *mer*TPC, achieved a maximum in vivo synthesis rate between 60 and 120 s after induction. In contrast, the synthesis rates of mRNA corresponding to the promoter-distal genes *mer*A and *mer*D were initially fivefold lower than the rates of the promoter-proximal genes.

Considering the $MerB_3$ protein, the four cysteine residues present in the sequence are also highly conserved (Cys96, Cys117, Cys159 and Cys160) but eight additional cysteine residues

(Cys58, Cys73, Cys120, Cys122, Cys126, Cys165, Cys172 and Cys175, plasmid pDU1358 numbering) are found in the protein. As Pitt *et al.* 2002 conclude, the three cysteine residues Cys96, Cys159 and Cys160 are important for the transformation of organomercurial compounds to mercuric ions. While the organomercurial substrate makes initial contact with Cys159 of MerB, Cys96 is then probably involved in cleavage of the carbon–mercury bond. The question whether the further cysteine residues are involved in the transformation is not clarified up to this date. The highly conserved Cys117 plays a structural role as previously suggested (Pitt *et al.* 2002). Therefore, it might be possible that cysteine residues (Cys120, Cys122 and Cys 126) close to Cys117 probably also plays a structural rather than a catalytic role. This hypothesis has to be confirmed by experiments such as site-directed mutagenesis of these three cysteines to acquire a loss or alteration in organomercurial resistance. Interestingly, the additional cysteine residues (Cys165, Cys172 and Cys175) in $MerB_3$ are located in the carboxyl-terminal region, which is a hydrophobic region large enough to accommodate a large aromatic group such as the one present in substrates like thiomersal. As shown in Figure A-11 there is also a CxxC motif (Cys179-Cys182) in this hydrophobic region that is known as a typical heavy-metal binding motif. Therefore, it is possible that this region, present in MerB, binds the hydrocarbon moiety of the organomercurial substrate, and it is structured so that it is able to accommodate a diverse range of potential organomercurial substrates. To understand more about the $MerB_3$ protein mutagenesis, studies have to be combined with an analysis of the protein structure by NMR spectroscopy (nuclear magnetic resonance spectroscopy) to develop a molecular picture for the binding of thiomersal, or even other organomercurials.

5 Summary

Thiomersal (TH), developed by Eli Lilly & Company has been used since 1930s for vaccine production and preventing bacterial contamination. Presently, there is no remediation for wastewater contaminated with TH available. Therefore, this study was conducted to assess the feasibility of aerobic treatment of thiomersal-contaminated solutions.

Comparison of TH resistant microorganisms

The potentialities for TH detoxification was determined by seven naturally mercury resistant isolates of *Pseudomonas* and two *Citrobacter* strains as well as two genetically engineered microorganisms (GEMs). Generally, all isolates showed resistance up to 2 ppm TH, however with different biotransformation rates (8-443 ng Hg· ml^{-1} · min^{-1}). The two GEMs (*Ps. putida* F1::*mer* and *Ps. putida* KT2442::*mer*-73) transformed thiomersal moderately well (69 and 71 ng Hg· ml^{-1} · min^{-1}) and were able to reduce TH given a certain cell density. Unforeseen well performed a wild type isolate, *Pseudomonas putida* Spi3. It tolerates and efficiently reduces very high concentrations of thiomersal up to 140 ppm.

Thiomersal detoxification capacity of *Ps. putida* Spi3

Spi3 proved in this study to be an excellent strain for TH detoxification. Analyzes demonstrated that the optimal transformation rate of TH was determined at a temperature of 30°C and pH of 7. Additionally, the results of the growth experiments showed that the cells at lag phase exhibited the highest TH transformation rates, followed by those at the exponential phase. At the stationary phase the cells had the lowest transformation rate. Throughout the experiments, it turned out that the TH transformation efficiency was found to be closely related to the initial cell density. A positive correlation of cell density on TH transformation rate was observed. As the cell number went below 10^5 cells · ml^{-1}, no sign of transformation could be observed. A rise in the initial density from 10^6 to 10^7 cells ml^{-1} resulted in an increase in the transformation rate of up to 67%. Thus, in dynamic systems, changes in cell number will have significant effects on the magnitude and timing of the transformation rate.

The effect of TH decomposition products on bacteria

As an ethylmercury derivate, it has been reported that TH has stability problems, especially in liquid solutions containing sodium chloride. The main decomposition products of TH undergoes, in the presence of sodium chloride, irreversible oxidation to 2,2'dithiosalicylic acid (dTHSA). This highly polar organic compound can serve as an energy or carbon source.

Therefore, experiments were carried out to determine the total amount of dTHSA utilization by *Ps. putida* Spi3 and *Ps. putida* KT2442::*mer*-73. The results of the investigation showed that dTHSA was not utilized by Spi3 and KT2442 as an energy source. Therefore, the effects of dTHSA in all TH experiments could be neglected.

Selection of a counter-ion for the ion-exchange membrane reactor

For membrane reactors it is of particular importance to use a suitable counter-ion to facilitate the flux of TH anions to the biocompartment. Therefore several carboxylic acids were analyzed in-depth experiments, indicating that 2,2'dimethylbutyric acetate (DMBA) was completely biologically inert, while in the presence of tert-butylacetate (TBA) the cell number slightly increased. Nevertheless, these carboxylic acids could be selected as candidates to be used as a counter-ion in an ion-exchange membrane bioreactor.

Biotransformation of thiomersal under the steady state condition

The aim of the experiment was to determine the TH transformation rate under steady state conditions with regard to TH dilution rate and residual TH at reactor outlet and consequently to provide a reasonable basis for an optimal and safe process design. Lab-scale bioreactors were set up using Spi3 and KT2442 and operated continuously. Both strains were able to reduce the high TH inflow concentration below the detection limit and the mercury removal was through out the experiment more than 99 %. Only a minimum of Hg^{2+} (5–20 $\mu g \cdot l^{-1}$) was detectable in both bioreactors at all dilution rates.

Analysis of the *mer* operon

The genetic structure of *mer* operons from Spi3 was studied with special attention to organomercurial lyase (MerB) and was compared to the *mer* operon of the different microorganisms.

All sequenced isolates carried clusters of functional and independently regulated mercury resistant genes (*mer*). The seven analyzed environmental strains harbour a narrow spectrum resistance *mer* operon beside their resistance to thiomersal that resulted in the presence of a broad spectrum resistant *mer* operon including the organomercurial lyase, MerB. The strain *Ps. putida* Spi3 however showed a special feature, since it carried four functional *mer* operons, one conferring narrow spectrum (*mer*NS), the others broad spectrum resistance (*mer*$BS_{1/2/3}$). The complete sequenced *mer*NS operon of Spi3 has essentially the same gene organization as transposon Tn501. The *mer*R gene is followed by sequences corresponding to a typical *mer* O/P region and followed downstream by *mer*TPAD genes. Analysis of the

broad spectrum resistance operon showed that Spi3 possesses three *mer*B genes which are probably located on different *mer* operons. The first *mer*B_1 gene which was mapped upstream of a regulatory gene (*mer*D) showed 100% identity to amino acid sequence of *Serratia marcescens* pDU1358. A second *mer*B_2 was also amplified upstream of a further *mer*D gene which encodes a deduced polypeptide of 209 amino acid residues that shows low similarity to MerB proteins in the databanks. In contrast to the both mentioned *mer*$B_{1/2}$, the gene arrangement of the third *mer*B_3 gene in the broad spectrum resistance operon is peculiar; *mer*B_3 is mapped between the *mer*R and *mer*T gene and the presence of two typical O/P regions, both upstream and downstream of *mer*B_3 was ascertained. Exactly this fact that the *mer*B gene has its own promoter and ribosomal binding site may account for Spi3's extremely high resistance to thiomersal. These four *mer* operons constitute Spi3's high resistant to mercuric ion and organomercurials.

6 References

Abramson J.J., Zable A.C., Favero T.G., G. Salama. Thimerosal interacts with the Ca^{2+} release channel ryanodine receptor from skeletal muscle sarcoplasmic reticulum. *Journal of biological chemistry* 1995; 270 (50): 29644-29647.

Abuqaddom A.I., R.M. Darwish, H. Muti. The effects of some formulation factors used in ophthalmic preparations on thiomersal activity against *Pseudomonas aeruginosa* and *Staphylococcus aureus*. *Journal of Applied Microbiology* 2003; 95: 250–255.

Akagi H., Malm O., Kinjo Y., Harado M., Branches F.J.P., Pfeiffer W.C., H. Kato. Methylmercury pollution in the Amazon, Brazil. *The Science of the total environment* 1995; 175: 85-95.

Akagi H., Malm O., Branches F.J.P. , Kinjo Y., Kashima, Y., Guimarães J.R.D., Oliveira R.B., Haraguchi K., Pfeiffer W.C., Takizawa Y., H. Kato. Human exposure to mercury due to goldmining in the Tapajós River Basin, Amazon, Brazil. *Water, air and soil pollution* 1995; 80: 85-94.

Allard A.S., M. Remberger, A.H. Neilson. Bacterial 0-Methylation of chloroguaiacols: effect of substrate concentration, cell density and growth conditions. *Applied and environmental microbiology* 1985; 49: 279-288.

Altschul S.F., Madden T.L., Schaffer A.A., Zhang J., Zhang Z., Miller W., D.J. Lipman. Gapped BLAST and PSI-BLAST: a new generation of protein database search programs. *Nucleic acids research* 1997; 25: 3389-3402.

American Academy of Pediatrics. Thiomersal in vaccines An Interim Report to Clinicians (RE9935). *Pediatrics* 1999; 104; 3: 570-574.

Ansari A.Z., Chael M.L., T.V. O'Halloran. Allosteric underwinding of DNA is a critical step in positive control of transcription by Hg-MerR. *Nature* 1992; 355: 87-89.

Arnesano F., Banci L., Bertini I., Ciofi-Baffoni S., Molteni E., Huffman D.L., T.V. O'Halloran. Metallochaperones and metal-transporting ATPases: a comparative analysis of sequences and structures. *2: Genome research* 2002; 12 (2): 255-271.

Arnon R. and E. Shapira. Crystalline papain derivative containing in intramolecular mercury bridge. *Journal of biological chemistry* 1969; 244: 1033-1038.

Axton J.M.H. Six cases of poisoning after a parenteral organic mercurial compound (merthiolate). *Journal of postgraduate medicine* 1972; 48: 417-421.

Bakir F., Damlugi S.F., Amin-Zaki L., Murtadha M., Khalidi A., Al-Rawi N.Y., Tikriti S., Dhahir H.I., Clarkson T.W., Smith J.C., R.A. Doherty. Methylmercury poisoning in Iraq. *Science* 1973; 181: 230-241.

Babiarz, C.L., Hurley J.P., Hoffmann S.R., Andren A.W., Shafer M.M., D.E. Armstrong. Partitioning of total mercury and methylmercury to the colloidal phase in freshwaters. *Environmental science & technology* 2001; 35; 24: 4773-4782.

Barkay T., Liebert C., M. Gillman. Environmental significance of the potential for mer(Tn21)-mediated reduction of Hg2+ to Hg0 in natural waters. *Applied and environmental microbiology* 1989; 55 (5): 1196-1202.

Barkay T., Miller S.M., A.O. Summers. Bacterial mercury resistance from atoms to ecosystems. *FEMS microbiology reviews* 2003; 27 (2-3): 355-84.

Baxter D.C. and W. Frech. Critical comparison of two standard digestion procedures for the determination of total mercury in natural water samples by cold vapor atomic absorption spectrometry. *Analytica chimica acta* 1990; 236: 377-384.

Begley T.P., Alan E.W., C.T. Walsh. Bacterial Organomercurial lyase: Overproduction, Isolation, and Characterization. *Biochemistry* 1986; 25 (22): 7186-7192.

Begley T.P., Walts A.E., C.T. Walsh. Mechanistic studies of a protonolytic organomercurial cleaving enzyme: bacterial organomercurial lyase. *Biochemistry* 1986; 25 (22): 7192-200.

Bernier R.H., Frank J.A., T.F. Nolan. Abscesses complicating DTP vaccination. *American journal of diseases of children* 1981; 135: 826-828.

Brooun A., Liu S. and K. Lewis. A dose-dependent study of antibiotic resistance in Pseudomonas aeruginosa biofilms. *Antimicrobial agents and chemotherapy* 2000; 44: 640-646.

Brown N.L., Misra T.K., Winnie J.N., Schmidt A., Seiff M., S. Silver. The nucleotide sequence of the mercuric resistance operons of plasmid R100 and transposon Tn501: further evidence for mer genes which enhance the activity of the mercuric ion detoxification system. *Molecular & general genetics* 1986; 202 (1):143-151.

Brown N.L., L.R. Evans. Transposition in prokaryotes: transposon Tn501. *Research in microbiology* 1991; 142 (6): 689-700.

Brown N.L., Camakaris J., Lee B.T., Williams T., Morby A.P., Parkhill J., D.A. Rouch. Bacterial resistances to mercury and copper. *Journal of cellular biochemistry* 1991; 46 (2): 106-14.

Caldwell D.E.. Cultivation and study of biofilm communities. In H. M. Lappin Scott and J. W. Costerton (ed.), *Microbial biofilms*. University Press, Cambridge, U.K. 1995; 64–79.

Cai, Y., Jaff R., R.D. Jones. Interactions between dissolved organic carbon and mercury species in surface waters of the Florida Everglades. *Applied geochemistry* 1999; 14: 395-407.

Caraballo I., Rabasco A.M., M. Fernández-Arévalo. Study of thiomersal degradation mechanism. *International Journal of pharmaceutics* 1993; 89: 213-221.

Carrithers S.L. and Hoffman. Sequential methylation of 2-mercaptoethanol to the dimethyl sulfonium ion, 2-(dimethylthio) ethanol, in vivo and in vitro. *Biochemical pharmacology* 1994; 48: 1017-1024.

Center of Disease Control. Uproar over a little-known preservative, thimerosal, jostles U.S. hepatitis B vaccination policy. *The hepatitis control report*. Summer 1999; 4: No 2.

Chang J.-S., Hong J., Ogunseitan O.A., B.H. Olson. Interaction of mercuric ions with the bacterial growth medium and its effects on enzymatic reduction of mercury. *Biotechnology progress* 1993; 9: 526–532.

Chang J.-S. and J. Hong. Estimation of kinetics of mercury detoxification from low-inoculum batch cultures of Pseudomonas aeruginosa PU21 (Rip64). *Journal of biotechnology* 1995; 42: 85-90.

Chang J.-S. and W.-S Law. Development of microbial mercury detoxification processes using a mercury-hyperresistant strain of *Pseudomonas aeruginosa* PU21. *Biotechnology and bioengineering* 1998; 57: 462–470.

Clark D.L., Weiss A.A., S. Silver. Mercury and organomercurial resistances determined by plasmids in *Pseudomonas*. *Journal of bacteriology* 1977; 132 (1):186-196.

Clever H.L., Johnson S.A., M.E. Derrick. The solubility of mercury and some sparingly soluble mercury salts in water and aqueous electrolyte solutions. *Journal of physical and chemical reference data* 1985; 14: 631-679.

Condee C.W. and A.O. Summers. A mer-lux transcriptional fusion for real-time examination of in vivo gene expression kinetics and promoter response to altered superhelicity. *Journal of bacteriology* 1992; 174 (24): 8094-8101.

Costerton J.W., Lewandowski Z., Caldwell D.E., Korber, D.R., H.M. Lappin-Scott. Microbial biofilms. *Annual review of microbiology* 1995; 49:711–745.

Costerton J. W., P. S. Stewart and E. P. Greenberg. Bacterial biofilms: a common cause of persistent infections. *Science* 1999; 284: 1318-1322.

Cox N.H. and A. Forsyth. Thimerosal Allergy and Vaccination Reactions. *Contact dermatitis* 1988; 18: 229-233.

Dahlberg C. and M. Hermansson. Abundance of Tn3, Tn21, and Tn501 transposase (tnpA) sequences in bacterial community DNA from marine environments, *Applied and environmental microbiology* 1995; 61: 3051–3056.

Davis L.G., Dibner M.D, J.F. Battey. DNA/RNA extraction and precipitation. In: *Basic methods in molecular biology*, Elsevier Science Publishers, 1986: 320-323.

Decicco B.T., Lee E.C., J.V. Sorrentino. Factors effecting Survival of *Pseudomonas cepacia* in Decongestant Nasal Sprays Containing thiomersal as Preservative. *Journal of pharmaceutical science* 1982, 71 (11): 1231-1234.

DeSilva T.M., Veglia G., Porcelli F., Prantner A.M., S.J. Opella. Selectivity in heavy metal-binding to peptides and proteins. *Biopolymers* 2002; 64 (4): 189-97.

Diaz E., Munthali M., de Lorenzo V., K.N. Timmis. Universal barriers to lateral spread of specific genes among microorganisms. *Molecular microbiology* 1994; 13: 855–861.

Drotar A.M., Burton G.A., Jr. Travenier J.E., R. Falls. Widespread occurrence of bacterial thiol methyltransferase and emission of methylated sulfur gases. *Applied and environmental microbiology* 1987; 53: 1626-1631.

Dym O. and D. Eisenberg. Sequence-structure analysis of FAD-containing proteins. *Protein science* 2001; 10; 9: 1712-28.

Elferink J.G. and B.M. de Koster. The effect of thimerosal on neutrophil migration: a comparison with the effect on calcium mobilization and CD11b expression. *Biochemical pharmacology* 1998; 55 (3):305-312.

Engst S. and S. M. Miller. Alternative routes for entry of HgX_2 into the active site of mercuric ion reductase depend on the nature of the X ligands. *Biochemistry* 1999; 38: 3519-3529.

Evans J.R. and K. Bielefeldt. Regulation of Sodium Currents through Oxidation and Reduction of Thiol Residues. *Neuroscience* 2000; 101 (1): 229–236.

Fagan D.G., Pritchard J.S., Clarkson T.W., M.R. Greenwood. Organ mercury levels in infants with omphaloceles treated with organic mercurial antiseptic. *Archives of disease in childhood* 1977; 52: 962-964.

Felske A.D., Fehr W., Pauling B.V., von Canstein H.F., I. Wagner-Dobler. Functional profiling of mercuric reductase (mer A) genes in biofilm communities of a technical scale biocatalyzer. *BMC microbiology* 2003; 27 (3): 22.

Firschein W. and P. Kim. Plasmid replication and partition in *Escherichia coli*: is the cell membrane the key? *Molecular microbiology* 1997; 23 (1): 1-10.

Ford C.Z., Sayler G.S., R.S. Burlage. Containment of a genetically engineered micro-organism during a field bioremediation application. *Applied microbiology and biotechnology* 1999; 5 (3): 397-400.

Fonseca A.D., Crespo J.G., Almeida J.S., A.M. Reis. Drinking water denitrification using a novel ion-exchange membrane bioreactor, *Environmental science and technology* 2000; 34: 1557.

Friese K.H., Roschig M., G. Wuenscher. A new calibration method for the determination of trace amounts of mercury in air and biological materials. *Fresenius' journal of analytical chemistry* 1990; 337 (8): 860-866.

Gambill B.D. and A.O. Summers. Versatile mercury-resistant cloning and expression vectors. *Gene* 1985; 39 (2-3): 293-7.

Gambill B.D. and A.O. Summers. Synthesis and degradation of the mRNA of the Tn21 mer operon. *Journal of molecular biology* 1992; 225: 251–259.

Garland J.L. and A.L. Mills. Classification and characterization of heterotrophic microbial communities on the basis of patterns of community-level-sole-carbon-source utilization. *Applied and environmental microbiology* 1991; 57:2351-2359.

Georgia Fisheries Management Section. Altamaha River 2000, 8-month creel survey total estimates. Department of Natural Resources, Wildlife Resources Division. Waycross, GA. 2001.

Gil-Turnes C., F.R. Conceição, O.A. Dellagostin. Production of pCB01, a plasmid for DNA immunization against the adhesion of *Escherichia coli* k88ab. *Brazilian iournal of microbiology* 2001; 32: 225-228.

Gilbert M. P. and A. 0. Summers. The distribution and divergence of DNA sequences related to the Tn2l and Tn501 operons. *Plasmid* 1988; 20:127-136.

Girkin R and D. Kirkpatrick. Report to Lyondell Chemicals Worldwide. 14C-[Tertiary-butyl acetate]: Metabolism and pharmacokinetic study in the rat after inhalation. *Huntingdon, Cambridgeshire, Huntingdon Life Sciences* 2000; 1-90.

Grabenstein J.D. Immunologic Necessities: diluents, adjuvants, and excipients. *Hospital pharmacy* 1996; 31:1387-1401.

Griffin H.G., Foster T.J., Silver S., T.K. Misra. Cloning and DNA sequence of the mercuric- and organomercurial-resistance determinants of plasmid pDU1358. *Proceedings of the National Academy of Sciences of the United States of America* 1987; 84 (10): 3112-3116.

Grinsted J. and N.L. Brown. A Tn21 terminal sequence within Tn501: complementation of tnpA gene function and transposon evolution. *Molecular and general genetics* 1984; 197: 497–502.

Gupta A., Phung L.T., Chakravarty L., S. Silver. Mercury resistance in Bacillus cereus RC607: transcriptional organization and two new open reading frames. *Journal of bacteriology* 1999; 181 (22): 7080-7086.

Hamlett N.V., Landale E.C., Davis B.H., A.O. Summers. Roles of the Tn21, *mer*T, *mer*P, and *mer*C gene products in mercury resistance and mercury binding. *Journal of bacteriology* 1992; 174: 6377-6385.

Hanna C.P., Tyson J.F., S. McIntosh. Determination of total mercury in waters and urine by flow injection atomic absorption spectrometry procedures involving on- and off-line oxidation of organomercury species. *Analytical chemistry* 1993; 65, 5: 653 – 656.

Harada M. Minamata diseases: Methylmercury poisoning in Japan caused by environmental pollution. *Critical reviews in toxicology* 1995; 25: 1-24.

Harayama S., Rekik M., A. Bairoch, E.L. Neidle., L.N. Ornston. Potential DNA slippage structures acquired during evolutionary divergence of *Acinetobacter calcoaceticus* chromosomal benABC and *Pseudomonas putida* TOL pwwo Plasmid xylXYZ, genes encoding benzoate dioxygenases. *Journal of bacteriology* 1991; 173: 7540-7548.

Harley C.B. and R.P. Reynolds. Analysis of *E. coli* promoter sequences. *Nucleic acids research* 1987; 15: 2343-2361.

Hatzelmann A., Haurand M., V. Ullrich. Involvement of calcium in thiomersal-stimulated formation of leukotriene by fMLP in human polymorphonuclear leucotyces. *Biochemical pharmacology* 1990. 38: 2129-2137.

Hecker M., Brüne B., Decker K., V. Ullrich. the Sulfhydryl reagent thiomersal elicits human platelet aggregation by mobilization of intercellular calcium and secondary prostaglandine endoperoxide formation. *Biochemical and biophysical research communications* 1989; 159: 961-968.

Helmann J.D., Wang Y., Mahler I., C.T. Walsh. Homologous metalloregulatory proteins from both gram-positive and gram-negative bacteria control transcription of mercury resistance operons. *Journal of bacteriology* 1989; 171 (1): 222-9.

Hendrickx L., M. Hausner and S. Wuertz. Natural genetic transformation in monoculture *Acinetobacter sp.* strain BD413 Biofilms. *Applied and environmental microbiology* 2003; 69: 1721–1727.

Hentzer, M., G. M. Teitzel, G. J. Balzer, A. Heydorn, S. Molin, M. Givskov, and M. R. Parsek. Alginate overproduction affects *Pseudomonas aeruginosa* biofilm structure and function. *Journal of bacteriology* 2001; 183: 5395–5401.

Higham D.P., Sadler P.J., and M.D. Scawen. Cadmium-resistant *Pseudomonas putida* synthesizes novel cadmium binding proteins. *Science* 1984; 225: 1043–1046.

Hill W.R., Stewart A.J., G.E. Napolitano. Mercury speciation and bioaccumulation in lotic primary producers and primary consumers. *Canadian journal of fisheries and aquatic sciences* 1996; 53: 812–819.

Hobman J., Kholodii G., Nikiforov V., Ritchie D.A., Strike P., O. Yurieva. The sequence of the mer operon of pMER327/419 and transposon ends of pMER327/419, 330 and 05. *Gene* 1994; 146 (1):73-78.

Hobman J.L., N.L. Brown. Overexpression of MerT, the mercuric ion transport protein of transposon Tn501, and genetic selection of mercury hypersensitivity mutations. *Molecular and general genetics* 1996; 250 (1): 129-134.

Horn JM., Brunke M, Deckwer W-D, KN. Timmis. *Pseudomonas putida* strains which constitutively overexpress mercury resistance for biodetoxification of organomercurial pollutants. *Applied and environmental microbiology* 1994; 60 (1): 357-362.

Hotta Y., S. Ezaki, H. Atomi, and T. Imanaka. Extremely stable and versatile carboxylesterase from a hyperthermophilic archaeon. *Applied environmental microbiology* 2002; 68: 3925-31.

Houben-Weyl 2000. Methoden der organischen Chemie (4^{th} Edition). Editor Eugen Müller. Thieme, Stuttgart, Germany.

Huang C.C., M. Narita, T. Yamagata, Y. Itoh, G. Endo. Structure analysis of a class II transposon encoding the mercury resistance of the Gram-positive bacterium *Bacillus megaterium* MB1, a strain isolated from Minamata Bay, Japan. *Gene* 1999; 234: 361–369.

Hutschinson T.W. and K.M. Meena. Lindberg S. Group report: Mercury. Ed. Lead, mercury, cadmium and arsenic in the environment. New York, Wiley 1987; 17-34.

Ikingura J.R. and H. Akagi. Methylmercury production and distribution in aquatic systems. *The science of the total environment* 1999; 234: 109-118.

Innis M.A. and D.H. Gelfand. Optimization of PCRs. PCR Protocols (Innis, Gelfand, Sninsky and White, eds.); Academic Press, New York 1990: 3-12.

Iohara K., Liyama R., Nakamura K., Silver S., Sakai M., Takeshita M., K. Furukawa. The *mer* operon of a mercury-resistant *Pseudoalteromonas haloplanktis* strain isolated from Minamata Bay, Japan. *Applied microbiology and biotechnology* 2001; 56: 736-741.

James G.A., Beaudette L., J.W. Costerton. Interspecies bacterial interactions in biofilms. *Journal of Industrial Microbiology* 1995; 15: 257–62.

Jobling M. G., Peters S.E., D.A. Ritchie. Plasmid borne mercury resistance in aquatic bacteria. *FEMS microbiology letters* 1988; 49: 31-37.

Jenkins K.B., Michelsen, D.L. J.T. Novak. Application of oxygen microbubbles for in situ biodegradation of p-xylene-contaminated groundwater in a soil column. American Institute of Chemical Engineers; Biotechnology progress 1993; 9 (4): 394-400.

Kaiser D. and R. Losick. How and why bacteria talk to each other. *Cell* 1993; 73: 873–885.

Kelly W.J. and D.C. Reanney. Mercury resistance among soil bacteria: ecology and transferability of genes encoding resistance. *Soil biology and biochemistry* 1984; 16: 1-8.

Kent A.D. and E.W. Triplett. Microbial communities and their interactions in soil and rhizosphere ecosystems. *Annual review of microbiology*, 2002; 56: 211-236.

Kiyono M, Omura T, Fujimori H, H. Pan-Hou. Organomercurial resistance determinats in *Pseudomonas* K-62 are present on two plasmids. *Archives of microbiology* 1995; 163: 242-247.

Kiyono M., Omura T., Inuzuka M., Fujimori H., H. Pan-Hou. Nucleotide sequence and expression of the organomercurial-resistance determinants from a Pseudomonas K-62 plasmid pMR26. *Gene* 1997; 189 (2): 151-157.

Kiyono M, H. Pan-Hou. The *mer*G Gene Product Is Involved in Phenylmercury Resistance in *Pseudomonas* Strain K-62. *Journal of bacteriology* 1999; 181 (3): 726-730.

Kholodii G.Y., Yurieva O.V., Lomovskaya O.L., Gorlenko Z., Mindlin S.Z., V.G. Nikiforov. Tn5053, a mercury resistance transposon with integron's ends. *Journal of molecular biology* 1993; 20: 230 (4): 1103-11037.

Kholodii G.Y., Gorlenko Z., Lomovskaya O.L., Mindlin S.Z., Yurieva O.V., V.G. Nikiforov. Molecular characterization of an aberrant mercury resistance transposable element from an environmental Acinetobacter strain. *Plasmid* 1993; 30 (3): 303-308.

Kholodii G.Y., Yurieva O.V., Gorlenko Z., Mindlin S.Z., Bass I.A., Lomovskaya O.L., Kopteva A.V., V.G. Nikiforov. Tn5041: a chimeric mercury resistance transposon closely related to the toluene degradative transposon Tn4651. *Microbiology* 1997; 143 (8):2549-2556.

Kholodii G., Yurieva O., Mindlin S., Gorlenko Z., Rybochkin V., V. Nikiforov. Tn5044, a novel Tn3 family transposon coding for temperature-sensitive mercury resistance. *Research in microbiology* 2000; 151: 291-302.

Kholodii G.Y., Gorlenko Z.M., Mindlin S.Z., Hobman J.L., V.G. Nikiforov. Tn5041-like transposons: molecular diversity, evolutionary relationships and distribution of distinct variants in environmental bacteria. *Microbiology* 2002; 148: 3569-3582.

Kholodii G.Y., Mindlin S., Gorlenko Z., Petrova M., Hobman J., V.G. Nikiforov. Translocation of transposition-deficient (TndPKLH2-like) transposons in the natural environment: mechanistic insights from the study of adjacent DNA sequences. *Microbiology* 2004; 150 (4):979-992.

Koch A.L. How bacteria face depression, recession and derepression. *Perspectives in biology and medicine* 1976; 20: 44–63.

Koch A.L. and C.H. Wang. How close to the theoretical diffusion limit do bacterial uptake systems function? *Archives of microbiology* 1982; 131 (1): 36-42.

Kondler-Budde R. Ist Thiomersal in Impfstoffen gefährlich? *Immunologie und Impfen* 1999; 2: 175-177.

Kovárová K., Käch A., Zehnder A.J., T. Egli. Cultivation of Escherichia coli with mixtures of 3-phenylpropionic acid and glucose: steady-state growth kinetics. *Applied and environmental microbiology* 1997; 63 (7): 2619-2624.

Kulikova V.V., Zakomirdina L.N., Bazhulina N.P., Dementieva I.S., Faleev N.G., Gollnick P.D.,T.V. Demidkina. Role of arginine 226 in the mechanism of tryptophan indole-lyase from *Proteus vulgaris*. *Biochemistry* (Mosc) 2003; 68 (11): 1181-1188.

Laddaga R.A., Chu L., Misra T.K., S. Silver. Nucleotide sequence and expression of the mercurial-resistance operon from *Staphylococcus aureus* plasmid pI258. *Proceedings of the National Academy of Sciences of the United States of America* 1987; 84 (15): 5106-5110.

Lee S.W., Glickmann E., D.A. Cooksey. Chromosomal locus for cadmium resistance in Pseudomonas putida consisting of a cadmium-transporting ATPase and a MerR family response regulator. *Applied and environmental microbiology* 2001; 67: 1437-1444.

Liebert C.A., Wireman J., Smith T., A.O. Summers. Phylogeny of mercury resistance (*mer*) operons of Gram-negative bacteria isolated from the fecal flora of primates. *Applied and environmental microbiology* 1997; 63: 1066-1076.

Liebert C.A., Hall R.M., A.O. Summers. Tn21, flagship of the floating genome. *Microbioloy and molecular biology reviews* 1999; 63 (3): 507-522.

Liebert C.A., Watson A.L. and A.O. Summers. The quality of *mer*C, a module of the *mer* mosaic. *Journal of molecular evolution* 2002; 51: 607-622.

Lowell H.J., Burgess S., Shenoy S., Peters M., T.K. Howard. Mercury poisoning associated with hepatitis B immunoglobulin. *Lancet* 1996: 347:480.

Magos L, Brown A.W., Sparrow S., Bailey E., Snowden R.T., W.R. Skipp. The Comparative Toxicology of Ethyl- and Methylmercury. *Archives of toxicology* 1985; 57:260-267.

Magos L. Review on the Toxicity of Ethylmercury, Including its Presence as a Preservative in Biological and Pharmaceutical Products. *Journal of applied toxicology* 2001; 21:1-5.

Mahaffey K.R. and G. Rice. An Assessment of Exposure to Mercury in the United States: Mercury Study Report to Congress. Washington, DC: *U.S. environmental protections agency*; 1997. Document EPA-452/R097-006.
Mahaffey K.R. Methylmercury: A new look at the risks. *Public health reports* 1999; 114: 397-413.

Martin F., Gaulberto A., Sorbrino F., E. Pintado. Thiomersal induces calcium mobilization, fructose 2,6-bisphosphate synthesis and cytoplasmic alkalinization in rat thymus lymphocytes. *Biochimica et biophysica acta* 1991; 1091: 110-114.

Massol-Deya A. A., Whallon J., Hickey R.F., J.M. Tiedje. Channel structure in aerobic biofilms of fixed film reactors treating contaminated groundwater. *Applied and environmental microbiology* 1995; 61:769–777.

Mason R.P. and W.F. Fitzgerald. Sources, sinks and biochemical cycling of mercury in the ocean. In: Baeyens W., Ebinghaus R. and Valiliev O. (eds.): Global and regional mercury cycles: Sources, fluxes and mass balances. *NATO ASI Series* 1996; 2. Environment. Vol. 21. Kluwer Academic Publishers, Dordrecht, The Netherlands.

Meakin B.J. and Z.M. Khammas. An observation on the determination of thiomersol at preservative concentration by flameless atomic absorption spectroscopy. *The Journal of pharmacy and pharmacology* 1979; 31: 653-654.

Mezna M. and F. Michelangeli. Effects of thimerosal on the transient kinetics of inositol 1,4,5-trisphosphate-induced Ca^{2+} release from cerebellar microsomes. *The Biochemical journal* 1997; 325 (1): 177-82.

Miller S. M., Moore M. J., Massey, V., Williams C. H., Jr., Distefano, M. D., Ballou, D. P. and C.T. Walsh. Evidence for the participation of Cys558 and Cys559 at the active site of mercuric reductase. *Biochemistry* 1989; 28: 1194-1205.

Ministry of Environment and Energy Denmark: The National Forest and Nature Agency. Risk assessment of genetically modified derivatives of *Pseudomonas fluorescens* F 113 for use in bioremediation of PCB contaminated soil. *Biotechnology* 2000.

Misra, T. K. Bacterial resistance to inorganic mercury salts and organomercurials. *Plasmid* 1992; 27:4–16.

Moore M. J. and C. T. Walsh. Mutagenesis of the N- and C-terminal cysteine pairs of Tn501 mercuric ion reductase: consequences for bacterial detoxification of mercurials. *Biochemistry* 1989; 28: 1183-1194.

Morby A.P., Hobman J.L., N.L.Brown. The role of cysteine residues in the transport of mercuric ions by the Tn501 MerT and MerP mercury-resistance proteins. *Molecular microbiology* 1995; 17 (1): 25-35.

Mukhopadhyay D.H., Yu H., Nucifora G., T.K. Misra. Purification and functional characterization of *mer*D: a coregulator of the mercury resistance operon in Gram-negative bacteria. *The Journal of biological chemistry* 1991; 266: 18538-18542.

Mulligan M.E., Brosius J. and W.R. McClure. Characterization in vitro of the effect of spacer length on the activity of Escherichia coli RNA polymerase at the TAC promoter. *The Journal of biological chemistry* 1985; 260: 3529-3538.

Nelson K.E., Weinel C., Paulsen I.T., Dodson R.J., Hilbert H., Martins dos Santos V.A.P., *et al.*. Complete genome sequence and comparative analysis of the metabolically versatile *Pseudomonas putida* KT2440. *Environmental microbiology* 2002 ; 4: 799–808.

Neumann G., R. Teras, L. Monson, M. Kivisaar, F. Schauer and H. J. Heipieper. Simultaneous degradation of atrazine and phenol *by Pseudomonas sp.* strain ADP: effects of toxicity and adaptation. *Applied and environmental microbiology* 2004; 70: 1907–1912.

Ngim, C.H. and S.C. Foo. Atomic Absorption Spectrophotometric Microdetermination of Total Mercury in Undigested Biological Samples. *Journal of analytical toxicology* 1988; 12: 132-135.

Nucifora G., Silver S., T.K. Misra. Down regulation of the mercury resistance operon by the most promoter-distal gene *mer*D. *Molecular & general genetics* 1990; 220: 69-72.

Nucifora G., Chu L., Misra T.K., S. Silver. Cadmium resistance from Staphylococcus aureus plasmid pI258 cadA gene results from a cadmium-efflux ATPase. *Proceedings of the National Academy of Sciences of the United States of America* 1989; 86 (10): 3544-3548.

Nucifora G., Chu L., Silver S., TK. Misra. Mercury operon regulation by the merR gene of the organomercurial resistance system of plasmid pDU1358. *Journal of bacteriology* 1989; 171 (8): 4241-4247.

Nucifora G., Silver S., T.K. Misra. Down regulation of the mercury resistance operon by the most promoter-distal gene merD. *Molecular and general genetics* 1989; 220 (1): 69-72.

O'Halloran T. and C. Walsh. Metalloregulatory DNA-binding protein encoded by the merR gene: isolation and characterization. *Science* 1987; 235 (4785): 211-4.

O'Halloran T.V., Frantz B., Shin M.K., Ralston D.M., J.G. Wright. The MerR heavy metal receptor mediates positive activation in a topologically novel transcription complex. *Cell* 1989; 56 (1): 119-129.

O'Halloran T.V. Transition metals in control of gene expression. *Science* 1993; 6 (261): 715-725.

Olson B. H., Cayless S. M., Ford S., J. N. Lester. Toxic element contamination and the occurrence of mercury resistant bacteria in Hg-contaminated soil, sediments, and sludges. *Archives of environmental contamination and toxicology* 1991; 20: 226-233.

Onat E. Solubility studies of metallic mercury in pure water at various temperatures. *Journal of inorganic and nuclear chemistry*1974; 36: 2029-2039.

Opella S.J., DeSilva T.M., G. Veglia. Structural biology of metal-binding sequences. *Current opinion in chemical biology* 2002; 6: 217-223.

Osborn M., Bruce K.D., Strike P., D.A. Ritchie. Distribution, diversity and evolution of the bacterial mercury resistance. *FEMS Microbiology reviews* 1997; 11: 145-152.

Oskarsson A., Schultz A., Skerfving S., Hallen I.P., Ohlin B., B.J. Lagerkvist. Total and inorganic mercury in breast milk in relation to fish consumption and amalgam in lactating women. *Archives of environmental health* 1996; 51 (3): 234–241.

Pabo C.O. and R.T. Sauer. Protein-DNA recognition. *Annual review of biochemistry* 1984; 53: 293-321.

Papadopoulos D., Schneider D., Meier-Eiss J., Arber W., Lenski R.E., M. Blot. Genomic evolution during a 10,000-generation experiment with bacteria. *Proceedings of the National Academy of Sciences of the United States of America* 1999; 96: 3807–3812.

Pardo R., Herguedas M., Barrado E., M. Vega. Biosorption of cadmium, copper, lead and zinc by inactive biomass of *Pseudomonas putida*. *Analytical and bioanalytical chemistry* 2003; 376: 26-32.

Park W., Jeon C.O., Hohnstock-Ashe A.M., Winans S.C., Zylstra G.J., E.L. Madsen. Identification and characterization of the conjugal transfer region of the pCg1 plasmid from naphthalene-degrading *Pseudomonas putida* Cg1. *Applied and environmental microbiology* 2003; 69 (6): 3263-3271.

Parkhill J. and N.L. Brown. Site-specific insertion and deletion mutants in the mer promoter-operator region of Tn501; the nineteen base-pair spacer is essential for normal induction of the promoter by MerR. *Nucleic acids research* 1990; 18 (17): 5157-5162.

Paulsson J.. Multileveled Selection on Plasmid Replication. *Genetics* 2002; 161: 1373-1384.

Pearson A.J., Bruce K.D., Osborn A.M., Ritchie D.A., P. Strike. Distribution of class II transposase and resolvase genes in soil bacteria and their association with mer genes, *Applied and environmental microbiology* 1996; 62: 2961–2965.

Pfab R., Muckter H., Roider G., T. Zilker. Clinical Course of Severe Poisoning with Thiomersal. *Clinical toxicology* 1996; 34: 453-460.

Philippidis G.P., Malmberg L.H., Hu W.S., J.L. Schottel. Effect of gene amplification on mercuric ion reduction activity of Escherichia coli. *Applied and environmental microbiology* 1991; 57 (12): 3558-64.

Pinedo C.A., B.F. Smets. Conjugal TOL transfer from *Pseudomonas putida* to *Pseudomonas aeruginosa*: effects of restriction proficiency, toxicant exposure, cell density ratios, and conjugation detection method on observed transfer efficiencies. *Applied and environmental microbiology* 2005; 71(1): 51-7.

Pintado E., Baquero-Leonis D., Conde M., F. Sobrino. Effect of Thiomersal and other Sylfhydryl Reagents on Calcium Permeability in Thymus Lymphocytes. *Biochemical Pharmacology* 1995, 49: 227-232.

Pirker C., Möslinger T., Wantke F., Götz M., R. Jarisch. Ethylmercuric chloride: The responsible agent in thiomersal hypersensitivity. *Contact dermatitis* 1993; 29: 152-154.

Pitts K.E., A.O. Summers. The roles of thiols in the bacterial organomercurial lyase (MerB). *Biochemistry* 2002; 41 (32): 10287-10296.

Powell H.M. and W.A. Jamieson. Merthiolate as a Germicide. *American journal of hygiene* 1931; 13: 296-310.

Ralston D.M. and T.V.O'Halloran. Ultrasensitivity and heavy-metal selectivity of the allosterically modulated MerR transcription complex. *Proceedings of the National Academy of Sciences of the United States of America* 1990; 87 (10): 3846-50.

Ramos J.L., Duque E., Huertas M.J. and A. Haïdour. Isolation and expansion of the catabolic potential of a *Pseudomonas putida* strain able to grow in the presence of high concentrations of aromatic hydrocarbons. *Journal of bacteriology* 1995; 177: 3911-3916.

Rasmussen L.D. and S.J. Sørensen. The effect of longterm exposure to mercury on the bacterial community in marine sediment. *Current microbiology* 1998; 36:291-297.

Ravatn R., Studer S., Springael D., Zehnder A.J., J.R. van der Meer. Chromosomal integration, tandem amplification, and deamplification in *Pseudomonas putida* F1 of a 105-kilobase genetic element containing the chlorocatechol degradative genes from *Pseudomonas sp.* Strain B13. *Journal of bacteriology* 1998; 180 (17): 4360-4369.

Ravel J., Di Ruggiero J., Robb F.T., R.T. Hill. Cloning and sequence analysis of the mercury resistance operon of *Streptomyces sp.* Strain CHR28 reveals a novel putative second regulatory gene. *Journal of bacteriology* 2000; 182 (8): 2345-2349.

Reader M.J. and C.B. Lines. Decomposition of Thiomersal in Aqueous Solution and its Determination by High-Performance Liquid Chromatography. *Journal of pharmaceutical Sciences* 1983; 72 (12): 1406-1409.

Reniero D., Galli E., P. Barbieri. Cloning and comparison of mercury- and organomercurial-resistance determinants from a Pseudomonas stutzeri plasmid. *Gene* 1995; 166 (1): 77-82.

Reniero D., Mozzon E., Galli E., P. Barbieri. Two aberrant mercury resistance transposons in the Pseudomonas stutzeri plasmid pPB. *Gene* 1998; 208 (1): 37-42.

Rensing C., Mitra B., B.P. Rosen. The zntA gene of Escherichia coli encodes a Zn(II)-translocating P-type ATPase. *Proceedings of the National Academy of Sciences of the United States of America* 1997; 94 (26): 14326-14331.

Ribaud 0. and M. Schwartz. Positive control of transcription initiation in bacteria. *Annual review of genetics* 1984; 18: 173-206.

Richardson M., Egyed E., D.J. Currie. In Mercury as a global pollutant. Porcella D.B., Huckabee J. W. and B. Wheatley, eds. Kluwer, Dordrecht. The Netherlands.1995; 499-508.

Rogers RD. Methylation of mercury in agriculture soils. *Journal of environmental quality* 1976; 5: 454-458.

Rohyans J., Walson P.D., Wood G.A., W.A. MacDonald. Mercury toxicity following merthiolate ear irrigations. *The Journal of pediatrics* 1994; 104: 311-313.

Ross W., Park S.J. and A.0. Summers. Genetic analysis of transcriptional activation and repression in the Tn2l mer operon. *Journal of bacteriology* 1989; 171: 4009-4018.

Rychlik W., Spencer W.J., R.E. Rhoads. Optimization of the Annealing Temperature for DNA Amplification in vitro. *Nucleic acids research.* 1990; 18: 640-6412.

Sahlman L., Lambeir A.M., Lindskog S. and H.B. Dunford. The reaction between NADPH and mercuric reductase from *Pseudomonas aeruginosa*. *Journal of biological chemistry* 1984; 259: 12403-12408.

Sahlman L., Wong W., J. A. Powlowski. Mercuric Ion Uptake Role for the Integral Inner Membrane Protein, MerC, Involved in Bacterial Mercuric Ion Resistance. *Journal of biological chemistry* 1997; 272: 29518-29526.

Schneiker S., Keller M., Droge M., Lanka E., Puhler A., W. Selbitschka. The genetic organization and evolution of the broad host range mercury resistance plasmid pSB102 isolated from a microbial population residing in the rhizosphere of alfalfa. *Nucleic acids research* 2001; 29 (24): 5169-5181.

Sedlmeier R. and J. Altenbuchner. Cloning and DNA sequence analysis of the mercury resistance genes of *Streptomyces lividans*. *Molecular and general genetics* 1992; 236 (1): 76-85.

Selifonova O.V. and R.W. Eaton. Use of an ipb-lux fusion to study regulation of the isopropylbenzene catabolism operon of *Pseudomonas putida* RE204 and to detect hydrophobic pollutants in the environment. *Applied and environmental microbiology* 1996; 62 (3): 778-783.

Senn H., Lendenmann U., Snozzi M., Hamer G., T. Egli. The growth of Escherichia coli in glucose-limited chemostat cultures: a reexamination of the kinetics. *Biochimica et biophysica acta* 1994; 1201: 424–436.

Shapiro J. A. Bacteria as multicellular organisms. *Scientific American* 1988; 256: 82-89.
Shapiro J. A. The significances of bacterial colony patterns. *Bioessays* 1995; 17(7): 597-607.

Shapiro J. A. Thinking about bacterial populations as multicellular organisms. *Annual review of microbiology* 1998; 52: 81-104.

Shewchuk L.M., Verdine G.L., C.T. Walsh. Transcriptional switching by the metalloregulatory MerR protein: initial characterization of DNA and mercury (II) binding activities. *Biochemistry* 1989; 28 (5): 2331-2339.

Shewchuk L.M., Helmann J.D., Ross W., Park S.J., Summers A.O., C.T. Walsh. Transcriptional switching by the MerR protein: activation and repression mutants implicate distinct DNA and mercury(II) binding domains. *Biochemistry* 1989; 28 (5): 2340-2344.

Short K.A., King R.J., Seidler R.J., R.H.Olsen. Biodegradation of phenoxyacetic acid in soil by *Pseudomonas putida* PP0301 (pR0103), a constitutive degrader of 2,4-dichlorophenoxy-acetate. *Molecular ecology* 1992; 1 (2): 89-94.

Shrager P. Slow sodium inactivation in nerve after exposure to sulfhydryl blocking reagents. *The Journal of general physiology* 1977; 69: 183-202.

Shrivasta K.P. and S. Singh. A New Method for Spectrophotometric Determination of Thiomersal in Biologicals. *Biologicals* 1995; 23: 65-69.

Silver S., Nucifora G., Chu L., T.K. Misra. Bacterial resistance ATPases: Primary pumps for exporting toxic cations and anions. *Trends in biochemical sciences* 1989; 14: 76-80.

Silver S.. Bacterial heavy metal resistancesystem and possibility of bioremediation. In Biotechnology: Bridging Research and Applications. Kulwer, Boston. 1991; 265-286.

Silver S, M. Walderhaug. Gene regulation of plasmid- and chromosome-determined inorganic ion transport in bacteria. *Microbiological reviews* 1992; 56 (1):195-228.

Silver S. and LT. Phung. Bacterial heavy metal resistance: new surprises. *Annual review of microbiology* 1996; 50: 753-789.

Simon P.A., Chen R.T., Elliot J.A., B. Schwartz. Outbreak of pyogenic abscesses after diphtheria and tetanus toxoids and pertussis vaccine. *The Pediatric infectious disease journal* 1993; 12: 368-371.

Sloan M.J. and R.S. Phillips. Effects of alpha-deuteration and of aza and thia analogs of L-tryptophan on formation of intermediates in the reaction of Escherichia coli tryptophan indole-lyase. *Biochemistry* 1996; 35 (50): 16165-16173.

Smalla K., Wachtendorf U., Heuer H., Liu W.-T., L.J. Forney. Analysis of Biolog-GN substrate utilization patterns by microbial communities. *Applied and environmental microbiology* 1998; 64:1220–1225.

Smit E., Wolters A., J.D. van Elsas. Self-transmissible mercury resistance plasmids with gene mobilizing capacity in soil bacterial population: Influence of wheat roots and mercury addition. *Applied and environmental microbiology* 1998; 64 (4): 1210-1219.

Solioz M. and C. Vulpe. CPx-type ATPases: a class of P-type ATPases that pump heavy metals. *Trends in biochemical sciences* 1996; 21: 237-241.

Song Jin-Ho, Yoon Young Jang, Yong Kyoo Shin, Moo Yeol Lee, Chung-Soo Lee. Inhibitory action of thimerosal, a sulfhydryl oxidant, on sodium channels in rat sensory neurons. *Brain research* 2000; 864: 105–113.

Spoering, A.L. and K. Lewis. Biofilms and planktonic cells of *Pseudomonas aeruginosa* have similar resistance to killing by antimicrobials. *Journal of bacteriology* 2001; 183: 6746-6751.

Stoodley P., Boyle J.D., Dodds I, H.M. Lappin-Scott. Consensus model of biofilm structure. Biofilms: community interactions and control. In: Wimpenny JWT, Gilbert PS, Lappin-Scott HM, Jones M, editors. Cardiff, UK: *Bioline* 1997; 1–9.

Stouten H. and W. Bogaerts. DECOS and SCG Basis for an Occupational Standard *n*-, *iso*-, *sec*-, and *tert*-Butyl acetate. Dutch Expert Committee on Occupational Standards and Swedish Criteria Group for Occupational Standards. Stockholm, *Arbetslivsinstitute* (National Institute for Working Life) (Arbete och Hälsa (Work and Health) NR 2002: II) available at: http://ebib.arbetslivsinstitutet.se/ah/2002/ah2002_11.pdf.

Stünning M., Brom J., W. König. Multiple Effects of Ethylmercurithiosalicylate on the Metabolization of Arachidonic Acid by Human Neutrophils. *Postaglandins leukotrines and essential fatty acid* 1988; 32: 1-7.

Summers A.O. Organization, expression, and evolution of genes for mercury resistance. *Annual review of microbiology* 1986; 40: 607-34.

Summers A.O. Generally Overlooked Fundamentals of Bacterial Genetics and Ecology. *Clinical infectious diseases* 2002; 34 (3): 85–92.

Suzuki T., Miyama T., H. Katsunuma. Comparative study of bodily distribution of mercury in mice after subcutaneous administration of methyl, ethyl, and n-propyl mercury acetate. *The Japanese journal of experimental medicine* 1963; 33: 277-282.

Swain E.B., D.D. Helwig., Mercury in fish from northeastern Minnesota lakes--historical trends, environmental correlates, and potential sources: *Journal of minnesota academy of science* 1989; 55 (1): 103-109.

Tempest D.W. The continuous cultivation of microorganisms. 1. Theory of the chemostat. *Methods in microbiology* 1970; 2: 259-276.

Tempest D. W. and O. M. Neijssel. Eco-physiological aspects of microbial growth in aerobic nutrient-limited environments. *Advances in microbial ecology* 1978; 2:105-153.

Thompson J.D., Gibson T.J., Plewniak F., Jeanmougin F., D.G. Higgins. The CLUSTAL_X windows interface: flexible strategies for multiple sequence alignment aided by quality analysis tools. *Nucleic acids research* 1997; 25: 4876-82.

Timmis K.N. *Pseudomonas putida*: a cosmopolitan opportunist par excellence. *Environmental microbiology* 2002; 4: 779–781.

Tosi A., Guerra L., F. Bardazzi. Hypposensitizing therapy with standart antigenic extracts: an important source of thiomersal sensitization. *Contact dermatitis* 1989: 20: 173-176.

Trakhtenberg I.M. In place of a conclusion. In: Chronic Effects of Mercury on Organisms. National Institutes of Health, DHEW Publication No. (NIH) 74-473, Stock Number 1753-00023. Published: 1974.

Truffault V., Coles M., Diercks T., Abelmann K., Eberhardt S., Lüttgen H., Bacher A., H. Kessler. The Solution Structure of the N-terminal Domain of Riboflavin Synthase. *Journal of molecular biology* 2001; 309 (4): 949-60.

Uhlin B.E. and K. Nordstrom. R plasmid gene dosage effects in Escherichia coli K-12: copy mutants of the R plasmic R1drd-19. *Plasmid.* 1977; 1 (1):1-7.

U.S. EPA. TMDL Development for Total Mercury and Fish Consumption Guidelines in the Middle and Lower Savannah River Watershed. *U.S. environmental protection agency* 2001; Region 4: February 28.

U.S. EPA. Total Mercury in Fish Tissue Residue in Talking Rock Creek (HUC 03150102): Ga. Highway 136 to Pickens/Gilmer County Line (Pickens County, GA). *U.S. environmental protection agency* 2003.

U.S. Geological Survey, Mineral Commodity Summaries, January 1998. http://minerals.usgs.gov/minerals/pubs/commodity/mercury/index.html#mcs.

U.S. Pharmacopeia 24, Rockville, MD: U.S. *Pharmacopeial convention*; 2001.

Van Beilen J.B., Panke S., Lucchini S., Franchini A.G., Röthlisberger M., B. Witholt. Analysis of *Pseudomonas putida* alkane degradation gene clusters and flanking insertion sequences: evolution and regulation of the alk genes. *Microbiology* 2001; 147:1621-163.

Van Driessche G., Koh M., Chen Z.W., Mathews F.S., Meyer T.E., Bartsch R.G., Cusanovich M.A., J.J Van Beeumen. Covalent structure of the flavoprotein subunit of the flavocytochrome c: sulfide dehydrogenase from the purple phototrophic bacterium Chromatium vinosum. *Protein science* 1996; 5 (9): 1753-1764.

Van Gorp R.M.A., Van Dam-Mieras M.C.E., Hornstra G., J.W.M. Heemskerk. Effect of Membrane-Permeable Sulfhydryl Reagents and Depletion of Glutathione on Calcium Mobilisation in Human Platelets. *Biochemical pharmacology* 1997; 53: 1533-1542.

Velizarov S., Rodrigues C.M., Reis A.M., J.G. Crespo. Mechanism of charged pollutants removal in an ion exchange membrane bioreactor: drinking water denitrification, *Biotechnology and bioengineering* 2001; 71: 245–254.

Vermeir G., Vandecasteele C., Temmerman E., Dams R., J. Versieck. Determination of mercury in biological materials by CV-AAS after wet digestion. *Mikrochimica acta* 1988; 3: 305-313.

Vermeir G., Vandecasteele C., R. Dams. Microwave dissolution for the determination of mercury in biological samples. *Analytica chimica acta* 1989; 220: 257-261.

Vesterberg O. Automatic method for quantitation of mercury in blood, plasma and urine. *J Journal of biochemical and biophysical methods* 1991; 23 (3): 227-236.

Vokounova M., Vacek O., F. Kunc. Degradation of the herbicide bromoxynil in *Pseudomonas putida*. *Folia microbiologica* 1992; 37:122-7.

von Canstein, H.F., Y. Li, Timmis K.N., Deckwer W.-D., and I. Wagner-Döbler. Removal of mercury from chlor-alkali electrolysis wastewater by a mercury-resistant *Pseudomonas putida* strain. *Applied and environmental microbiology* 1999; 65: 5279-5284.

von Canstein, H.F., Y. Li, and I. Wagner-Döbler. Long-term stability of mercury reducing microbial biofilm communities analysed by 16S-23S rDNA interspacer region polymorphism. *Microbial ecology* 2001, 42: 624–634.

von Canstein H.F., S. Kelly, Y. Li, I. Wagner-Döbler. Species Diversity improves efficiency of mercury reducing biofilms under changing environmental conditions. *Applied and environmental microbiology* 2002a; 68: 2829-2837.

von Canstein H.F., Y. Li, A. Felske, I. Wagner-Döbler. Long-term stability of mercury-reducing microbial biofilm communities analyzed by 16s-23s rdna interspacer region polymorphism. *Microbial ecology* 2002b; 42: 624-634.

Wagner-Döbler I., H.F. von Canstein, Y. Li, K.N. Timmis, W.-D. Deckwer. Removal of mercury from chemical wastewater by microorganisms in technical scale. *Environmental science and technology* 2000; 34: 4628–4634.

Wagner-Dobler I. Pilot plant for bioremediation of mercury-containing industrial wastewater. *Applied microbiology and biotechnology* 2003; 62 (2-3):124-33.

Walsh C.T., Distefano M.D., Moore M.J., Shewchuk L.M., G. L. Verdine. Molecular basis of bacterial resistance to organomercurial and inorganic mercuric salts. *The FASEB journal* 1988; 2: 124-130.

Walts A.E. and C. Walsh. Bacterial Organomercury Lyase: Novel Enzymatic Protonolysis of Organostannanes. *Journal of the american chemical society* 1988; 110: 1950-1953.

Wantke F., Demmer C.M., Götz M., R. Jarish. Contact dermatitis from Thiomersal. 2 years experimence with ethylmercuric chloride inpatch testing Thiomersal-sensitive patients. *Contact dermatitis* 1994; 30: 115-117.

Wang Y., Moore M.J., Levinson H.S., Silver S., C.T. Walsh. Nucleotide sequence of a chromosomal mercury resistance determinant from a Bacillus sp. with broad-spectrum mercury resistance. *Journal of bacteriology* 1989; 171: 83-92.

Warne S.E., P. L. deHaseth. Promoter recognition by *Escherichia coli* RNA polymerase. Effects of single base pair deletions and insertions in the spacer DNA separating the -10 and -35 regions are dependent on spacer DNA sequence. *Biochemistry* 1993; 32 (24): 6134-6140.

Weber, J.H. Review of possible paths for abiotic methylation of mercury (II) in the aquatic environment. *Chemosphere* 1993; 26: 2063.

Weber F.J., Isken S., J.A.M. de Bont. Cis/trans isomerization of fatty acids as a defence mechanism of *Pseudomonas putida* strains to toxic concentrations of toluene. *Microbiology* 1994; 140: 2013-2017.

Weisiger R.A., Pinkus L.M., W.B. Jakoby. Thiol S-methyltransfrase: suggested role in detoxification of intestinal hydrogen sulfide. *Biochemical pharmacology* 1980; 29: 2885-2887.

Wekkeli M., Hippmann G., Rosenkranz A.R., Jarisch R., M. Götz. Mercury as a contact allergen. *Contact dermatitis* 1990; 22: 295.

Williams P.A. and K. Murray. Metabolism of benzoate and the methylbenzoates by Pseudomonas putida (arvilla) mt-2: evidence for the existence of a TOL plasmid. *Journal of Bacteriology* 1974; 120: 416–423.

Wilson G.S. The Hazards of Immunization. New York, NY: *The Athlone Press* 1967: 75-84.

Wilson J.R., Leang C., Morby A.P., Hobman J.L., N.L. Brown. MerF is a mercury transport protein: different structures but a common mechanism for mercuric ion transporters? *FEBS Letters* 2000; 472: 78-82.

Wood J.M. and H.K. Wang. Microbial resistance to heavy metals. *Environmental science and technology* 1983: 17: 82a-90a.

World Health Organization. Mercury. Geneva: World Health Organization; *Environmental Health Criteria* 1976: 1.

World Health Organization. Inorganic Mercury. Geneva: World Health Organization; *Environmental Health Criteria* 1991: 118.

World Health Organization. Trace elements and human nutrition and health. Geneva: *World Health Organization*; 1996: 209.

World Health Organization. Methylmercury: Food Additives Series 44. Geneva: *International program on chemical safety* 2000.

Yu H., Mukhopadhyay D. and T.K. Misra. Purification and Characterization of a Novel Organometallic Receptor Protein Regulating the Expression of the Broad Spectrum Mercury-resistant Operon of Plasmid pDU1358. *Journal of biological chemistry* 1994; 269 (22): 15697-15702.

Figures

Table

Symbols and Abbreviations

AAS	Atomic absorption spectroscopie
AFS	Atomic fluorescence spectrometry
bp	Basepairs
C	Concentration ($g \cdot l^{-1}$)
cfu	Colony forming units
CVAAS	Cold-vapor atomic absorption spectrometry
D	Dilution rate
DOT	Dissolved oxygen tension
DMBA	2,2' dimethylbutyric acetate
DMHg	dimethylmercury
DNA	Deoxyribonucleic acid
dNTP	2'-desoxyribonucleoside-5' triphosphat
DtaP	Diphtheria, tetanus, and pertussis vaccine
DSM	Deutsche Sammlung für Microorganism
dTHSA	2,2' dithiosalicylic acid
EDTA	Ethylendiamine tetra acetate
etc.	et cetera, Latin for : and so on
EHg	Ethylmercury
FAD	Flavin adenine dinucleotide
FIAS 200	Flow injection system
× g	Times gravity
GC	Gas chromatography
GEM	Genetically engineered microorganism
GMO	Genetically modified organism
Hg	Mercury
Hg^0	Elemental mercury
Hg^{2+}	Divalent ionic mercury
Hib	Haemophilus influenzae type b bacteria
HPLC	High performance liquid chromatography
ICP	Inductively coupled plasma-mass spectrometry
iVA	iso Valeric acid
iBA	iso Buturic acid

kb	Kilobases
λ	Wavelength lambda
L	Litre
LB	Luria Bertani Medium
M	Molecular mass (g·mol)
M9	minimal medium for Pseudomonad
MHg	Methylmercury
MMHg	Monomethylmercury
MPD	Microwave-induced plasma atomic emission detection
mer	Mercury resistance operon
ms	Mismatch
ν	Kinematic viscosity
NAA	Neutron activation analysis
NADH	Nicotinamide-adenine dinucleotide
NCBI	National Center for Biotechnology Information
NMS	Bacterial medium containing yeast, sucrose and NaCl
OD_{600}	Optical density at 600 nm
ORF	Open reading frame
PA	Pivalic acid
PCR	Polymerase chain reaction
PMA	Phenyl mercuric acetate
PPA	Propylphosphonic acid
ppb	Parts per billion [$\mu g\ L^{-1}$]
ppm	Parts per million [$mg\ L^{-1}$]
Rif	Rifampicin
rpm	Revolution per minute
SCSUP	Sole Carbon Substrate Utilization Profiles
SDS	Sodium Dodecyl Sulfate
SSC	Sodium chloride, sodium citrate
t	Time
t½	Halflife
TAE	Tris-Acetate-EDTA
TBA	Tert-butylacetate
TBPA	Tert-butylphosphonic acid

TE	Tris-EDTA
TH	Thiomersal
THSA	Thiosalicylic acid
Tn5	Transposon 5
U	Velocity
UV	Ultra violet
v/v	Volume per volume
wt	Wildtype
w/v	Weight per volum

Appendix

A. The *mer* gene alignments

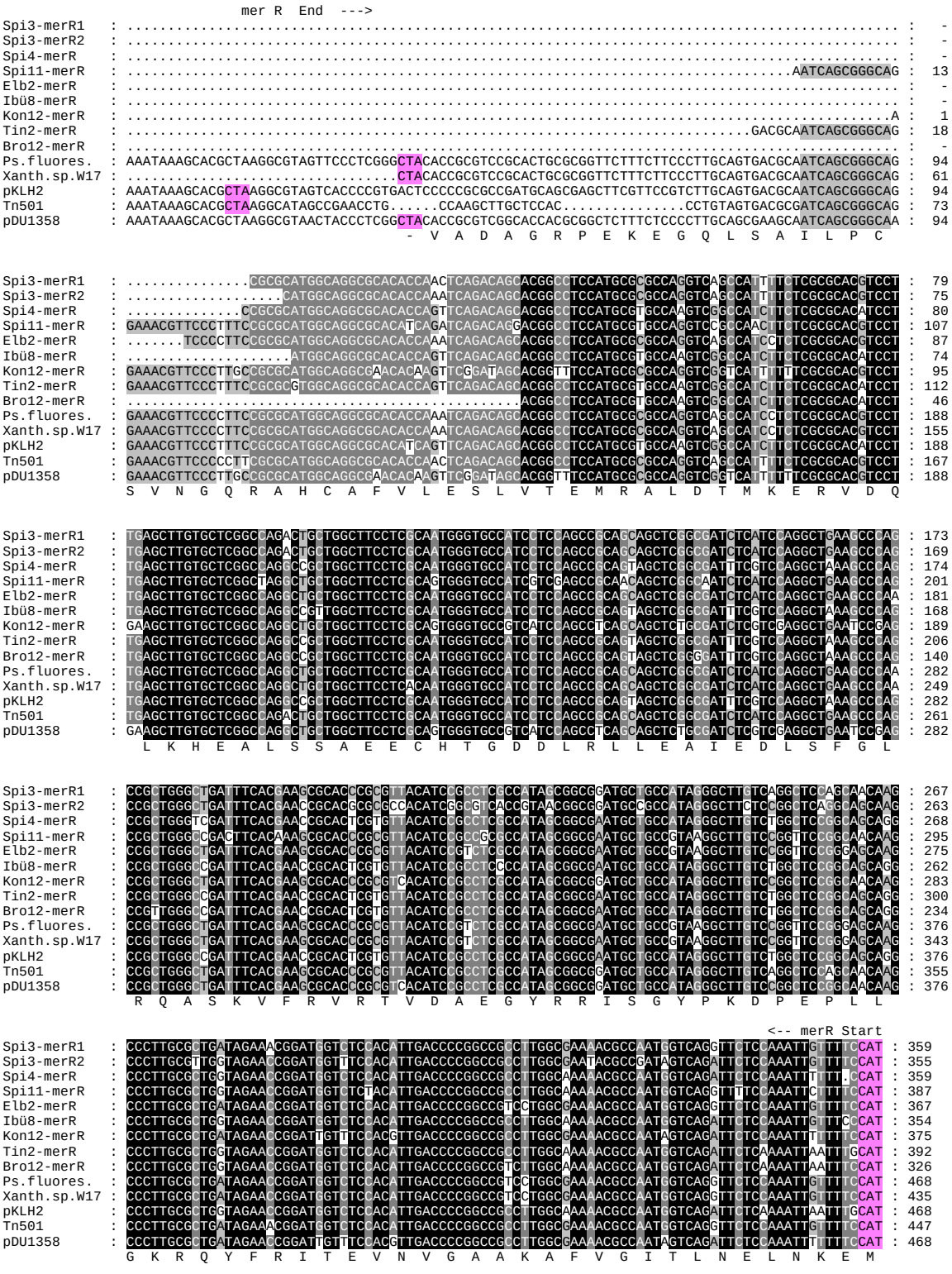

Figure A-1. Alignment of *mer*R from 8 environmental mercury resistant isolates with published genes. The references are *Ps. flourescens*: X73112; *Xanthomonas sp. W17*: Tn5053: L40585; Tn501: *Pseudomonas aeruginosa*: Z00027; Plasmid pKLH2: *Acinetobacter calcoaceticus*: AF213017; Plasmid pDU1358: *Serratia marcescens*: M24940. The amino acid sequence of Plasmid pDU1358 is shown as standard single letter below the DNA sequence line. The stop codon is represented as (-). Black shade: 100% similarity; gray: 80% similarity; light gray 60% similarity.

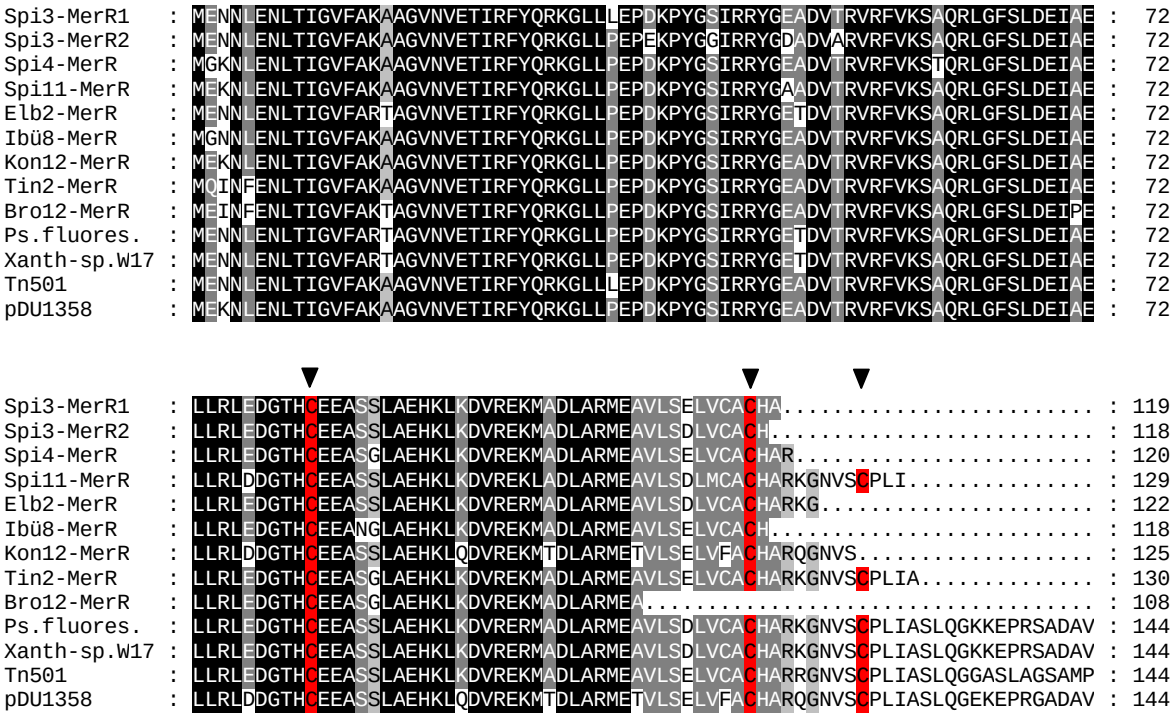

Figure A-2. Alignment of the MerR protein of the 9 environmental isolates with published MerR proteins. References are Plasmid *Ps. flourescens*: X73112; *Xanthomonas sp. W17*: Tn5053: L40585; Tn501: *Pseudomonas aeruginosa*: Z00027; Plasmid pKLH2: *Acinetobacter calcoaceticus*: AF213017; Plasmid pDU1358: *Serratia marcescens*: M24940. The highly conserved cysteines residues (Cys82, Cys117 and Cys126) are red marked. By the use of primer R3 approximately 24 bp of the end of MerR proteins were not sequenced. Black shade: 100% similarity; Gray: 80% similarity; Light gray 60% similarity.

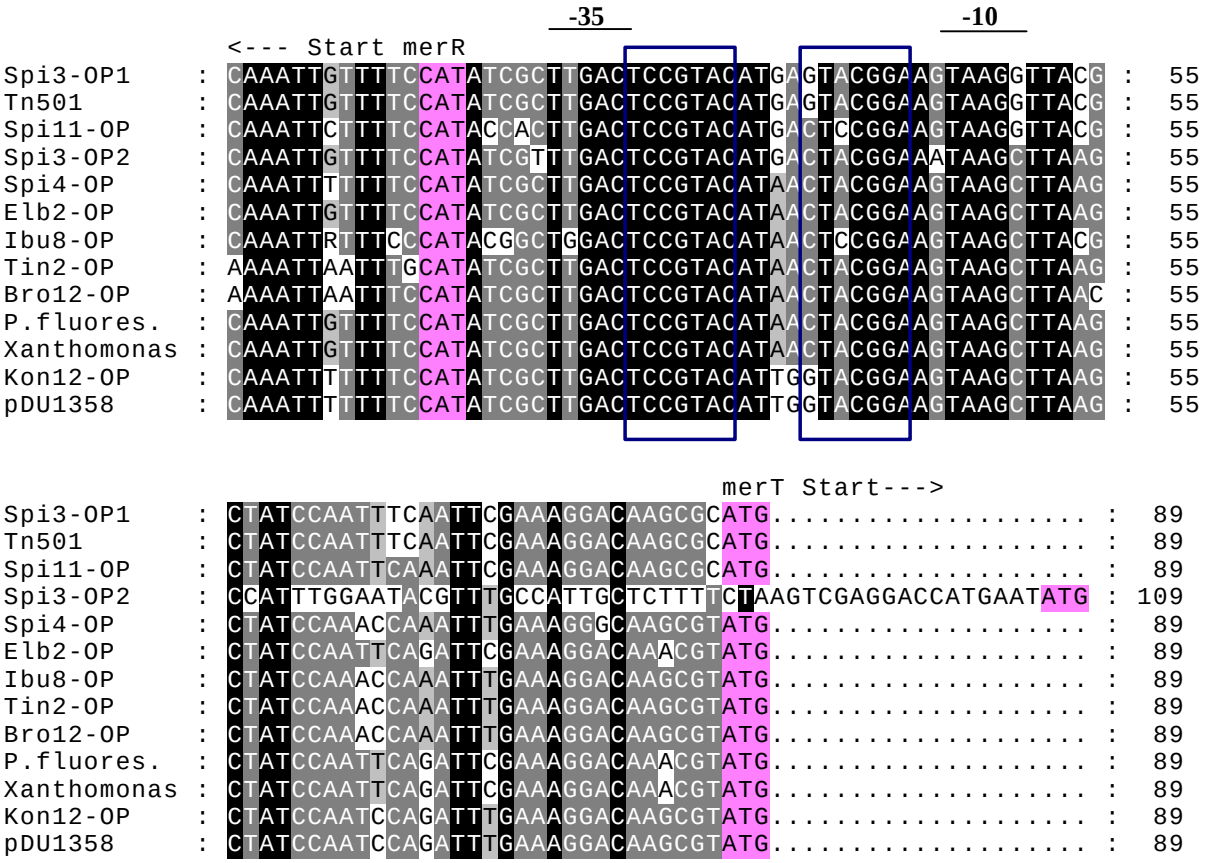

Figure A-3. Alignment of the *mer*O/P amino acid sequence of the 9 environmental isolates with published MerO/P sequence. References are Plasmid *Ps. flourescens*: X73112; *Xanthomonas sp. W17*: Tn5053: L40585; Tn501: *Pseudomonas aeruginosa*: Z00027; Plasmid pDU1358: *Serratia marcescens*: M24940. Regions with similarity to the consensus -35 and -10 recognition elements for RNA polymerase are lined above the nucleotide sequences, and elements of dyad symmetry (conserved GTAC: TCC**GTAC**....**GTAC**GGA) are boxed. Black shade: 100% similarity; Gray: 80% similarity; Light gray 60% similarity.

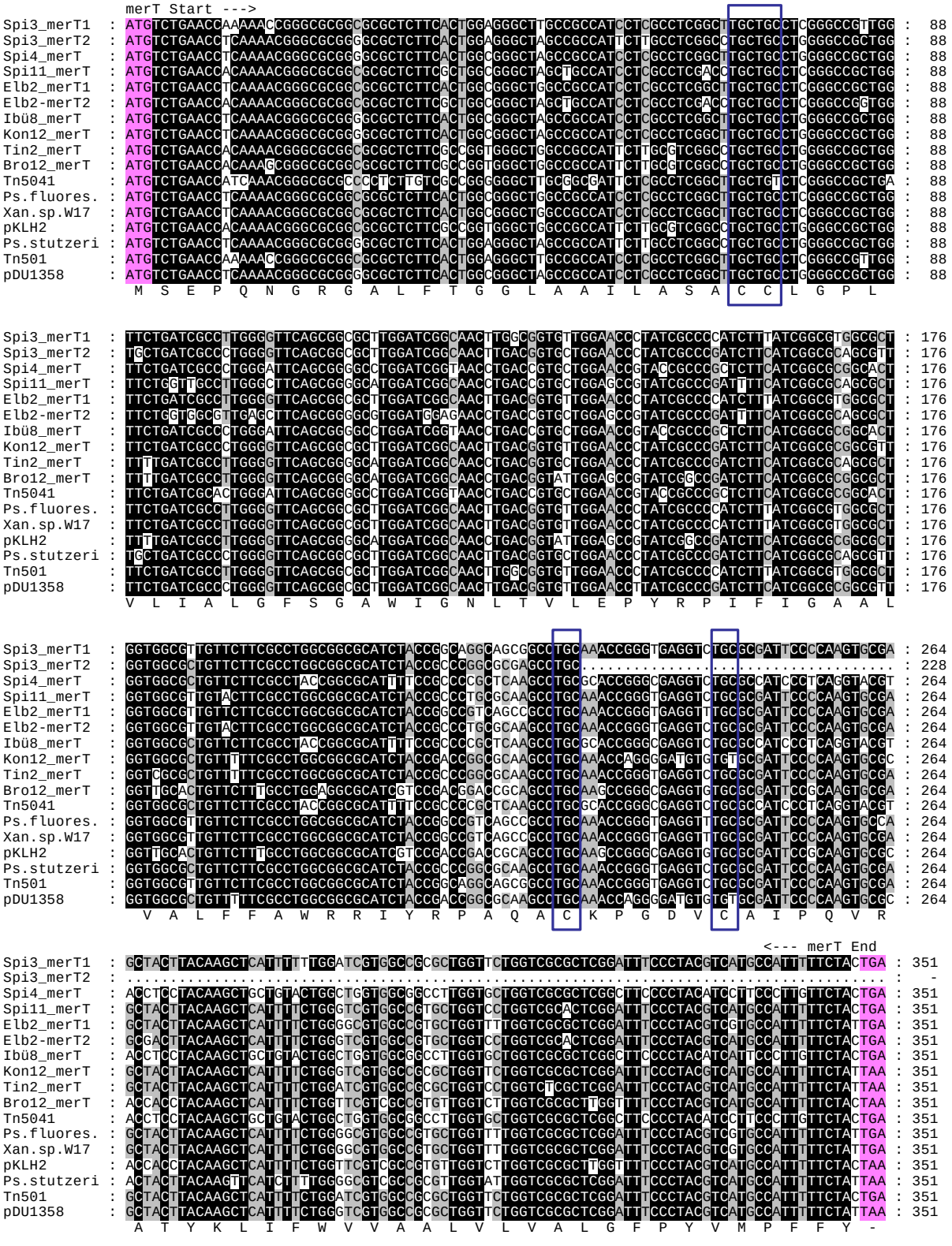

Figure A-4. Alignment of the *mer*T genes of the 8 environmental isolates and published *mer*T genes. The references are *Pseudomonas sp.*: Tn5041: X98999; *Ps. fluorescens*: X73112; *Xanthomonas sp. W17*: Tn5053: L40585; Tn501: *Pseudomonas aeruginosa*: Z00027; Plasmid pKLH2: *Acinetobacter calcoaceticus*: AF213017; Plasmid pDU1358: *Serratia marcescens*: M24940. Amino acid sequence of Plasmid pDU1358 polypeptide is shown as standard single letter below the DNA sequence line. The conserved cysteine residues are boxed. The stop codon is represented as (-). Black shade: 100% similarity; Gray: 80% similarity; Light gray 60% similarity. Start and stop codon are colored pink.

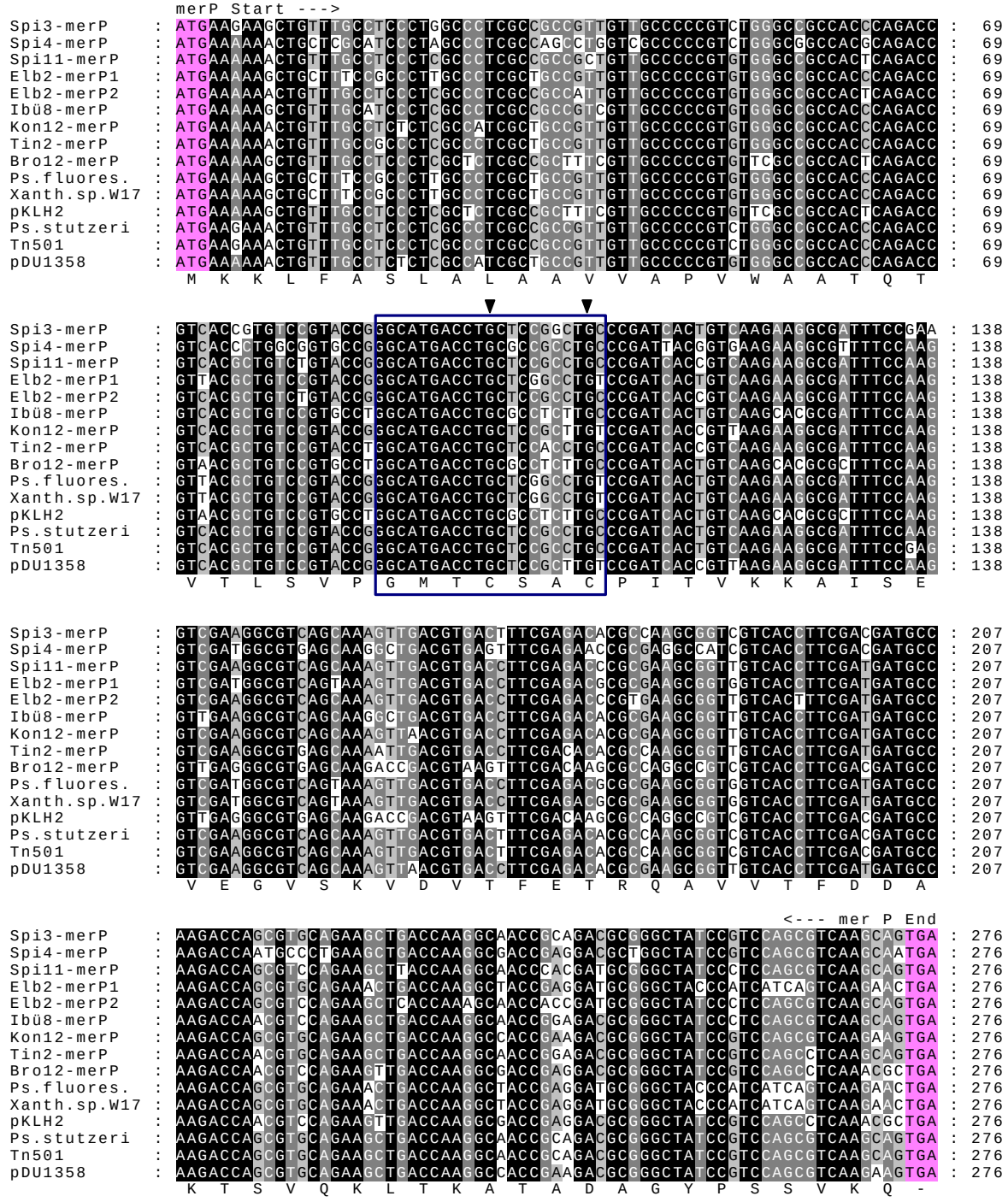

Figure A-5. Alignment of the *mer*P genes of the 8 environmental isolates and published *mer*P genes. The references are *Ps. fluorescens*: X73112; *Xanthomonas sp. W17*: Tn5053: L40585; Tn501: *Pseudomonas aeruginosa*: Z00027; Plasmid pKLH2: *Acinetobacter calcoaceticus*: AF213017; Plasmid pDU1358: *Serratia marcescens*: M24940. Amino acid sequence of Tn501 polypeptide is shown as standard single letter below the DNA sequence line. The stop codon is represented as (-). The two cysteine residues are marked with arrows and the metal binding motif GMTCxxC is boxed. Black shade: 100% similarity; Gray: 80% similarity; Light gray 60% similarity. Start and stop codon are colored pink.

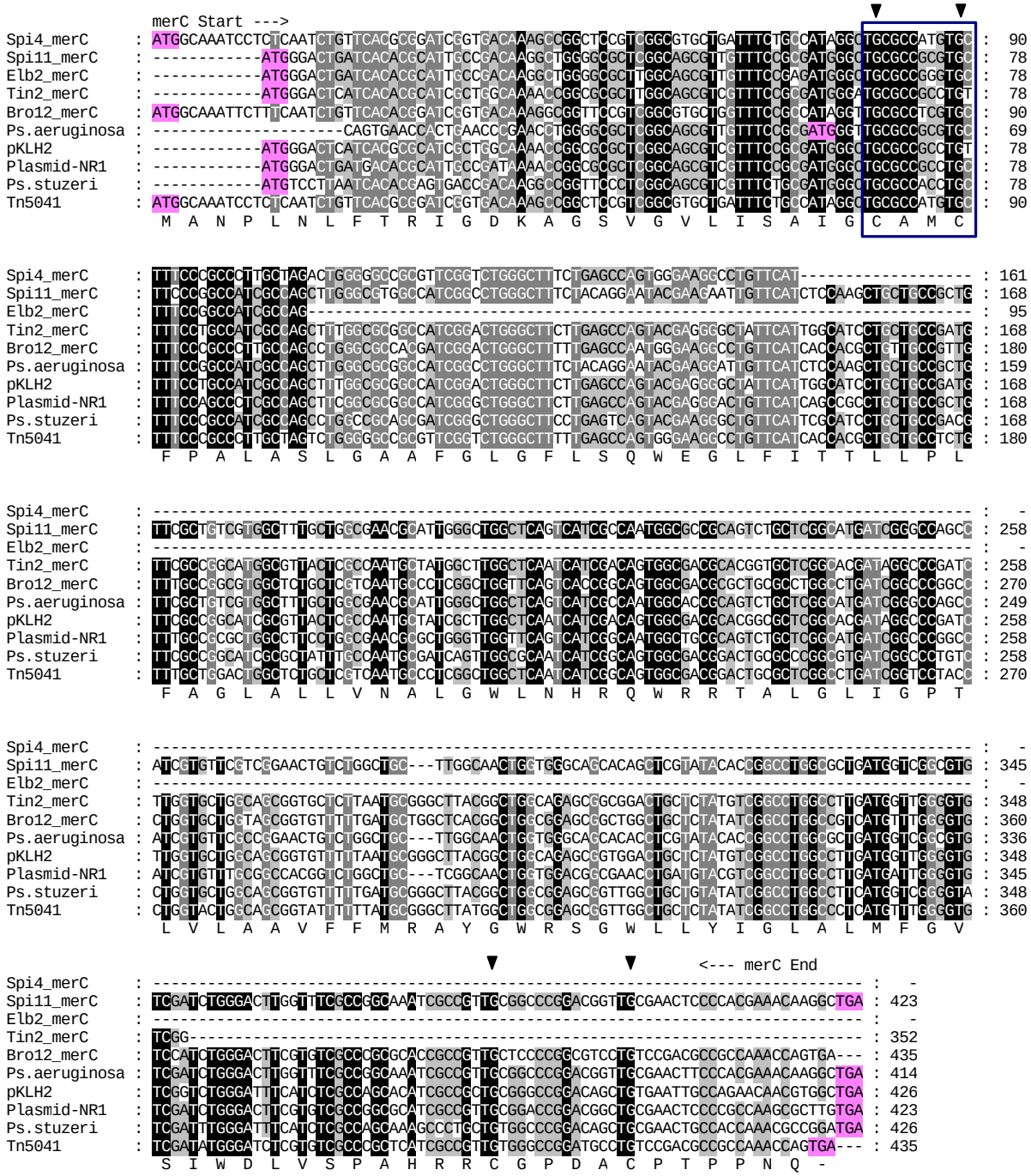

Figure A-6. Alignment of the *mer*C genes of the 5 isolates and published *mer*C genes. The references are *Pseudomonas sp.*: Tn5041: X98999; Plasmid pKLH2: *Pseudomonas sp.*: Tn5041: X98999; *Ps. stutzeri*: plasmid pPB: U90263; Plasmid pKLH2: *Acinetobacter calcoaceticus*: AF213017; Ps. aeruginosa: AF120971. Amino acid sequence of Tn5041 polypeptide is shown as standard single letter below the DNA sequence line. The four cysteine residues are marked with arrows above sequences and the typical metal binding motif (CxxC) on the N-termini of MerC is boxed. The stop codon is represented as (-). Black shade: 100% similarity; Gray: 80% similarity; Light gray 60% similarity. Start and stop codon are colored pink.

A.

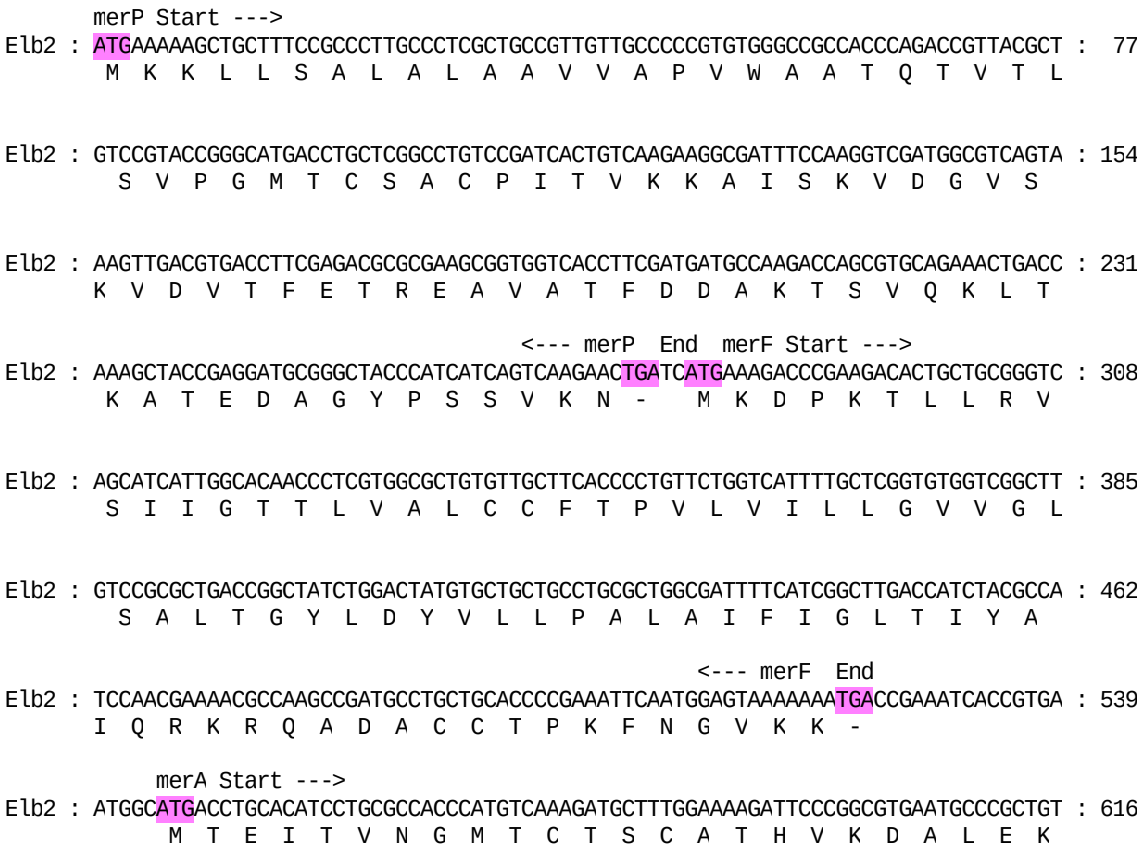

B.

Figure A-7. Nucleotide sequence of 246 bp of *Ps. putida* Elb2 narrow spectrum mercury resistance gene cluster. A: The region includes the genes *mer*P, *mer*F and 5' end of *mer*A gene. B: Alignment of merF and 24 bp sequence of merP with published nucleotide sequence of Tn5053 from *Xanthomonas sp.* W17: AAA98325. Start and stop codons are colored in pink and the predicted polypeptide (aa) sequences are shown. Stop codon is represented as (-).

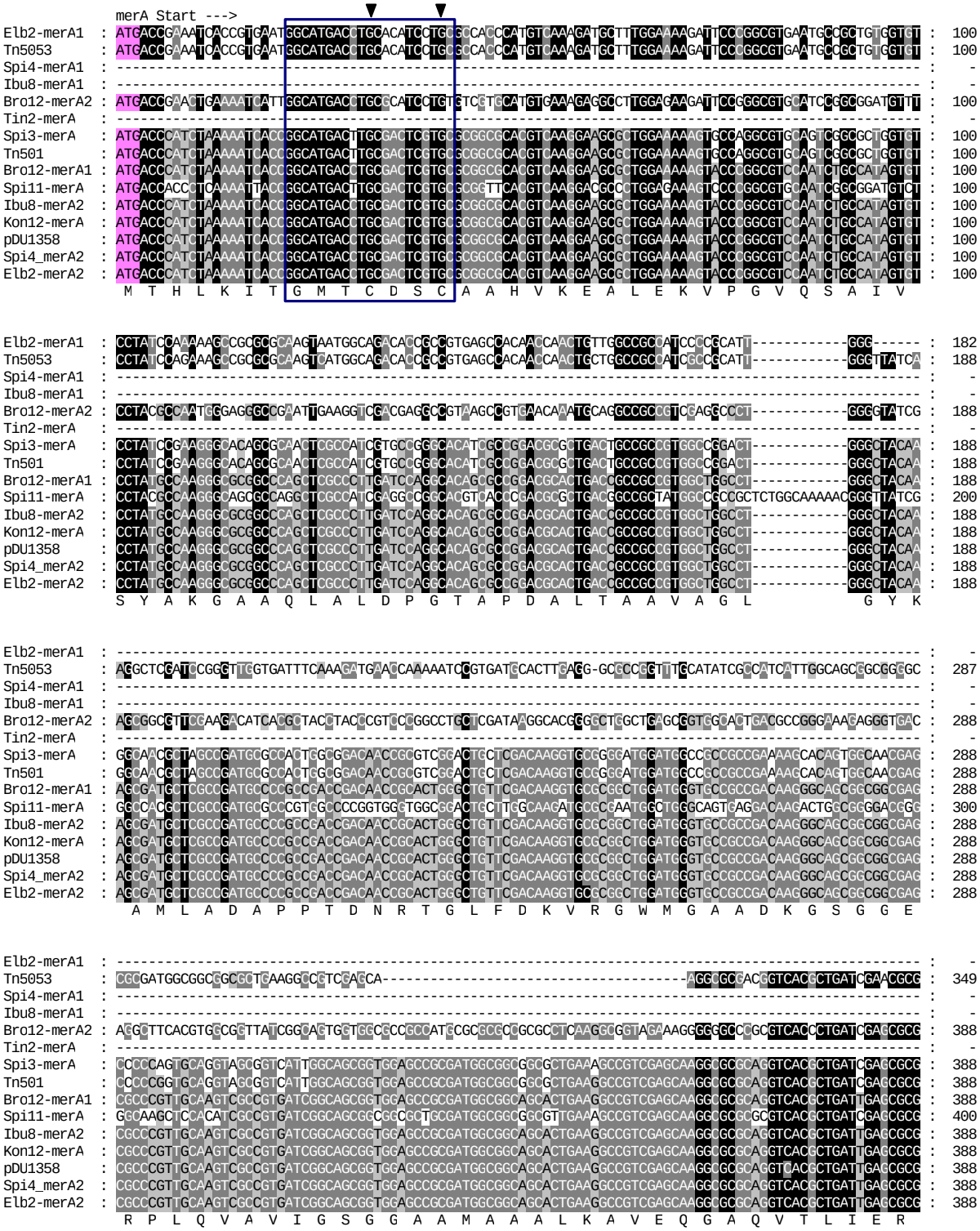

Figure A-8a. Alignment of the *mer*A genes of the eight environmental isolates and published *mer*A genes. The references are Plasmid pDU1358: *Serratia marcescens*: M24940; *Xanthomonas sp. W17*: Tn5053: L40585; Transposon Tn501: *Pseudomonas aeruginosa* plasmid pVS1: Z00027. Spi4-merA1, Ibu8-merA1, Tin2-merA, Ibu8-merA2 and Bro12-merA1 are only partly sequenced. Amino acid sequence of pDU135 polypeptide (accession no. M15049, Z49200 and M24940) is shown as standard single letter below the DNA sequence line. The metal bind motif (GMTCxxC) with two cysteine residues (Cys11 and Cys 14) is boxed. Black shade: 100% similarity; Gray: 80% similarity; Light gray 60% similarity. Start and stop codon are colored pink.

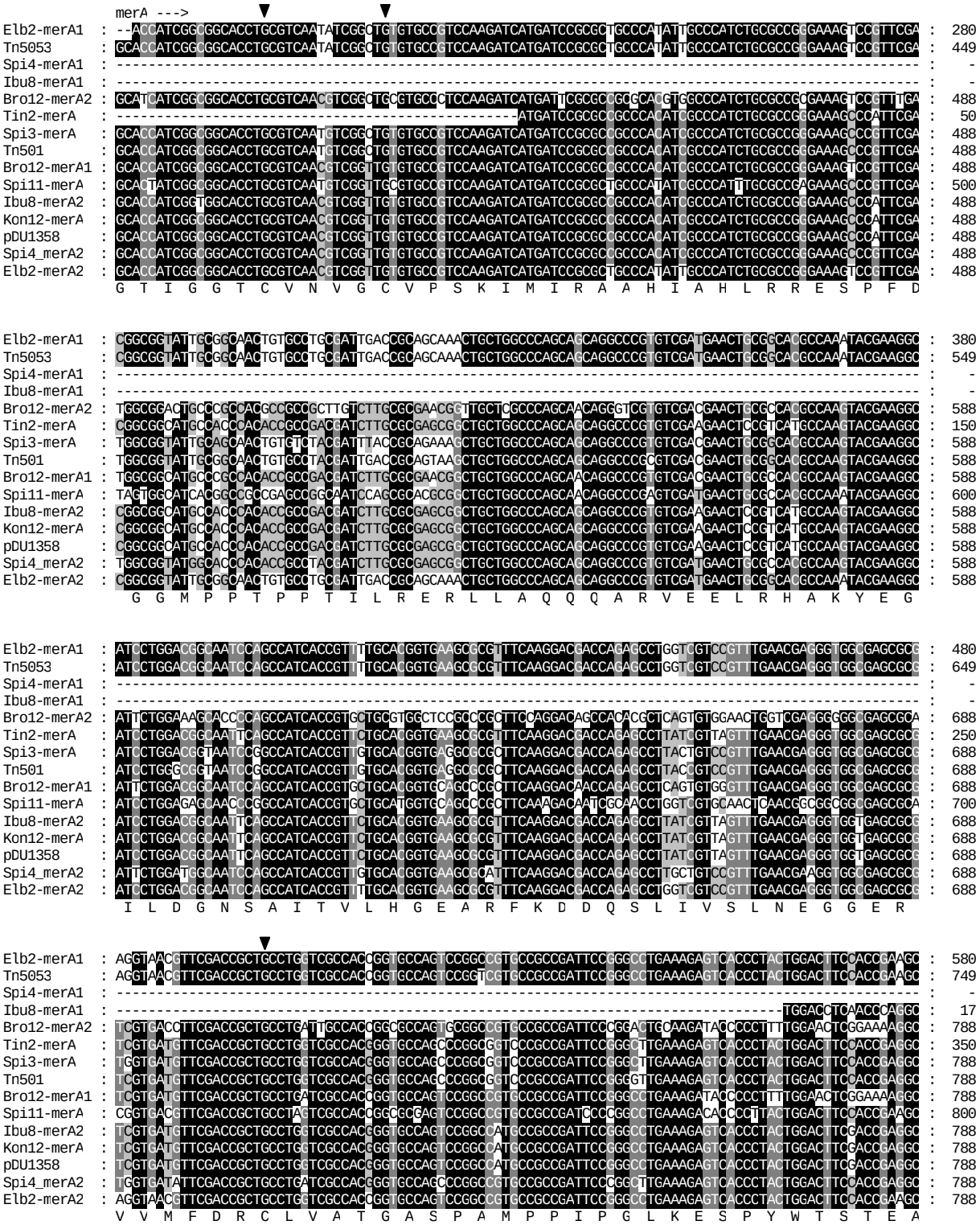

Figure A-8b. Continuation of *mer*A sequence alignment from environmental isolates and published genes (389 bp-788 bp numbering from pDU1358). The isolates Spi4-merA1, Ibu8-merA1 and Tin2 are partly sequenced. The cysteine residues are marked with arrows above sequences.

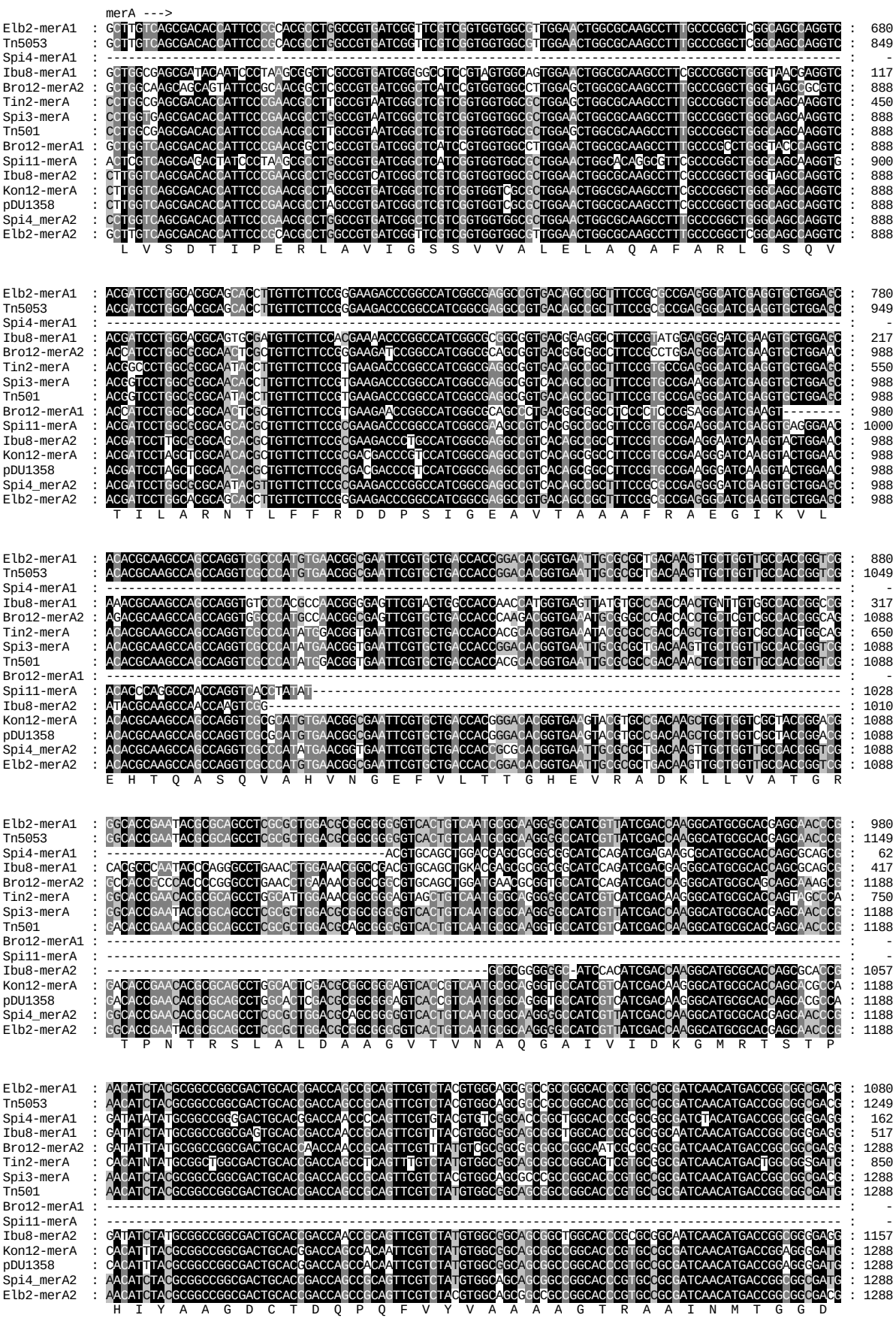

Figure A-8c. Continuation of *mer*A sequence alignment from environmental isolates and published genes (789 bp- 1288 bp from pDU1358). The isolates Spi4-merA1, Bro12-merA1, Spi11-merA and Ibu8-merA2 are partly sequenced.

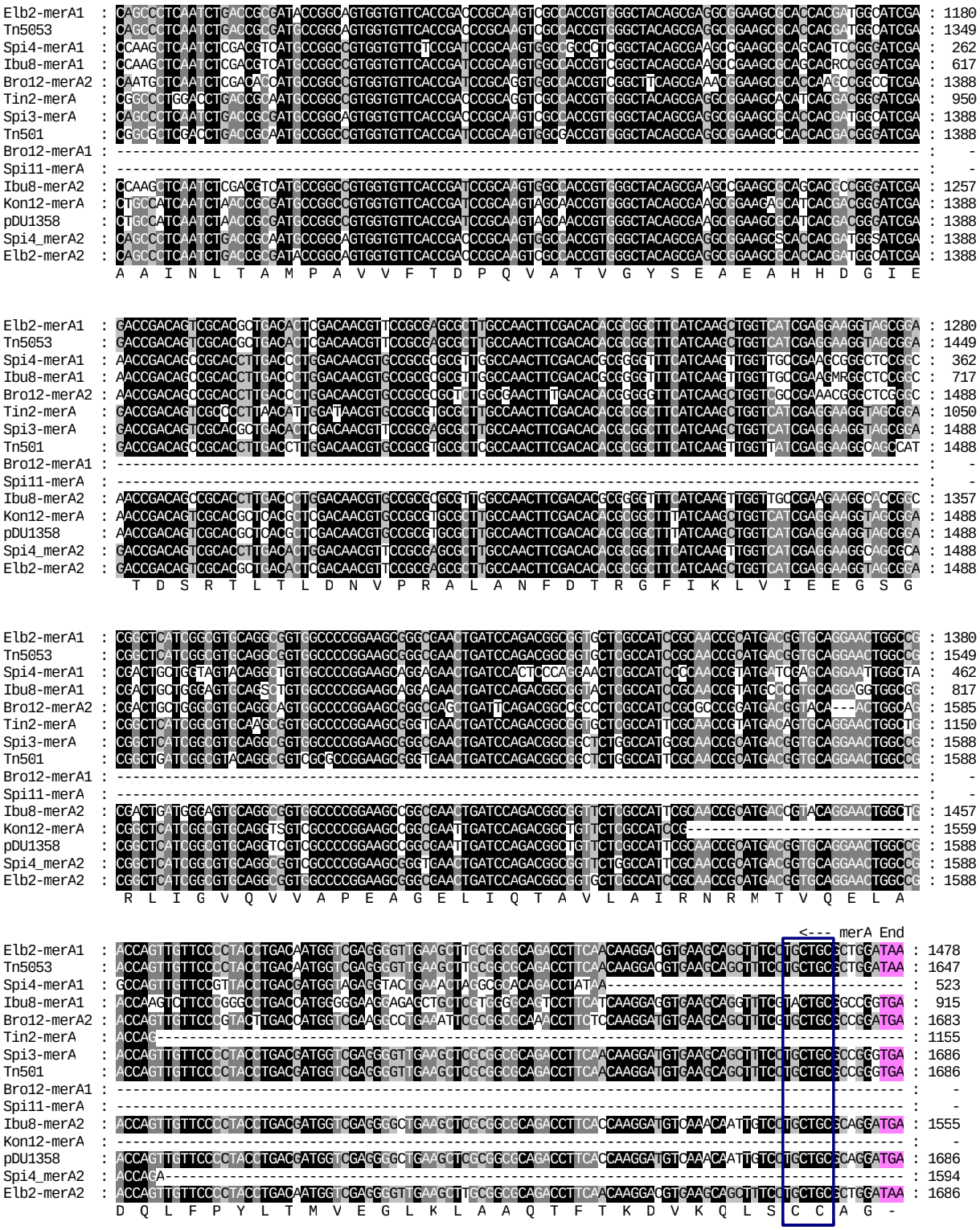

Figure A-8d. Continuation of *mer*A sequence alignment from environmental isolates and published genes (1289 bp -1686 bp). Stop codon is colored pink. By the use of primer A9 and A5 the end of *mer*A gene from Spi4-merA1, Tin2-merA, Kon12-merA and Spi4-merA2 were not sequenced. The two conserved Cysteine residues (Cys558 and Cys559) are boxed.

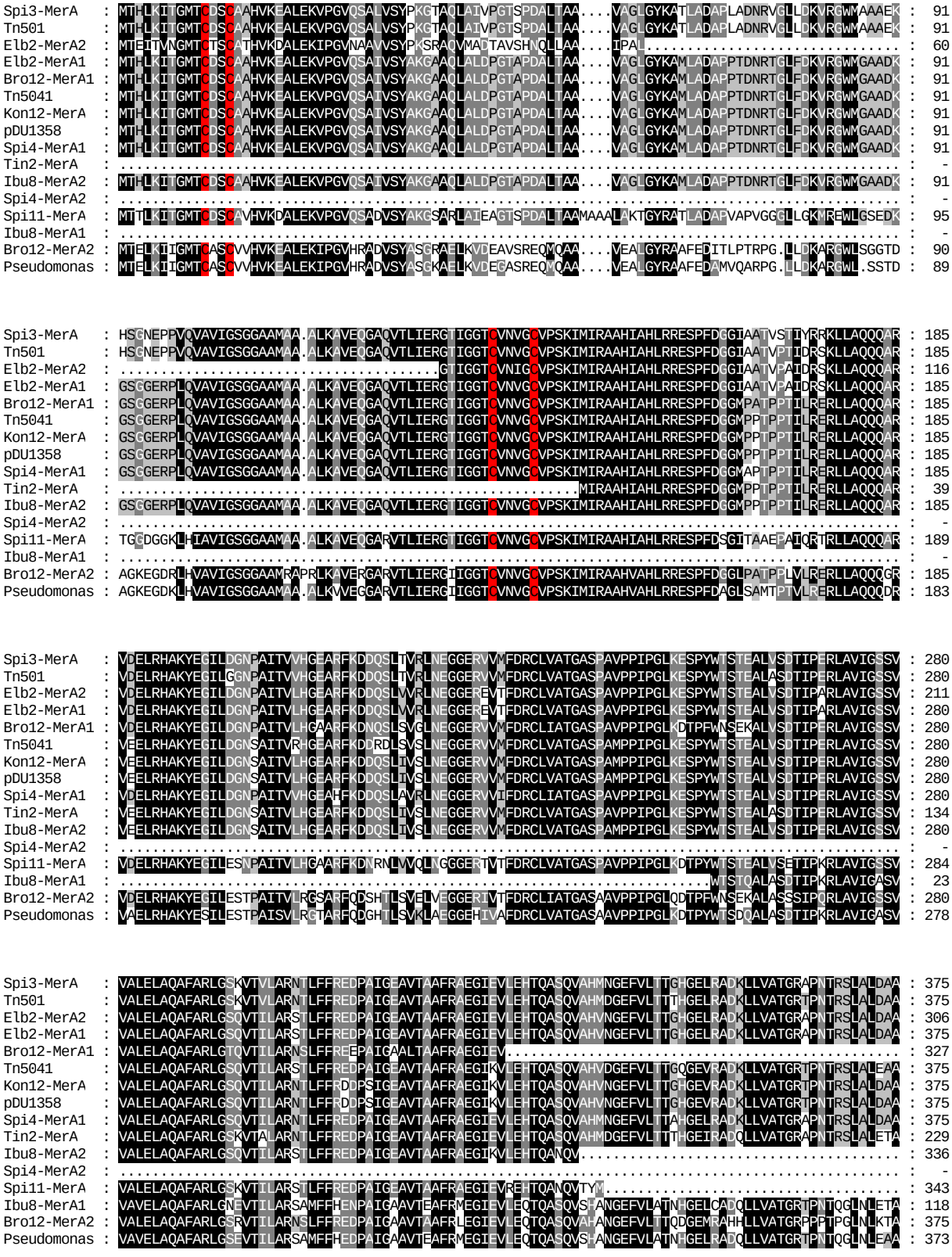

Figure A-9a. Alignment of the MerA protein sequence of all eight isolates and published MerA proteins. The references are Plasmid pDU1358: *Serratia marcescens*: P08662; Tn501: *Pseudomonas aeruginosa*: P08332; and *Pseudomonas sp.* KHP41: CAA67451. The cysteines residues (Cys10-Cys13; Cys135-Cys140 and Cys558-Cys559) are marked red. The Gaps in protein sequence of Elb2-MerA2, Tin2-MerA, Bro12-MerA1, Spi4-MerA2, Spi11-MerA and Ibu8-MerA1 are only partly sequencing. Black shade: 100% similarity; Gray: 80% similarity; Light gray 60% similarity.

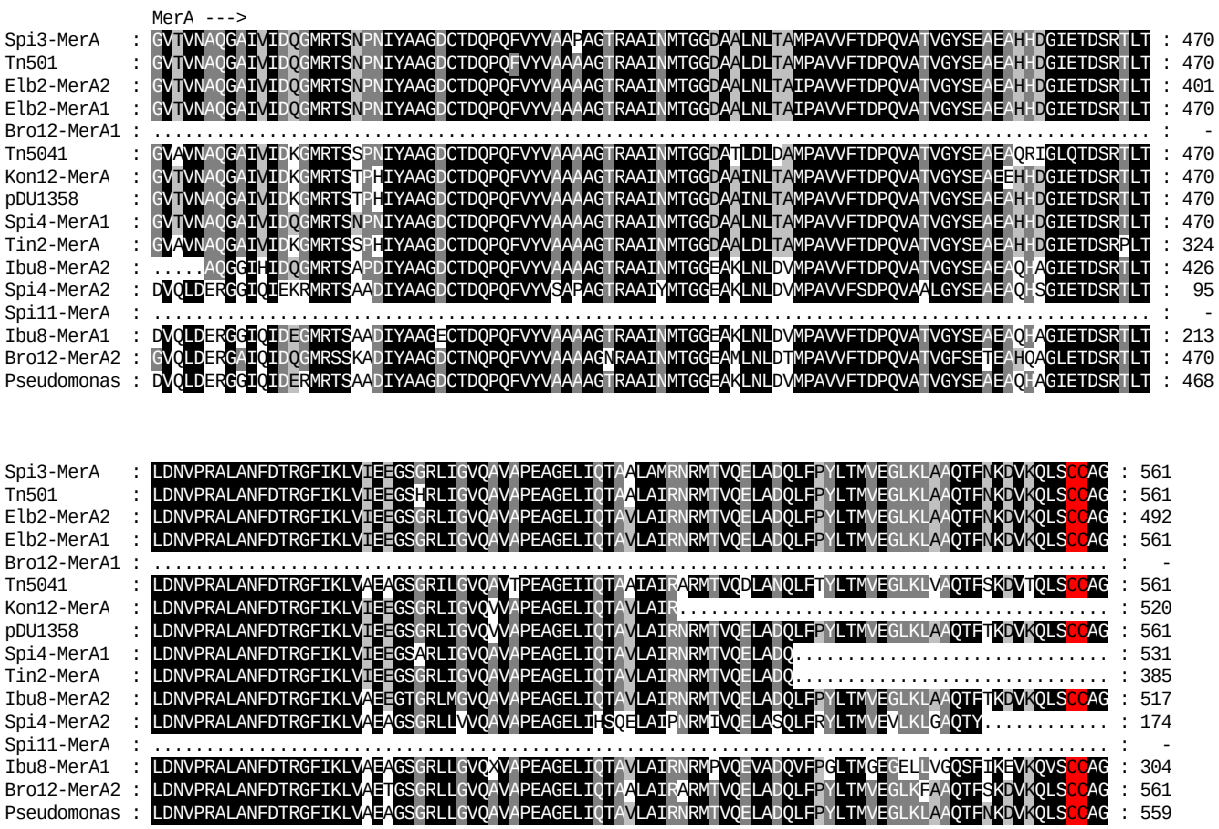

Figure A-9b. Continuing the Alignment of the MerA protein of all eight isolates and published MerA proteins. The Gaps in protein sequence of Elb2-MerA2, Tin2-MerA, Bro12-MerA1, Kon12-Mer-A, Spi4-MerA1 and Spi4-MerA2 are due to incomplete sequencing. Black shade: 100% similarity; Gray: 80% similarity; Light gray 60% similarity. The cysteine residues (Cys10-Cys13; Cys135-Cys140 and Cys558-Cys559) are marked red.

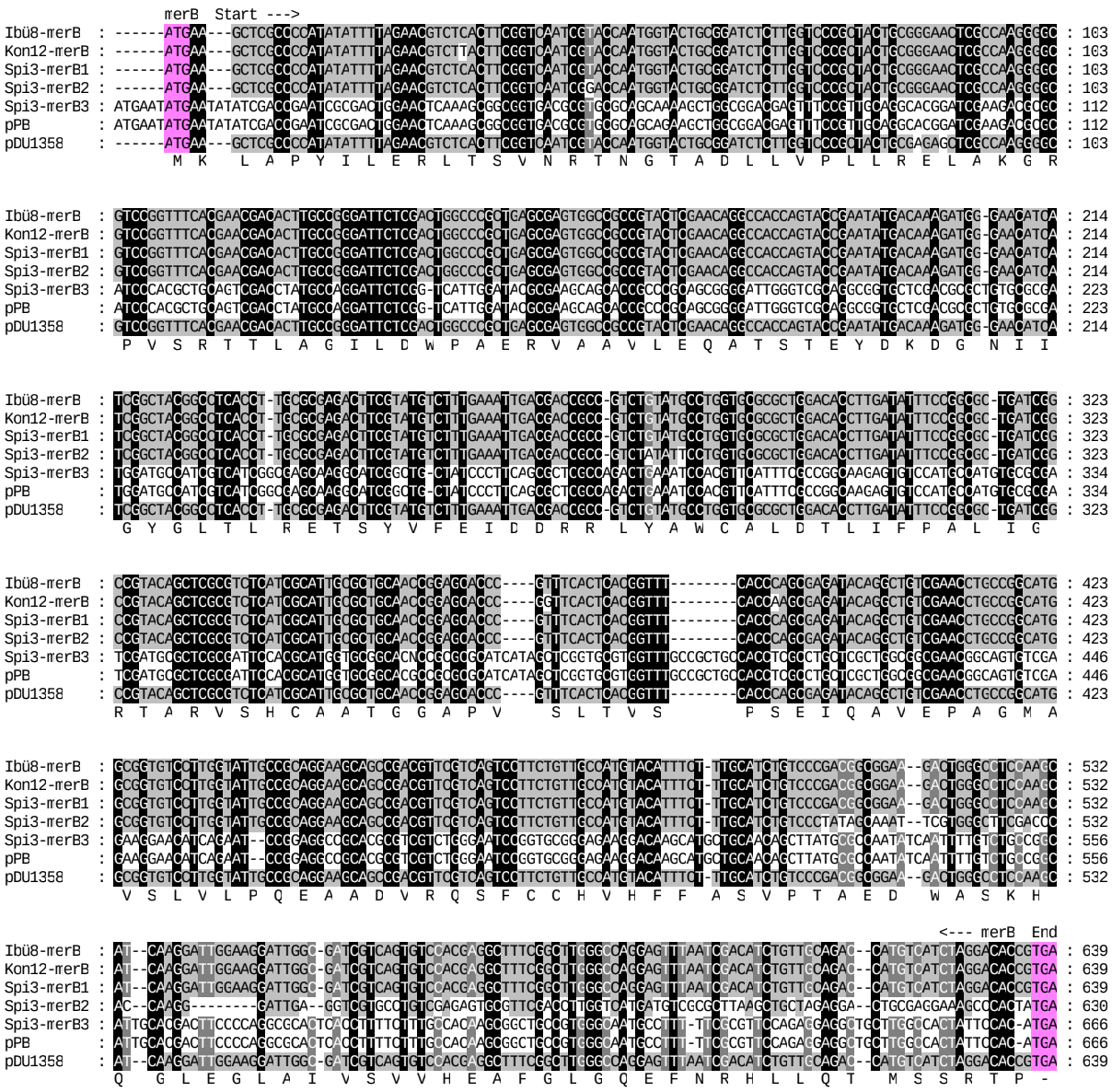

Figure A-10. Alignment of the *mer*B genes of three environmental isolates (Ibü8, Kon12 and Spi3) and published *mer*B genes. The references are Plasmid pDU1358: *Serratia marcescens*: M15049; Plasmid pPB: *Ps. stutzeri*: *mer*RBT: U90263. Amino acid sequence of Plasmid pDU1358 polypeptide is shown as standard single letter below the DNA sequence line. The stop codon is represented as (–). Black shade: 100% similarity; Gray: 80% similarity; Light gray 60% similarity. Start and stop codon are colored pink.

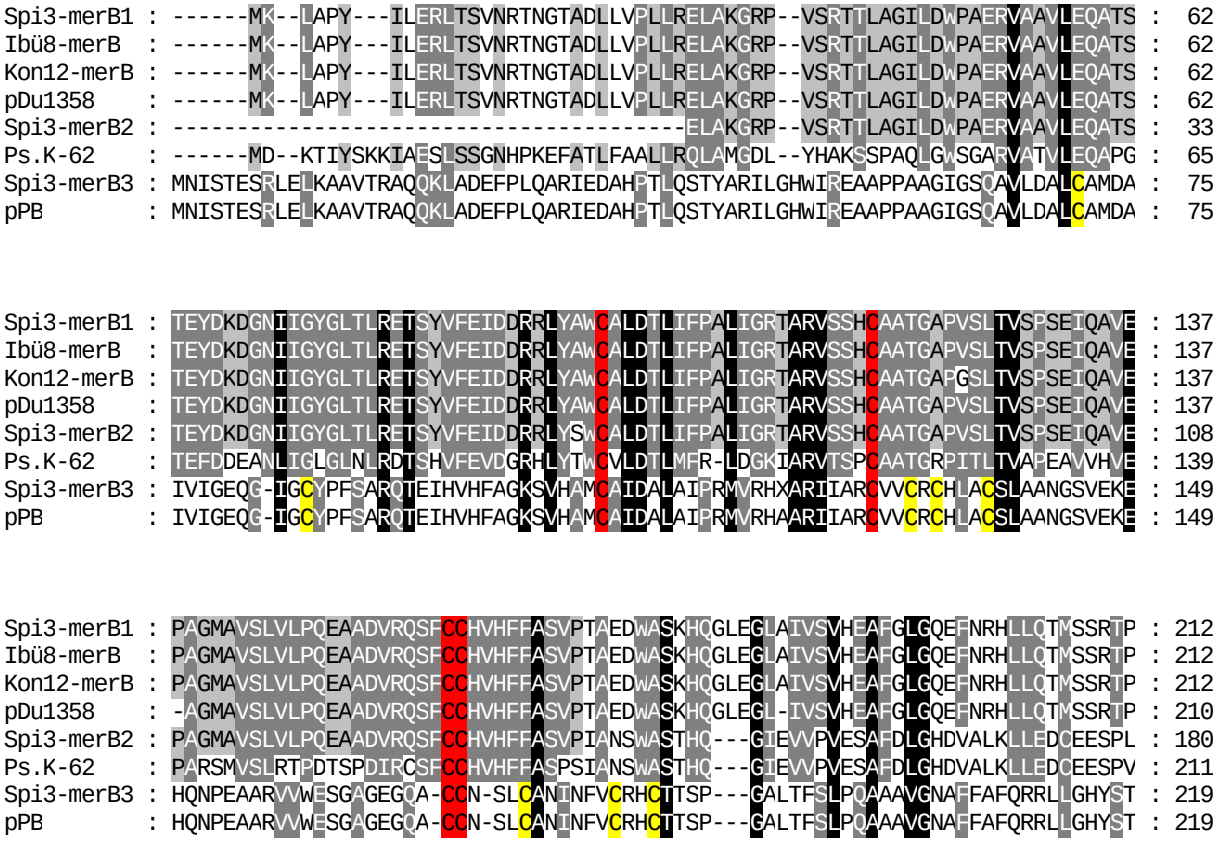

Figure A-11. Alignment of the MerB protein of three isolates possessing MerB and published MerB proteins. References are Plasmid pDU1358: *Serratia marcescens*: P08662; *Pseudomonas K-62 plasmid pMR26*: BAA20338; and plasmid pPB: *Pseudomonas stutzeri*: AAC38230. The highly conserved cysteines residues (Cys96, Cys117, Cys159 and Cys160) are red marked. MerB proteins of plasmid pPB and Spi3 have eight further cysteine residues (Cys71, Cys84, Cys131, Cys133, Cys137, Cys172, Cys179 and Cys182, referring to plasmid pPB) which are yellow marked. Black shade: 100% similarity; Gray: 80% similarity; Light gray 60% similarity.

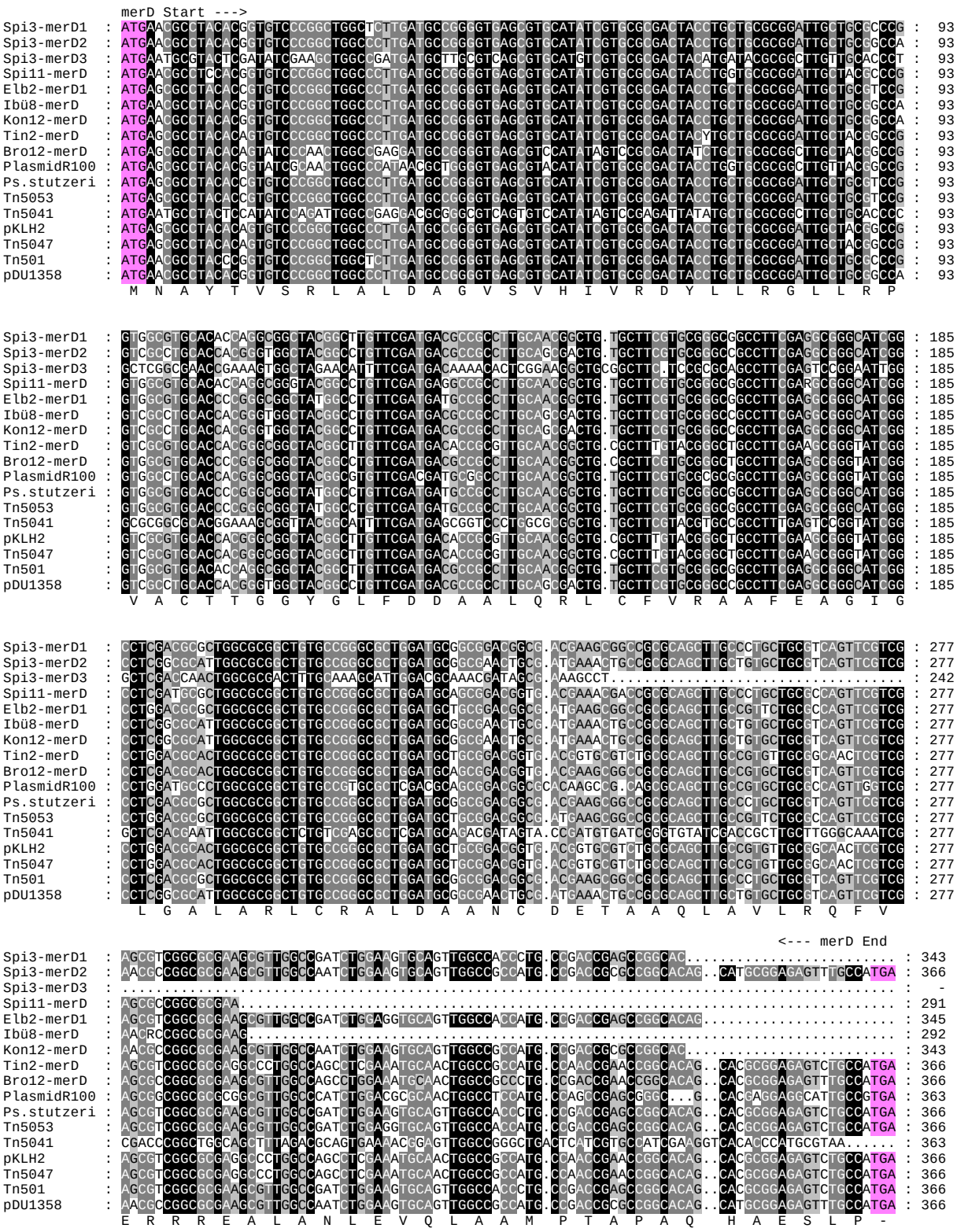

Figure A-12. Alignment of the *mer*D genes of environmental isolates and published *mer*D genes. References are *Pseudomonas sp.*: Tn5041: X98999; *Ps. fluorescens*: X73112; *Xanthomonas sp. W17*: Tn5053: L40585; Tn501: *Pseudomonas aeruginosa*: Z00027; Plasmid pKLH2: *Acinetobacter calcoaceticus*: AF213017; Plasmid pDU1358: *Serratia marcescens*: M15049; *Acinetobacter calcoaceticus* KHW14: Tn5047. Spi3-merD1 and D3 als well as Spi11, Ibu8 and Kon12 are partly sequenced. Amino acid sequence of Plasmid pDU1358 polypeptide is shown as standard single letter below the DNA sequence line. Black shade: 100% similarity; Gray: 80% similarity; Light gray 60% similarity. Start and stop codon are colored pink.

B. Position of Specific *mer* Gene Primers

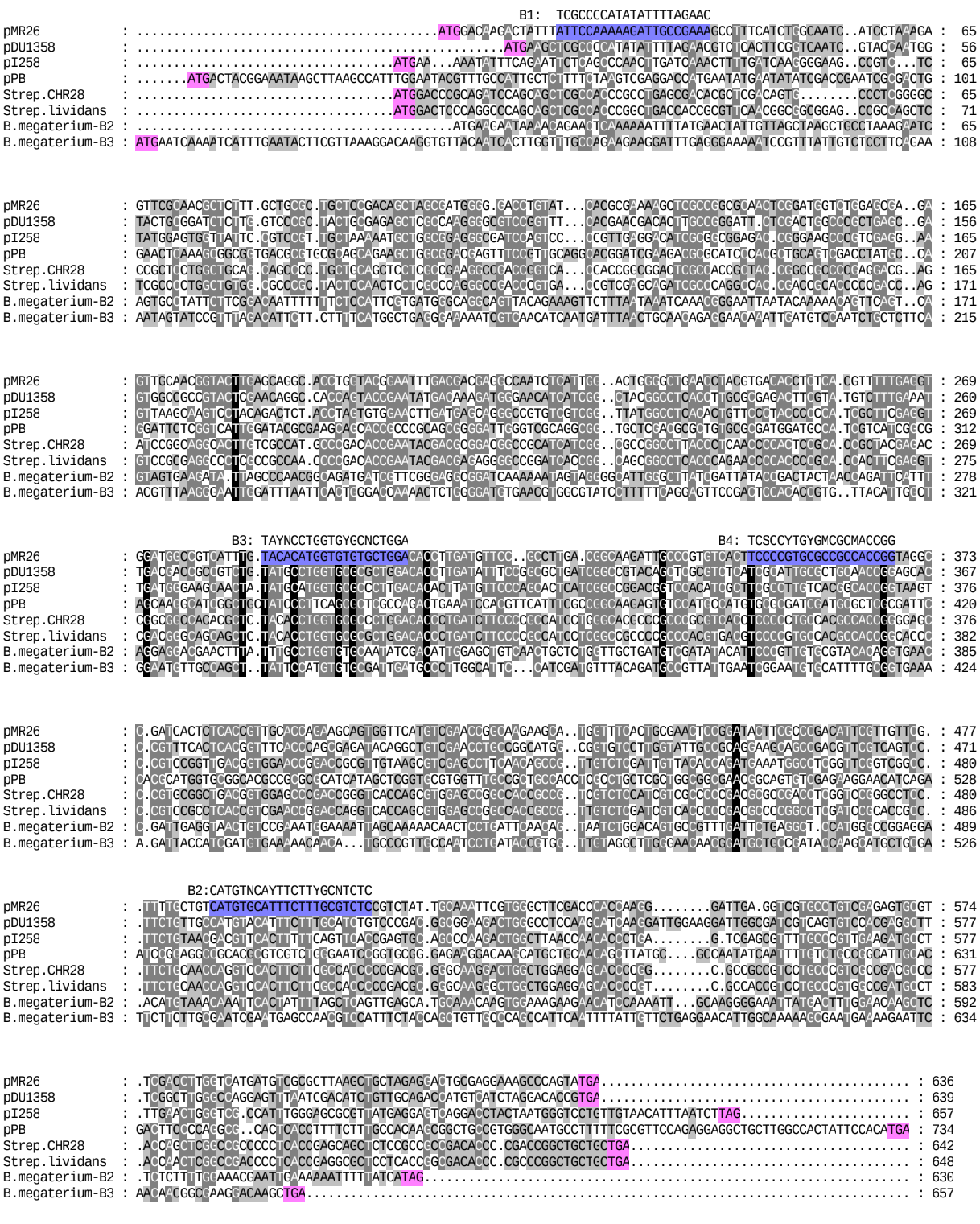

Figure B-13. Alignment of the published *mer*B sequences with specific primers. The primers (forward primer: B1 and B3; reverse primer: B2 and B4) are colored in green. Plasmid pDU1358: *Serratia marcescens*: M24940; Plasmid pMR26: *Pseudomonas sp.* K62: MerB$_2$: AB013925; Plasmid pPB: *Ps. stutzeri*: *mer*RBT: U90263; Plasmid pRJ28: *Streptomyces sp.* CHR28: AF222792; *Strep. lividans*: X65467; *Bacillus megaterium*: *mer*B2: AB027307; *Bacillus megaterium*: *mer*B3: AB027306. Black shade: 100% similarity; Gray: 80% similarity; Light gray 60% similarity. Start and stop codon are colored pink.

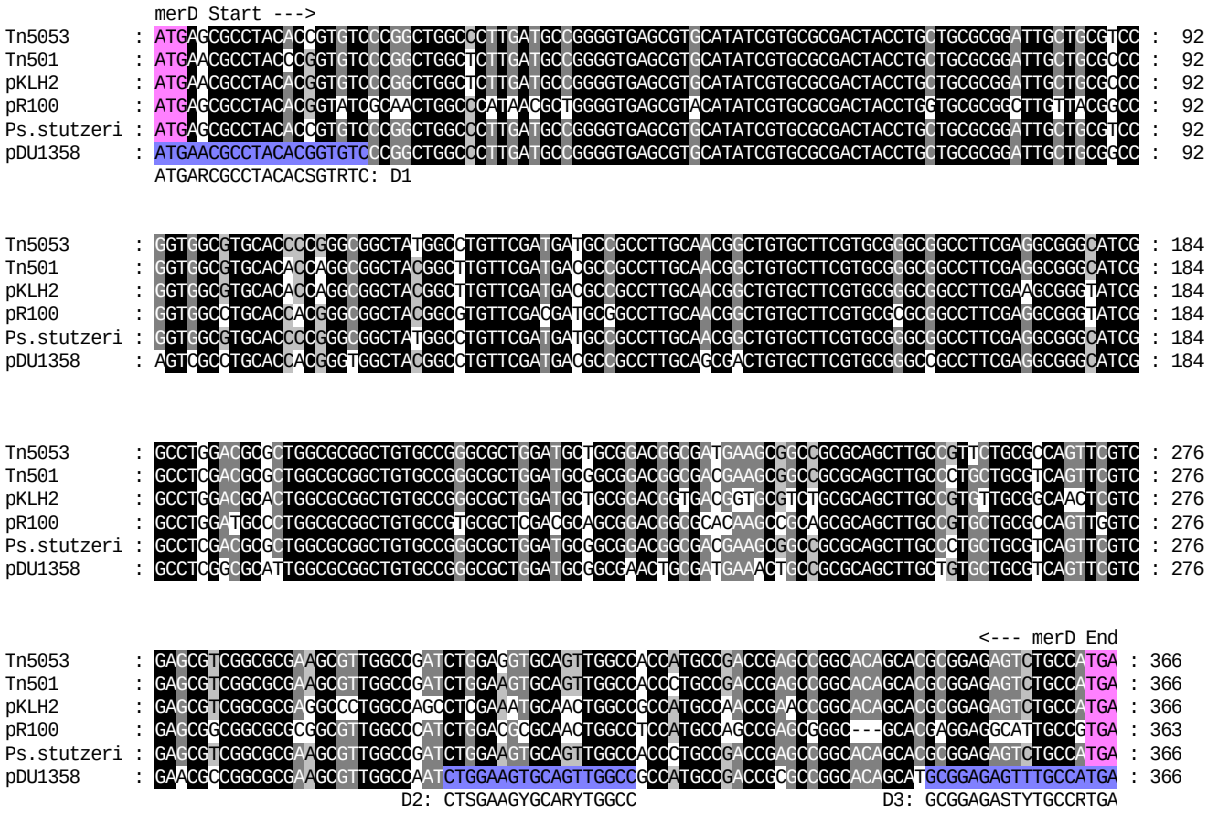

Figure B-14. Alignment of the published *mer*D sequences with specific primers. The primers (forward primer: D1; reverse primer: D2 and D3) are colored in blue. Plasmid pDU1358: *Serratia marcescens*: M24940; Plasmid pPB: *Ps. stutzeri*: *mer*RBT: U90263; *Xanthomonas sp. W17*: Tn5053: L40585; Tn501: *Pseudomonas aeruginosa*: Z00027; Plasmid pKLH2: *Acinetobacter calcoaceticus*: AF213017; Plasmid R100: NC002134. Black shade: 100% similarity; Gray: 80% similarity; Light gray 60% similarity. Start and stop codon are colored pink.

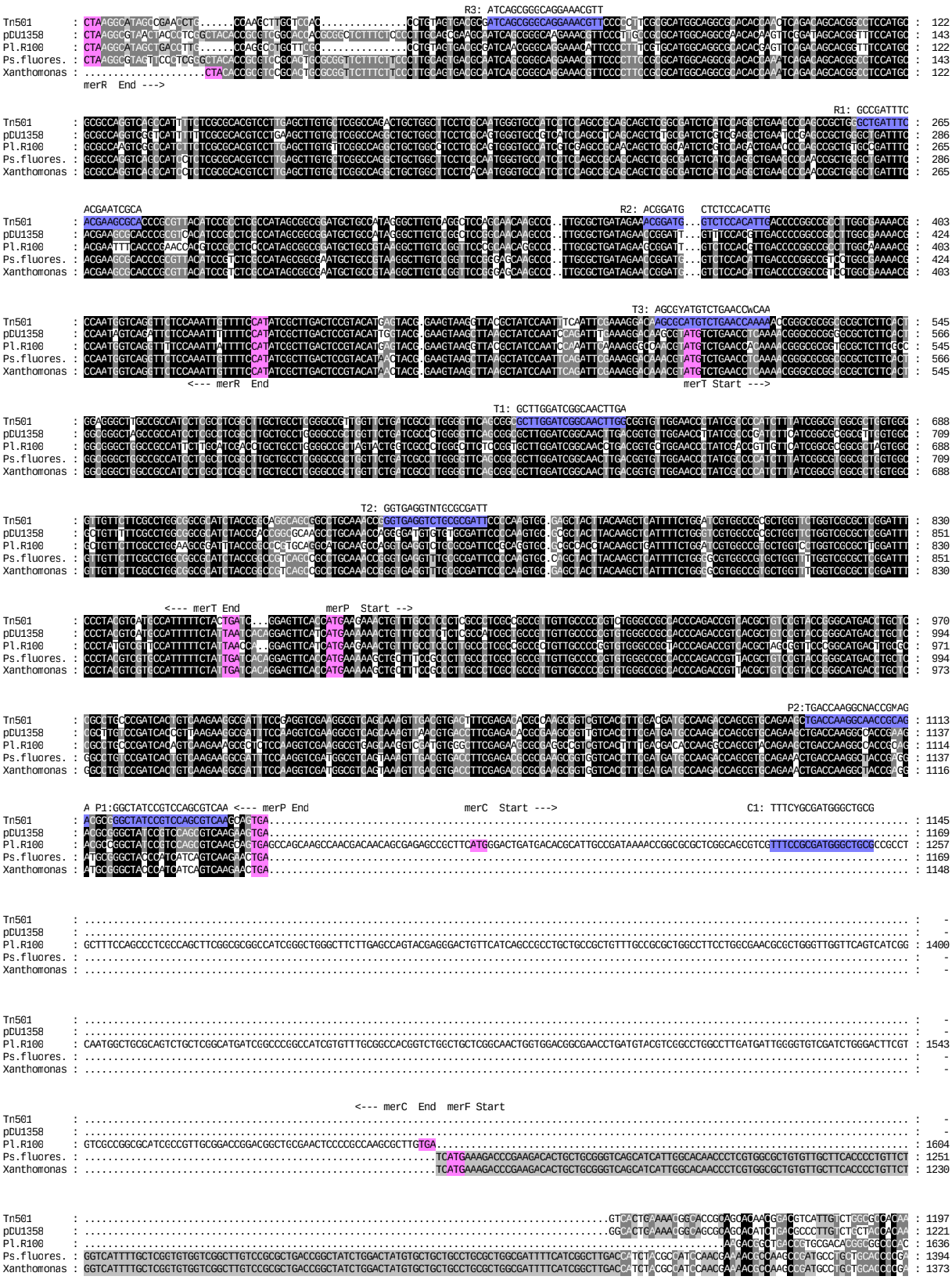

Figure B-15a. **Alignment of the published *mer* operon with specific primers.** The primers are colored in blue. Plasmid pDU1358: *Serratia marcescens*: M24940; Plasmid pPB: *Xanthomonas sp. W17*: Tn5053: L40585; Tn501: *Pseudomonas aeruginosa*: Z00027; *Ps. flourescens*: X73112; Plasmid R100: NC002134. Black shade: 100% similarity; Gray: 80% similarity; Light gray 60% similarity. Start and stop codon are colored pink.

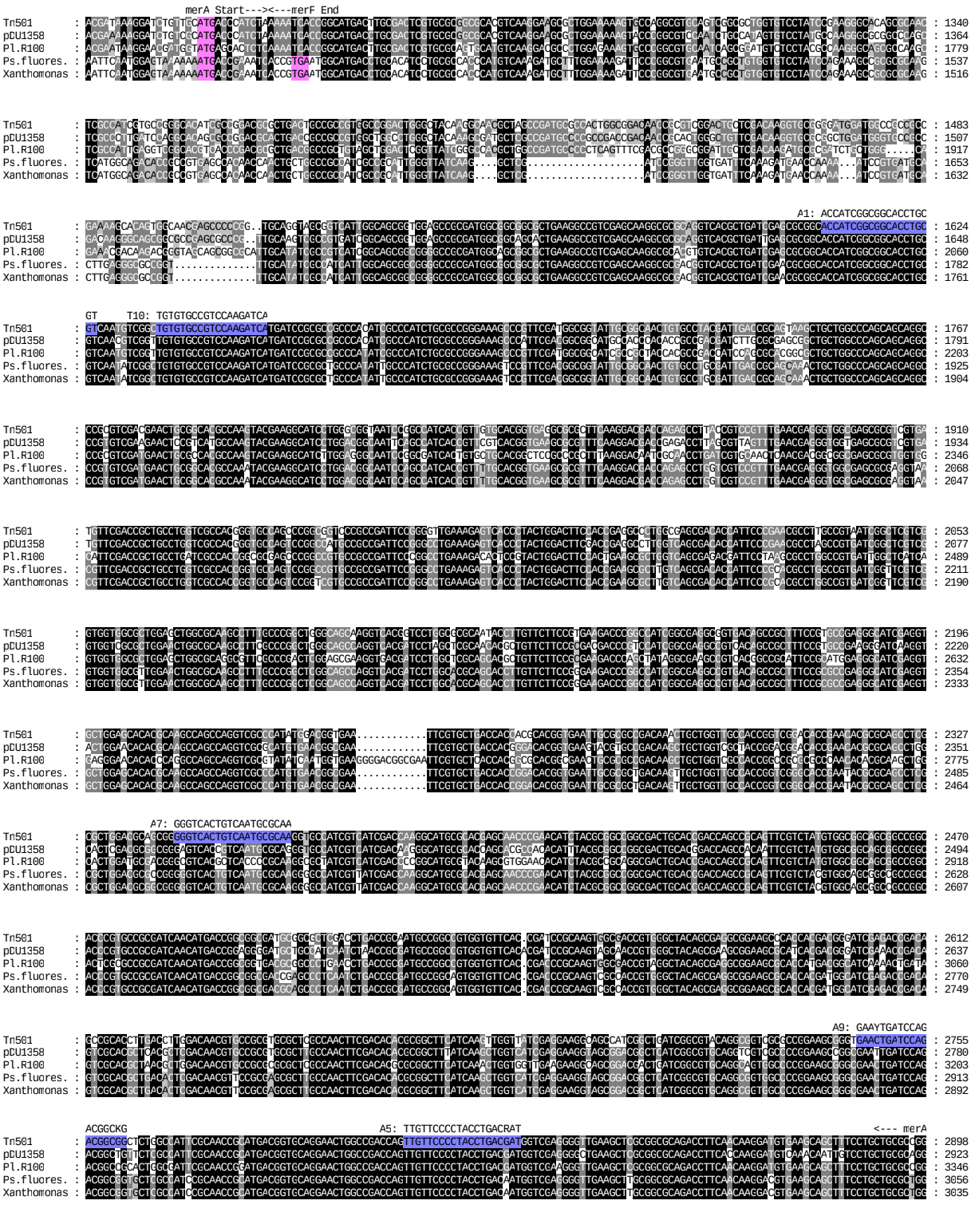

Figure B-15b. Continuation of the published *mer* operon sequence alignment with specific primers. The primers are colored in blue. The stop codon is represented as (-). Black shade: 100% similarity; Gray: 80% similarity; Light gray 60% similarity. Start and stop codon are colored pink.

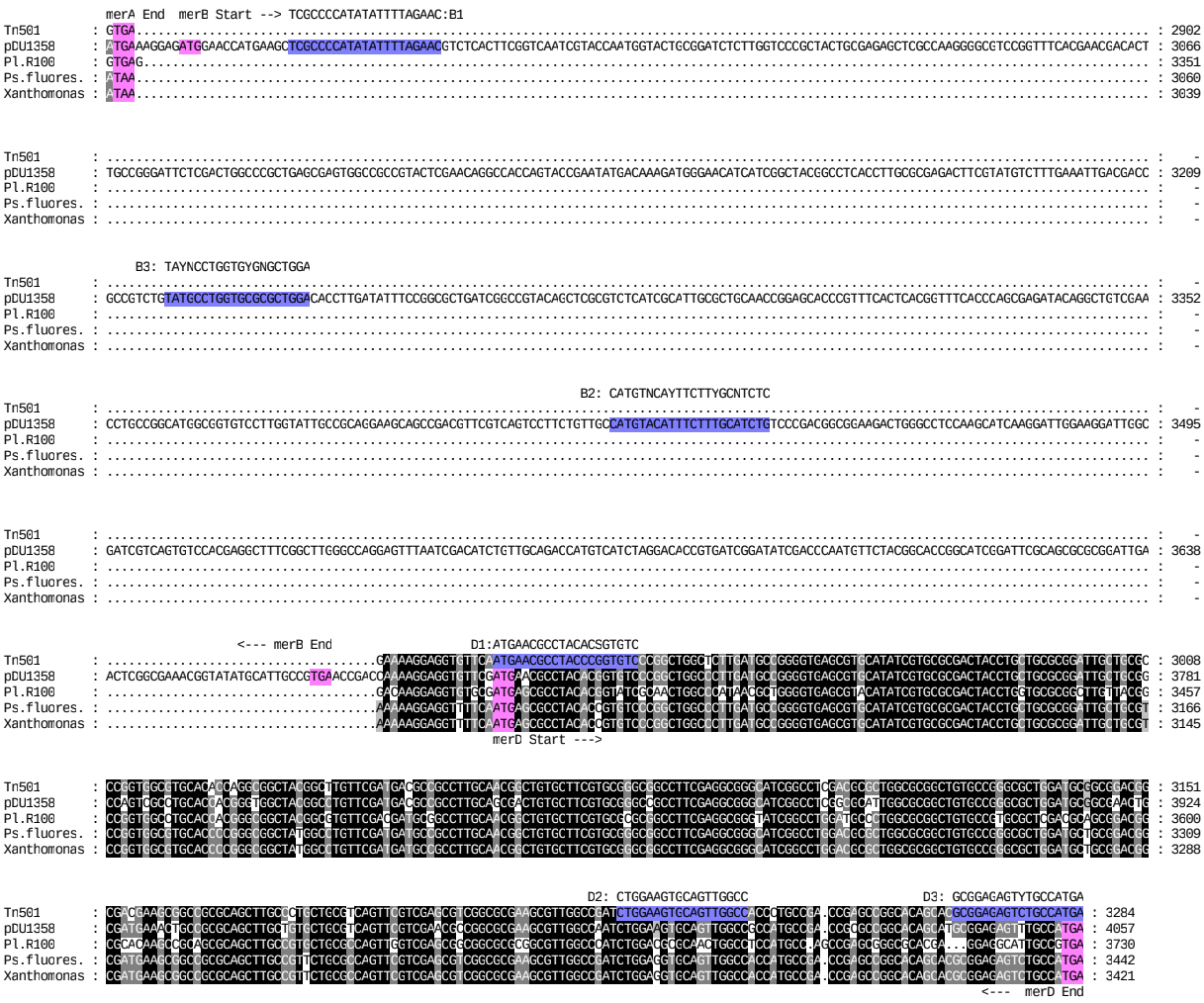

Figure B-15c. Continuing the published *mer* operon sequence alignment with specific primers. The primers are colored in blue. Black shade: 100% similarity; Gray: 80% similarity; Light gray 60% similarity. Start and stop codon are colored pink.

C. The *mer*Gene Arrangements of the Isolates

1. Pseudomonas putida Spi3

- 1st *mer* operon:

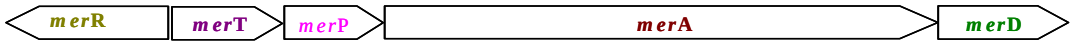


```
                                                  merR End --->
Spi3  : ..................................................................................................... :    -
Tn501 : CTAAGGGGTCGTCTCAGAAAACGGAAAATAAAGCACGCTAAGGCATAGCCGAACCTGCCAAGCTTGCTCCACCCTGTAGTGACGCGATCAGCGGGCAGGA :  100
                                                    -  P  M  A  S  G  A  L  S  A  G  G  Q  L  S  A  I  L  P  C  S

Spi3  : ............CGCGCATGGCAGGCGCACACCAACTCAGACAGCACGGCCTCCATGCGCGCCAGGTCAGCCATTTTCTCGCGCACGTCCTTGAGCTTG :   87
Tn501 : AACGTTCCCCCTTCGCGCATGGCAGGCGCACACCAACTCAGACAGCACGGCCTCCATGCGCGCCAGGTCAGCCATTTTCTCGCGCACGTCCTTGAGCTTG :  200
         V  N  G  R  R  A  H  C  A  C  V  L  E  S  L  V  A  E  M  R  A  L  D  A  M  K  E  R  V  D  K  L  K

Spi3  : TGCTCGGCCAGACTGCTGGCTTCCTCGCAATGGGTGCCATCCTCCAGCCGCAGCAGCTCGGCGATCTCATCCAGGCTGAAGCCCAGCCGCTGGGCTGATT :  187
Tn501 : TGCTCGGCCAGACTGCTGGCTTCCTCGCAATGGGTGCCATCCTCCAGCCGCAGCAGCTCGGCGATCTCATCCAGGCTGAAGCCCAGCCGCTGGGCTGATT :  300
         H  E  A  L  S  S  A  E  E  C  H  T  G  D  E  L  R  L  L  E  A  I  E  D  L  S  F  G  L  R  Q  A  S  K

Spi3  : TCACGAAGCGCACCCGCGTTACATCCGCCTCGCCATAGCGGCGGATGCTGCCATAGGGCTTGTCAGGCTCCAGCAACAAGCCCTTGCGCTGATAGAAACG :  287
Tn501 : TCACGAAGCGCACCCGCGTTACATCCGCCTCGCCATAGCGGCGGATGCTGCCATAGGGCTTGTCAGGCTCCAGCAACAAGCCCTTGCGCTGATAGAAACG :  400
         V  F  R  V  R  T  V  D  A  E  G  Y  R  R  I  S  G  Y  P  K  D  P  E  L  L  L  G  K  R  Q  Y  F  R

                                                                                  <--- merR Start
Spi3  : GATGGTCTCCACATTGACCCCGGCCGCCTTGGCGAAAACGCCAATGGTCAGGTTCTCCAAATTGTTTTCCATATCGCTTGACTCCGTACATGAGTACGGA :  387
Tn501 : GATGGTCTCCACATTGACCCCGGCCGCCTTGGCGAAAACGCCAATGGTCAGGTTCTCCAAATTGTTTTCCATATCGCTTGACTCCGTACATGAGTACGGA :  500
         I  T  E  V  N  V  G  A  A  K  A  F  V  G  I  T  L  N  E  L  N  N  E  M

                                                        merT Start --->
Spi3  : AGTAAGGTTACGCTATCCAATTTCAATTCGAAAGGACAAGCGCATGTCTGAACCAAAAACCGGGCGCGGCGCGCTCTTCACTGGAGGGCTTGCCGCCATC :  487
Tn501 : AGTAAGGTTACGCTATCCAATTTCAATTCGAAAGGACAAGCGCATGTCTGAACCAAAAACCGGGCGCGGCGCGCTCTTCACTGGAGGGCTTGCCGCCATC :  600
                                       ----          M  S  E  P  K  T  G  R  G  A  L  F  T  G  G  L  A  A  I
                                       RBS

Spi3  : CTCGCCTCGGCTTGCTGCCTCGGGCCGTTGGTTCTGATCGCCTTGGGGTTCAGCGGCGCTTGGATCGGCAACTTGGCGGTGTTGGAACCCTATCGCCCCA :  587
Tn501 : CTCGCCTCGGCTTGCTGCCTCGGGCCGTTGGTTCTGATCGCCTTGGGGTTCAGCGGCGCTTGGATCGGCAACTTGGCGGTGTTGGAACCCTATCGCCCCA :  700
         L  A  S  A  C  C  L  G  P  L  V  L  I  A  L  G  F  S  G  A  W  I  G  N  L  A  V  L  E  P  Y  R  P

Spi3  : TCTTTATCGGCGTGGCGCTGGTGGCGTTGTTCTTCGCCTGGCGGCGCATCTACCGGCAGGCAGAGGCCTGCAAACCGGGTGAGGTCTGCGCGATTCCCCA :  687
Tn501 : TCTTTATCGGCGTGGCGCTGGTGGCGTTGTTCTTCGCCTGGCGGCGCATCTACCGGCAGGCAGCGGCCTGCAAACCGGGTGAGGTCTGCGCGATTCCCCA :  800
         I  F  I  G  V  A  L  V  A  L  F  F  A  W  R  R  I  Y  R  Q  A  A  A  C  K  P  G  E  V  C  A  I  P  Q

                                                                                                  <--- merT End
Spi3  : AGTGCGAGCTACTTACAAGCTCATTTTTTGGATCGTGGCCGCGCTGGTTCTGGTCGCGCTCGGATTTCCCTACGTCATGCCATTTTTCTACTGATCGGAG :  787
Tn501 : AGTGCGAGCTACTTACAAGCTCATTTTCTGGATCGTGGCCGCGCTGGTTCTGGTCGCGCTCGGATTTCCCTACGTCATGCCATTTTTCTACTGATCGGAG :  900
         V  R  A  T  Y  K  L  I  F  W  I  V  A  A  L  V  L  V  A  L  G  F  P  Y  V  M  P  F  F  Y  -

              merP Start --->
Spi3  : TTCACCATGAAGAAGCTGTTTGCCTCCCTGGCCCTCGCCGCCGTTGTTGCCCCCGTCTGGGCCGCCACCCAGACCGTCACCGTGTCCGTACCGGGCATGA :  887
Tn501 : TTCACCATGAAGAACTGTTTGCCTCCCTCGCCCTCGCCGCCGTTGTTGCCCCCGTCTGGGCCGCCACCCAGACCGTCAGCGCTGTCCGTACCGGGCATGA : 1000
                M  K  K  L  F  A  S  L  A  L  A  A  V  V  A  P  V  W  A  A  T  Q  T  V  T  L  S  V  P  G  M

Spi3  : CCTGCTCCGGCTGCCCGATCACTGTCAAGAAGGCGATTTCCGAAGTCGAAGGCGTCAGCAAAGTTGACGTGACTTTCGAGACACGCCAAGCGGTCGTCAC :  987
Tn501 : CCTGCTCCGCCTGCCCGATCACTGTCAAGAAGGCGATTTCCGAGGTCGAAGGCGTCAGCAAAGTTGACGTGACTTTCGAGACACGCCAAGCGGTCGTCAC : 1100
         T  C  S  A  C  P  I  T  V  K  K  A  I  S  E  V  E  G  V  S  K  V  D  V  T  F  E  T  R  Q  A  V  V  T

                                                                                  <--- merP End
Spi3  : CTTCGACGATGCCAAGACCAGCGTGCAGAAGCTGACCAAGGCAACCGCAGACGCGGGCTATCCGTCCAGCGTCAAGCAGTGAGTCACTGAAAACGGCACC : 1087
Tn501 : CTTCGACGATGCCAAGACCAGCGTGCAGAAGCTGACCAAGGCAACCGCAGACGCGGGCTATCCGTCCAGCGTCAAGCAGTGAGTCACTGAAAACGGCACC : 1200
         F  D  D  A  K  T  S  V  Q  K  L  T  K  A  T  A  D  A  G  Y  P  S  S  V  K  Q  -

                                                        merA Start --->
Spi3  : GCAGCACAACGGACGTCATTGTCTGGCGCCACAAACGATAAAGGATCTGTTGGCATGACCCATCTAAAAATCACCGGCATGACTTGCGACTCGTGCGCGGC : 1187
Tn501 : GCAGCACAACGGACGTCATTGTCTGGCGCCACAAACGATAAAGGATCTGTTGGCATGACCCATCTAAAAATCACCGGCATGACTTGCGACTCGTGCGCGGC : 1300
                                          ----          M  T  H  L  K  I  T  G  M  T  C  D  S  C  A  A
                                          RBS

Spi3  : GCACGTCAAGGAAGCGCTGGAAAAAGTGCCAGGCGTGCAGTCGGCGCTGGTGTCCTATCCGAAGGGCACAGCGCAACTCGCCATCGTGCCGGGCACATCG : 1287
Tn501 : GCACGTCAAGGAAGCGCTGGAAAAAGTGCCAGGCGTGCAGTCGGCGCTGGTGTCCTATCCGAAGGGCACAGCGCAACTCGCCATCGTGCCGGGCACATCG : 1400
         H  V  K  E  A  L  E  K  V  P  G  V  Q  S  A  L  V  S  Y  P  K  G  T  A  Q  L  A  I  V  P  G  T  S
```

Figure C-16a. **Alignment of the complete narrow spectrum resistant operon (NS) of the strain *Ps. p*. Spi3, including the *mer* genes R, T, P, A, D.** Amino acid sequence of Tn501 polypeptide (accession no. Z00027) is shown as standard single letter below the DNA sequence line. Black shade: 100% similarity. Start and stop codon are colored pink.

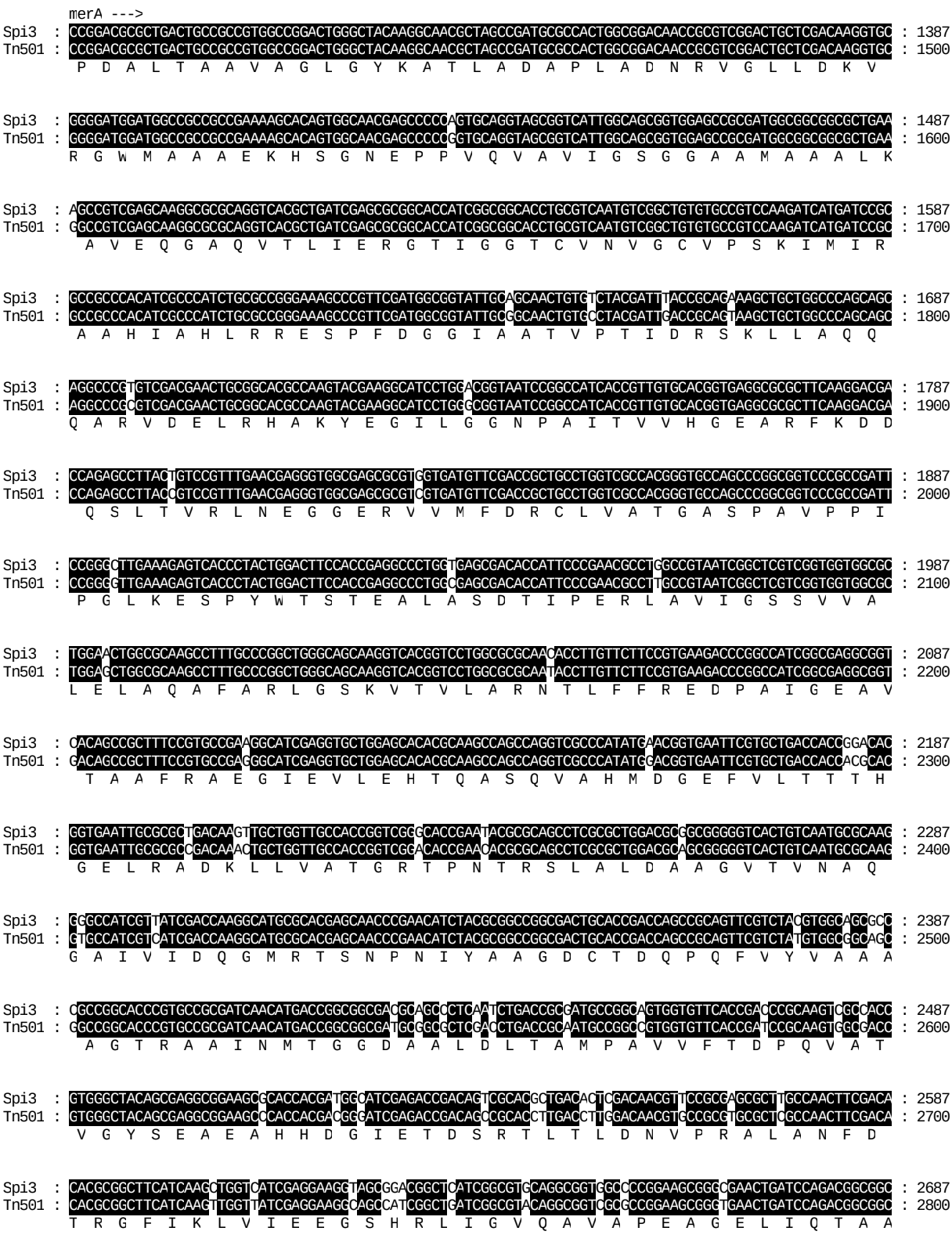

Figure C-16b. Continuing of alignment of the *mer* genes from Spi3 with Tn501. Amino acid sequence of Tn501 polypeptide (accession no. Z00027) is shown as standard single letter below the DNA sequence line. Black shade: 100% similarity. Start and stop codon are colored pink.

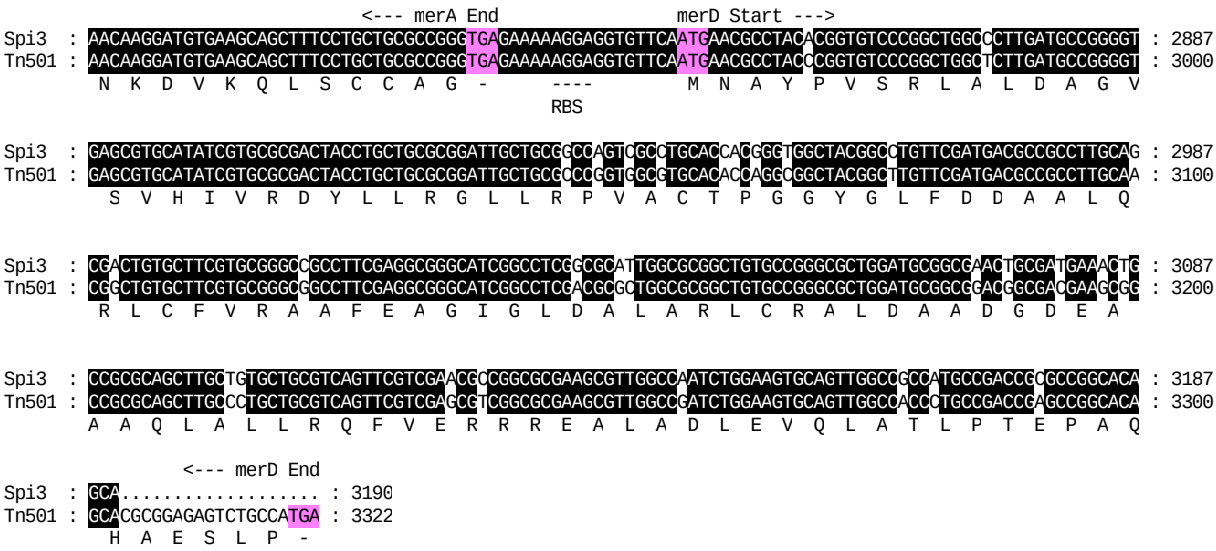

Figure C-16c. Continuing the alignment of the *mer* genes from Spi3 with Tn501. Amino acid sequence of Tn501 polypeptide (accession no. Z00027) is shown as standard single letter below the DNA sequence line. Black shade: 100% similarity. Start and stop codon are colored pink.

- 2nd *mer* operon:

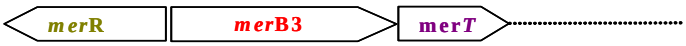

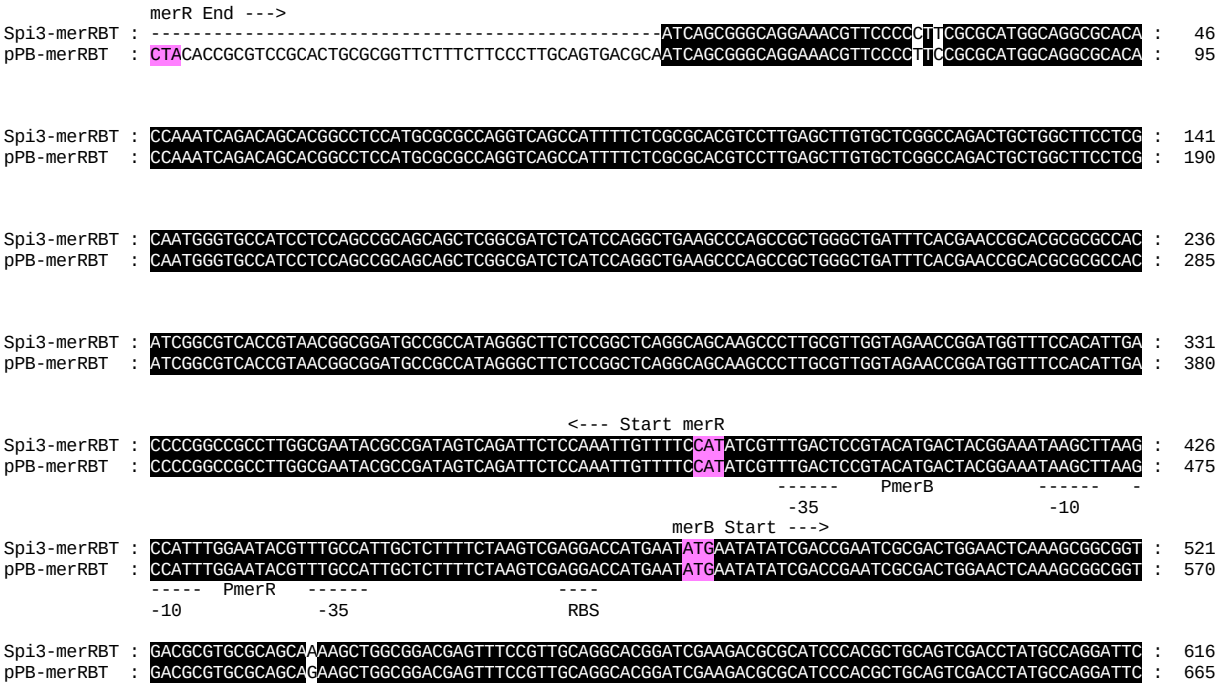

Figure C-17a. **Alignment of partly sequenced broad spectrum mercury resistant operon from *Ps. putida* Spi3 with plasmid pPB from *Ps. Stutzeri* (accession no. PSU90263), including the genes *mer*R$_2$, *mer*B and the 5' end of *mer*T$_2$ gene.** Promoters, ribosomal binding site and the poly peptide sequence of plasmid pPB are shown below the DNA sequence. The stop codon is represented as (-). Black shade: 100% similarity. Start and stop codon are colored pink.

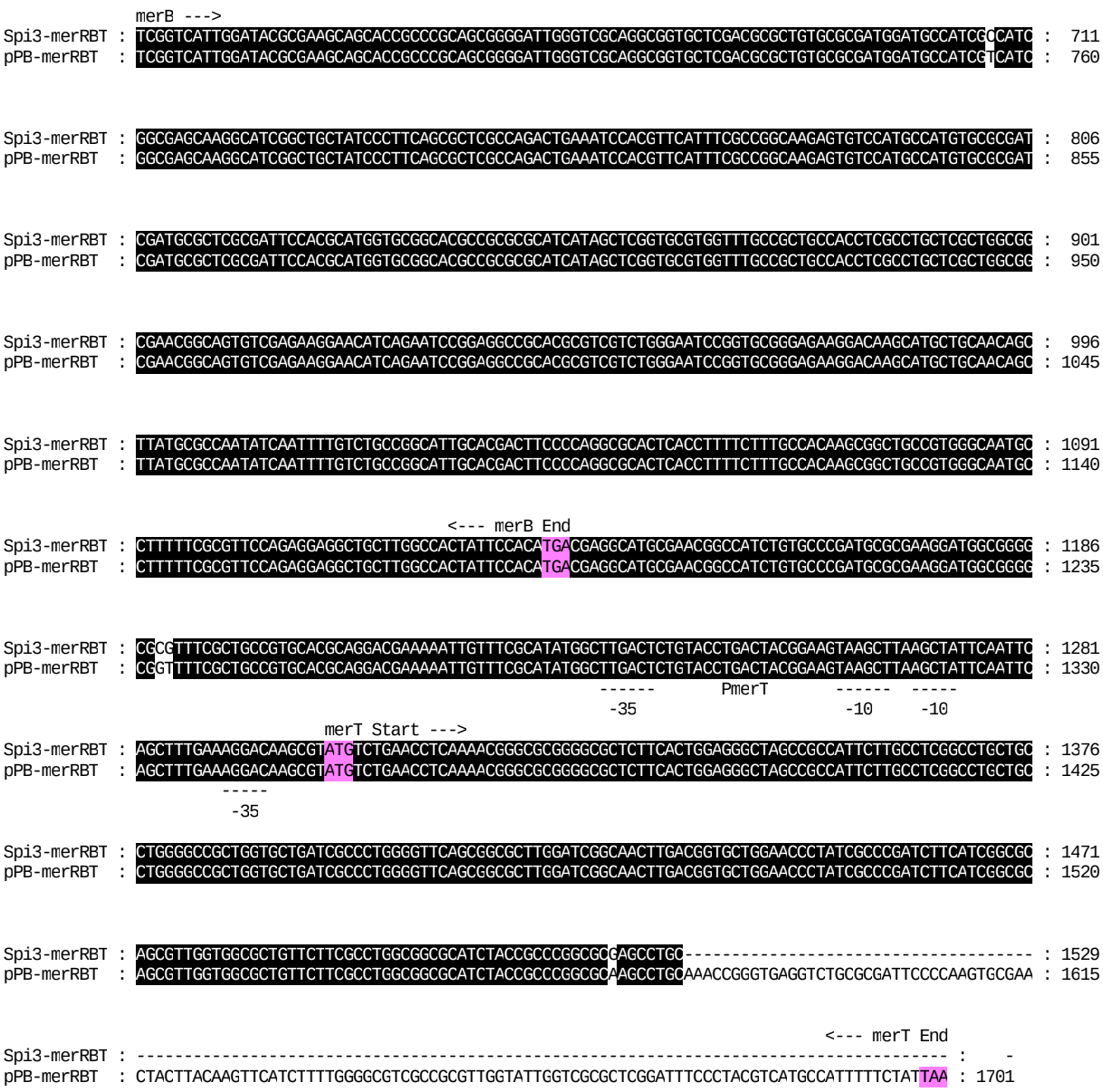

Figure C-17b. Continuing the alignment of *mer*B and *mer*T from Spi3 with plasmid pPB. Amino acid sequence of Tn501 polypeptide (accession no. Z00027) is shown as standard single letter below the DNA sequence line. Black shade: 100% similarity. Start and stop codon are colored pink.

- 3rd *mer* operon:

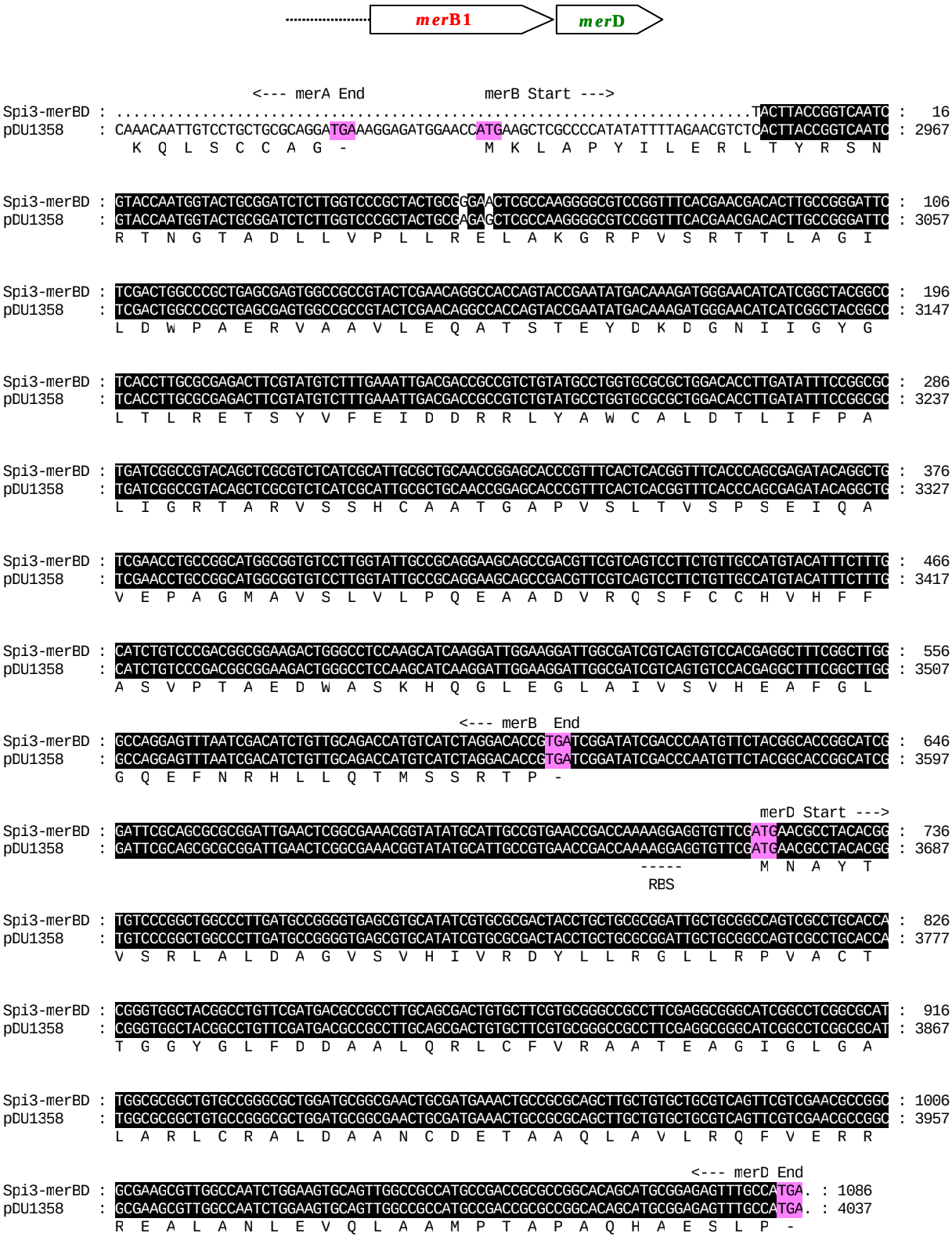

Figure C-18. **Alignment of partly sequenced broad spectrum mercury resistant operon from *Ps. putida* Spi3 with plasmid pDU1358 (accession no. M15049), including the *mer*B and *mer*D gene.** Ribosomal binding site and the poly peptide sequence of plasmid pDU1358 is shown below the DNA sequence. The stop codon is represented as (-). Black shade: 100% similarity. Start and stop codon are colored pink.

- 4th *mer* operon:

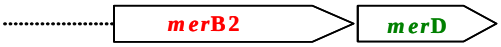


```
                                                                merB Start --->
Spi3-merBD : CCAAGGATGTCAAACAATTGTCCTGGTGCGCAGGATGAAAGGAGATGGAACCATGAAGCTCGCCCCATATATTTTAGAACGTCTCACTTCGGT :   93
                                                    -----        M  K  L  A  P  Y  I  L  I  R  L  T  S  V
                                                    RBS

Spi3-merBD : CAATCGGACCAATGGTACTGCGGATCTCTTGGTCCCGCTACTGCGGGAACTCGCCAAGGGGCGTCCGGTTTCACGAACGACACTTGCCGGGAT :  186
               N  R  T  N  G  T  A  D  L  L  V  P  L  L  R  E  L  A  K  G  R  P  V  S  R  T  T  L  A  G  I

Spi3-merBD : TCTCGACTGGCCCGCTGAGCGAGTGGCCGCCGTACTCGAACAGGCCACCAGTACCGAATATGACAAAGATGGGAACATCATCGGCTACGGCCT :  279
               L  D  W  P  A  E  R  V  A  A  V  L  E  Q  A  T  S  T  E  Y  D  K  D  G  N  I  I  G  Y  G  L

Spi3-merBD : CACCTTGCGCGAGACTTCGTATGTCTTTGAAATTGACGACCGCCGTCTATATTCCTGGTGCGCGCTGGACACCTTGACATTCCCGGCGTTCAT :  372
               T  L  R  E  T  S  Y  V  F  E  I  D  D  R  R  L  Y  S  W  C  A  L  D  T  L  T  F  P  A  F  I

Spi3-merBD : CGGCCGTACAGCTCGCGTCTCATCGCATTGCGCTGCAACCGGTAGACCCGTTTCACTCACGGTTTCACCCAACGAGATACAGGCTGTCGAACC :  465
               G  R  T  A  R  V  S  S  H  C  A  A  T  G  R  P  V  S  L  T  V  S  P  N  E  I  Q  A  V  E  P

Spi3-merBD : TGCCGGCATGGCGGTGTCCTTGGTATTGCCGCAAGAAGCAGCCGACGTTCGTCAGTCCTTCTGCTGCCATGTGCATTTCTTTGCATCTCCGCC :  558
               A  G  M  A  V  S  L  V  L  P  Q  E  A  A  D  V  R  Q  S  F  C  C  H  V  H  F  F  A  S  P  P

Spi3-merBD : TATTGCAAATTCGTGGGCTTCGACCCACCAAGGGATTGAGGTCGTGCCTGTCGAGAGTGCGTTCGACCTTGGTCATGATGTCGCGCTTAAGCT :  651
               I  A  N  S  W  A  S  T  H  Q  G  I  E  V  V  P  V  E  S  A  F  D  L  G  H  D  V  A  L  K  L

                                  <--- merB End
Spi3-merBD : GCTAGAGGACTGCGAGGAAAGCCCACTATGAATGCGTACTCGATATCGAAGCTGGCTGATGATGCTTGCGTCGCGTGCATGTCGTGCGCGACT :  744
               L  E  D  C  E  E  S  P  L  -

               merD Start --->
Spi3-merBD : ACATGATACGCGGCTTGTTGCACCCTGCTCGGCGAACCGAAAGTGGCCAGAACATTTTCGATGACAAAACACTCGGAAGGCTGCGGCTTCTCC :  837
                M  I  R  G  L  L  H  P  A  R  R  T  E  S  G  Q  N  I  F  D  D  K  T  L  G  R  L  R  L  L

Spi3-merBD : GCGCAGCCTTCGAGTCCGGAATTGGGCTCGACCAACTGGCGCGACTTTGCAAAGCATTGGACGCAAACGATAGCGAAAGCCTGGACCGATGCG :  930
             R  A  A  F  E  S  G  I  G  L  D  Q  L  A  R  L  C  K  A  L  D  A  N  D  S  E  S  L  D  R  C

Spi3-merBD : TCGAGCGCGTGCGATGGAAGATCGACGTGCGTCGAACAGTTTTGACTGTCGCCGAGGCCTCTTTGAATGAAATGGCGGCCGGTGCAGCTACTT : 1023
             V  E  R  V  R  W  K  I  D  V  R  R  T  V  L  T  V  A  E  A  S  L  N  E  M  A  A  G  A  A  T

                                                                                        <--- merD End
Spi3-merBD : CAGGTCCGGCCGGTAAAAGCGTTGGAATTAGCCACTTCGTATATAATATATCGATTAATACATTCTCTCTACTCAATGTAACGTCTGCCTAAA : 1116
             S  G  P  A  G  K  S  V  G  I  S  H  F  V  Y  N  I  S  I  N  T  F  S  L  L  N  V  T  S  A  -
```

Figure C-19. Nucleotide sequence of the second broad spectrum mercury resistant operon from *Ps. putida* Spi3, including the genes *mer*B_2, *mer*D_2. Ribosomal binding site and the predicted polypeptide sequence is shown below the DNA sequence. The stop codon is represented as (-). Black shade: 100% similarity. Start and stop codon are colored pink.

2. *Ps. aeruginosa* Bro12

- 1st *mer* operon:

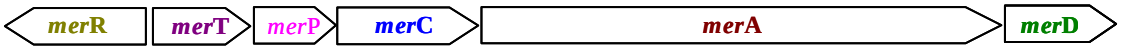

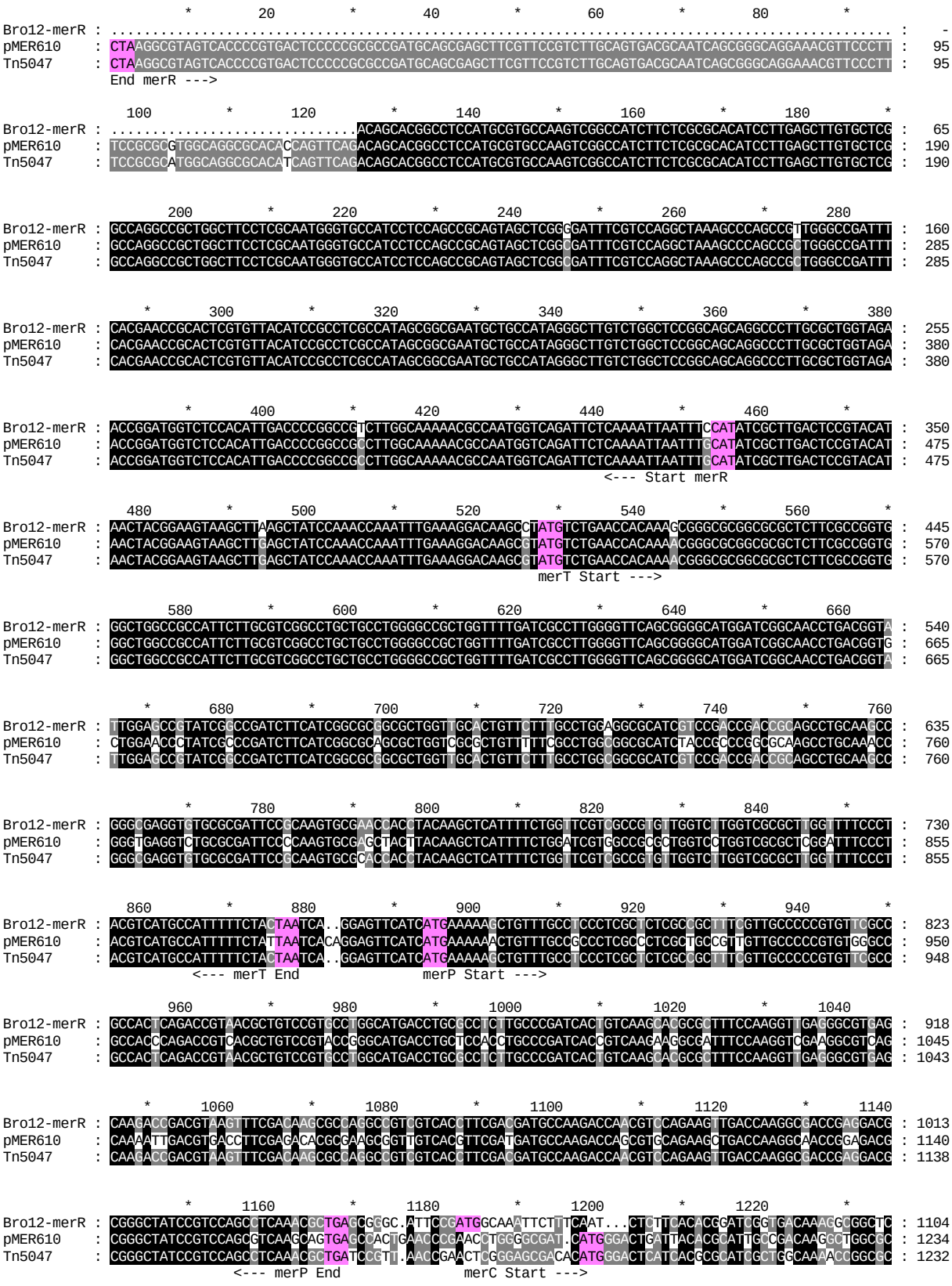

Figure C-20a. **Alignment of the complete narrow spectrum (NS) operon of the strain *Ps. aeruginosa* Bro12, including the *mer* genes R, T, P, C, A, D**. The nucleotide sequence is aligned with published *mer* operon of Tn5047 (accession no. AJ251307) and plasmid pMER610 (accession no. Y08993). Black shade: 100% similarity. Start and stop codon are colored pink.

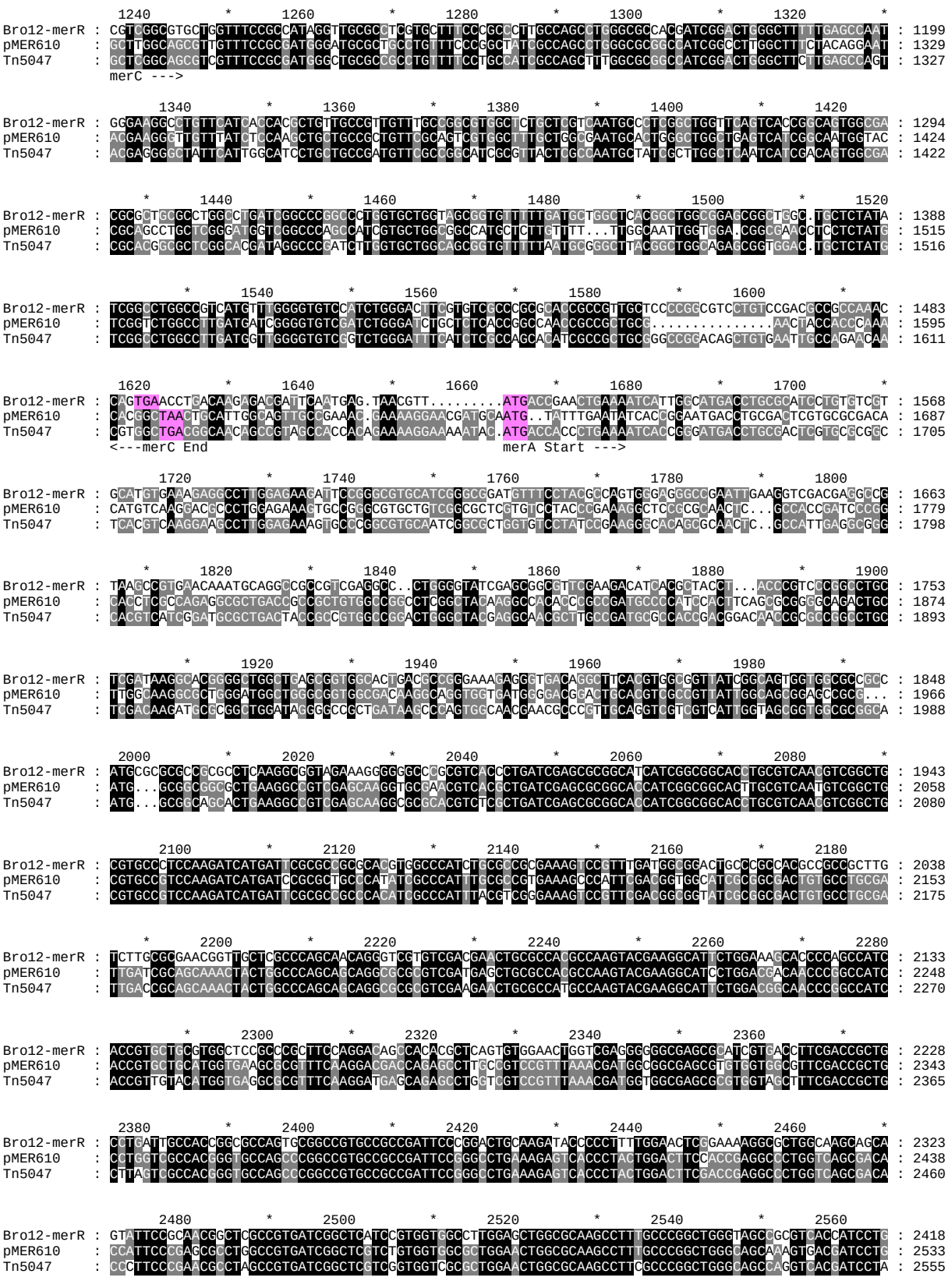

Figure C-20b. Continuing of alignment of the *mer* genes from Bro12 (accession no. AJ251307) and plasmid pMER610 (accession no. Y08993). Black shade: 100% similarity. Start and stop codon are colored pink.

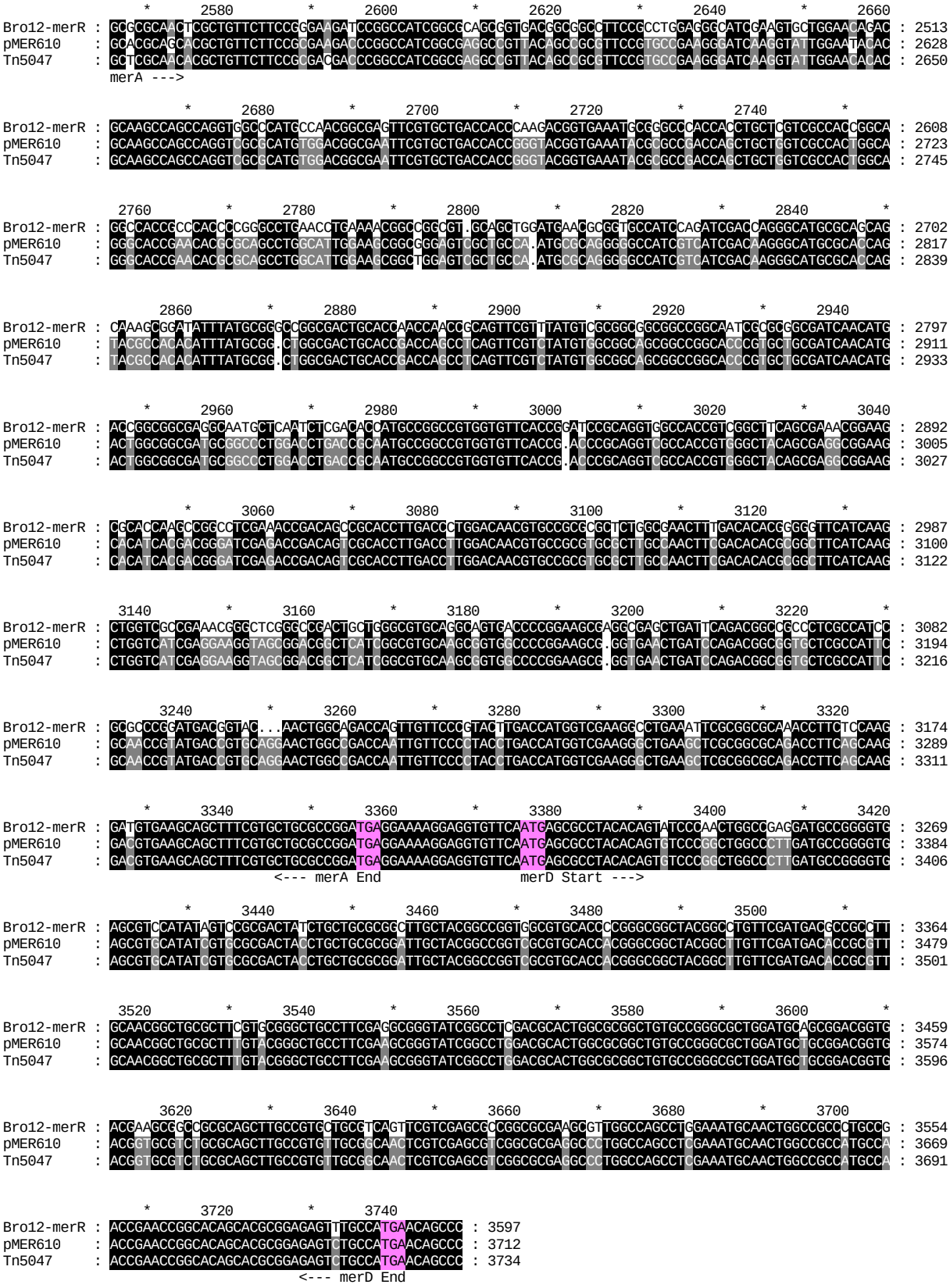

Figure C-20c. Continuing of alignment of the *mer* genes from Bro12 with Tn5047 (accession no. AJ251307) and plasmid pMER610 (accession no. Y08993). Black shade: 100% similarity. Start and stop codon are colored pink.

- 2nd *mer* operon:


```
                  *        20         *        40         *        60         *        80
Bro12-534-merPA : ..................................................................................... :    -
pDU1358         : ATGAAAAAACTGTTTGCCTCTCTCGCCATCGCTGCCGTTGTTGCCCCCGTGTGGGCCGCCACCCAGACCGTCACGCTGTCCGTAC :   85
                  merP Start --->

                     *       100         *       120         *       140         *       160         *
Bro12-534-merPA : ..................................................................................... :    -
pDU1358         : CGGGCATGACCTGCTCCGCTTGTCCGATCACCGTTAAGAAGGCGATTTCCAAGGTCGAAGGCGTCAGCAAAGTTAACGTGACCTT :  170

                        180         *       200         *       220         *       240         *
Bro12-534-merPA : ..................................................................................... :    -
pDU1358         : CGAGACACGCGAAGCGGTTGTCACCTTCGATGATGCCAAGACCAGCGTGCAGAAGCTGACCAAGGCCACCGAAGACGCGGGCTAT :  255

                  260         *       280         *       300         *       320         *       340
Bro12-534-merPA : ....................................CGCAGCACATCTGACGCCCTTGTCTGCTACCACAAACGAAAAAGGAT :   47
pDU1358         : CCGTCCAGCGTCAAGAAGTGAGGCACTGAAAACGGCAGCGCAGCACATCTGACGCCCTTGTCTGCTACCACAAACGAAAAAGGAT :  340
                                                    <--- merP End

                     *       360         *       380         *       400         *       420
Bro12-534-merPA : CTGTCGCATGACCCATCTAAAAATCACCGGCATGACCTGCGACTCGTGCGCGGCGCACGTCAAGGAAGCGCTGGAAAAAGTACCC :  132
pDU1358         : CTGTCGCATGACCCATCTAAAAATCACCGGCATGACCTGCGACTCGTGCGCGGCGCACGTCAAGGAAGCGCTGGAAAAAGTACCC :  425
                        merA Start --->

                     *       440         *       460         *       480         *       500         *
Bro12-534-merPA : GGCGTCCAATCTGCCATAGTGTCCTATGCCAAGGGCGCGGCCCAGCTCGCCCTTGATCCAGGCACAGCGCCGGACGCACTGACCG :  217
pDU1358         : GGCGTCCAATCTGCCATAGTGTCCTATGCCAAGGGCGCGGCCCAGCTCGCCCTTGATCCAGGCACAGCGCCGGACGCACTGACCG :  510

                        520         *       540         *       560         *       580         *
Bro12-534-merPA : CCGCCGTGGCTGGCCTGGGCTACAAAGCGATGCTCGCCGATGCCCCGCCGACCGACAACCGCACTGGGCTGTTCGACAAGGTGCG :  302
pDU1358         : CCGCCGTGGCTGGCCTGGGCTACAAAGCGATGCTCGCCGATGCCCCGCCGACCGACAACCGCACTGGGCTGTTCGACAAGGTGCG :  595

                  600         *       620         *       640         *       660         *       680
Bro12-534-merPA : CGGCTGGATGGGTGCCGCCGACAAGGGCAGCGGCGGCGAGCGCCCGTTGCAAGTCGCCGTGATCGGCAGCGGTGGAGCCGCGATG :  387
pDU1358         : CGGCTGGATGGGTGCCGCCGACAAGGGCAGCGGCGGCGAGCGCCCGTTGCAAGTCGCCGTGATCGGCAGCGGTGGAGCCGCGATG :  680

                     *       700         *       720         *       740         *       760
Bro12-534-merPA : GCGGCAGCACTGAAGGCCGTCGAGCAAGGCGCGCAGGTCACGCTGATTGAGCGCGGCACCATCGGCGGCACCTGCGTCAACGTCG :  472
pDU1358         : GCGGCAGCACTGAAGGCCGTCGAGCAAGGCGCGCAGGTCACGCTGATTGAGCGCGGCACCATCGGCGGCACCTGCGTCAACGTCG :  765

                     *       780         *       800         *       820         *       840         *
Bro12-534-merPA : GTTGTGTGCCGTCCAAGATCATGATCCGCGCCGCCCACATCGCCCATCTGCGCCGGGAAAGTCCGTTCGATGGCGGCATGCCCGC :  557
pDU1358         : GTTGTGTGCCGTCCAAGATCATGATCCGCGCCGCCCACATCGCCCATCTGCGCCGGGAAAGCCCATTCGACGGCGGCATGCCACC :  850

                        860         *       880         *       900         *       920         *
Bro12-534-merPA : CACACCGCCGACGATCTTGCGCGAACGGCTGCTGGCCCAGCAACAGGCCCGTGTCGACGAACTGCCCCACGCCAAGTACGAAGGC :  642
pDU1358         : CACACCGCCGACGATCTTGCGCGAGCGGCTGCTGGCCCAGCAGCAGGCCCGTGTCGAAGAACTCCGTCATGCCAAGTACGAAGGC :  935

                  940         *       960         *       980         *      1000         *      1020
Bro12-534-merPA : ATTCTGGACGGCAATCCAGCCATCACCGTGCTGCACGGTGCAGCCCGCTTCAAGGACAACCAGAGCCTCAGTGTGGGTTTGAACG :  727
pDU1358         : ATCCTGGACGGCAATTCAGCCATCACCGTTCTGCACGGTGAAGCGCGTTTCAAGGACGACCAGAGCCTTATCGTTAGTTTGAACG : 1020

                     *      1040         *      1060         *      1080         *      1100
Bro12-534-merPA : AGGGTGGCGAGCGCGTCGTGATGTTCGACCGCTGCCTGATCGCCACCGGTGCCAGTCCGGCGGTGCCGCCGATTCCGGGCCTGAA :  812
pDU1358         : AGGGTGGTGAGCGCGTCGTGATGTTCGACCGCTGCCTGGTCGCCACGGGTGCCAGTCCGGCGATGCCGCCGATTCCGGGCCTGAA : 1105

                     *      1120         *      1140         *      1160         *      1180         *
Bro12-534-merPA : AGATACCCCCTTTTGGAACTCGGAAAAGGCGCTGGTCAGCGACACCATTCCCGAACGGCTCGCCGTGATCGGCTCATCCGTGGTG :  897
pDU1358         : AGAGTCACCCTACTGGACTTCGACCGAGGCCTTGGTCAGCGACACCATTCCCGAACGCCTAGCCGTGATCGGCTGGTCGGTGGTC : 1190
```

Figure C-21a. **Alignment of the partly sequenced broad spectrum resistant (BS) operon of the strain *Ps. aeruginosa* Bro12, including the *mer* genes *mer*P and *mer*A.** Black shade: 100% similarity. Start and stop codon are colored pink.

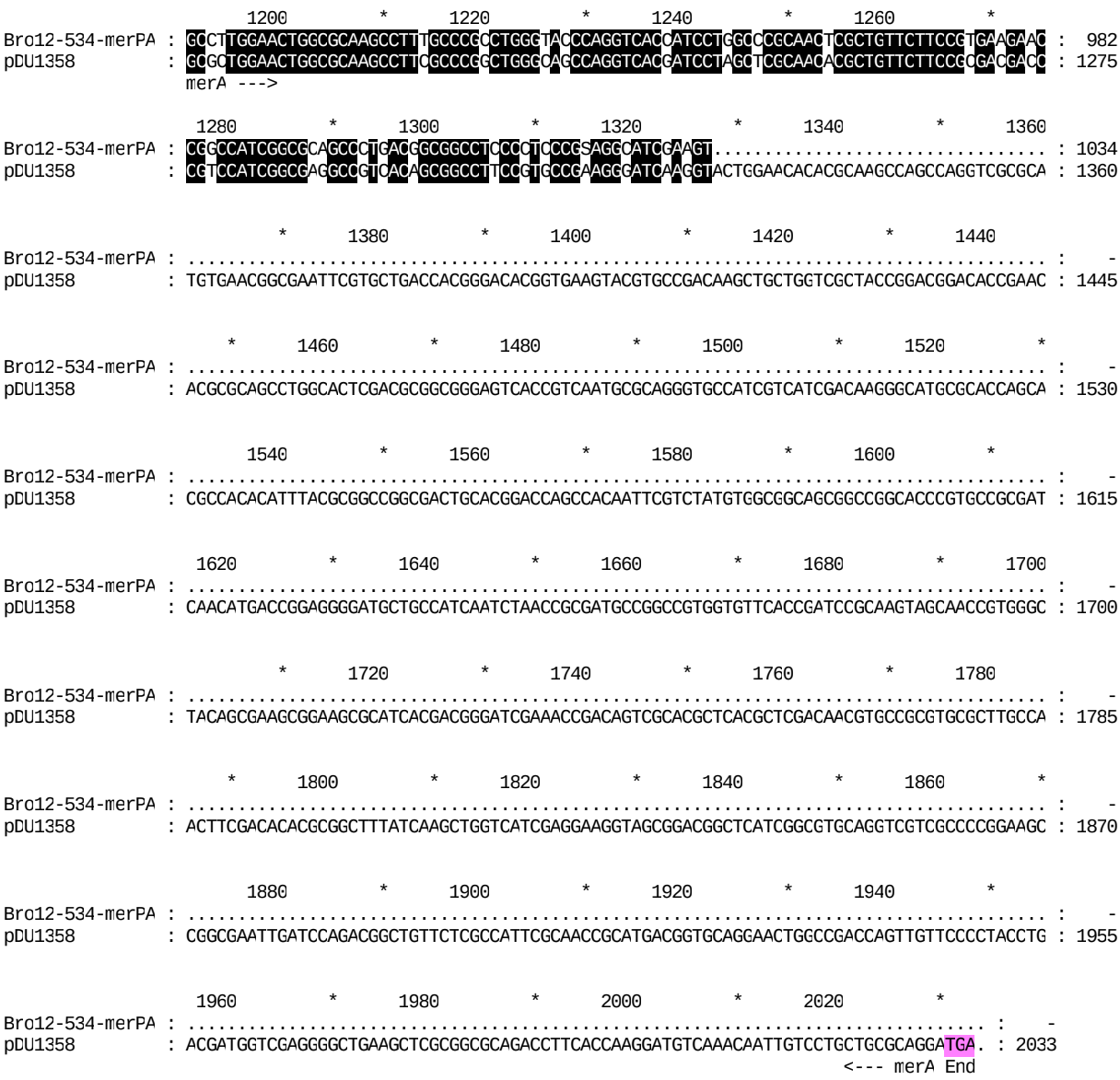

Figure C-21b. Continuing the alignment of the *mer* genes from Bro12 with plasmid pDU1358. Black shade: 100% similarity. Start and stop codon are colored pink.

3. Ps. stutzeri Ibu8

- 1st *mer* operon:

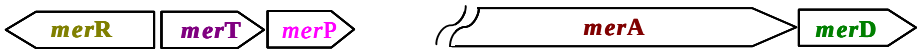


```
                End merR --->
Ibü8_merRTP : ..................................................................................... :   -
Ibu8-merAD  : ..................................................................................... :   -
Tn5047      : CTAAGGCGTAGTCACCCCGTGACTCCCCCGCGCCGATGCAGCGAGCTTCGTTCCGTCTTGCAGTGACGCAATCAGCGGGCAGGAAACGTTCCCT :  94
                - P T T V G H S G R A S A A L K T G D Q L S A I L P C S V N G

Ibü8_merRTP : ........ATGGCAGGCGCACACAGTTCAGACAGCACGGCCTCCATGCGTGCCAAGTCGGCCATCTTCTCGCGCACATCCTTGAGCTTGTGCT :  86
Ibu8-merAD  : ..................................................................................... :   -
Tn5047      : TTCCGCGCATGGCAGGCGCACATCAGTTCAGACAGCACGGCCTCCATGCGTGCCAAGTCGGCCATCTTCTCGCGCACATCCTTGAGCTTGTGCT :  188
                K R A H C A C V L E S L V A E M R A L D A M K E R V D K L K H E

Ibü8_merRTP : CGGCCAGGCCGTTGGCTTCCTCGCAATGGGTGCCATCCTCCAGCCGCAGTAGCTCGGCGATTTCGTCCAGGCTAAAGCCCAGCCGCTGGGCCGA :  180
Ibu8-merAD  : ..................................................................................... :   -
Tn5047      : CGGCCAGGCCGCTGGCTTCCTCGCAATGGGTGCCATCCTCCAGCCGCAGTAGCTCGGCGATTTCGTCCAGGCTAAAGCCCAGCCGCTGGGCCGA :  282
                A L G S A E E C H T G D E L R L L E A I E D L S F G L R Q A S

Ibü8_merRTP : TTTCACGAACCGCACTCGTGTTACATCCGCCTCCCATAGCGGCGAATGCTGCCATAGGGCTTGTCTGGCTCCGGCAGCAGGCCCTTGCGCTGG :  274
Ibu8-merAD  : ..................................................................................... :   -
Tn5047      : TTTCACGAACCGCACTCGTGTTACATCCGCCTCGCCATAGCGGCGAATGCTGCCATAGGGCTTGTCTGGCTCCGGCAGCAGGCCCTTGCGCTGG :  376
                K V F R V R T V D A E G Y R R I S G Y P K D P E P L L G K R Q

                                                                  <--- merR start
Ibü8_merRTP : TAGAACCGGATGGTCTCCACATTGACCCCGGCCGCCTTGGCAAAAACGCCAATGGTCAGATTCTCCAAATTATTTCCCATACGGCTTGACTCCG :  368
Ibu8-merAD  : ..................................................................................... :   -
Tn5047      : TAGAACCGGATGGTCTCCACATTGACCCCGGCCGCCTTGGCAAAAACGCCAATGGTCAGATTCTCAAAATTAATTGCATATCGCTTGACTCCG :  470
                Y F R I T E V N V G A A K A F V G I T L N E F N I Q M

                                                        merT Start --->
Ibü8_merRTP : TACATAACTCCGGAAGTAAGCTTACGCTATCCAAACCAAATTTCAAAGGACAAGCGTATGTCTGAACCTCAAAACGGGCGCGGCGCGCTCTTCC :  462
Ibu8-merAD  : ..................................................................................... :   -
Tn5047      : TACATAACTACGGAAGTAAGCTTGAGCTATCCAAACCAAATTTGAAAGGACAAGCGTATGTCTGAACCACAAAACGGGCGCGGCGCGCTCTTCG :  564
                                                  ----      M S E P Q N G R G A L F
                                                  RBS

Ibü8_merRTP : CTGGCGGGCTAGCCGCCATCCTCGCGTCGGCTTGCTGCCTGGGGCCGCTGGTTTTGATCGCCTTGGGGTTCAGCGGGGCATGGATCGGCAACCT :  556
Ibu8-merAD  : ..................................................................................... :   -
Tn5047      : CCGGTGGGCTGCCGCCATTCTTGCGTCGGCCTGCTGCCTGGGGCCGCTGGTTTTGATCGCCTTGGGGTTCAGCGGGGCATGGATCGGCAACCT :  658
                A G G L A A I L A S A C C L G P L V L I A L G F S G A W I G N L

Ibü8_merRTP : GACGGTATTGGAGCCGTATCGGCCGATCTTCATCGGCGCGGCGCTGGTTGCACTGTTCTTTGCCTGGCGGCGCATTTTCCGACCGGCTCAAGCC :  650
Ibu8-merAD  : ..................................................................................... :   -
Tn5047      : GACGGTATTGGAGCCGTATCGGCCGATCTTCATCGGCGCGGCGCTGGTTGCACTGTTCTTTGCCTGGCGGCGCATCGTCCGACCGACGCGCAGCC :  752
                T V L E P Y R R P I F I G A A L V A L F F A W R R I V R P T A A

Ibü8_merRTP : TGGCACCGGGCGAGGTCTGCGCCATCCCTCAGGTGCCTACCACCTACAAGCTGCTGTACTGGTTGGTGGCCGCGTTGGTGTTGGTCGCGCTCG :  744
Ibu8-merAD  : ..................................................................................... :   -
Tn5047      : TGCAAGCCGGGCGAGGTGTGCGGCATCCGCAAGTGCGCACCACCTACAAGCTCATTTTCTGGTTCGTCGCCGTGTTGGTCTTGGTCGCGCTTG :  846
                C K P G E V C A I P Q V R T T Y K L I F W F V A V L V L V A L

                                  <--- merT End            merP Start --->
Ibü8_merRTP : GCTTTCCCTACGTCATGCCATTTTTCTACTAATCAGGAGTTCATCATGAAAAAGCTGTTTGCATCCCTCGCCCTCGCCGCCGTCGTTGCCCCCG :  838
Ibu8-merAD  : ..................................................................................... :   -
Tn5047      : GTTTTCCCTACGTCATGCCATTTTTCTACTAATCAGGAGTTCATCATGAAAAAGCTGTTTGCCTCCCTCGGTCTCGCCGCTTCGTTGCCCCCG :  940
                G F P Y V M P F F Y -            M K K L F A S L A L A A F V A P

Ibü8_merRTP : TGTGGGCCGCCACCCAGACCGTCACGCTGTCCGTGCCTGGCATGACCTGCGCCTCTTGCCCGATCACTGTCAAGCACGCGATTTCCAAGGTTGA :  932
Ibu8-merAD  : ..................................................................................... :   -
Tn5047      : TGTTCGCCGCCACTCAGACCGTAACGCTGTCCGTGCCTGGCATGACCTGCGCCTCTTGCCCGATCACTGTCAAGCACGCGCTTTCCAAGGTTGA : 1034
                V F A A T Q T V T L S V P G M T C A S C P I T V K H A L S K V E
```

Figure C-22a. **Alignment of the partly sequenced narrow spectrum resistant operon (NS) of the strain *Ps. stutzeri* Ibu8, including the *mer* genes *mer*R, *mer*T and *mer*P.** The merC gene and 5' end of meA could not be sequenced. Amino acid sequence of Tn5047 from *Acinetobacter calcoaceticus* KHP18 (accession no. AF213017) polypeptide is shown as standard single letter below the DNA sequence line. Black shade: 100% similarity. Start and stop codon are colored pink.

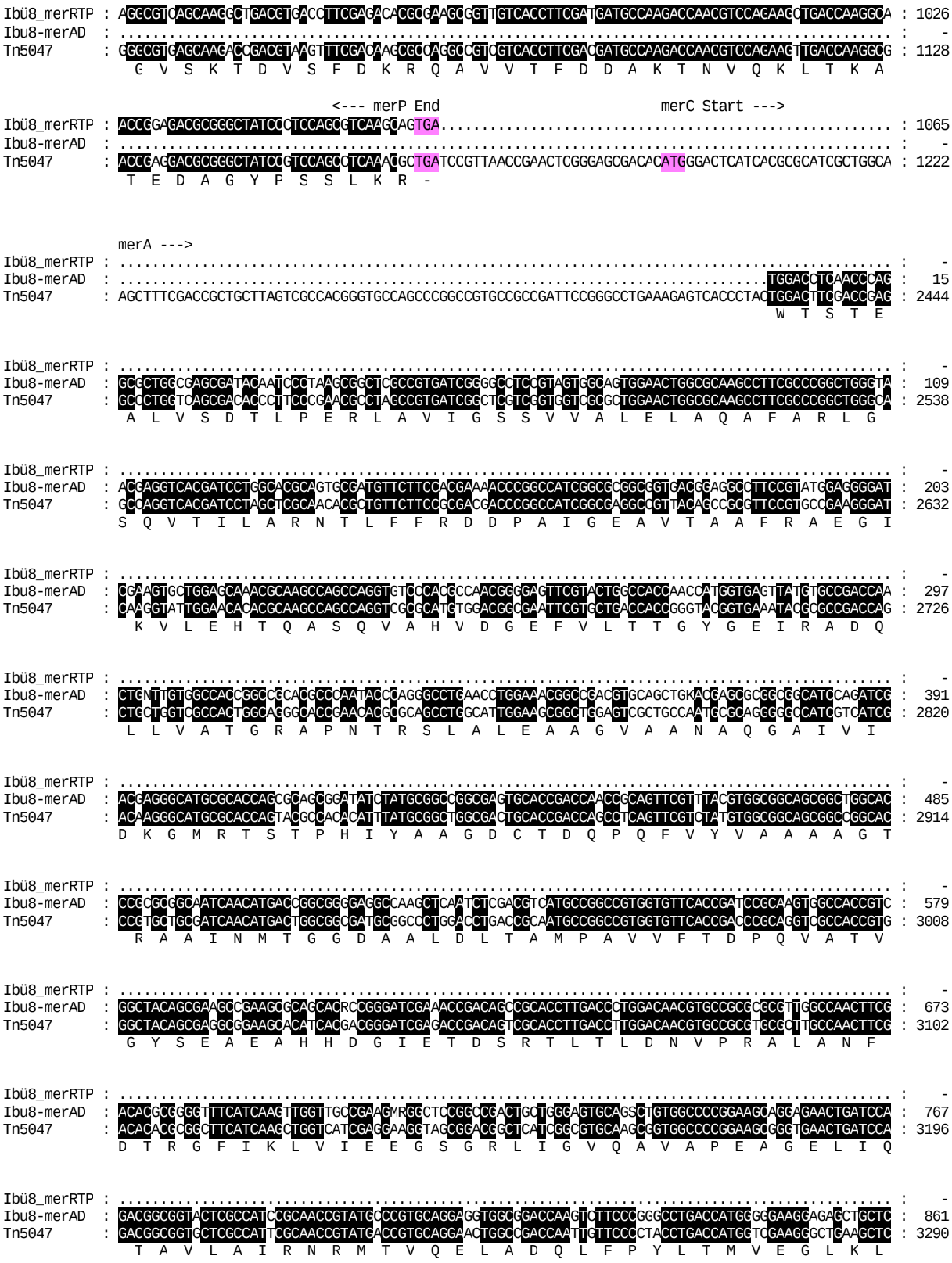

Figure C-22b. Continuing the alignment of the *mer* genes from Ibu8 with Tn5053, including the sequel of *mer*A and *mer*D. Amino acid sequence of Tn5047 from *Acinetobacter calcoaceticus* KHP18 (accession no. AF213017) polypeptide is shown as standard single letter below the DNA sequence line. Black shade: 100% similarity. Start and stop codon are colored pink.

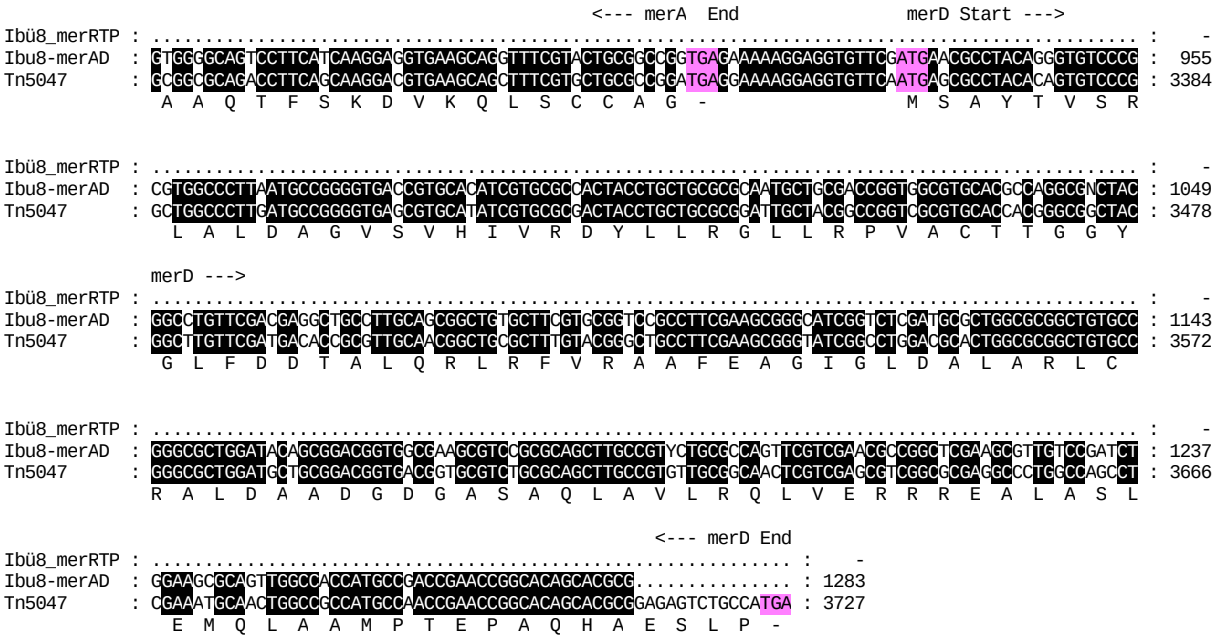

Figure C-22c. Continuing the alignment of the *mer* genes from Ibu8 with Tn5053, including the sequel of *mer*D. Amino acid sequence of Tn5047 from *Acinetobacter calcoaceticus* KHP18 (accession no. AF213017) polypeptide is shown as standard single letter below the DNA sequence line. Black shade: 100% similarity. Start and stop codon are colored pink.

- 2nd *mer* operon:

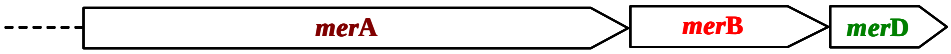


```
                merA Start --->
Ibü8-merA   : ATGACCCATCTAAAAATCACCGGCATGACCTGCGACTCGTGCGCGGCGCACGTCAAGGAAGCGCTGGAAAAAGTACCCGGCGTCCAATCTGCCA :  94
Ibü8-merABD : ............................................................................................... :   -
pDU1358     : ATGACCCATCTAAAAATCACCGGCATGACCTGCGACTCGTGCGCGGCGCACGTCAAGGAAGCGCTGGAAAAAGTACCCGGCGTCCAATCTGCCA :  94
                M  T  H  L  K  I  T  G  M  T  C  D  S  C  A  A  H  V  K  E  A  L  E  K  V  P  G  V  Q  S  A

Ibü8-merA   : TAGTGTCCTATGCCAAGGGCGCGGCCCAGCTCGCCCTTGATCCAGGCACAGCGCCGGACGCACTGACCGCCGCCGTGGCTGGCCTGGGCTACAA :  188
Ibü8-merABD : ............................................................................................... :   -
pDU1358     : TAGTGTCCTATGCCAAGGGCGCGGCCCAGCTCGCCCTTGATCCAGGCACAGCGCCGGACGCACTGACCGCCGCCGTGGCTGGCCTGGGCTACAA :  188
                I  V  S  Y  A  K  G  A  A  Q  L  A  L  D  P  G  T  A  P  D  A  L  T  A  A  V  A  G  L  G  Y  K

Ibü8-merA   : AGCGATGCTCGCCGATGCCCCGCCGACCGACAACCGCACTGGGCTGTTCGACAAGGTGCGCGGCTGGATGGGTGCCGCCGACAAGGGCAGCGGC :  282
Ibü8-merABD : ............................................................................................... :   -
pDU1358     : AGCGATGCTCGCCGATGCCCCGCCGACCGACAACCGCACTGGGCTGTTCGACAAGGTGCGCGGCTGGATGGGTGCCGCCGACAAGGGCAGCGGC :  282
                A  M  L  A  D  A  P  P  T  D  N  R  T  G  L  F  D  K  V  R  G  W  M  G  A  A  D  K  G  S  G

Ibü8-merA   : GGCGAGCGCCCGTTGCAAGTCGCCGTGATCGGCAGCGGTGGAGCCGCGATGGCGGCAGCACTGAAGGCCGTCGAGCAAGGCGCGCAGGTCACGC :  376
Ibü8-merABD : ............................................................................................... :   -
pDU1358     : GCCGAGCGCCCGTTGCAAGTCGCCGTGATCGGCAGCGGTGGAGCCGCGATGGCGGCAGCACTGAAGGCCGTCGAGCAAGGCGCGCAGGTCACGC :  376
                G  E  R  P  L  Q  V  A  V  I  G  S  G  G  A  A  M  A  A  A  L  K  A  V  E  Q  G  A  Q  V  T

Ibü8-merA   : TGATTGAGCGCGGCACCATCGGTGGCACCTGCGTCAACGTCGGTTGTGTGCCGTCCAAGATCATGATCCGCGCCGCCCACATCGCCCATCTGCG :  470
Ibü8-merABD : ............................................................................................... :   -
pDU1358     : TGATTGAGCGCGGCACCATCGGCGGCACCTGCGTCAACGTCGGTTGTGTGCCGTCCAAGATCATGATCCGCGCCGCCCACATCGCCCATCTGCG :  470
                L  I  E  R  G  T  I  G  G  T  C  V  N  V  G  C  V  P  S  K  I  M  I  R  A  A  H  I  A  H  L  R

Ibü8-merA   : CCGGGAAAGCCCATTCGACGGCGGCATGCCACCCACACCGCCGACGATCTTGCGCGAGCGGCTGCTGGCCCAGCAGCAGGCCCGTGTCGAAGAA :  564
Ibü8-merABD : ............................................................................................... :   -
pDU1358     : CCGGGAAAGCCCATTCGACGGCGGCATGCCACCCACACCGCCGACGATCTTGCGCGAGCGGCTGCTGGCCCAGCAGCAGGCCCGTGTCGAAGAA :  564
                R  E  S  P  F  D  G  G  M  P  P  T  P  P  T  I  L  R  E  R  L  L  A  Q  Q  Q  A  R  V  E  E

Ibü8-merA   : CTCCGTCATGCCAAGTACGAAGGCATCCTGGACGGCAATTCAGCCATCACCGTTGTGCACGGTGAAGCGCGTTTCAAGGACGACCAGAGCCTTA :  658
Ibü8-merABD : ............................................................................................... :   -
pDU1358     : CTCCGTCATGCCAAGTACGAAGGCATCCTGGACGGCAATTCAGCCATCACCGTTGGTCACGGTGAAGCGCGTTTCAAGGACGACCGAGACCTTA :  658
                L  R  H  A  K  Y  E  G  I  L  D  G  N  S  A  I  T  V  L  H  G  E  A  R  F  K  D  D  R  D  L

Ibü8-merA   : TCGTTAGTTTGAACGAGGGTGGTGAGCGCGTCGTGATGTTCGACCGCTGCCTGGTCGCCACGGGTGCCAGTCCGGCCATGCCGCCGATTCCGGG :  752
Ibü8-merABD : ............................................................................................... :   -
pDU1358     : GCGTTAGTTTGAACGAGGGTGGTGAGCGCGTCGTGATGTTCGACCGCTGCCTGGTCGCCACGGGTGCCAGTCCGGCCATGCCGCCGATTCCGGG :  752
                S  V  S  L  N  E  G  G  E  R  V  V  M  F  D  R  C  L  V  A  T  G  A  S  P  A  M  P  P  I  P  G

Ibü8-merA   : CCTGAAAGAGTCACCCTACTGGACTTCGACCGAGGCCTTGGTCAGCGACACCATTCCCGAACGCCTGGCCGTCATCGGCTCGTCGGTGGTGGCG :  846
Ibü8-merABD : ............................................................................................... :   -
pDU1358     : CCTGAAAGAGTCACCCTACTGGACTTCGACCGAGGCCTTGGTCAGCGACACCATTCCCGAACGCCTAGCCGTGATCGGCTCGTCGGTGGTCGCG :  846
                L  K  E  S  P  Y  W  T  S  T  E  A  L  V  S  D  T  I  P  E  R  L  A  V  I  G  S  S  V  V  A

Ibü8-merA   : CTGGAACTGGCGCAAGCCTTCGCCCGGCTGGGTAGCCAGGTCACGATCCTTGCGCGCAGCACGCTGTTCTTCCGCGAAGACCGTGCCATCGGCG :  940
Ibü8-merABD : ............................................................................................... :   -
pDU1358     : CTGGAACTGGCGCAAGCCTTCGCCCGGCTGGGCAGCCAGGTCACGATCCTAGCTCGCAACACGCTGTTCTTCCGCGACGACCGTCCATCGGCG :  940
                L  E  L  A  Q  A  F  A  R  L  G  S  Q  V  T  I  L  A  R  N  T  L  F  F  R  D  D  P  S  I  G
```

Figure C-23a. Alignment of the partly sequenced broad spectrum resistant (BS) operon of the strain *Ps. stutzeri* Ibu8, including the *mer* genes *mer*A, *mer*B and *mer*D. Amino acid sequence of pDU1358 polypeptide (accession no. M15049, Z49200 and M24940) is shown as standard single letter below the DNA sequence line. Black shade: 100% similarity. Start and stop codon are colored pink.

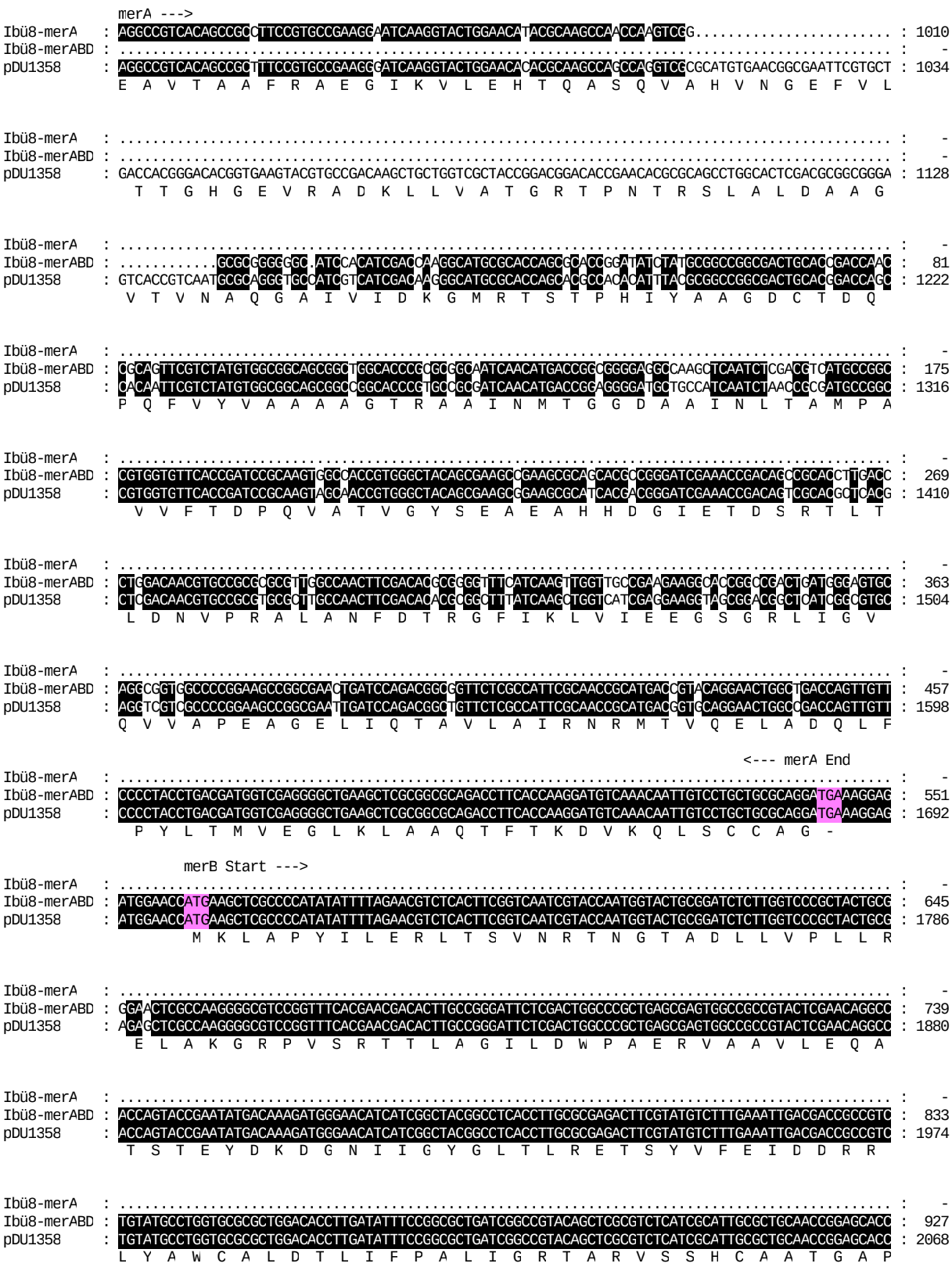

Figure C-23b. Continuing the alignment of the *mer* genes from Ibu8 with plasmid pDU1358. Amino acid sequence of reference polypeptide (accession no. M15049, Z49200 and M24940) is shown as standard single letter below the DNA sequence line. Black shade: 100% similarity. Start and stop codon are colored pink.

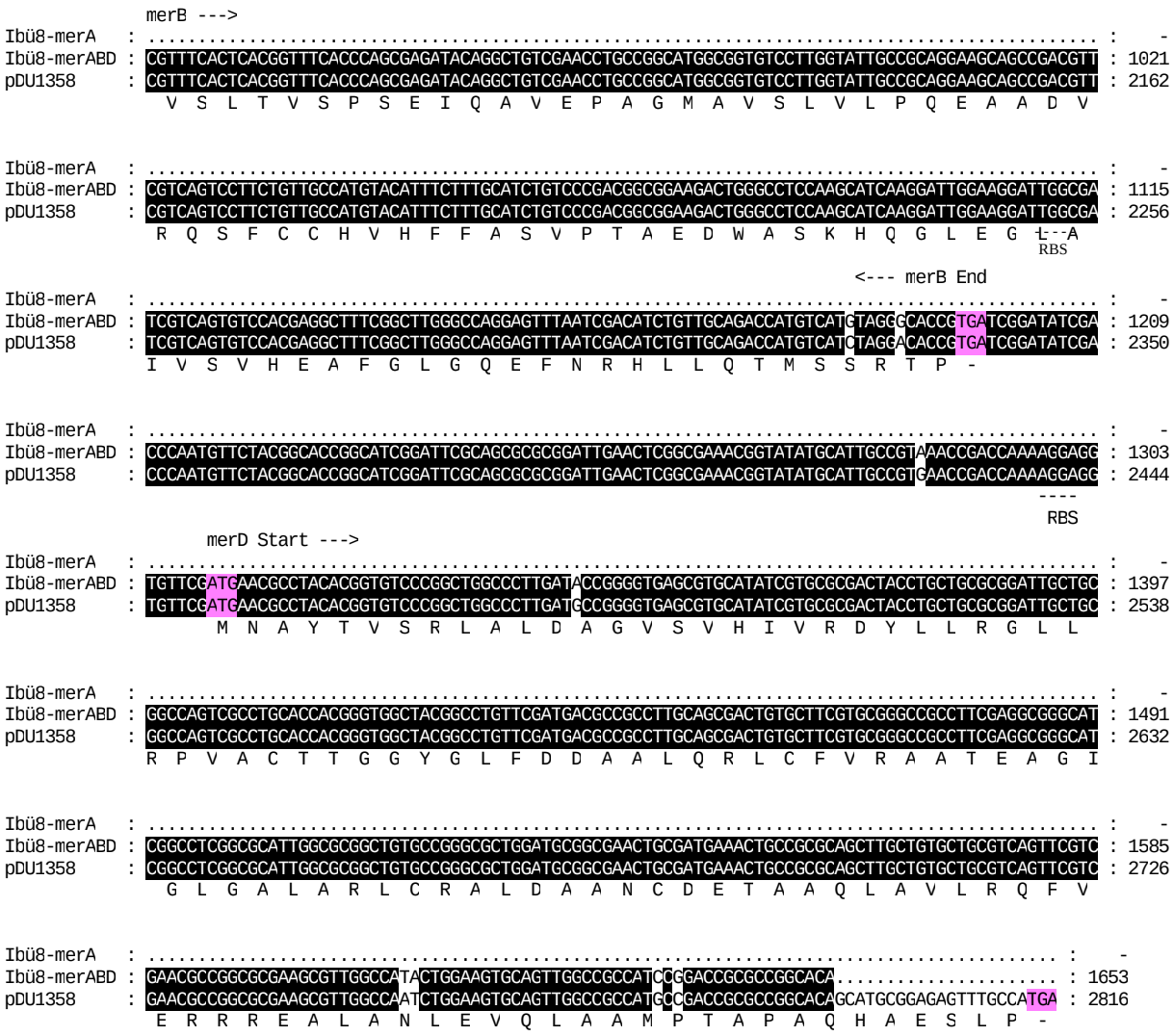

Figure C-23c. Continuing the alignment of the *mer* genes from Ibu8 with plasmid pDU1358. Amino acid sequence of pDU135 polypeptide (accession no. M15049, Z49200 and M24940) is shown as standard single letter below the DNA sequence line. Black shade: 100% similarity. Start and stop codon are colored pink.

4. Ps. putida Elb2

- 1st *mer* operon:

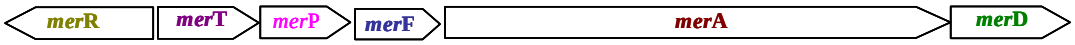


```
                End merR --->
Elb2-merRTPFA : ----------------------------------------------------GGGCAGGAAACGTTCCCCTTCCGCGCATGGCAGGCG :  36
Elb2-merAD    : ------------------------------------------------------------------------------------- :   -
Tn5053        : CTACACCGCGTCCGCACTGCGCGGTTCTTTCTTCCCTTGCAGTGACGCAATCAGCGGGCAGGAAACGTTCCCCTTCCGCGCATGGCAGGCG :  91
                  -  V  A  D  A  S  R  P  E  K  K  G  Q  L  S  A  I  L  P  C  S  V  N  G  K  R  A  H  C  A

Elb2-merRTPFA : CACACCAAATCAGACAGCACGGCCTCCATGCGCGCCAGGTCAGCCATCCTCTCGCGCACGTCCTTGAGCTTGTGCTCGGCCAGGCTGCTGG :  127
Elb2-merAD    : ------------------------------------------------------------------------------------- :   -
Tn5053        : CACACCAAATCAGACAGCACGGCCTCCATGCGCGCCAGGTCAGCCATCCTCTCGCGCACGTCCTTGAGCTTGTGCTCGGCCAGGCTGCTGG :  182
                  C  V  L  D  S  L  V  A  E  M  R  A  L  D  A  M  R  E  R  V  D  K  L  K  H  E  A  L  S  S  A

Elb2-merRTPFA : CTTCCTCGCAATGGGTGCCATCCTCCAGCCGCAGCAGCTCGGCGATCTCATCCAGGCTGAAGCCCAACCGCTGGGCTGATTTCACGAAGCG :  218
Elb2-merAD    : ------------------------------------------------------------------------------------- :   -
Tn5053        : CTTCCTCACAATGGGTGCCATCCTCCAGCCGCAGCAGCTCGGCGATCTCATCCAGGCTGAAGCCCAACCGCTGGGCTGATTTCACGAAGCG :  273
                  E  E  C  H  T  G  D  E  L  R  L  L  E  A  I  E  D  L  S  F  G  L  R  Q  A  S  K  V  F  R

Elb2-merRTPFA : CACCCGCGTTACATCCGTCTCGCCATAGCGGCGAATGCTGCCGTAAGGCTTGTCCGGTTCCGGGAGCAAGCCCTTGCGCTGATAGAACCGG :  309
Elb2-merAD    : ------------------------------------------------------------------------------------- :   -
Tn5053        : CACCCGCGTTACATCCGTCTCGCCATAGCGGCGAATGCTGCCGTAAGGCTTGTCCGGTTCCGGGAGCAAGCCCTTGCGCTGATAGAACCGG :  364
                  V  R  T  V  D  T  E  G  Y  R  R  I  S  G  Y  P  K  D  P  E  P  L  L  G  K  R  Q  Y  F  R

                                                                  <--- merR Start
Elb2-merRTPFA : ATGGTCTCCACATTGACCCCGGCCGTCCTGGCGAAAACGCCAATGGTCAGGTTCTCCAAATTGTTTTCCATATCGCTTGACTCCGTACATA :  400
Elb2-merAD    : ------------------------------------------------------------------------------------- :   -
Tn5053        : ATGGTCTCCACATTGACCCCGGCCGTCCTGGCGAAAACGCCAATGGTCAGGTTCTCCAAATTGTTTTCCATATCGCTTGACTCCGTACATA :  455
                  I  T  E  V  N  V  G  A  T  R  A  F  V  G  I  T  L  N  E  L  N  N  E  M

                                                                  merT Start --->
Elb2-merRTPFA : ACTACGGAAGTAAGCTTAAGCTATCCAATTCAGATTCGAAAGGACAAACGTATGTCTGAACCTCAAAACGGGCGCGGCGCGCTCTTCACTG :  491
Elb2-merAD    : ------------------------------------------------------------------------------------- :   -
Tn5053        : ACTACGGAAGTAAGCTTAAGCTATCCAATTCAGATTCGAAAGGACAAACGTATGTCTGAACCTCAAAACGGGCGCGGCGCGCTCTTCACTG :  546
                                                  ----          M  S  E  P  Q  N  G  R  G  A  L  F  T
                                                  RBS

Elb2-merRTPFA : GCGGGCTGGCCGCCATCCTCGCCTCGGCTTGCTGCCTCGGGCCGCTGGTTCTGATCGCCTTGGGGTTCAGCGGCGCTTGGATCGGCAACTT :  582
Elb2-merAD    : ------------------------------------------------------------------------------------- :   -
Tn5053        : GCGGGCTGGCCGCCATCCTCGCCTCGGCTTGCTGCCTCGGGCCGCTGGTTCTGATCGCCTTGGGGTTCAGCGGCGCTTGGATCGGCAACTT :  637
                  G  G  L  A  A  I  L  A  S  A  C  C  L  G  P  L  V  L  I  A  L  G  F  S  G  A  W  I  G  N  L

Elb2-merRTPFA : GACGGTGTTGGAACCCTATCGCCCCATCTTTATCGGCGTGGCGCTGGTGGCGTTGTTCTTCGCCTGGCGGCGCATCTACCGGCCGTCAGCC :  673
Elb2-merAD    : ------------------------------------------------------------------------------------- :   -
Tn5053        : GACGGTGTTGGAACCCTATCGCCCCATCTTTATCGGCGTGGCGCTGGTGGCGTTGTTCTTCGCCTGGCGGCGCATCTACCGGCCGTCAGCC :  728
                  T  V  L  E  P  Y  R  P  I  F  I  G  V  A  L  V  A  L  F  F  A  W  R  R  I  Y  R  P  S  A

Elb2-merRTPFA : GCCTGCAAACCGGGTGAGGTTTGCGCGATTCCCCAAGTGCGAGCTACTTACAAGCTCATTTTCTGGGGCGTGGCCGTGCTGGTTTTGGTCG :  764
Elb2-merAD    : ------------------------------------------------------------------------------------- :   -
Tn5053        : GCCTGCAAACCGGGTGAGGTTTGCGCGATTCCCCAAGTGCGAGCTACTTACAAGCTCATTTTCTGGGGCGTGGCCGTGCTGGTTTTGGTCG :  819
                  A  C  K  P  G  E  V  C  A  I  P  Q  V  R  A  T  Y  K  L  I  F  W  G  V  A  V  L  V  L  V
```

Figure C-24a. **Alignment of the narrow spectrum resistant *mer* operon of *Ps. putida* Elb2.** Amino acid sequence of Tn5053 polypeptide from *Xanthomonas sp. W17* (accession no. L40585) is shown as standard single letter below the DNA sequence line. Black shade: 100% similarity. Start and stop codon are colored pink.

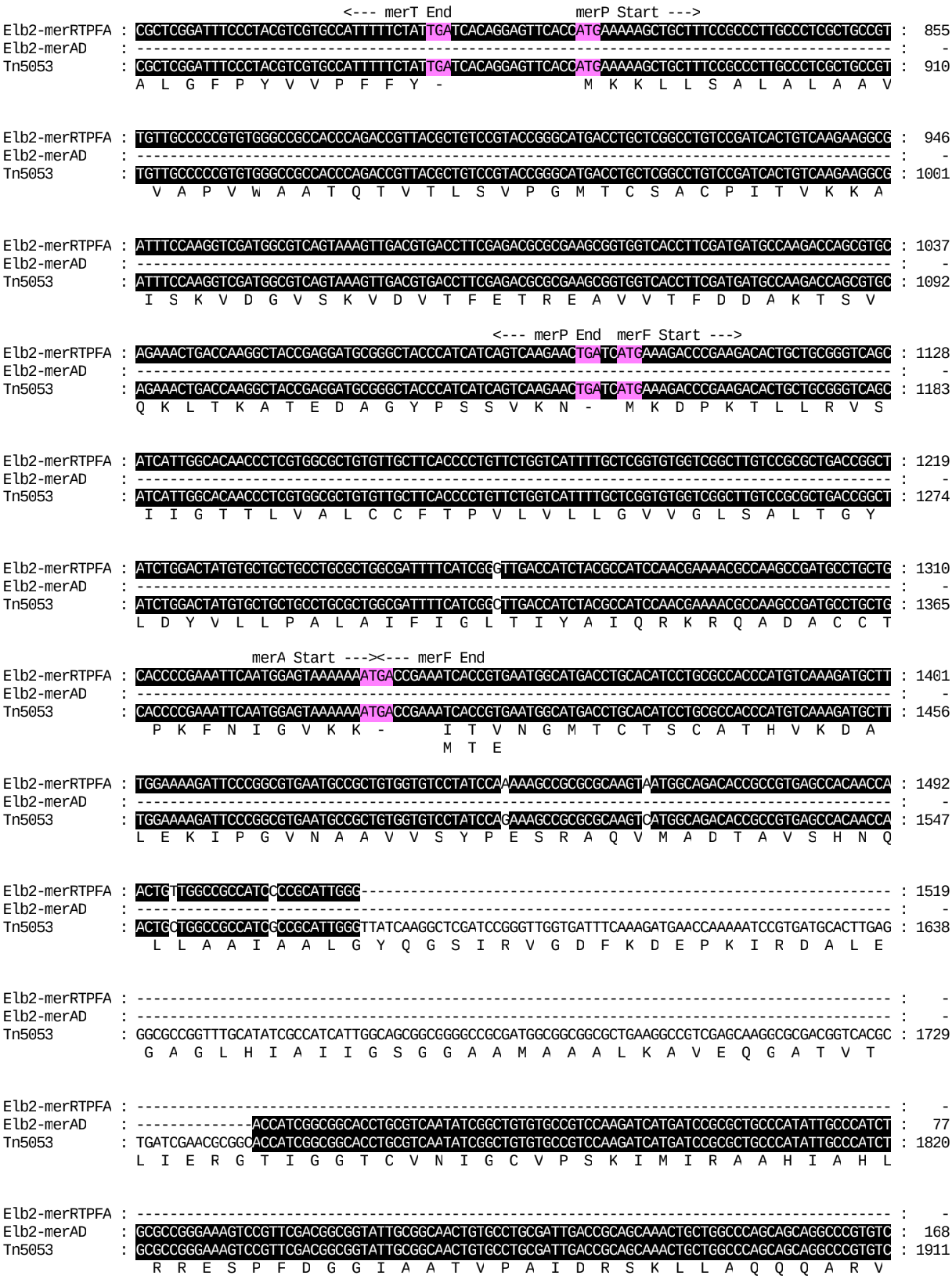

Figure C-24b. Continuing the alignment of the *mer* genes (*mer*F and *mer*A) from Elb2 with plasmid Tn5053. In *mer*A is a gap of 168 nucleotide which could not be sequenced (1575 bp – 1743 bp). Amino acid sequence of reference polypeptide (accession no. L40585) is shown as standard single letter below the DNA sequence line. Black shade: 100% similarity. Start and stop codon are colored pink.

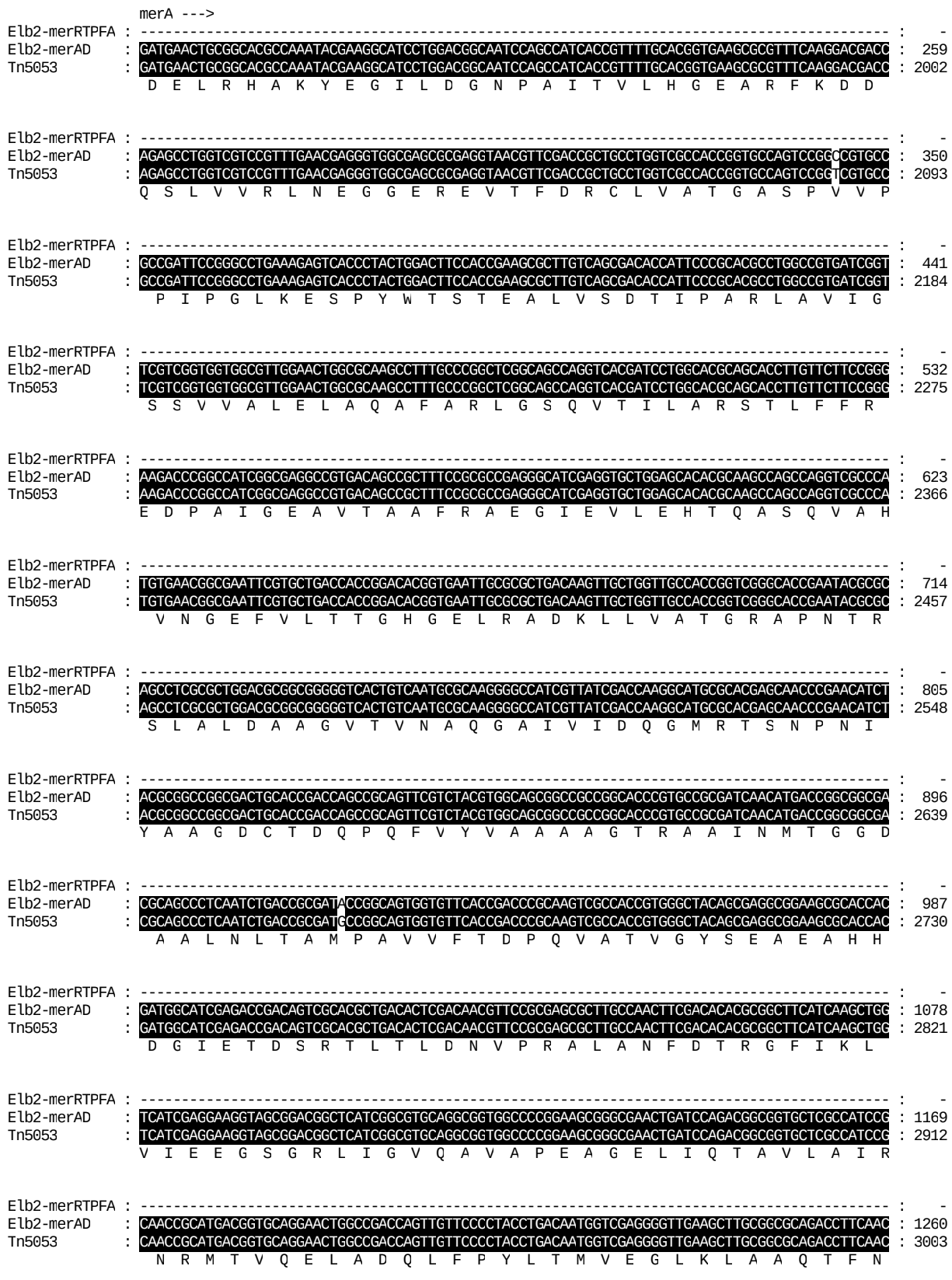

Figure C-24c. Continuing the alignment of the *mer* genes (*mer*A) from Elb2 with plasmid Tn5053. Amino acid sequence of reference polypeptide (accession no. L40585) is shown as standard single letter below the DNA sequence line. Black shade: 100% similarity. Start and stop codon are colored pink.

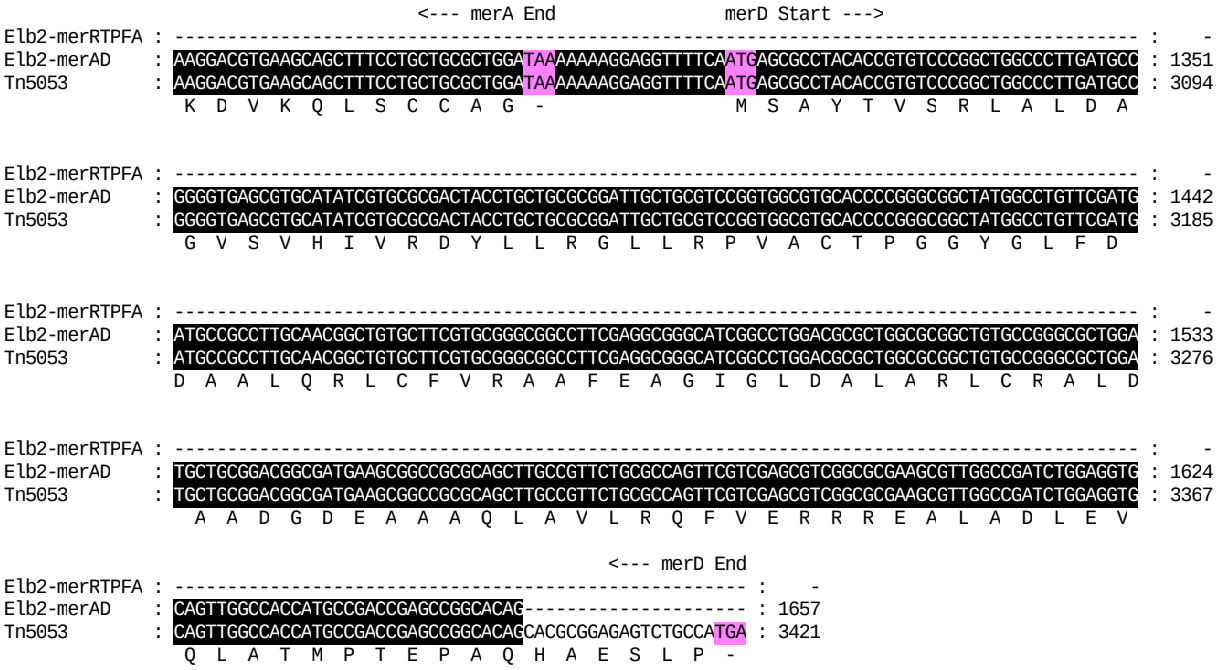

Figure C-24d. Continuing the alignment of the *mer* genes (*mer*A and *mer*D) from Elb2 with plasmid Tn5053. Amino acid sequence of reference polypeptide (accession no. L40585) is shown as standard single letter below the DNA sequence line. Black shade: 100% similarity. Start and stop codon are colored pink.

- 2nd *mer* operon:

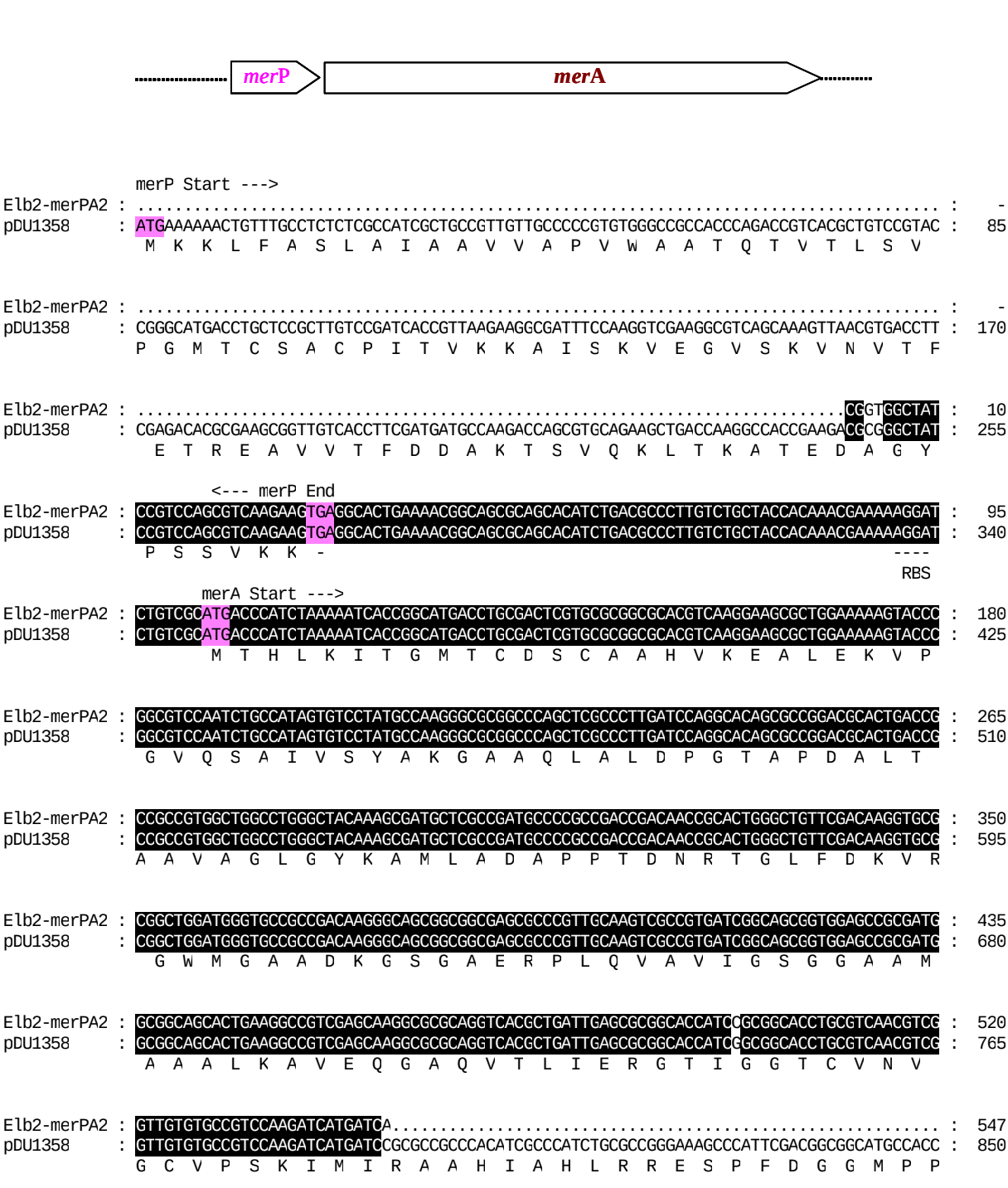

Figure C-25. **Alignment of the partly sequenced *mer* operon of the strain *Ps.putida* Elb2, including the *mer* genes *mer*P and *mer*A$_2$ with pDU1358.** Presumably a broad spectrum resistant operon (BS). Amino acid sequence of pDU1358 polypeptide (accession no. M15049, Z49200 and M24940) is shown as standard single letter below the DNA sequence line. Black shade: 100% similarity. Start and stop codon are colored pink.

- 3rd *mer* operon:

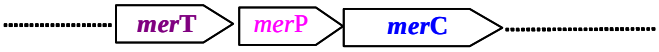

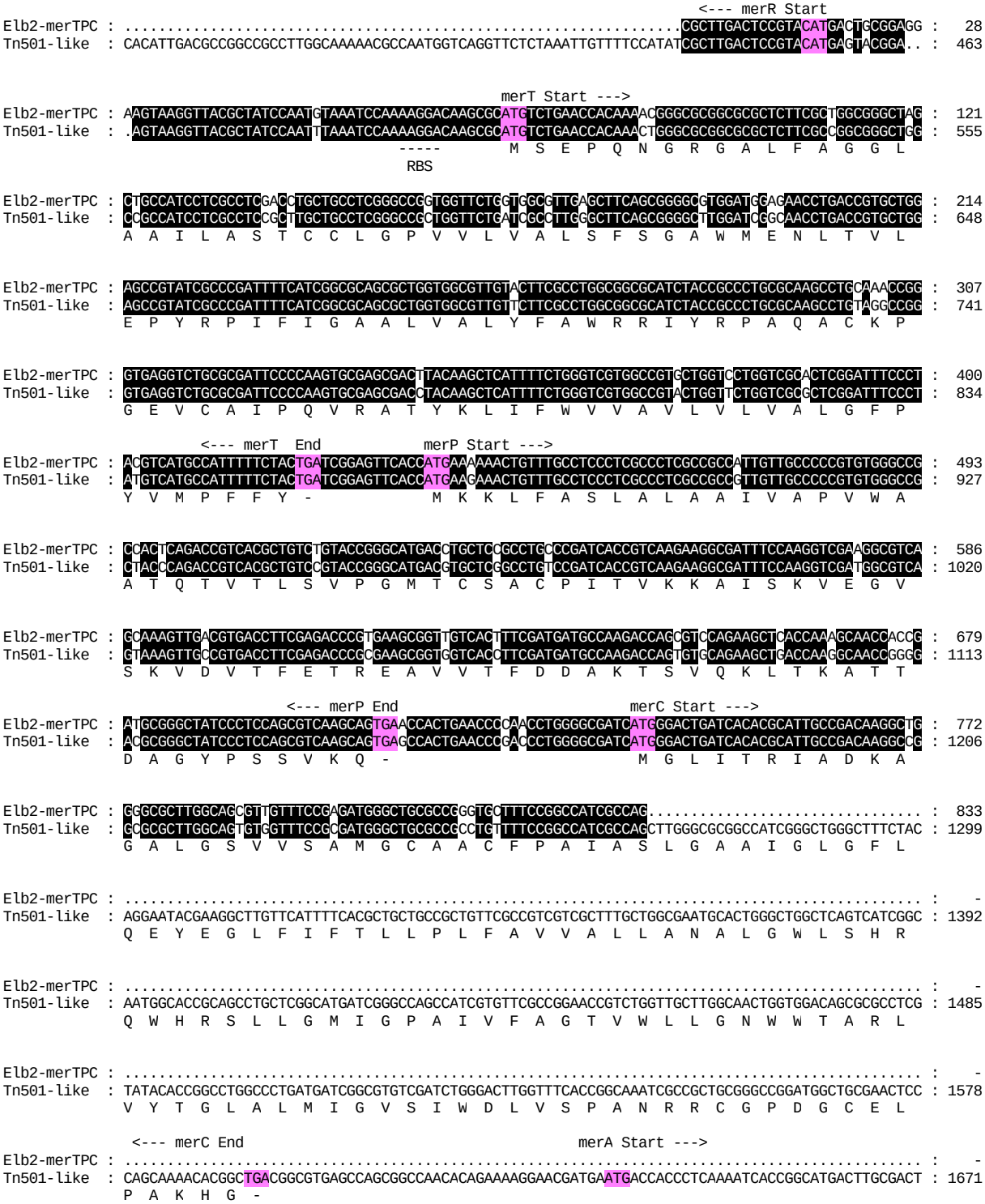

Figure C-26. **Alignment of partly sequenced mer operon of *Ps. putida* Elb2, including the *mer* genes *mer*T, *mer*P and *mer*C.** Amino acid sequence of Tn501-like polypeptide from *Delftia acidovorans* (accession no. AAP88279, AAP88280 and AAP88281) is shown as standard single letter below the DNA sequence line. Black shade: 100% similarity. Start and stop codon are colored pink.

5. *Ps. putida Kon12*

- 1st *mer* operon:


```
          End merR --->
Kon12   : ..........................................................AGAAACGTTCCCTTGCCGCGCATGGCAGGC :   30
pDU1358 : CTACACCGCGTCGGCACCACGCGGCTCTTTCTCCCCTTGCAGCGAAGCAATCAGCGGGCAAGAAACGTTCCCTTGCCGCGCATGGCAGGC :   90
            -  V  A  D  A  G  R  P  E  K  E  G  Q  L  S  A  I  L  P  C  S  V  N  G  Q  R  A  H  C  A

Kon12   : GAACACAAGTTCGGATAGCACGGTTTCCATGCGCGCCAGGTCGGTCATTTTTTCGCGCACGTCCTGAAGCTTGTGCTCGGCCAGGCTGCT :  120
pDU1358 : GAACACAAGTTCGGATAGCACGGTTTCCATGCGCGCCAGGTCGGTCATTTTTTCGCGCACGTCCTGAAGCTTGTGCTCGGCCAGGCTGCT :  180
            F  V  L  E  S  L  V  T  E  M  R  A  L  D  T  M  K  E  R  V  D  Q  L  K  H  E  A  L  S  S

Kon12   : GGCTTCCTCGCAGTGGGTGCCGTCATCCAGCCTCAGCAGCTCTGCGATCTCGTCGAGGCTGAATCCGAGCCGCTGGGCTGATTTCACGAA :  210
pDU1358 : GGCTTCCTCGCAGTGGGTGCCGTCATCCAGCCTCAGCAGCTCTGCGATCTCGTCGAGGCTGAATCCGAGCCGCTGGGCTGATTTCACGAA :  270
            A  E  E  C  H  T  G  D  D  L  R  L  L  E  A  I  E  D  L  S  F  G  L  R  Q  A  S  K  V  F

Kon12   : GCGCACCCGCGTCACATCCGCCTCGCCATAGCGGCGGATGCTGCCATAGGGCTTGTCCGGCTCCGGCAACAAGCCCTTGCGCTGATAGAA :  300
pDU1358 : GCGCACCCGCGTCACATCCGCCTCGCCATAGCGGCGGATGCTGCCATAGGGCTTGTCCGGCTCCGGCAACAAGCCCTTGCGCTGATAGAA :  360
            R  V  R  T  V  D  A  E  G  Y  R  R  I  S  G  Y  P  K  D  P  E  P  L  L  G  K  R  Q  Y  F

                                                                                <--- merR Start
Kon12   : CCGGATTGTTTCCACGTTGACCCCGGCCGCCTTGGCGAAAACGCCAATAGTCAGATTCTCCAAATTTTTTTCCATATCGCTTGACTCCGT :  390
pDU1358 : CCGGATTGTTTCCACGTTGACCCCGGCCGCCTTGGCGAAAACGCCAATAGTCAGATTCTCCAAATTTTTTTCCATATCGCTTGACTCCGT :  450
            R  I  T  E  V  N  V  G  A  A  K  A  F  V  G  I  T  L  N  E  L  N  K  E  M

                                                                    merT Start --->
Kon12   : ACATTGGTACGGAAGTAAGCTTAAGCTATCCAATCCAGATTTGAAAGGACAAGCGTATGTCTGAACCTCAAAACGGGCGCGGGGCGCTCT :  480
pDU1358 : ACATTGGTACGGAAGTAAGCTTAAGCTATCCAATCCAGATTTGAAAGGACAAGCGTATGTCTGAACCTCAAAACGGGCGCGGGGCGCTCT :  540
                                                  ----          M  S  E  P  Q  N  G  R  G  A  L
                                                  RBS

Kon12   : TCACTGGCGGGCTAGCCGCCATCCTCGCCTCGGCTTGCTGCCTGGGGCCGCTGGTTCTGATCGCCCTGGGGTTCAGCGGCGCTTGGATCG :  570
pDU1358 : TCACTGGCGGGCTAGCCGCCATCCTCGCCTCGGCTTGCTGCCTGGGGCCGCTGGTTCTGATCGCCCTGGGGTTCAGCGGCGCTTGGATCG :  630
            F  T  G  G  L  A  A  I  L  A  S  A  C  C  L  G  P  L  V  L  I  A  L  G  F  S  G  A  W  I

Kon12   : GCAACTTGACGGTGTTGGAACCCTATCGCCCGATCTTCATCGGCGCGGCGTTGGTGGCGCTGTTTTTCGCCTGGCGGCGCATCTACCGAC :  660
pDU1358 : GCAACTTGACGGTGTTGGAACCTTATCGCCCGATCTTCATCGGCGCGGCGTTGGTGGCGCTGTTTTTCGCCTGGCGGCGCATCTACCGAC :  720
            G  N  L  T  V  L  E  P  Y  R  P  I  F  I  G  A  A  L  V  A  L  F  F  A  W  R  R  I  Y  R

Kon12   : CGGCGCAAGCCTGCAAACCAGGGGATGTGTGTGCGATTCCCCAAGTGCGCGCTACTTACAAGCTCATTTTCTGGGTCGTGGCCGCGCTGG :  750
pDU1358 : CGGCGCAAGCCTGCAAACCAGGGGATGTGTGTGCGATTCCCCAAGTGCGCGCTACTTACAAGCTCATTTTCTGGGTCGTGGCCGCGCTGG :  810
            P  A  Q  A  C  K  P  G  D  V  C  A  I  P  Q  V  R  A  T  Y  K  L  I  F  W  V  V  A  A  L

                                                <--- merT End                merP Start --->
Kon12   : TTCTGGTCGCGCTCGGATTTCCCTACGTCATGCCATTTTTCTATTAATCACAGGAGTTCATCATGAAAAAACTGTTTGCCTCTCTCGCCA :  840
pDU1358 : TTCTGGTCGCGCTCGGATTTCCCTACGTCATGCCATTTTTCTATTAATCACAGGAGTTCATCATGAAAAAACTGTTTGCCTCTCTCGCCA :  900
            V  L  V  A  L  G  F  P  Y  V  M  P  F  F  Y  -                M  K  K  L  F  A  S  L  A

Kon12   : TCGCTGCCGTTGTTGCCCCCGTGTGGGCCGCCACCCAGACCGTCACGCTGTCCGTACCGGGCATGACCTGCTCCGCTTGTCCGATCACCG :  930
pDU1358 : TCGCTGCCGTTGTTGCCCCCGTGTGGGCCGCCACCCAGACCGTCACGCTGTCCGTACCGGGCATGACCTGCTCCGCTTGTCCGATCACCG :  990
            L  A  A  V  V  A  P  V  W  A  A  T  Q  T  V  T  L  S  V  P  G  M  T  C  S  A  C  P  I  T

Kon12   : TTAAGAAGGCGATTTCCAAGGTCGAAGGCGTCAGCAAAGTTAACGTGACCTTCGAGACACGCGAAGCGGTTGTCACCTTCGATGATGCCA : 1020
pDU1358 : TTAAGAAGGCGATTTCCAAGGTCGAAGGCGTCAGCAAAGTTAACGTGACCTTCGAGACACGCGAAGCGGTTGTCACCTTCGATGATGCCA : 1080
            V  K  K  A  I  S  E  V  E  G  V  S  K  V  D  V  T  F  E  T  R  Q  A  V  V  T  F  D  D  A
```

Figure C-27a. **Alignment of the broad spectrum resistant operon (BS) of the strain *Ps. p*. Kon12,** including the *mer* genes R, T, P, A, B and D. Amino acid sequence of the plasmid pDU1358 polypeptide (accession no. M15049, Z49200 and M24940) is shown as standard single letter below the DNA sequence line. Black shade: 100% similarity. Start and stop codon are colored pink.

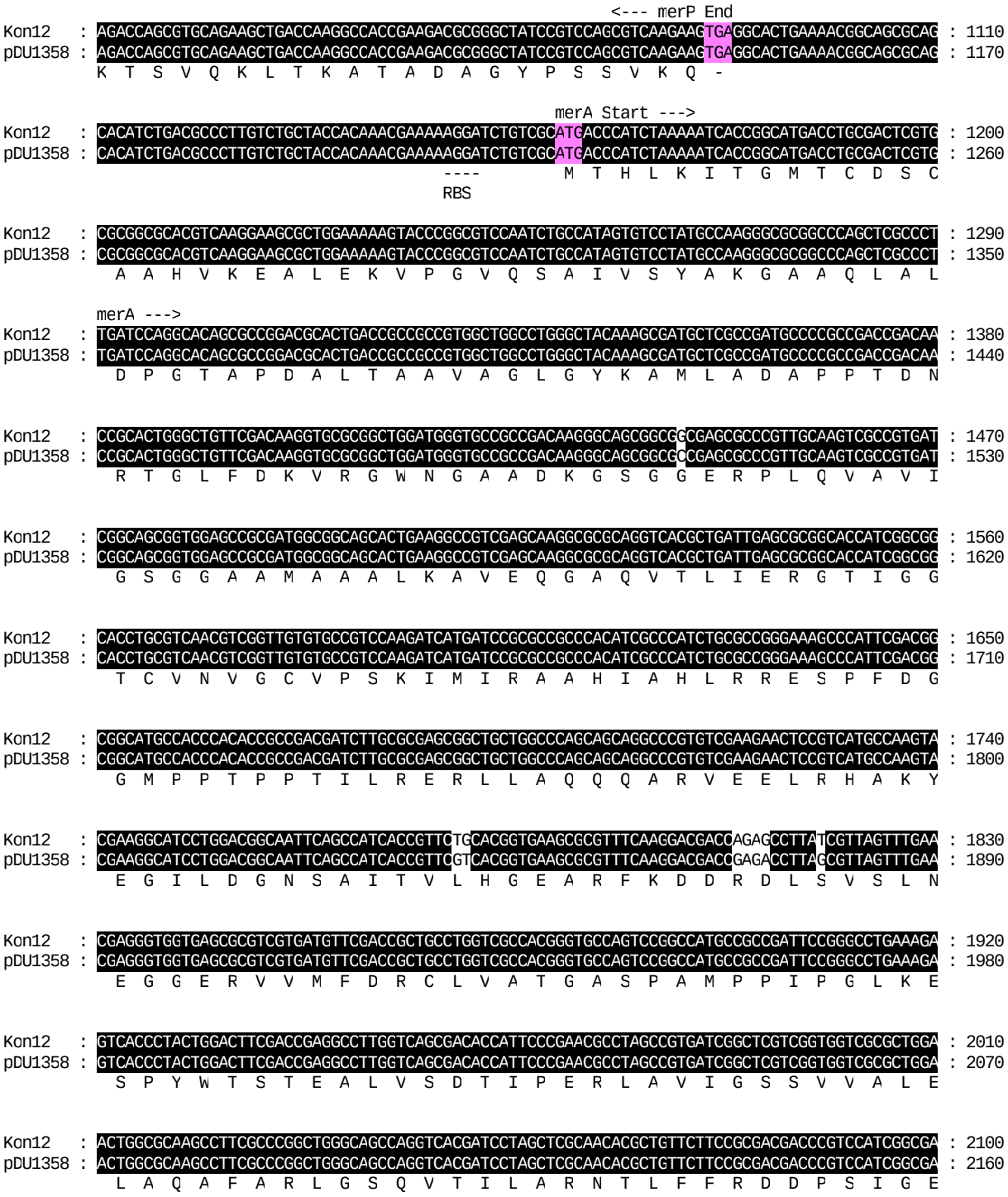

Figure C-27b. Continuing the alignment of the *mer*A gene from Kon12 with plasmid pDU1358. In *mer*A is a gap of 168 nucleotide which could not be sequenced (1575 bp – 1743 nt). Amino acid sequence of reference polypeptide (accession no. M15049, Z49200 and M24940) is shown as standard single letter below the DNA sequence line. Black shade: 100% similarity. Start and stop codon are colored pink.

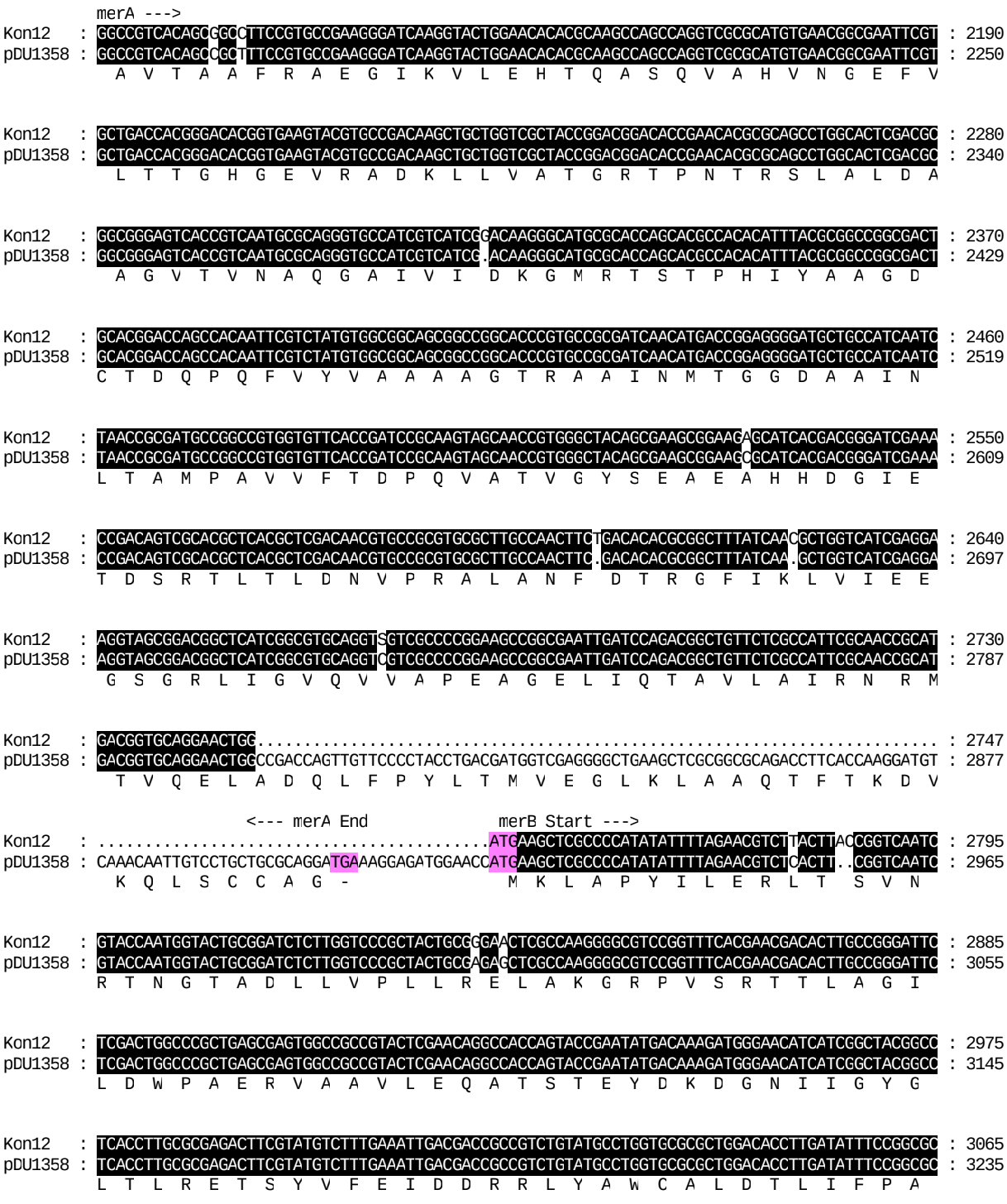

Figure C-27c. Continuing the alignment of the *mer* genes (*mer*A and *mer*B) from Kon12 with plasmid pDU1358. In *mer*A is a gap of 114 nucleotide which was not be sequenced (2919 bp – 2805 bp). Amino acid sequence of pDU1358 polypeptide (accession no. M15049, Z49200 and M24940) is shown as standard single letter below the DNA sequence line. Black shade: 100% similarity. Start and stop codon are colored pink.

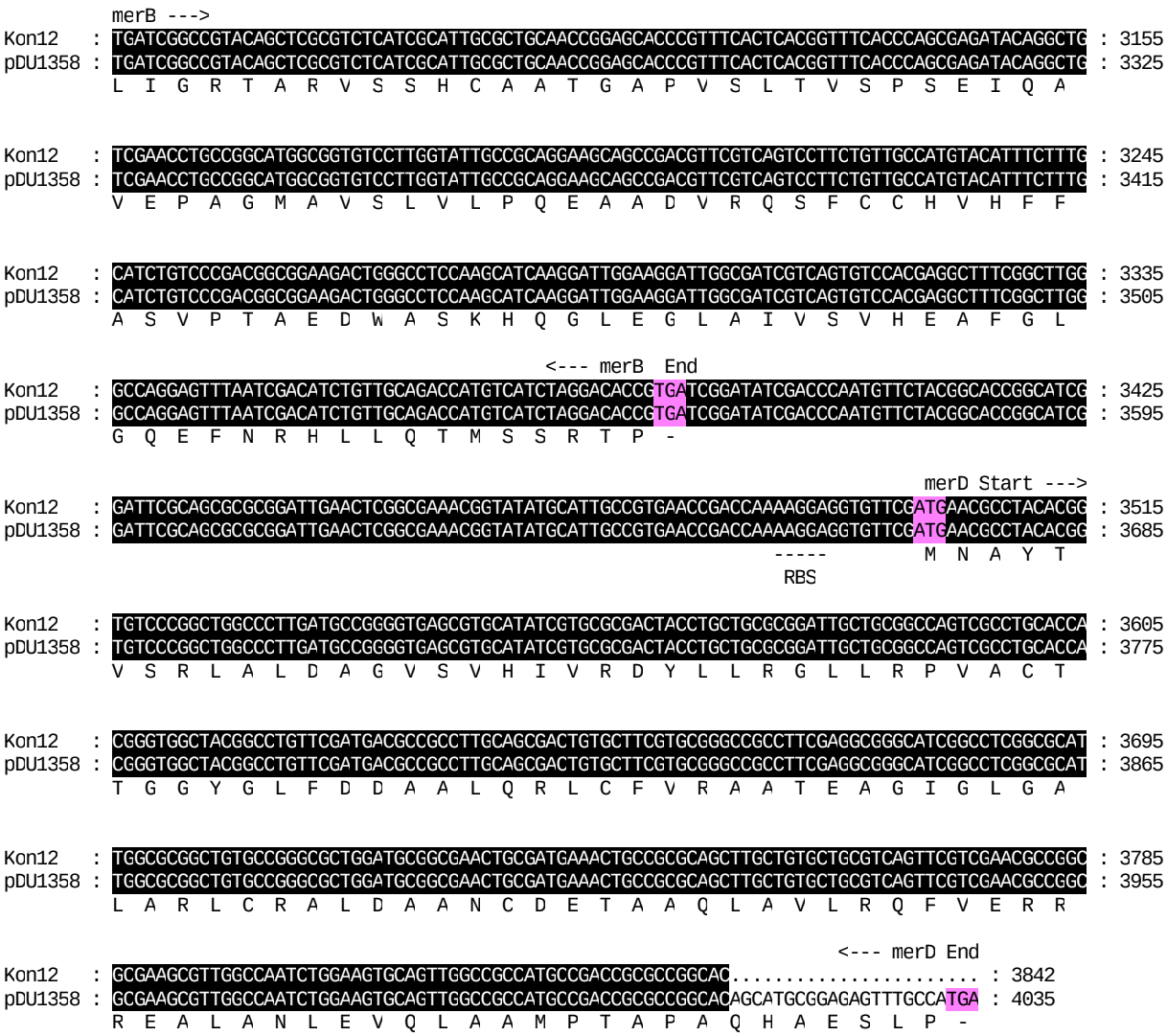

Figure C-27d. Continuing the alignment of the *mer*B and *mer*D gene from Kon12 with plasmid pDU1358. Amino acid sequence of pDU1358 polypeptide (accession no. M15049, Z49200 and M24940) is shown as standard single letter below the DNA sequence line. Black shade: 100% similarity. Start and stop codon are colored pink.

6. Citrobacter freundii Tin2

- 1st *mer* operon:

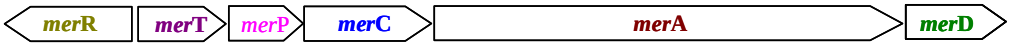

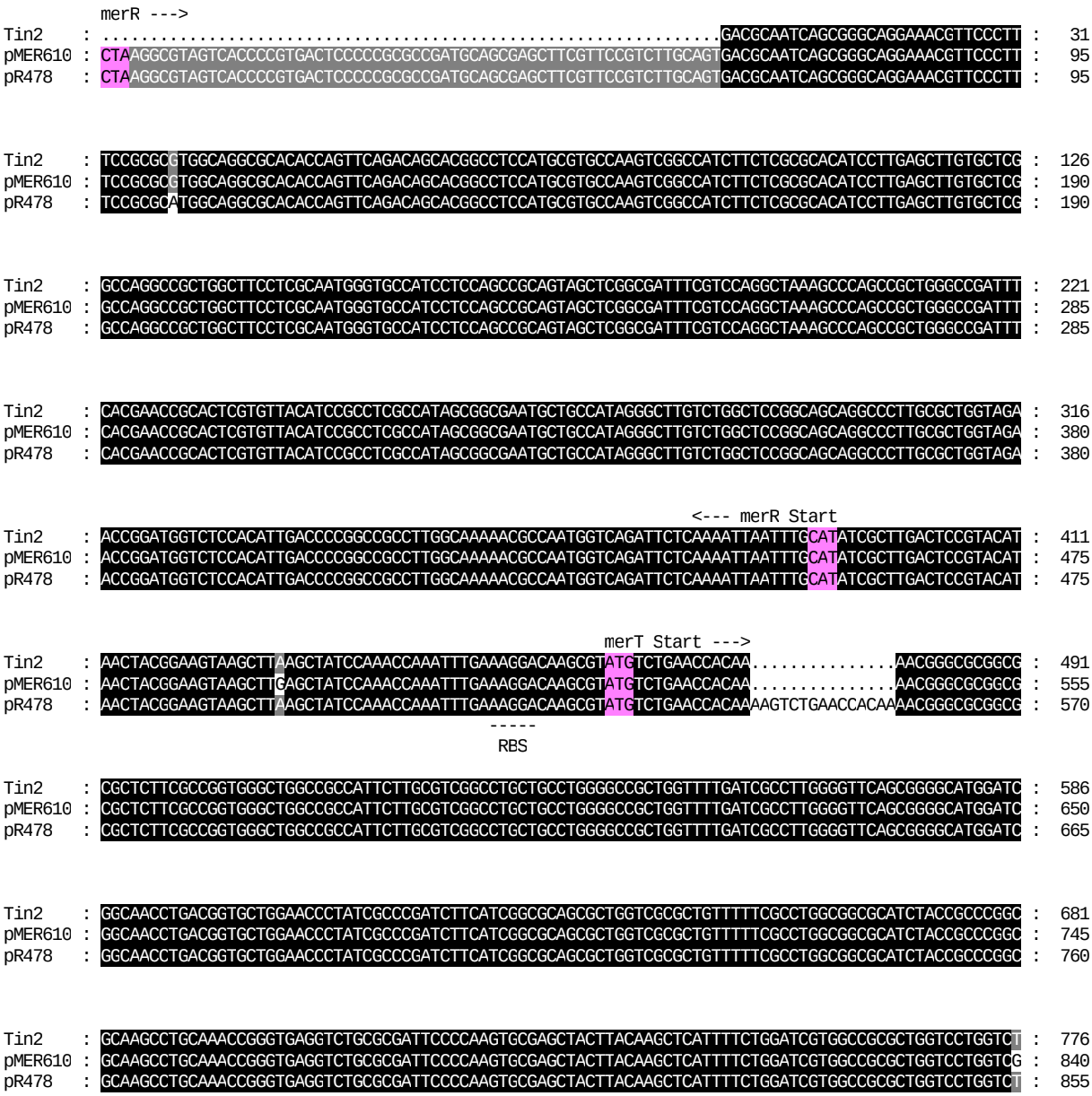

Figure C-28a. **Alignment of the narrow spectrum resistant *mer* operon of *Citrobacter freundii* Tin2**. The nucleotide sequence is aligned with plasmid pMER610 from *Alcaligenes sp.* (accession no.Y08993) and plasmid pR478 from *Serratia marcescens* (accession no. BX664015), including the *mer* genes R, T, P, C, A and D. Ribosomal binding site are shown below the DNA sequence. Black shade: 100% similarity. Start and stop codon are colored pink.

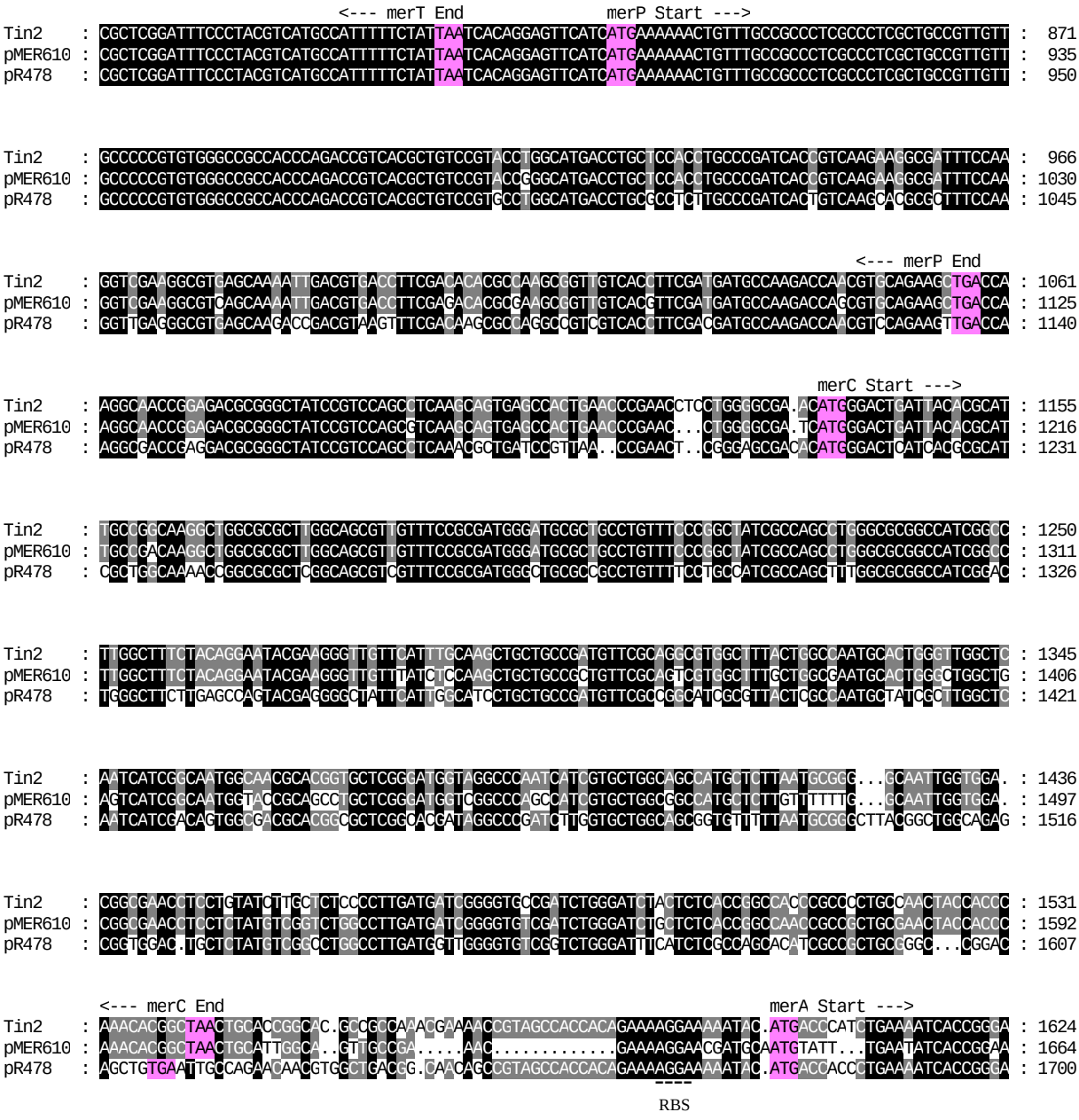

Figure C-28b. Continuing the alignment of *mer*TPCA from *Citrobacter freundii* Tin2 with plasmids pMER and pR478. Ribosomal binding site are shown below the DNA sequence. Black shade: 100% similarity. Start and stop codon are colored pink.

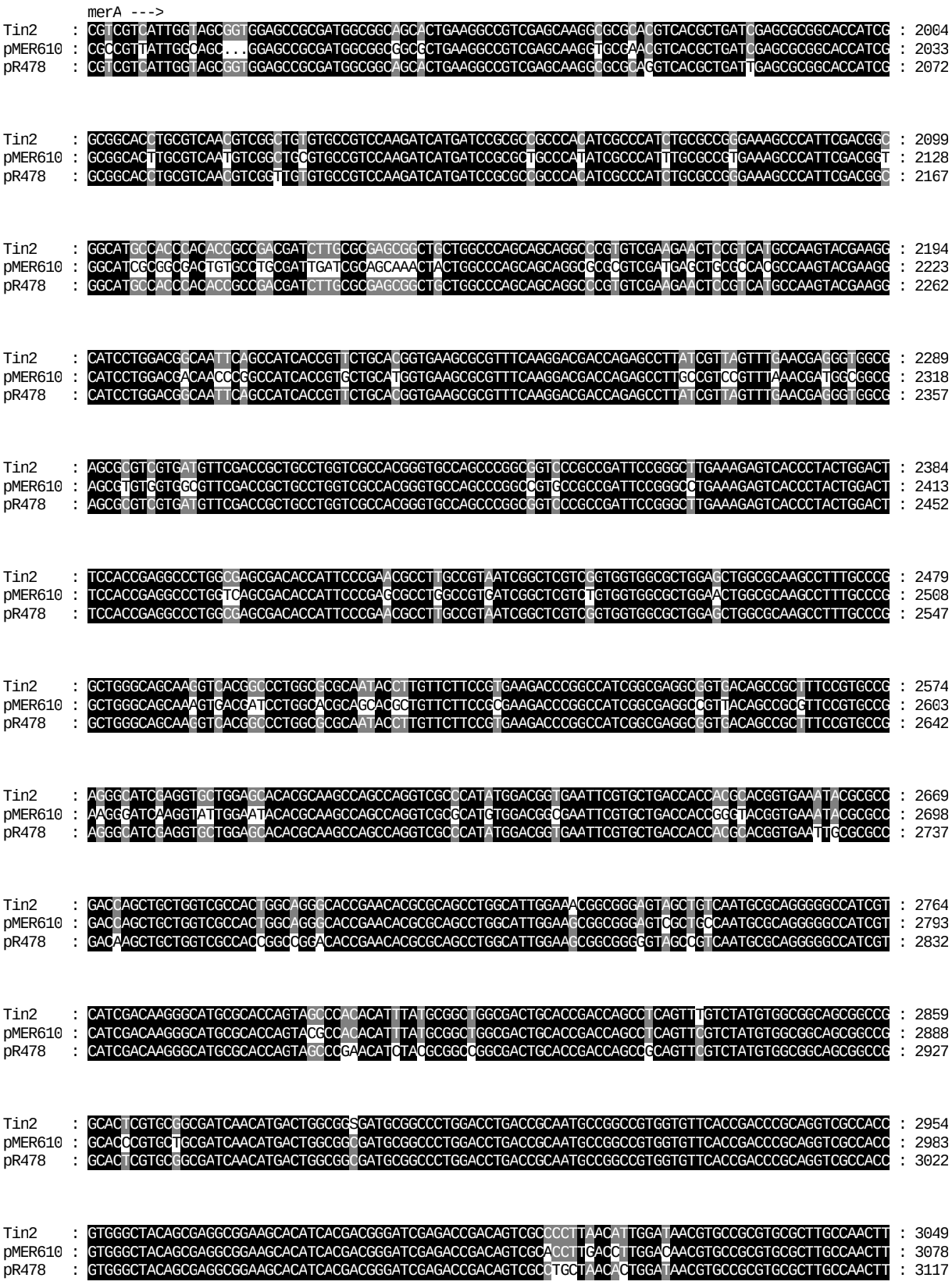

Figure C-28c. Continuing the alignment of the *mer*A gene from *Citrobacter freundii* Tin2 with plasmids pMER and pR478. Black shade: 100% similarity. Start and stop codon are colored pink.

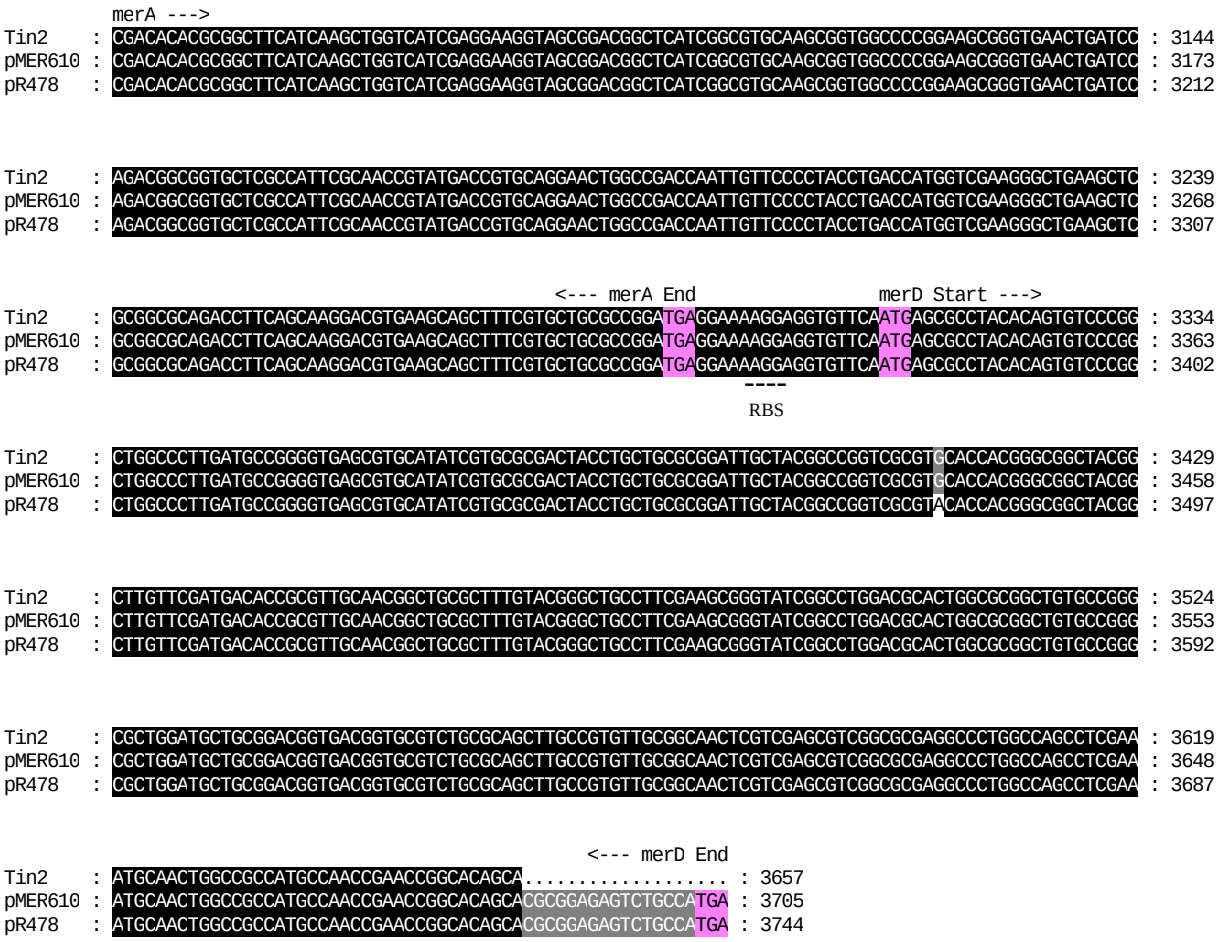

Figure C-28d. Continuing the alignment of the *mer*A and *mer*D gene from *Citrobacter freundii* Tin2. Black shade: 100% similarity. Start and stop codon are colored pink.

7. Ps. fulva Spi11

- 1st *mer* operon:

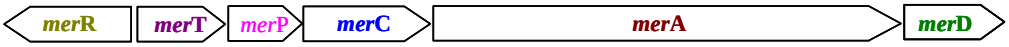


```
                End merR --->
Spi11-merRTPCA : ------------------------------------------------ATCAGCGGGCAGGAAACGTTCCCTTTCCGCGCATGGCAGGCGC :   44
D.acidovorans  : CTAAGGCATAGCCGACCCTGCCAGGCTTGTTCCGCCCTGTAGCGACGCGATCAGCGGGCAGGAAACATTCCCCTTCCGCGCATGGCAGGCGC :   92
Spi11-merAD    : ---------------------------------------------------------------------------------------- :    -

Spi11-merRTPCA : ACATCAGATCAGACAGGACGGCCTCCATGCGTGCCAGGTCCGCCAACTTCTCGCGCACGTCCTTGAGCTTGTGCTCGGCTAGGCTGCTGGCT :  136
D.acidovorans  : ACACCAGTTCAGACAGCACGGTTTCCATGCGCGCCAGGTCGGCCATCTTTTCGCGCACGTTCTGAAGCTTGTGCTCGGCCAGGCTGCTGGCT :  184
Spi11-merAD    : ---------------------------------------------------------------------------------------- :    -

Spi11-merRTPCA : TCCTCGCAGTGGGTGCCATCGTCGAGCCGCAACAGCTCGGCAATCTCATCCAGGCTGAAGCCCAGCCGCTGGGCCGACTTCACAAAGCGCAC :  228
D.acidovorans  : TCCTCGCAGTGGGTGCCGTCGTCGAGCCGCAGCAGATCGGCTATTTCATCCAGGCTGAAGCCCAGCCGCTGGGCCGATTTCACGAATCGCAC :  276
Spi11-merAD    : ---------------------------------------------------------------------------------------- :    -

Spi11-merRTPCA : CCGCGTTACATCCGCCGCGCCATAGCGGCGAATGCTGCCGTAAGGCTTGTCCGGTTCCGGCAACAAGCCCTTGCGCTGGTAGAACCGGATGG :  320
D.acidovorans  : TCGCGTCACATCCGCCGCGCCATAGCGGCGAATGCTGCCGTAAGGCTTATCCGGTTCCGGCAGCAAGCCCTTACGCTGATAGAACGGGATCG :  368
Spi11-merAD    : ---------------------------------------------------------------------------------------- :    -

                                                  <--- merR Start
Spi11-merRTPCA : TCTCTACATTGACCCGGCCGCCTTGGAAAAAACGCCAATGGTCAGGTTTTCCAAATTCTTTTCCATACCACTTGACTCCGTACATGACTCC :  412
D.acidovorans  : TTTCCACATTGACCCGGCCGCCTTGGCAAAAACGCCAATGGTCAGGTTCTCTAAATTCTTTTCCATATCGCTTGACTCCGTACATGAGTAC :  460
Spi11-merAD    : ---------------------------------------------------------------------------------------- :    -

                                                  merT Start --->
Spi11-merRTPCA : GGAAGTAAGGTTACGCTATCCAATTCAAATTCGAAAGGACAAGCGCATGTCTGAACCACAAAACGGGCGCGGCGCGCTCTTCGCTGGCGGGC :  504
D.acidovorans  : GGAAGTAAGGTTACGCTATCCAATTTAAATCCAAAAGGACAAGCGCATGTCTGAACCACAAACTGGGCGCGGCGCGCTCTTCGCCGGCGGGC :  552
Spi11-merAD    : ---------------------------------------------------------------------------------------- :    -
                                          ----
                                          RBS

Spi11-merRTPCA : TAGCTGCCATCCTCGCCTCGACTTGCTGCCTCGGGCCGCTGGTTCTGGTTGCCTTGGGCTTCAGCGGGGCATGGATCGGCAACCTGACCGTG :  596
D.acidovorans  : TGGCCGCCATCCTCGCCTCCGCTTGCTGCCTCGGGCCGCTGGTTCTGATCGCCTTGGGCTTCAGCGGGGCTTGGATCGGCAACCTGACCGTG :  644
Spi11-merAD    : ---------------------------------------------------------------------------------------- :    -

Spi11-merRTPCA : CTGGAGCCGTATCGCCCGATTTTCATCGGCGCAGCGCTGGTGGCGTTGTACTTCGCCTGGCGGCGCATCTACCGCCCTGCGCAAGCCTGCAA :  688
D.acidovorans  : CTGGAGCCGTATCGCCCGATTTTCATCGGCGCAGCGCTGGTGGCGTTGTTCTTCGCCTGGCGGCGCATCTACCGCCCTGCGCAAGCCTGTAG :  736
Spi11-merAD    : ---------------------------------------------------------------------------------------- :    -

Spi11-merRTPCA : ACCGGGTGAGGTCTGCGCGATTCCCCAAGTGCGAGGTACTTACAAGCTCATTTTCTGGGTCGTGGCCGTGCTGGTCCTGGTCGCACTCGGAT :  780
D.acidovorans  : GCCGGGTGAGGTCTGCGCGATTCCCCAAGTGCGAGCGACCTACAAGCTCATTTTCTGGGTCGTGGCCGTACTGGTTCTGGTCGCGCTCGGAT :  828
Spi11-merAD    : ---------------------------------------------------------------------------------------- :    -
```

Figure C-29a. Alignment of the narrow spectrum resistant *mer* operon of *Ps. fulva* Spi11. The nucleotide sequence is aligned with Tn501-like mercury resistance transposon from *Delftia acidovorans* strain MC1 (accession no. AY327575) including the *mer* genes R, T, P, C, A and D. Ribosomal binding site are shown below the DNA sequence. Black shade: 100% similarity. Start and stop codon are colored pink.

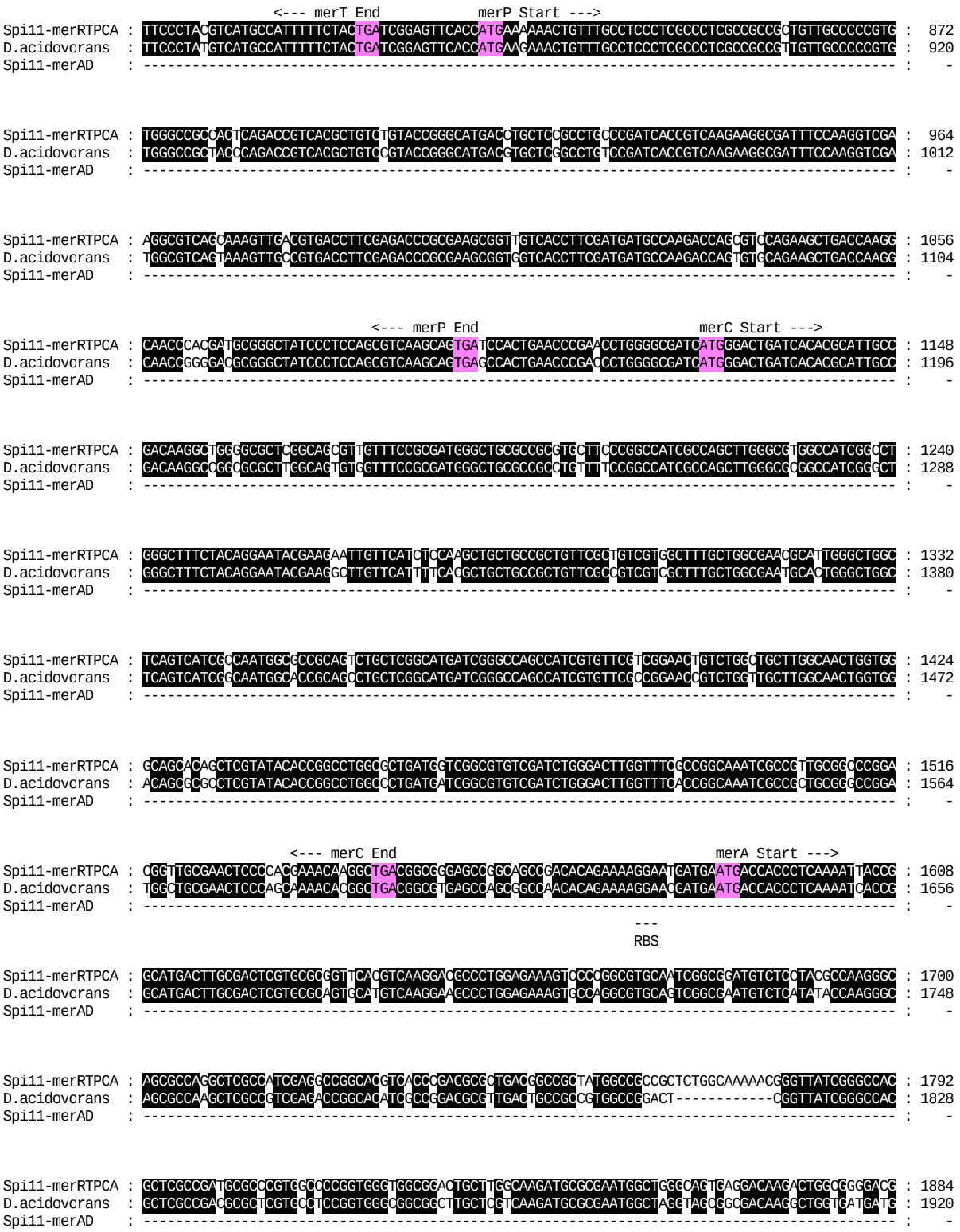

Figure C-29b. Continuing the alignment of the *mer*TPCA gene from *Ps. fulva* Spi11 with Tn501-like mercury resistance transposon from *Delftia acidovorans* strain MC1 (accession no. AY327575). Ribosomal binding site are shown below the DNA sequence. Black shade: 100% similarity. Start and stop codon are colored pink.

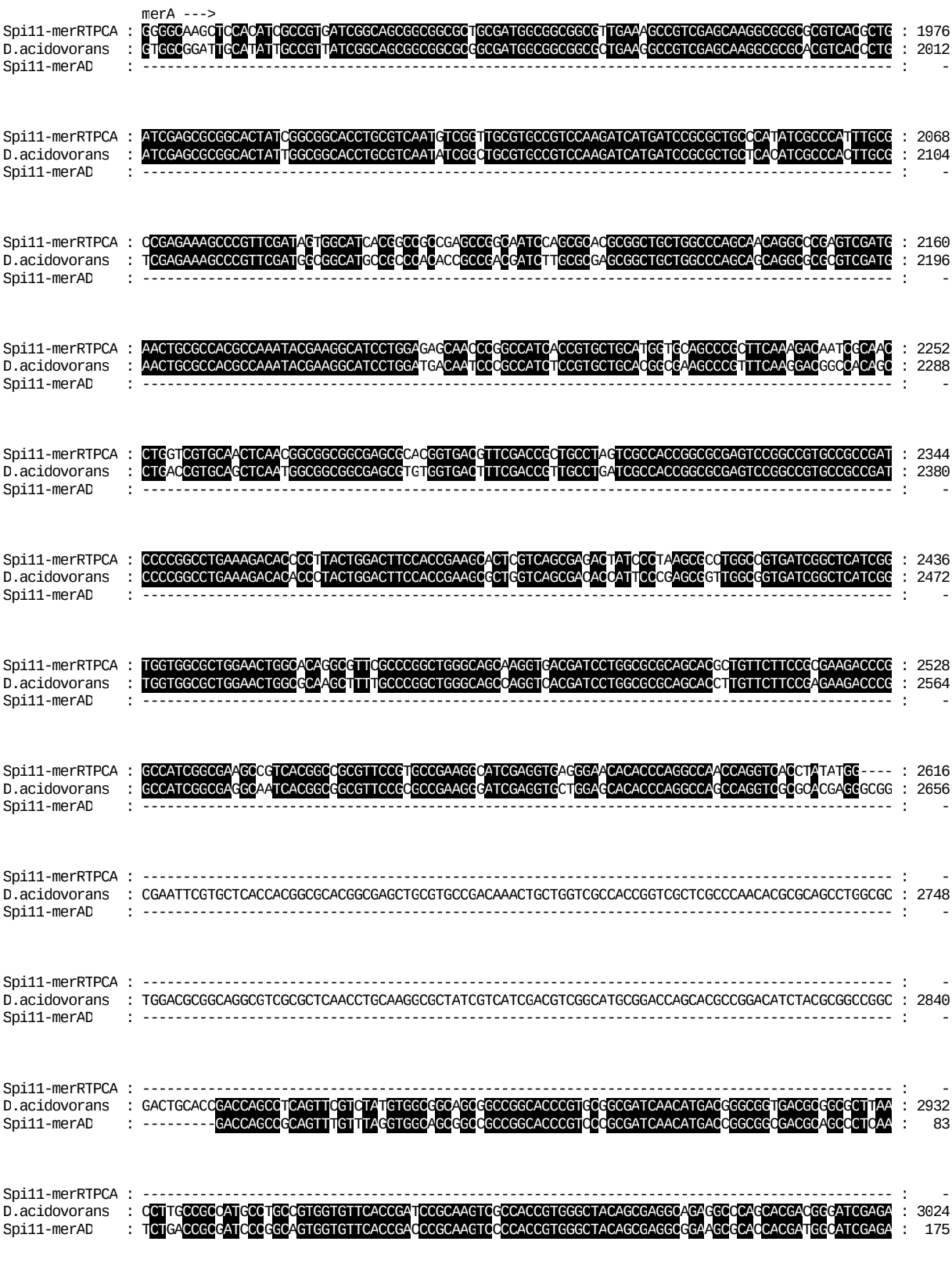

Figure C-29c. Continuing the alignment of the *mer*A gene from Spi11 with Tn501-like. In *mer*A is a gap of 196 nucleotide, which was not be sequenced (2653 bp – 2849 bp). Black shade: 100% similarity. Start and stop codon are colored pink.

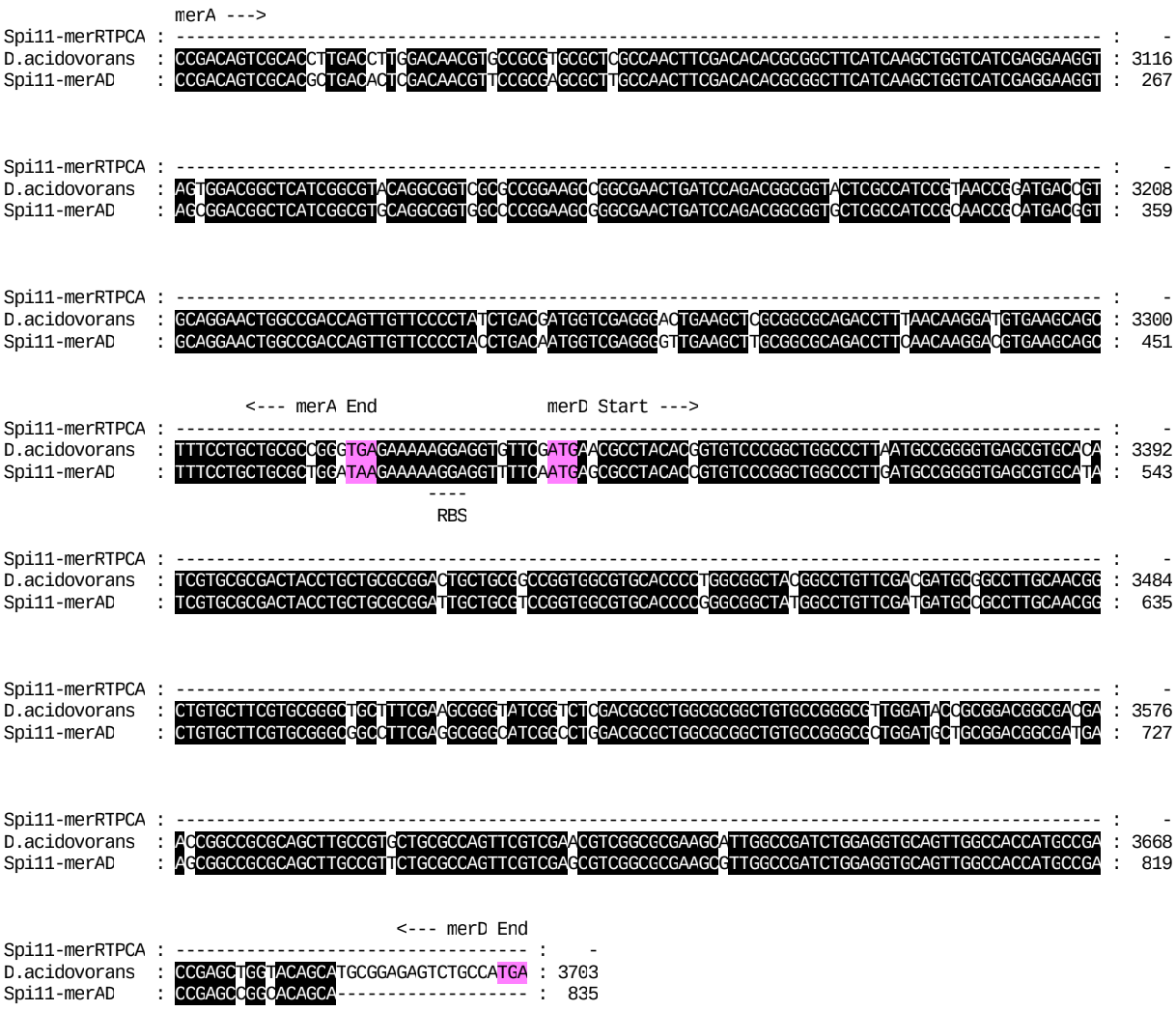

Figure C-29d. Continuing the alignment of the *mer*A and *mer*D gene from Spi11 with Tn501-like transposon from *Delftia acidovorans* strain MC1 (accession no. AY327575). Ribosomal binding site are shown below the DNA sequence. Black shade: 100% similarity. Start and stop codon are colored pink.

8. Ps. putida Spi4

- 1st *mer* operon:

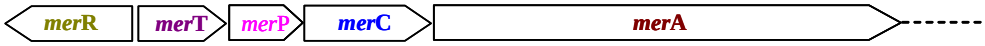


```
                 merR Start --->
Spi4-merRTPC     : ..............................................................CGCGGCATGGCAG :  13
Sp.paucimobilis  : ..............................................................             :   -
Tn5041           : TACGCAACGGGAAATCCTCGGTTAACGCCCGAGTTGTCCCCATGCAGCGAAACGATCAGCGGACAGGAAACAGTCCCGTGGCTGGCACAACAG :  93
Spi4-merA        : ..............................................................             :   -

Spi4-merRTPC     : GCGCACACCAGTTCAGACAGCACGGCCTCCATGCGTGCCAAGTCGGCCATCTTCTCGCGGCACATCCTTGAGCTTGTGCTCGGGCAGGCCGCTG :  106
Sp.paucimobilis  : ..............................................................             :   -
Tn5041           : TCGTGAACCAGTTGCTCCAAAACTGACTCGATCCGTCGCAGATCCGCGGACGTTGCCACGGCACATCCCCAAGCTTCTGCTCGGGGAGCCACAGGC :  186
Spi4-merA        : ..............................................................             :   -

Spi4-merRTPC     : GCTTCCTCGCAATGGCTGCCATCCTCCAGCCGCAGTAGGTCGGCGATTTCGTCCAGGCTAAAGCCCAGCCGCTGGCTCGATTTCACGAACCGC :  199
Sp.paucimobilis  : ..............................................................             :   -
Tn5041           : GCTTCATCGCAGTGACCACCGTCATCCAGCCTCAACAGGCCGGCCACTTCATCGAGGCTAAAGCCCAGCCGTTGCCCGGATTTAACGAATTTC :  279
Spi4-merA        : ..............................................................             :   -

Spi4-merRTPC     : ACTCCTGTTACATCCGCCTGCCATAGCGGCGAATGCTGCCATAGGGCTTGTCTGGCTCCGGCAGCAGGCCTTGCGCTGGTAGAACCGGATG :  292
Sp.paucimobilis  : ..............................................................             :   -
Tn5041           : ACCCGGCCGACATCCGCCTCACCGTAACGGCGAATGCTGCCGTAGGGCTTGTCCGGTTCGGGTAACAGCGCCTTGCGTTGATAGAACCGGATG :  372
Spi4-merA        : ..............................................................             :   -

Spi4-merRTPC     : GTCTCCACATTGACCCCGGCCGCCTTGGCAAAAACGCCAATGGTCAGATTCTCCAAATTTTTTTCCATATCGCTTGACTCCGTACATAACTAC :  385
Sp.paucimobilis  : ...................GCCGCCTTGGCAAAAACGCCAATGGTCAGATTCTCCAAATTTTTTTCCATATCGCTTGACTCCGTACATAACTAC :   75
Tn5041           : GTTTCCACGTTGACCCCGGCCGCCTTGGCGAAAGCGCCCAATGGTCAGGCTTTCCAAATTGTTTTTCATACCGCTTGATTCCGTACATGACTAC :  465
Spi4-merA        : ..............................................................             :   -

                                                          merT Start --->
Spi4-merRTPC     : GGAAGTAAGCTTAAGCTATCCAAACCAAATTTGAAAGGGCAAGCGTATGTCTGAACCTCAAAACGGGCGCGGGGCGCTCTTCACTGGCGGGCT :  478
Sp.paucimobilis  : GGAAGTAAGCTTAAGCTATCCAAACCAAATTTGAAAGGGCAAGCGTATGTCTGAACCTCAAAACGGGCGCGGGGCGCTCTTCACTGGCGGGCT :  168
Tn5041           : GGGACTAACCTTAAACCATCGATCAAATGCTCGAAAGCAGAAATGCATGTCTGAACCATCAAACGGGCGCGCCCCTCTTGTCGCCGGGGGCT :  558
Spi4-merA        : ..............................................................             :   -
                                                     ---
                                                     RBS

Spi4-merRTPC     : AGCCGCCATCCTCGCCTCGGCTTGCTGCCTGGGGCCGCTGGTTCTGATCGCCCTGGGATTCAGCGGGGCCTGGATCGGTAACCTGACCGTGCT :  571
Sp.paucimobilis  : AGCCGCCATCCTCGCCTCGGCTTGCTGCCTGGGGCCGCTGGTTCTGATCGCCCTGGGATTCAGCGGGGCCTGGATCGGTAACCTGACCGTGCT :  261
Tn5041           : TGCGGCGATTCTCGCCTCGGCTTGCTGTCTGGGGCCGCTGATTCTGATCGCACTGGGATTCAGCGGGGCCTGGATCGGTAACCTGACCGTGCT :  651
Spi4-merA        : ..............................................................             :   -

Spi4-merRTPC     : GGAACCGTACCGCCCGCTCTTCATCGGCGCGGCACTGGTGGCGCTGTTCTTCGCCTACCGGCGCATTTTCCGCCCCGCTCAAGCCTGCGCACC :  664
Sp.paucimobilis  : GGAACCGTACCGCCCGCTCTTCATCGGCGCGGCACTGGTGGCGCTGTTCTTCGCCTACCGGCGCATTTTCCGCCCCGCTCAAGCCTGCGCACC :  354
Tn5041           : GGAACCGTACCGCCCGCTCTTCATCGGCGCGGCACTGGTGGCGCTGTTCTTCGCCTACCGGCGCATTTTCCGCCCCGCTCAAGCCTGCGCACC :  744
Spi4-merA        : ..............................................................             :   -

Spi4-merRTPC     : GGGCGAGGTCTGCGCCATCCCTCAGGTACGTACCTCCTACAAGCTGCTGTACTGGCTGGTGGCGGCCTTGGTGCTGGTCGCGCTCGGCTTCCC :  757
Sp.paucimobilis  : GGGCGAGGTCTGCGCCATCCCTCAGGTACGTACCTCCTACAAGCTGCTGTACTGGCTGGTGGCGGCCTTGGTGCTGGTCGCGCTCGGCTTCCC :  447
Tn5041           : GGGCGAGGTCTGCGCCATCCCTCAGGTACGTACCTCCTACAAGCTGCTGTACTGGCTGGTGGCGGCCTTGGTGCTGGTCGCGCTCGGCTTCCC :  837
Spi4-merA        : ..............................................................             :   -
```

Figure C-30a. **Alignment of the partly sequenced narrow spectrum resistant *mer* operon from *Ps. putida* Spi4**. The nucleotide sequence of Spi4 is aligned with partly sequenced and published *Sphingomonas paucimobilis* strain 660H (accession no. AF120972) and *Pseudomonas sp.* transposon Tn5041 (accession no. X98999), including the *mer* genes R, T, P, C and *mer*A. Ribosomal binding site are shown below the DNA sequence. Black shade: 100% similarity. Start and stop codon are colored pink.

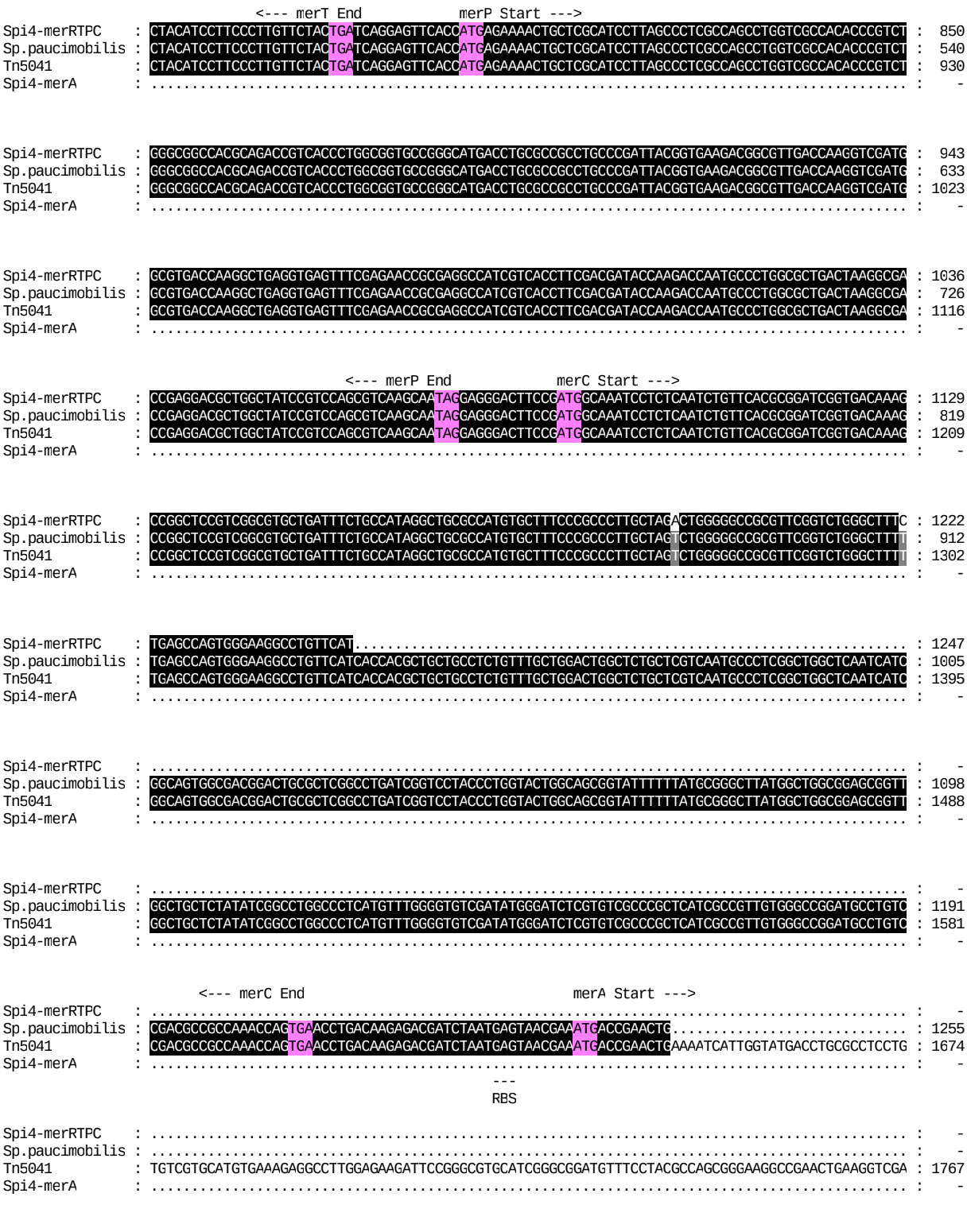

Figur C-30b. Continuing the alignment of the *mer* genes T, P, C and partly sequenced *mer*A gene from *Ps. putida* Spi4 with *Sphingomonas paucimobilis* strain 660H (accession no. AF120972) and Tn5041 (accession no. X98999). Ribosomal binding site are shown below the DNA sequence. Black shade: 100% similarity. Start and stop codon are colored pink.

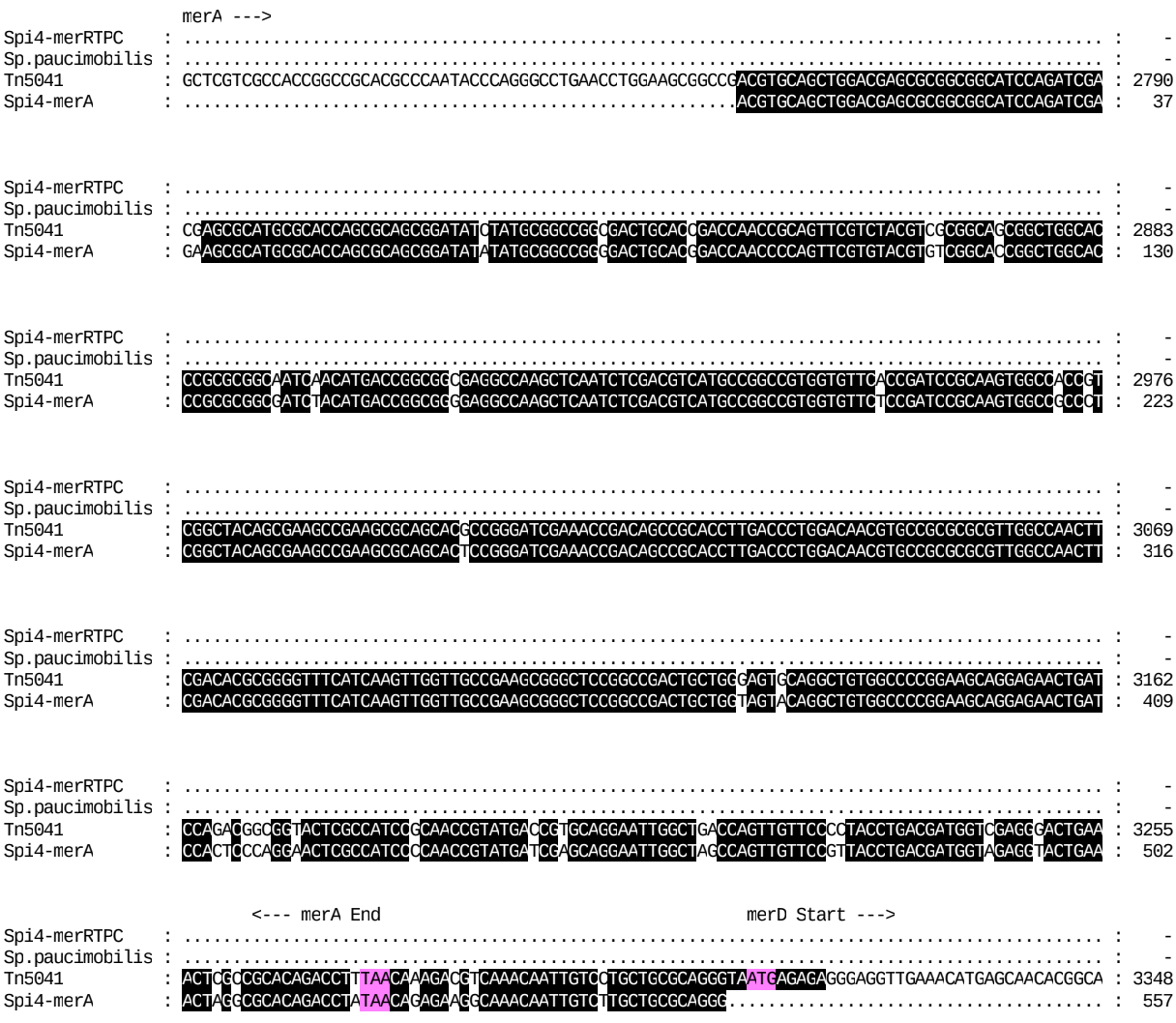

Figure C-30c. Continuing the alignment of the partly sequenced *mer*A gene from Spi4 with Tn5041 (accession no. X98999). No *mer*D gene could be detected though all standard strains possessed the *mer*D gene. Ribosomal binding site are shown below the DNA sequence. Black shade: 100% similarity. Start and stop codon are colored pink.

- 2nd *mer* operon:


```
                                                                  <--- merP End
Spi4-merA : ..........................................................GAACTGAAAACGGCAGCGCAG :   21
pDU1358   : AGACCAGCGTGCAGAAGCTGACCAAGGCCACCGAAGACGCGGGCTATCCGTCCAGCGTCAAGAAGTGAGGAACTGAAAACGGCAGCGCAG : 1170
              K  T  S  V  Q  K  L  T  K  A  T  A  D  A  G  Y  P  S  S  V  K  Q  -

                                                          merA Start --->
Spi4-merA : CACATCTGACGCCCTTGTCTGCTACCACAAACGAAAAAGGATCTGTCGCATGACCCATCTAAAAATCACCGGCATGACCTGCGACTCGTG :  111
pDU1358   : CACATCTGACGCCCTTGTCTGCTACCACAAACGAAAAAGGATCTGTCGCATGACCCATCTAAAAATCACCGGCATGACCTGCGACTCGTG : 1260
                                              ----          M  T  H  L  K  I  T  G  M  T  C  D  S  C
                                              RBS

Spi4-merA : CGCGGCGCACGTCAAGGAAGCGCTGGAAAAAGTACCCGGCGTCCAATCTGCCATAGTGTCCTATGCCAAGGGCGCGGCCCAGCTCGCCCT :  201
pDU1358   : CGCGGCGCACGTCAAGGAAGCGCTGGAAAAAGTACCCGGCGTCCAATCTGCCATAGTGTCCTATGCCAAGGGCGCGGCCCAGCTCGCCCT : 1350
              A  A  H  V  K  E  A  L  E  K  V  P  G  V  Q  S  A  I  V  S  Y  A  K  G  A  A  Q  L  A  L

            merA --->
Spi4-merA : TGATCCAGGCACAGCGCCGGACGCACTGACCGCCGCCGTGGCTGGCCTGGGCTACAAAGCGATGCTCGCCGATGCCCCGCCGACCGACAA :  291
pDU1358   : TGATCCAGGCACAGCGCCGGACGCACTGACCGCCGCCGTGGCTGGCCTGGGCTACAAAGCGATGCTCGCCGATGCCCCGCCGACCGACAA : 1440
              D  P  G  T  A  P  D  A  L  T  A  A  V  A  G  L  G  Y  K  A  M  L  A  D  A  P  P  T  D  N

Spi4-merA : CCGCACTGGGCTGTTCGACAAGGTGCGCGGCTGGATGGGTGCCGCCGACAAGGGCAGCGGCGCGAGCGCCCGTTGCAAGTCGCCGTGAT :  381
pDU1358   : CCGCACTGGGCTGTTCGACAAGGTGCGCGGCTGGATGGGTGCCGCCGACAAGGGCAGCGGCCCGAGCGCCCGTTGCAAGTCGCCGTGAT : 1530
              R  T  G  L  F  D  K  V  R  G  W  N  G  A  A  D  K  G  S  G  G  E  R  P  L  Q  V  A  V  I

Spi4-merA : CGGCAGCGGTGGAGCCGCGATGGCGGCAGCACTGAAGGCCGTCGAGCAAGGCGCGCAGGTCACGCTGATTGAGCGCGGCACCATCGGCGG :  471
pDU1358   : CGGCAGCGGTGGAGCCGCGATGGCGGCAGCACTGAAGGCCGTCGAGCAAGGCGCGCAGGTCACGCTGATTGAGCGCGGCACCATCGGCGG : 1620
              G  S  G  G  A  A  M  A  A  A  L  K  A  V  E  Q  G  A  Q  V  T  L  I  E  R  G  T  I  G  G

Spi4-merA : CACCTGCGTCAACGTCGGTTGTGTGCCGTCCAAGATCATGATCCGCGCCGCCCACATCGCCCATCTGCGCCGGGAAAGCCCGTTCGATGG :  561
pDU1358   : CACCTGCGTCAACGTCGGTTGTGTGCCGTCCAAGATCATGATCCGCGCCGCCCACATCGCCCATCTGCGCCGGGAAAGCCCATTCGACGG : 1710
              T  C  V  N  V  G  C  V  P  S  K  I  M  I  R  A  A  H  I  A  H  L  R  R  E  S  P  F  D  G

Spi4-merA : CGGTATGGCACCCACACCGCCTACGATCTTGCGCGAGCGGCTGCTGGCCCAGCAGCAGGCCCGTGTCGATGAACTGCGCCACGCCAAGTA :  651
pDU1358   : CGGCATGGCACCCACACCGCCGACGATCTTGCGCGAGCGGCTGCTGGCCCAGCAGCAGGCCCGTGTCGAAGAACTCCGTCATGCCAAGTA : 1800
              G  M  P  P  T  P  P  T  I  L  R  E  R  L  L  A  Q  Q  Q  A  R  V  E  E  L  R  H  A  K  Y

Spi4-merA : CGAAGGCATTCTGGATGGCAATGCAGCCATCACCGTTGTGCACGGTGAAGCGCATTTCAAGGACGACCAGAGCCTTGCTGTCCGTTTGAA :  741
pDU1358   : CGAAGGCATCCTGGACGGCAATTCAGCCATCACCGTTCGTCACGGTGAAGCGCGTTTCAAGGACGACCGAGACCTTAGCGTTAGTTTGAA : 1890
              E  G  I  L  D  G  N  S  A  I  T  V  L  H  G  E  A  R  F  K  D  D  R  D  L  S  V  S  L  N

Spi4-merA : CGAAGGTGGCGAGCGCGTGGTGATATTCGACCGCTGCCTGATCGCCACGGGTGCCAGCCCGGCCGTGCCGCCGATTCCCGGCTTGAAAGA :  831
pDU1358   : CGAGGGTGGCTGAGCGCGTCGTGATGTTCGACCGCTGCCTGGTCGCCACGGGTGCCAGTCCGGCCATGCCGCCGATTCCGGGCCTGAAAGA : 1980
              E  G  G  E  R  V  V  M  F  D  R  C  L  V  A  T  G  A  S  P  A  M  P  P  I  P  G  L  K  E
```

Figure C-31a. **Alignment of the partly sequenced *mer*A gene from *Ps. putida* Spi4 with plasmid pDU1358.** In *mer*A is a gap of 168 nucleotide which could not be sequenced (1575 bp – 1743 nt). Ribosomal binding site and amino acid sequence of reference polypeptide (accession no. M15049, Z49200 and M24940) is shown as standard single letter below the DNA sequence line. Black shade: 100% similarity. Start and stop codon are colored pink.

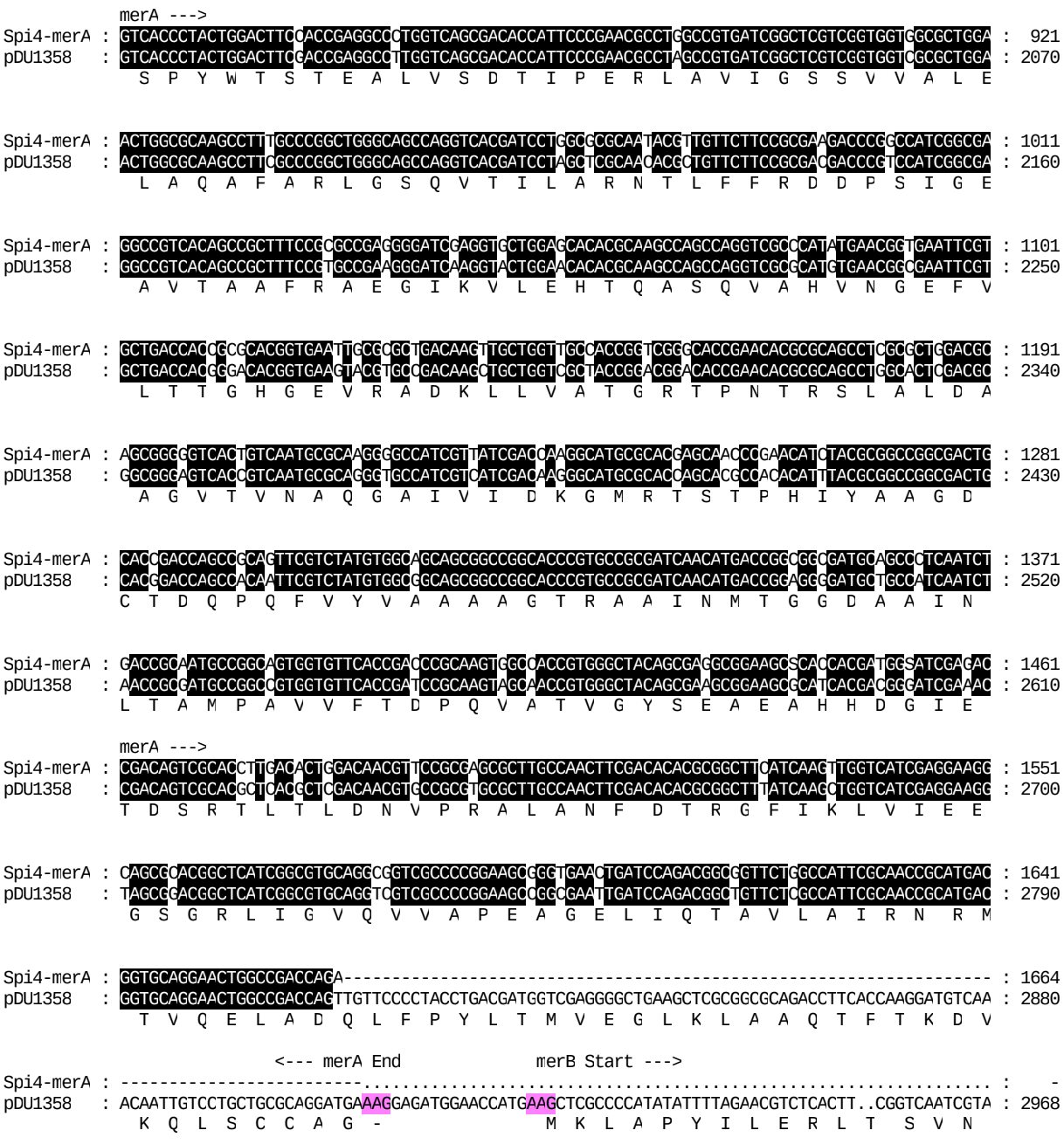

Figure C-31b. Continuing the alignment of the partly sequenced *mer*A gene from Spi4. Amino acid sequence of pDU1358 polypeptide (accession no. M15049, Z49200 and M24940) is shown as standard single letter below the DNA sequence line. Black shade: 100% similarity. Start and stop codon are colored pink.

D. Mercury Calibration Curves

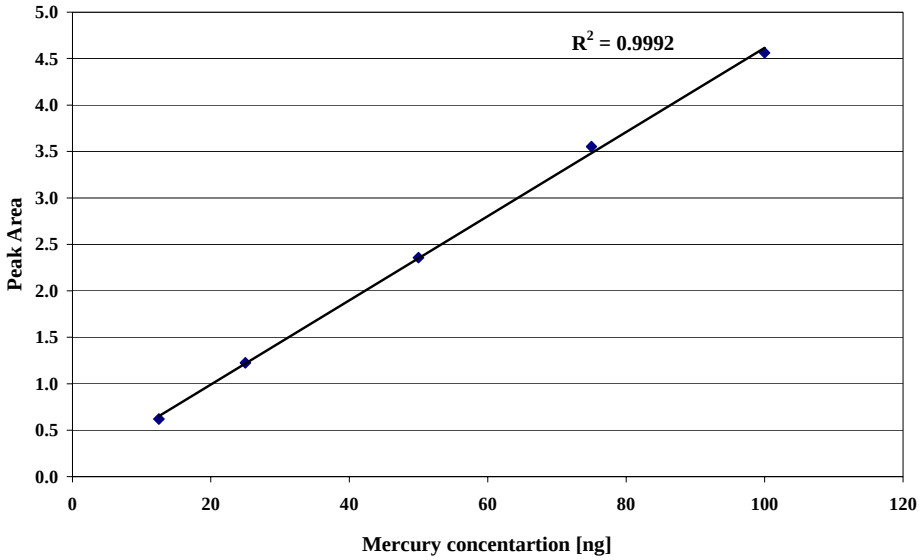

Figure D-32. Calibration curve of total mercury measurement on CVAAS. The mercury standard concentration was between 12.5 and 100 ng.

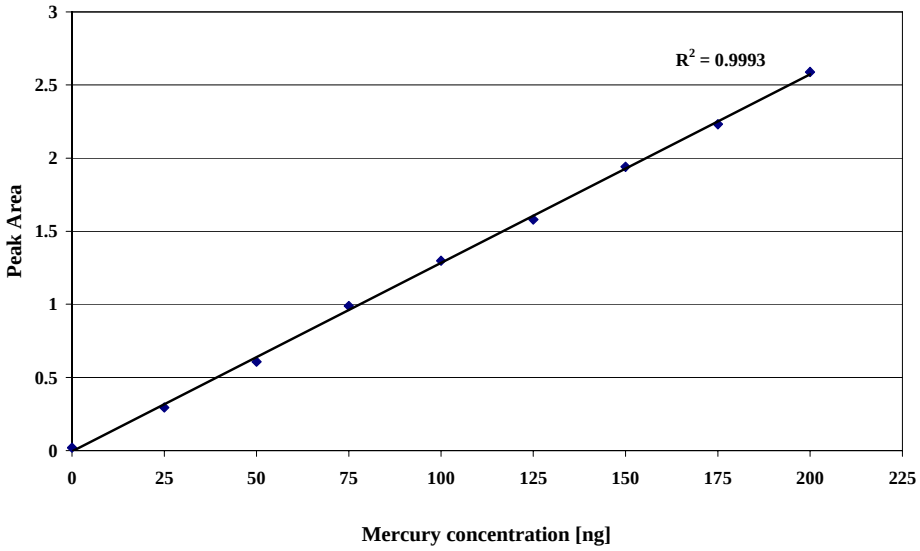

Figure D-33. Calibration curve of thiomersal transformation rate measurement. The mercury standard concentration was between 0-200 ng.

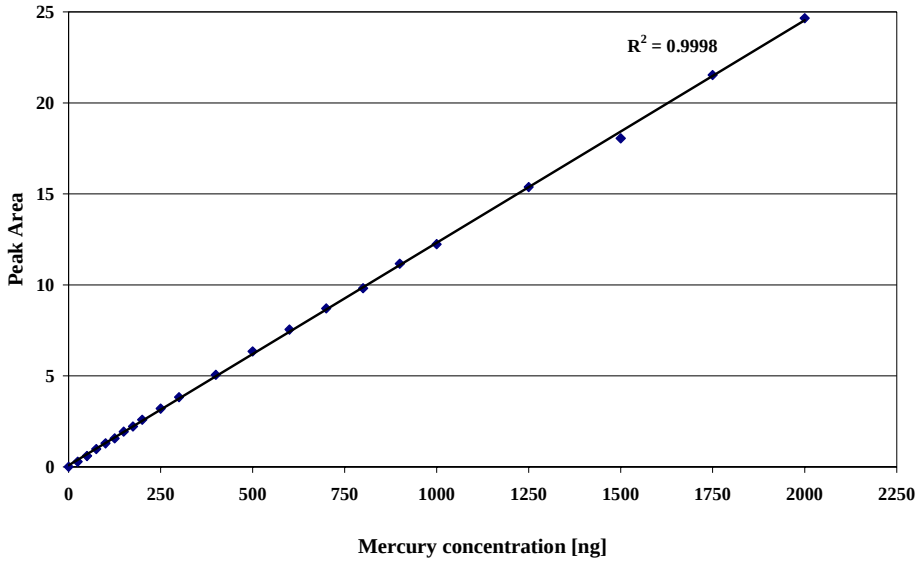

Figure D-34. Calibration curve of thiomersal transformation rate measurement. The mercury standard concentration was between 0-2000 ng.

ACKNOWLEDGEMENTS

The work described in this thesis was done in the Gesellschaft für Biotechnologische Forschung (GBF) under supervision Prof. Dr. K. N. Timmis. However, this thesis could not have been written without the kind support of several people, not only scientifically but also socially. I would like to take the opportunity to thank everybody who supported me during this time. I would like to thank the people that were of most help personally.

Mein besonderer Dank gilt Frau PD Dr. Irene Wagner-Döbler für die Überlassung des Themas, Ermöglichung selbständigen wissenschaftlichen Arbeitens, sowie für ihr Interesse am Fortgang dieser Arbeit und die gewährte Unterstützung.

Der Europäischen Union bin ich für die Finanzierung dieses Projekts n^{o} QLK3-1999-01213 zu Dank verpflichtet.

Herrn Prof. Dr. Dieter Jahn danke ich für die Übernahme des Zweitgutachtens.

Herrn Prof. Deckwer und Dr. Rolf-Joachim Müller danke ich für die ausgesprochen herzliche Aufnahme in die Räume der Umweltverfahrenstechnik der GBF im Y-Gebäude, 2. Stock.

Mein größter Dank gilt Björg Pauling und Christa Hoch für Unterstützung und das Interesse an meiner Arbeit. Ihre Geduld und ihr Optimismus haben zum Gelingen dieser Arbeit beigetragen. Außerdem danke ich für die stetige Diskussions- und Hilfsbereitschaft sowie die gewissenhafte Durchsicht des Manuskripts.

I would like to acknowledge Victor A. Pires Martins dos Santos for his help and encouragment with the reactor operation and maintenance.

Ein ganz herzlicher Dank geht Johannes Leonhäuser, für die Fortführung des Reaktors und seine Hilfsbereitschaft.

Mein herzlicher Dank gilt René Huppmann für die analytischen Messungen an HPLC, und für seine Hilfsbereitschaft.

Bei allen ehemaligen Mitgliedern des Labors D011, Ina Pubantz, Harald von Canstein, Ingrid Brümmer, Andreas Felske, Marita Sylla und Verena Heindl, sowie Daniela Regenhardt und Stefanie Tilmann, möchte ich mich für die besonders angenehme Arbeitsatmosphäre bedanken, so dass ich gerne ins Labor ging.

Mit Herrn Possins Hilfsbereitschaft und seinem unendlich großen Herzen waren etliche Probleme und Umzüge viel leichter lösbar. Ihm sei dafür ganz besonders herzlich gedankt.

Bedanken möchte ich mich nicht zuletzt bei meiner großen Familie und meinem Mann Folkert. Ohne deren Unterstützung und Motivation wäre die Arbeit nie geschrieben worden.